

ACCELEROMETER-BASED GAIT ANALYSIS FOR THE QUANTITATIVE
ASSESSMENT OF RUNNING PERFORMANCE FOR POTENTIAL
APPLICATION OUTSIDE THE LABORATORY

Danielle T. Charles

PhD Thesis

Submitted in accordance with the requirements for the degree of
Doctor of Philosophy

The University of Leeds
School of Biomedical Sciences

July 2024

INTELLECTUAL PROPERTY RIGHTS

The candidate confirms that the work submitted is her own and that appropriate credit has been given where reference has been made to the work of others.

This copy has been supplied on the understanding that it is copyright material and that no quotation from the thesis may be published without proper acknowledgement.

The right of Danielle T. Charles to be identified as Author of this work has been asserted by her in accordance with the Copyright, Designs and Patents Act 1988.

Behold the heaven, the earth, the sea; all that is bright in them or above them; all that creep or fly or swim; all have forms because all have number.

Take away number and they will be nothing... Ask what delights you in dancing and number will reply: 'Lo, here I am.' Examine the beauty of bodily form, and you will find everything is in its place by number. Examine the beauty of bodily motion and you will find everything in its due time by number.

- St. Augustine

ACKNOWLEDGEMENTS

I would like to express my deepest gratitude to the remarkable individuals whose unwavering support and encouragement have played an instrumental role in the completion of this doctoral journey.

First and foremost, I extend my heartfelt thanks to my dear friends Tim, Conny, Hanna, Nat, Maddie, Rachel, Nicole and Jordan. Your camaraderie, intellectual discussions and moments of respite were invaluable throughout this challenging academic pursuit. Your friendship made the long hours of research and writing not only bearable but enjoyable.

I am grateful to my parents and family members for their endless encouragement, understanding and belief in my abilities. Your sacrifices and unwavering support have been the bedrock of my academic journey. I am truly fortunate to have you as my pillars of strength.

Special appreciation goes to my supervisors, Dr. Graham Askew and Professor Andy Brown, for their guidance, wisdom, expertise and willingness to jump on the treadmill whenever needed. Your insightful feedback and mentorship have been invaluable in shaping the trajectory of my research. I am deeply grateful for the learning and grow opportunities under your guidance.

To all the participants that excitedly volunteered; bouncing in, in the morning but crawling out in the afternoon after a tougher than anticipated training protocol.

To my dedicated tutor, Diane, for her patience, constructive feedback and commitment to my academic development. Your guidance has been indispensable in refining my academic skills.

To all those mentioned and to the countless others who supported me along the way, your contributions were pivotal to the successful completion of this epic task. Without your encouragement, understanding and belief in my abilities, this achievement would not have been possible. As I stand on the precipice of this academic milestone, I am reminded that this journey was not taken alone. The collective support of friends, family, mentors and loved ones has been my anchor. Thank you!

With heartfelt gratitude,

Danielle

ABSTRACT

Running gait analysis is often achieved using motion capture (MC), however this is largely confined to laboratories with costly and space-intensive equipment. This study investigates measuring radial acceleration against time on a runner's leg, using a sensitive wearable accelerometer as a simpler alternative. Stride Frequency (SF) and Spectral Purity (SP) were identified as key parameters extracted using Fast Fourier Transformation (FFT) of accelerometry data as potential quantitative indicators of running gait quality. To assess these parameters as measures of gait quality and whether they are related to performance, Running Economy (RE) benefits from wearing the Nike® Vaporfly ZoomX Next% (VFN%) versus the Saucony® ProGrid Jazz 12 (JAZ) running shoes were determined using a Cardiopulmonary Exercise Test (CPET) of 25 participants running at a fixed speed of 12 km/h on a treadmill over various inclines from 0-5%. The RE benefits of the VFN% were confirmed to be 4.4% at 0% incline and shown to exponentially decline to a predicted minimum benefit of 2.3% by 16% incline and above. The FFT of the corresponding accelerometer movement waves revealed that runners always have a lower SF and generally a better SP when wearing the VFN% running shoes. As incline increased the difference between the lower SF in the VFN% vs the JAZ parallels the declining RE benefit of wearing VFN% over the JAZ whilst running at a fixed speed. This novel analysis emphasises the potential of accelerometry as a tool for understanding gait quality and predicting performance outside the laboratory. Further testing and optimisation are

required to make this type of gait analysis affordable and accessible for all athletes.

TABLE OF CONTENTS

1.	General Introduction.....	2
1.1.	Running.....	3
1.2.	Basic mechanics of running	5
1.3.	Mechanical energetics - Potential Energy (PE) and Kinetic Energy (KE)	7
1.4.	Mechanical energetics - Elastic Stored Energy (ESE)	10
1.5.	Energetics of running and Running Economy (RE)	12
1.6.	Energetics of running and footwear	18
1.7.	Incline running.....	27
1.8.	Stride Length (SL) and Stride Frequency (SF)	30
1.9.	Gait analysis.....	32
1.10.	Wearable devices	33
1.11.	Analytical techniques.....	38
1.12.	Aims.....	41
1.13.	Objectives	41
2.	Formulation and Optimisation of General Methods	44
2.1.	Introduction	45
2.1.1.	Aim	46
2.1.2.	Objectives	46
2.2.	General methods	48
2.2.1.	Wearable device technical specification.....	48
2.2.2.	Participant inclusion criteria.....	49
2.2.3.	Ethics.....	50

2.2.4.	Statistical testing	51
2.2.5.	Data extraction	52
2.3.	Premise.....	55
2.3.1.	Aim	55
2.3.2.	Hypothesis testing	56
2.3.3.	Objectives	57
2.4.	Method.....	57
2.4.1.	protocol	57
2.4.2.	Data extraction	58
2.4.3.	Data processing.....	58
2.5.	Results and discussion	60
2.5.1.	Next steps	65
2.6.	Premise.....	67
2.6.1.	Aim	67
2.6.2.	Hypotheses	67
2.6.3.	Objectives	68
2.6.4.	Method.....	68
2.6.5.	General methods	68
2.6.6.	Protocol	68
2.6.7.	Data extraction	69
2.6.8.	Data processing.....	69
2.7.	Results and discussion	70
2.7.1.	Next steps	76
2.8.	Premise.....	78

2.9.	Aim	78
2.9.1.	Hypotheses	78
2.9.2.	Objectives	79
2.10.	Data processing.....	80
2.10.1.	Filtering.....	80
2.10.2.	Rotation matrices	81
2.11.	Analytical techniques.....	86
2.11.1.	Fast Fourier Transformation (FFT) for Fundamental Frequency (FF) ..	86
2.11.2.	Cumulative Distribution Function (CDF) for Spectral Purity (SP)	89
2.11.3.	Cross-correlation for gait symmetry.....	92
2.12.	Protocol	96
2.12.1.	Data extraction	98
2.13.	Results and discussion	98
2.13.1.	Placement style and device colour on Fundamental Frequency (FF) and Spectral Purity (SP)	106
2.14.	Limitations	107
2.15.	Conclusion.....	108
2.15.1.	Next steps	108
3.	Study 4: Nike® Vaporfly ZoomX NEXT% running shoes have running economy benefits over various inclines compared to conventional running shoes	
	110	
3.1.	Introduction	111
3.1.1.	Running Economy (RE)	111
3.1.2.	Breaking2 Campaign	112

3.1.3.	Running on an incline	113
3.1.4.	Running shoe composition	114
3.1.5.	Aim	118
3.1.6.	Hypotheses	118
3.1.7.	Objectives	119
3.2.	Method.....	120
3.2.1.	General methods	120
3.2.2.	Statistical power	120
3.2.3.	Participants	120
3.2.4.	Protocol	121
3.2.5.	Data extraction	124
3.2.6.	Data processing.....	124
3.3.	Results.....	126
3.3.1.	Variance.....	126
3.3.2.	Parametric testing	126
3.4.	Discussion	137
3.4.1.	Summary of findings	137
3.4.2.	Hypothesis one; running on the level (0%)	138
3.4.3.	Hypothesis two; running on an incline (1%, 3% and 5%).....	139
3.4.4.	Hypothesis three; relationship of the data - exponential decay model 142	
3.5.	Application	145
3.6.	Conclusion.....	147
3.7.	Limitations	148

4.	Study 5: The Global gait analysis Tool (GaiT) for the quantification of running performance using accelerometry	152
4.1.	Premise.....	153
4.1.1.	Aim	154
4.1.2.	Hypotheses	154
4.1.3.	Objectives	155
4.2.	General methods	155
4.2.1.	Statistical power	155
4.2.2.	Participants	156
4.2.3.	Protocol	157
4.2.4.	Data extraction	159
4.2.5.	Data processing and analytical techniques	159
4.3.	Results.....	161
4.3.1.	Variance.....	161
4.3.2.	Statistical testing.....	161
4.4.	Discussion	180
4.4.1.	Hypothesis one; for males and females the VFN% will produce a lower Fundamental Frequency (FF) than the JAZ over all inclines, thus lower Stride Frequency (SF).....	180
4.4.2.	Hypothesis two; for males and females Fundamental Frequency (FF) will increase with increasing incline in both running shoes.....	181
4.4.3.	Hypothesis three; for males and females lower Running Economy (RE) values will be associated with lower Fundamental Frequency (FF) values.....	183

4.4.4.	Hypothesis four; for males and females the VFN% will produce lower Spectral Purity (SP) levels than the JAZ, ergo have better gait quality.....	184
4.4.5.	Hypothesis five; for males and females higher Spectral Purity (SP) values will be seen with increasing incline.	186
4.4.6.	Hypothesis six; for males and females lower Running Economy (RE) values will be associated with lower Spectral Purity (SP) values.	187
4.5.	Conclusion and next steps	188
4.5.1.	Summary of findings	188
4.5.2.	Future work	190
5.	General Discussion.....	193
5.1.	Project Aim.....	193
5.2.	Chapter 1: General Introduction	193
5.3.	Chapter 2: Formulation and Optimisation of General Methods.....	194
5.4.	Chapter 3: Nike® Vaporfly ZoomX NEXT% running shoes have running economy benefits over various inclines compared to conventional running shoes	196
5.5.	Chapter 4: The Global gait analysis Tool (GaiT) for the quantification of performance differences between running wearing VFN% and JAZ shoes using accelerometry	198
5.6.	Philosophical and speculative impacts	200
5.6.1.	Revolutionising sports and athletic training.....	200
5.6.2.	Transforming healthcare and rehabilitation.....	200
5.6.3.	Consumer fitness market.....	201
5.6.4.	Public health initiatives	201

5.6.5.	Scientific research and technological advancements	202
5.6.6.	Product development and innovation	202
5.6.7.	Conclusion.....	202
5.7.	Limitations	204
5.7.1.	Samples size and representation.....	204
5.7.2.	Randomisation process	204
5.7.3.	Gender differences	205
5.7.4.	Methodological constraints.....	205
5.7.5.	Technological and instrumentation limitations.....	205
5.7.6.	Longitudinal considerations	206
5.8.	Future work	206
5.9.	Conclusion.....	209
	Section 1: Basic project details.....	215
	Section 2: Contact details	216
	Section 3: Summary of the research	216
	Section 4: Research data and impact.....	219
	Section 5: Protocols.....	222
	Section 6: Additional ethical issues	222
	Section 7: Recruitment and consent process	225
	Section 8: Data protection, confidentiality and anonymisation.....	228
	Section 9: Other ethical issues	230
	Section 10: Further details for student projects (complete if applicable).....	231
	Section 11: Other members of the research team (complete if applicable) ...	232
	Section 12: Supporting documents	233

Section 13: Sharing information for training purposes	234
Section 14: Declaration.....	234

LIST OF FIGURES

Figure 1: Running gait cycle, consisting of Initial Contact (IC), mid-Stance (mid-ST), Toe-Off (TO), mid-Swing (mid-SW), finishing with Initial Contact (IC) again (Houglum, 2016).	6
Figure 2: Variation in gait cycle parameters with speed of movement showing two complete gait cycles or strides. As speed increases, SW time (clear) increases, followed by ST time (shaded) decreases and DF increases with the overall gait cycle time shortening (Novacheck, 1998).	7
Figure 3: The relationship between Potential Energy (PE) and Kinetic Energy (KE) in running noting Stance Phase Reversal (STR) and Double Float (DF) (Novacheck, 1998).	9
Figure 4: The spring-mass model for running (Li, 2011).	12
Figure 5: Factors affecting running economy (Barnes and Kilding, 2015).	15
Figure 6: Example of results from cardiopulmonary exercise testing. (CPET) within the laboratory. These curves are based on a male participant locomoting at different speeds. A. When displaying metabolic power for walking and running as a function of speed. B. When displaying energy cost in joules per meter for walking and running as a function of speed (Alexander, 1992).	18
Figure 7: The effect of shoe mass on oxygen uptake ($\dot{V}O_2$ %). Where 100 g increase (per pair) in running shoe mass equates to approximately an additional 1% in $\dot{V}O_2$ uptake (Cavanagh and Kram, 1985).	19
Figure 8: Change in oxygen uptake for running in shoes of different mass compared with barefoot running. Shoe mass values are the combined mass of	

a one shoe pair. Standardised mean difference (SMD) on the y-axis and $\dot{V}O_2$ is on the x-axis (Fuller et al., 2015).	20
Figure 9: The effect of cushioning on running economy (RE). Two similar weighted running shoes, with shoe two having more cushioning than shoe one. Shoe two utilised less $\dot{V}O_2$ than shoe one, thus had better RE (Cavanagh and Kram, 1985).	22
Figure 10: Exploded view of the Nike® prototype shoe that incorporates a newly developed midsole material and a full-length carbon-fibre midsole plate with forefoot curvature, embedded in the midsole (Hoogkamer et al., 2018).	23
Figure 11: Estimated change in race time, compared with a previous result, when switching shoes (Quealy and Katz, 2019).....	25
Figure 12: Optimal velocity for locomotion over several inclines. For a 65 kg participant, the most economical grade was about -10% decline, with energy cost increasing linearly with increasing incline and decline. Adapted for this project by changing the units from cal/m/kg to $\dot{V}O_2$ ml/kg/min (Cavanagh and Kram, 1985).	27
Figure 13: Elastic Stored Energy (ESE) differences with incline. The solid curves are the mechanical energy fluctuations of the BCoM throughout stance, the black dashed lines represent the maximum possible elastic stored and returned energy (MPESE), the grey dashed lines, the anatomically estimated elastic energy storage (AESE). Both mechanical energy generation and dissipation occur, with more generation occurring uphill, elastic stored energy decreases, thus the body must generate additional energy to account for this decrease. Adapted for this project from Snyder, Kram and Gottschall, (2012).	29

Figure 14: The curvilinear relationship between $\dot{V}O_2$ and stride length (SL). The dashed line represents the optimal SL which produces the least $\dot{V}O_2$ uptake at a given running speed. The preferred SL is close to the optimal meaning self-optimisation occurs. Adapted for this project (Cavanagh and Kram, 1985).	30
Figure 15: The relationship between stride frequency (SF) and metabolic cost. Trials were run at 2.8 m/s with SF calculated for the preferred stride frequency (PSF) then 85%, 92%, 108% and 115% of PSF. The arrow represents optimal stride frequency (OSF) where the metabolic cost is at its lowest (Snyder and Farley, 2011).....	31
Figure 16: MEMS accelerometer (Rao et al., 2019).	34
Figure 17: The x-, y- and z-axes with the corresponding angular system of roll, pitch and yaw respectively (Ellis et al., 2014).....	36
Figure 18: Eight gait features highlighted in the accelerometer movement wave. Corresponds to the walking gait events that are defined in figure 1; 1. IC, 2. Load Response (LR), 3. mid-ST, 4. Terminal-ST, 5. TO, 6. IS, 7. Mid-SW and 8. terminal-SW (Anway, Yu and Vassallo, 2018).	39
Figure 19: Fast Fourier Transform (FFT)(A and C) and Cumulative Distribution Function (CDF) (B and D) plots from which Spectral Purity (SP) is determined. Where figures A and B represent a child with low SP (higher gait quality), commonly displayed as a left (negative) skew with few, high amplitude, low frequency peaks, being classed as cleaner spectra. C and D are from a child with a high SP (low gait quality) commonly displayed as many, lower amplitude, higher frequency peaks (Barnes, 2017).	40

Figure 20: The two, custom made wearable devices (SlamTracker, Swansea University, UK).	49
Figure 21: Orientations from 1-6 in which the wearable device was positioned for one minute each.	58
Figure 22: Tilt test gravitational effect on the each of tri-axial accelerometer axes (blue = x-axis, green = y-axis and red = z-axis) positioned in the six different orientations as noted, in	61
Figure 23: The resultant right-hand coordinate system is shown for the device in each of the six orientations. Gravity is demonstrated as a vertical, downward arrow.	63
Figure 24: A. The wearable device schematic containing x-, y- and z-axes with corresponding counter clockwise rotations, roll (ϕ), pitch (ρ) and yaw (ψ) respectively. B. The red and blue wearable devices marked with their corresponding coordinate system, top upper left corner marker, and top and bottom orientation.	63
Figure 25: Image depicting the radial and transverse axis of the lower limb and converging point where the wearable device will be fitted.	64
Figure 26: Bland-Altman plot of the internal versus the external clock sampling frequency results. Where the black line shows the bias, and the dashed black line the upper and lower limits of agreement (LOA).	72
Figure 27: Bland-Altman plot of red versus the blue device sampling frequency results. Where the black line shows the bias, and the dashed black line the upper and lower limits of agreement (LOA).	72

Figure 28: Graphical representation of the blue (LL) and the red (RL) devices x-, y- and z- accelerometer waves set at a 0.025 wave scaling (40 Hz). The red (RL) device waves are on the left of the figure and the blue (LL) device waves are on the right side of the figure with seconds (s) along the x-axis and gravitational acceleration (g) on the y-axis. There is an observable variation in the time and end point of the blue and red waves. This can only be corrected after the data is extracted in the Igor Pro v8 processing software by changing the wave scaling as in Equation 6.....74

Figure 29: A. and B. show a two second radial accelerometry sample from the uninjured left leg (LL) (solid line) and injured right leg (RL) (dotted line). C. and D. show the fast Fourier transform (FFT) of the two second accelerometry sample from A. and B. respectively. A. and C. represent 4 km/h and B. and D. represent 15 km/h (Jenner et al., no date).88

Figure 30: Sequency of the generation of a CDF: A. one-minute movement wave from an individual with good motion, B. with poor motion, C. and D. are the corresponding FFT from the movement waves, E. and F. are the corresponding CDFs from the FFT (Barnes, 2017).....91

Figure 31: Auto-correlation of the non-injured leg against itself (black line) against the cross-correlation of the injured leg against the non-injured leg (dotted red line) at 11, 19 and 48-weeks post-surgery (Jenner et al., no date). .95

Figure 32: Raw accelerometry data graphed to show x-, y- and z-axis movement waves from one of the test-retest repeatability trials. The figure shows the protocol including the initial shaking movement of the wearable device, after fitting the participant standing in a static position, the participant building up

their running speed as the treadmill was gradually increased to 16 km/h, the 120 second segment running at 16 km/h, the winding down of the runner as the treadmill was gradually decreased to 0 km/h, and the removal and final shake of the wearable devices to show the end of the trial.....99

Figure 33: Two strides from the x-axis movement wave recorded via the blue accelerometer (Ac_x_LL) during a running trial at 16 km/h. It is possible to identifying calculable gait parameters; push off, leg swing and maximum impact force (Barnes, 2017).....100

Figure 34: Raw accelerometry wave for the x-axis for a 100 second sample of running at 16 km/h from the LL and RL, where the blue Acc_x_LL wave is for the accelerometry x-axis movement wave of the left leg (LL), and red Acc_x_RL is the same for the right leg (RL) which was extracted from Figure 32.101

Figure 35: FFT in the frequency domain from a 100 second sample of running at 16 km/h where blue FFT_Acc_x_LL represents the FFT wave for the accelerometry x-axis movement wave of the left leg (LL), and red FFT_Acc_x_RL is the same for the right leg (RL) from Figure 34. FF is Fundamental Frequency in Hz and SF is stride frequency in Hz.102

Figure 36: CDF of LL (blue) and RL (red) FFT during RE protocol at 16 km/h with black dashed line demonstrating 0.5 CDF probability and first blue dashed line representing LL normalised frequency and second red dashed line RL normalised frequency.103

Figure 37: Auto-correlation of the RL vs RL (blue line) against the cross-correlation of the RL vs LL (red line) of x axis data during the RE protocol at 16 km/h. Where Acc_x_16kmh_Auto (RLRL) is the original 100 s epoch of the

accelerometry wave for the RL that has been correlated against itself (auto-correlation) and Acc_x_16kmh_Auto (RLLL) is the original 100 s epoch of the accelerometry movement wave for the RL that has been correlated against the accelerometry wave for the LL (cross-correlation).	105
Figure 38: Breakdown of the Vaporfly (VF) running shoe build composition which contains the upper, upper midsole foam layer, carbon-fibre midsole plate, lower midsole foam layer and rubber outsole (Healey and Hoogkamer, 2021).....	115
Figure 39: Saucony®'s ProGrid Jazz 12, schematic view of the running shoe construction (Saucony® Inc., 2017).....	117
Figure 40: Incline protocol schematic. The full protocol demonstrating time spent testing the first, followed by the second randomised running shoe, at 12 km/h over four randomised intervals.....	123
Figure 41: Mean gross rate of submaximal oxygen uptake ($\dot{V}O_2$ ml/kg/min) for the Nike® Vaporfly ZoomX NEXT% (VFN%) and Saucony® ProGrid Jazz 12 (JAZ) running shoes, averaged over all inclines, for males (blue) and females (orange) showing standard error (S.E.). On average, the JAZ had a higher $\dot{V}O_2$ uptake for both males and females than the VFN%.....	127
Figure 42: Gross submaximal rate oxygen uptake (ml/kg/min) at 0%, 1%, 3% and 5% incline in VFN% (orange line) and JAZ (blue line) with S.E., bars. Gross $\dot{V}O_2$ uptake was significantly less in VFN% than the JAZ ($P < 0.01$).	130
Figure 43: Mean and individual gross oxygen uptake ($\dot{V}O_2$ ml/kg/min) between the Vaporfly ZoomX NEXT% (VFN%) and Saucony® ProGrid Jazz 12 (JAZ) whilst running on a treadmill at 12 km/h at 0%, 1%, 3% and 5%. The black line reports	

the mean gross $\dot{V}O_2$ of all participants and the grey lines are for each individual participant.....	131
Figure 44: Mean $\dot{V}O_2$ uptake for those that "yes" can and "no" cannot run 10 km ≤ 40 -minute, against various inclines (0-5%). The JAZ and VFN% for yes and no are not significantly different..	133
Figure 45: Running economy (RE) benefit/ penalty. The difference between $\dot{V}O_2$ uptake VFN% and JAZ divided by the JAZ to give the benefit of the VFN%. The individual grey lines are for each of the 18 participants with the thick black line being the mean result for all participants.	135
Figure 46: Gross mean $\dot{V}O_2$ uptake difference (%) (blue dots) including standard error bars. The exponential decay fit (black line), where under the fit line depicts the fixed effect of the running shoe; the mass effect being a constant 1% RE penalty per 100 g per shoe of additional running shoe weight, and the midsole effect at 1.3% benefit of the VFN% running shoe regardless of incline.	136
Figure 47: The RE benefit (%) of the VFN% versus the JAZ from this study (blue line) and from the VF4% versus the Nike® Streak 6 (grey line), over inclines 0-5%.	140
Figure 48: New York City Marathon course profile; Implication of current research on calculating VF RE benefits based on the exponential decay results from this study (New York Road Runners, 2024).	146
Figure 49: Fundamental Frequency (FF) for the VFN% and the JAZ running shoe over incline 0%, 1%, 3% and 5%. Mean FF for all participants (black line), mean FF for females (orange line), mean FF for males (blue line) and FF for each	

individual participant (grey line). Mean FF is lower for the VFN% than the JAZ over all inclines.	164
Figure 50: Mean Fundamental Frequency (FF) for the VFN% (orange) and the JAZ (blue) running shoe, where the VFN% facilitates a lower FF, thus SF than the JAZ whilst running on all inclines.	165
Figure 51: Fundamental Frequency (FF) benefit/ penalty. The difference between FF in the VFN% and the JAZ divided by the FF in JAZ, times 100 to give the benefit of the FF in the VFN% (Equation 23). The individual grey lines are for each of the male and female participants, with the thick black line being the combined mean result for all participants.	167
Figure 52: Fundamental Frequency (FF) benefit expressed as a percentage between the VFN% and the JAZ running shoe. This shows the mean benefit of all participant data (black), female data (orange) and male data (blue) over all inclines tested.	168
Figure 53: Correlation for males running data at 0% incline for $\dot{V}O_2$ uptake (ml/kg/min) vs FF (Hz) whilst running in the JAZ running shoes. This figure shows a statistically significant strong, positive relationship, where $\dot{V}O_2$ uptake increases, FF increases.....	170
Figure 54: Correlation for females running data at 0% incline for $\dot{V}O_2$ uptake (ml/kg/min) vs FF (Hz) for VFN% running shoes. This figure shows a statistically significant strong, negative relationship, where when $\dot{V}O_2$ uptake increases, FF decreases.	170
Figure 55: Running Economy (RE) benefit versus Fundamental Frequency (FF) benefit. The difference between FF in the VFN% and the JAZ divided by the FF in	

JAZ times 100 to give the percentage benefit of the FF in the VFN% (Equation 23).	
The black line is the exponential decay fitted data, the blue dots are the mean RE benefit and the grey squares are the FF benefit.....	171
Figure 56: Mean Spectral Purity (SP) for the VFN% (orange) and the JAZ (blue) running shoe, where on average the VFN% facilitates lower SP, compared to the JAZ, over all inclines but 0%. This means that typically the VFN% have superior gait quality.....	173
Figure 57: Spectral Purity (SP) benefit/ penalty. The difference between SP in the VFN% and the JAZ divided by the SP in JAZ, times 100 to give the percentage benefit of the SP in the VFN%. The individual grey lines are for each of the male and female participants, with the thick black line being the combined mean result for all participants.	175
Figure 58: Spectral Purity (SP) expressed as a percentage benefit between the VFN% and the JAZ running shoes, where the mean difference of all participant data (black) showing S.E., female data (orange) and male data (blue) over all inclines tested.	176
Figure 59: Females treadmill running at 5% incline; gross $\dot{V}O_2$ uptake (ml/kg/min) vs SP (Hz) for JAZ running shoes. A statistically significant strong, negative relationship, where when gross $\dot{V}O_2$ uptake increases, SP decreases.....	178
Figure 60: Running Economy (RE) benefit versus Spectral Purity (SP) benefit imposed over VFN% exponential decay modelled data for RE benefit. The difference between SP in the VFN% and the JAZ divided by the SP in JAZ to give the percentage benefit of the SP in the VFN% (Equation 23). The black line is the	

exponential decay fitted data, the blue dots are the mean RE benefit and the grey
squares are the superimposed SP benefit. 179

LIST OF TABLES

Table 1: Normative Running Economy (RE) values for male and female runners of varying ability despite the challenge of accumulating this information due to varied protocols, differing gas-analysis equipment, data averaging techniques and maximal aerobic capacity categorisation (Barnes and Kilding, 2015).....	16
Table 2: tilt test results showing the gravitational (g) effect on each of the three accelerometer axes during the six orientations, performed on the red and blue wearable devices. Sensitivity (S) and the subsequent sensor bias (B) were calculated with a worked example to correct the accelerometer coordinates (<i>AStatic_calibrated</i>).....	62
Table 3: Results of three frequency tests with n=12; frequency (Hz) for each test, mean and S.D. frequency for each device and clock type.....	71
Table 4: Descriptive statistics for the strict and varied placement of the wearable devices and the analytical processing techniques. Where N = number of participants, S.D. = standard deviation and S.E. = standard error, LL is left leg and RL is right leg.	106
Table 5: Mass of lead shoelace weight added to each shoe size (Colloff, 2022).	117
Table 6: Participant descriptive statistics.	121
Table 7: Testing results for n = 18 participants for gross $\dot{V}O_2$ (ml/kg/min) for running in the Nike® Vaporfly ZoomX NEXT% (VFN%) and Saucony® Jazz (JAZ) running shoes. The table shows the minimum, maximum, mean and standard deviation (S.D.) for each result.....	128

Table 8: Participant descriptive statistics.	157
Table 9: Results for Fundamental Frequency (FF) for the VFN% and JAZ running shoes over 0%, 1%, 3% and 5% incline, including the N, mean, S.D. and mean difference.	166
Table 10: Results for Fundamental Frequency (FF) benefit for the VFN% over 0%, 1%, 3% and 5% incline, including the N, mean and S.D.	168
Table 11: Results for Spectral Purity (SP) for the VFN% and the JAZ running shoes over 0%, 1%, 3% and 5% incline, including the N, mean, S.D. and mean difference.	174
Table 12: Results for Spectral Purity (SP) benefit for the VFN% over 0%, 1%, 3% and 5% incline, including the N, mean and S.D.	176

ABBREVIATIONS

ACF	Auto-Correlation Function
AESE	Anatomically Estimated Elastic Stored Energy
B	Bias
BCoM	Body Centre of Mass
CCF	Cross-Correlation Function
CDF	Cumulative Distribution Function
CI	Confidence Interval
CO₂	Carbon Dioxide
CoV	Coefficient of Variation
CPET	Cardiopulmonary Exercise Testing
DF	Double Float
DFT	Discrete Fourier Transform
ESE	Elastic Stored Energy
EVA	Ethylene-Vinyl Acetate
F	Finish
FF	Fundamental Frequency
FFT	Fast Fourier Transform
g	Gravitational Acceleration
GaiT	Global Gait Analysis Tool
GCT	Ground Contact Time
GRF	Ground Reaction Force
hh:mm:ss	Hours, Minutes and Seconds
HRC	High Rebound Compound
HRM	Heart Rate Max

Hz	Hertz (Frequency Unit)
I	Initial
IC	Initial Contact
J/kg	Joules per Kilogram
J/m	Joules per Meter
JAZ	Saucony® ProGrid Jazz 12
KE	Kinetic Energy
km/h	Kilometres per Hour
LBS	Longitudinal Bending Stiffness
LL	Left Leg
LOA	Limits Of Agreement
m/s	Meters per Second
MC	Motion Capture
MEMS	Micro Mechanical Electronic Systems
ml/kg/min	Millilitres per Kilogram per Minute
MPESE	Maximum Possible Elastic Stored and Returned Energy
MTP	Metatarsophalangeal
O₂	Oxygen
OSF	Optimal Stride Frequency
p	Point
PAR-Q	Physical Activity Readiness Questionnaire
PE	Potential Energy
PEBA	Polyether Block Amide
PSF	Preferred Stride Frequency
R	Recovery Score

RE	Running Economy
RER	Respiratory Exchange Ratio
RHR	Resting Heart Rate
RL	Right Leg
s	Seconds
S	Sensitivity
S.D.	Standard Deviation
S.E.	Standard Error
SF	Stride Frequency
SI	Gait Symmetry Index
SL	Stride Length
SMD	Standardised Mean Difference
SP	Spectral Purity
SRC	Super Rebound Compound
ST	Stance
STR	Stance Phase Reversal
SW	Swing
TO	Toe-Off
TPU	Thermoplastic Polyurethane
VF	Nike® Vaporfly/ Vaporfly Prototype
VF4%	Nike® Vaporfly 4%
VFN%	Nike® Vaporfly ZoomX NEXT%
$\dot{V}CO_2$	Rate of Carbon Dioxide Expired
$\dot{V}O_2$	Rate of Oxygen Uptake
$\dot{V}O_{2max}$	Maximal Rate of Oxygen Uptake
$\dot{V}O_{2submax}$	Submaximal Rate of Oxygen Uptake

W Watts

W/kg Watts per Kilogram

W/kg/m Watts per Kilogram per Minute

W/s Watts per Second

CHAPTER ONE

1. GENERAL INTRODUCTION

SUMMARY

This chapter covers the growing popularity of running and resultant increased interest in gait research. While gait research laboratories offer valuable data, they are costly and not widely accessible. Wearable devices are emerging as a low-cost alternative for gait analysis, though their consistency is debated, especially for high-speed movements. There is a great deal of importance for energy efficiency leading to performance enhancement in running. Where running shoe characteristics such as shoe mass, cushioning and midsole properties, is of growing interest due to their impact on running economy (RE) and associated improvement in performance. The introduction of the carbon-fibre midsole plate into running shoes, exemplified by the Nike® Vaporfly series revolutionised the market, demonstrating a 4% improvement in RE. The impact of shoe design on uphill RE and gait characteristics warrants further investigation. Gait analysis, using accelerometers within wearable devices, offer a cost-effective alternative to laboratory-based methods. This project aims to investigate accelerometer-based gait analysis for the quantitative assessment of running performance for potential application outside the laboratory. The resolution of this research question would be particularly useful for recreation and professional runners, and coaches with an interest in objectively quantifying gait and running performance.

1.1. RUNNING

The late 1960s and early 1970s saw a notable surge in distance running engagement (Novacheck, 1998), with Jim Fixx and his revolutionary book “the complete book of running” credited for facilitating America's fitness revolution by popularizing the sport of running and demonstrating the health benefits of regular jogging (Plymire, 2002). Running became popular in the UK in the 1980's through the introduction of Chris Brasher and John Disley's London Marathon, and Brendon Foster's Great North Run (Scheerder J., Breedveld and Borgers J., 2015). Recent statistics indicate that four in 10 individuals identify themselves as runners, with 30% engaging in running at least once weekly (Rizzo, 2021). Running stands as one of the most favoured forms of physical activity globally, owing to its minimal equipment requirements and flexible structure. According to the latest data from the International Association of Athletics Federation, running events drew over 107.9 million participants across 70,000 races in 2019, marking a 60% increase in popularity over the last decade (DeJong, Fish and Hertel, 2021). The grassroots growth of initiatives like Parkrun, established in 2004, has contributed to this upward trend. This free 5 km run, held weekly in 28 countries, boasts over 5 million registered participants as of 2018 (Wiltshire, Fullagar, & Stevinson, 2018). Its appeal lies in its inclusivity, welcoming participants of all abilities. Runners can track their progress by scanning a barcode to log their performance time.

The upsurge in both recreational and professional running has in turn fuelled increased interest in gait research and performance analysis which has been facilitated by technological advancements such as faster cameras and marker

systems, streamlining the once labour-intensive process of frame-by-frame digitisation (Menolotto *et al.*, 2020).

Knowledge is required on running gait variables to monitor and improve performance. Historically, coaches used fast and simplistic visual assessment to capture and improve running gait variables, such as Stride Frequency (SF)¹, which when improved can significantly enhance performance (Hoogkamer *et al.*, 2018). However, beyond measuring SF, visual assessment is highly subjective, with moderate validity and moderate test-retest repeatability (Kluge *et al.*, 2017). It is challenging to compare data sets within and between individuals to identify relationships between technique alterations and performance outcomes (Lissiana *et al.*, 2017; Brahms *et al.*, 2018). This is especially true after implementing interventions, such as changes in footwear. Since 2017, the composition of running shoes significantly changed, with increases in the foam midsole volume plus the addition of a carbon-fibre midsole plate that has yielded the most successful racing shoes yet. Those wearing running shoes of this composition have achieved several marathon world records, facilitating the breaking of the 2-hour marathon barrier (Hoogkamer *et al.*, 2016; Hoogkamer, Kram and Arellano, 2017; Whiting, Hoogkamer and Kram, 2022). However, as performance plateaus, other methods for improvement were adopted, such as seeking the in-depth knowledge and specialised equipment within gait research laboratories. These laboratories have the means to objectively identify running gait variables; unfortunately, this information is expensive to gather and not readily

¹ the number of strides taken in a unit of time, often per minute or per second.

accessible to much of the running community (Norris, Anderson and Kenny, 2014).

Wearable devices are being investigated as a low-cost and portable alternative for gait analysis due to their ability to record variables, such as gait cycle events, SF and peak impact force, that have already been validated against 3-D motion capture (MC) (Hu and Soh, 2014; Joukov, Karg and Kulic, 2014; Bötzel *et al.*, 2016, 2018). Such wearable devices have provided a portable and convenient method enabling athletes and coaches to objectively identify and improve specific gait variables that inform performance. The novelty of the wearable device is its ability to capture data within the field permitting the evaluation of such gait variables (Jenner *et al.*, no date; Norris, Anderson and Kenny, 2014; Caldas *et al.*, 2017). Debate remains regarding the methodological consistency of wearable devices, specifically the capture of information from high-speed testing, such as performance running.

1.2. BASIC MECHANICS OF RUNNING

The analysis of gait is broken down into gait cycles, encompassing a series of lower limb movements. One gait cycle is one stride, beginning with initial contact (IC) of the reference leg with the ground and ends with IC of the reference leg for the second time (Figure 1) (Novacheck, 1998).

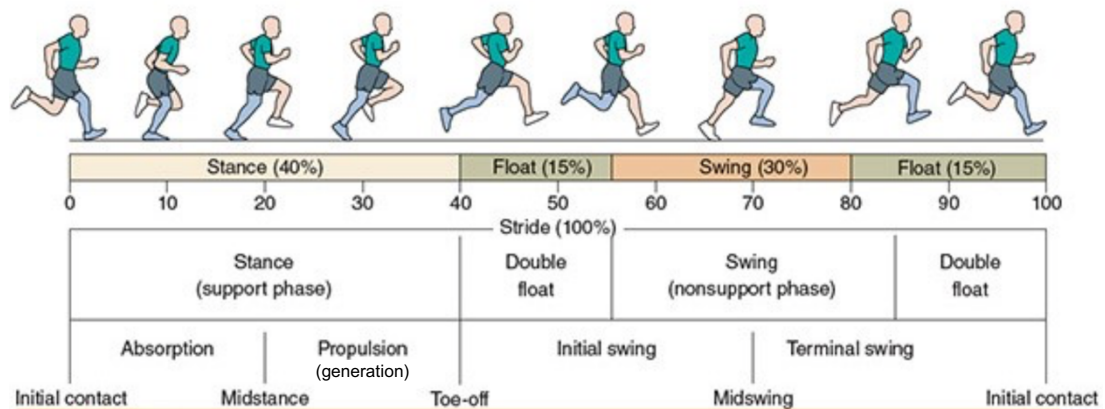


Figure 1: Running gait cycle, consisting of Initial Contact (IC), mid-Stance (mid-ST), Toe-Off (TO), mid-Swing (mid-SW), finishing with Initial Contact (IC) again (Houghlum, 2016).

In running, toe-off (TO) occurs before 50% of the gait cycle is completed, thus both feet are airborne twice during the gait cycle at the beginning and end of swing (SW), known as double float (DF). DF has an overlapping SW phase during each stride (Figure 2) (Novacheck, 1998). As speed increases during running, ST² time decreases, SW³ time typically remains relatively constant or may decrease slightly. This is because higher running speeds are often associated with a shorter duration of the entire gait cycle, including both ST and SW phases. To maintain a consistent stride frequency and overall pace, the duration of both ST and SW phases may be reduced proportionally. This reduction in ST time allows for quicker transitions between strides and facilitates a faster cadence.

Maintaining a consistent cadence (stride rate) at different speeds optimises efficiency and minimises ground contact time. Thus, while ST time decreases

² the time when the foot is in contact with the ground.

³ the time when the foot is in the air.

with increasing speed, SW time is adjusted to ensure a smooth transition between strides while maintaining the desired cadence. As speed increases, SF increases, meaning the time spent in the SW phase decreases because the leg must move quicker to keep up with the faster pace. This is accompanied by the decreased duration of the ST phase allowing for a quicker transition from ST phase to SW phase, contributing to the overall decrease in SW time (Novacheck, 1998).

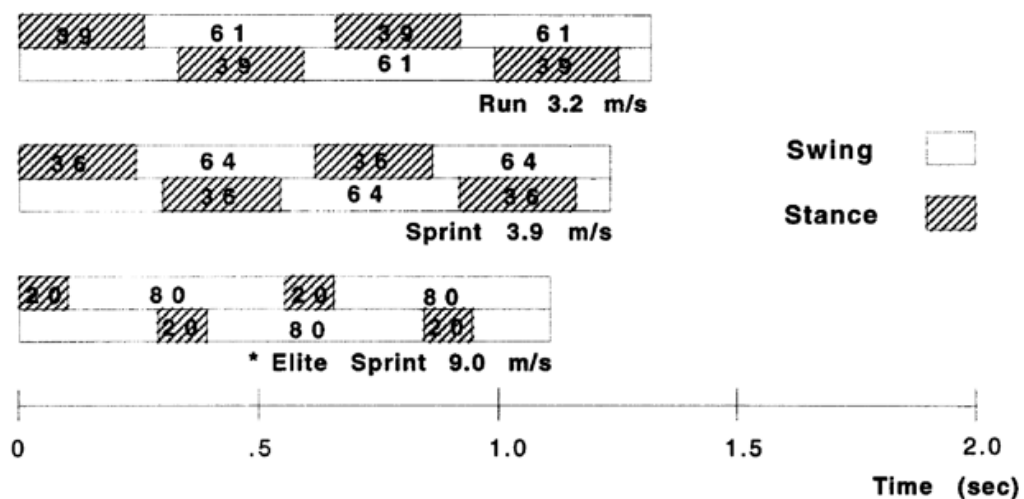


Figure 2: Variation in gait cycle parameters with speed of movement showing two complete gait cycles or strides. As speed increases, SW time (clear) increases, followed by ST time (shaded) decreases and DF increases with the overall gait cycle time shortening (Novacheck, 1998).

1.3. MECHANICAL ENERGETICS - POTENTIAL ENERGY (PE) AND KINETIC ENERGY (KE)

The process of energy transference between potential energy (PE) and kinetic energy (KE) involves the conversion of stored energy into the energy for motion. This often occurs in the context of objects experiencing gravitational

forces. PE is the stored energy an object possesses due to its position or state. In the context of gravitational PE, an object can be calculated as the product of its mass (m), gravitational acceleration (g), and height (h) above a reference point (Equation 1) (Novacheck, 1998).

Equation 1: Gravitational potential energy (PE) equation measured in joules (J) where m is the mass of an object, g is gravitational acceleration at 9.81 m/s² and h is height above a reference point (Novacheck, 1998).

(1)

$$PE (J) = mgh$$

Kinetic energy (KE) refers to the energy that an object possesses due to its motion by virtue of its velocity (v) and mass (m) (Equation 2) (Novacheck, 1998).

Equation 2: Kinetic energy (KE) equation measured in joules (J) where m is mass and v is velocity (Novacheck, 1998).

(2)

$$KE (J) = \frac{1}{2}mv^2$$

PE and KE can be interconverted, for instance, when an object is elevated to a certain height (h) it has the capacity to do work but it is not currently in motion, thus possesses gravitational PE. As the object falls under the influence of gravity, its PE is converted into KE. KE increases until it reaches its maximum whilst PE decreases until it has zero gravitational PE and vice versa during upward motion. In running, the KE and PE energy cycle are in

phase; springing from the lowest point during mid-stance (mid-ST), to the highest point in mid-swing (mid-SW). This is where DF occurs, the point in running where both feet are off the ground (Figure 3) (Novacheck, 1998).

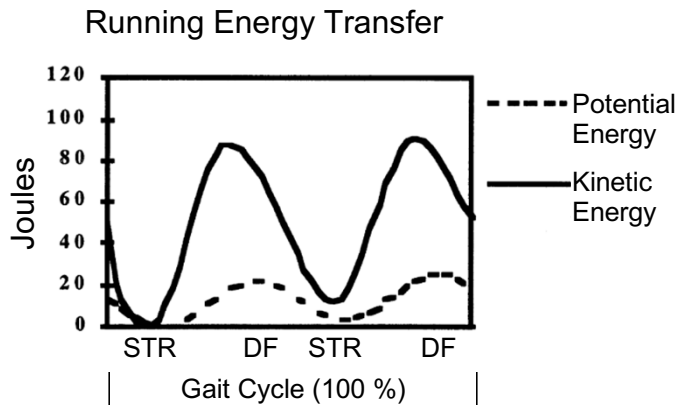


Figure 3: The relationship between Potential Energy (PE) and Kinetic Energy (KE) in running noting Stance Phase Reversal (STR) and Double Float (DF) (Novacheck, 1998).

The running gait cycle consists of two phases; the stance (ST) phase and the swing (SW) phase (Figure 1). ST starts with IC, where KE from the previous stride is converted into PE as the leg starts to decelerate (Figure 3). As the leg decelerates, the KE decreases. Generation phase (the period when the foot is actively pushing off the ground, generating the force necessary to propel the body forward) at mid-ST, the PE continues to increase as the runner's body centre of mass (BCoM) gains height, contributing to the storage of PE as the body mass transitions over the supporting foot, moving from weight absorption to propulsion (Figure 1). The KE is lower during mid-ST compared to IC. At toe-off (TO), as the foot leaves the ground, PE is at its maximum and the KE is minimal. The leg is now pushing off, converting PE into KE. The propulsion

phase at late ST sees the BCoM shift forwards and upwards facilitating forward propulsion. PE decreases as the BCoM starts to descend followed by KE increases as the runner gains velocity.

At SW there is a moment of PE as the leg swings forward, lifting and preparing for the next stride. The BCoM follows a parabolic trajectory, descending from its highest point in mid-ST to lowest during SW contributing to forward momentum. The KE is relatively low during the initial SW. At mid-SW PE is minimal, the BCoM continues to descend as the leg continues its forward SW with KE increasing as the leg accelerates during mid-SW. By terminal SW, PE starts to build again, the BCoM remains low aiding stability as the leg prepares for the next IC. KE reaches its peak just before IC. The sum of KE and PE remains relatively constant in an isolated system, demonstrating the conservation of energy during the gait cycle (Alexander, 1991; Novacheck, 1998; Bramble and Lieberman, 2004).

1.4. MECHANICAL ENERGETICS - ELASTIC STORED ENERGY (ESE)

The running gait cycle involves the storage and release of elastic stored energy (ESE) in various anatomical structures, particularly tendons, to enhance the efficiency of the movement. At IC as the foot contacts the ground, the Achilles tendon undergoes elongation, storing elastic PE (Figure 1). The triceps surae, including the gastrocnemius and soleus muscles, contract eccentrically to control the rate of ankle dorsiflexion and contribute to ESE storage. At mid-ST, the Achilles tendon continues to elongate storing additional ESE. Muscles, like the gastrocnemius and soleus, work

isometrically to maintain tension to control the descent of the BCoM, contributing to further ESE storage. At TO, the ESE in the Achilles tendon is released and the triceps surae, specifically the gastrocnemius, contract concentrically, aiding in ankle plantarflexion and release of ESE to propel the body forwards.

At initial SW, the leg swings forward, the biarticular muscles such as the hip flexor (iliopsoas) and quadriceps muscle (rectus femoris), eccentrically contract to continue leg lift forwards. ESE is stored through the stretching of the tendons around the hip and knee joints. By mid-SW ESE continues to be stored in tendons, preparing for ST. Muscles such as the hamstrings (comprising the biceps femoris, semitendinosus, and semimembranosus muscles) and the iliopsoas, primarily contract eccentrically to indirectly control knee extension through controlling the position of the pelvis and trunk during the descent of the thigh during running. These eccentric contractions play a crucial role in managing movement and contribute to the storage of elastic strain energy, which aids in enhancing movement efficiency and conserving metabolic energy. At terminal SW just before IC, the ESE in the tendons, particularly around the hip and knee joints, is released. The hamstrings contract concentrically and quadriceps contract eccentrically, to control the leg's descent and contribute to a smooth transition to the next stance phase. The entire process then repeats with each step, creating a continuous cycle of ESE storage and release (Alexander, 1991; Novacheck, 1998; Bramble and Lieberman, 2004). The up and down oscillation of the BCoM is often referred to using the spring mass model and simplistically mimics the motion of a pogo stick (Figure 4) (Li, 2011).

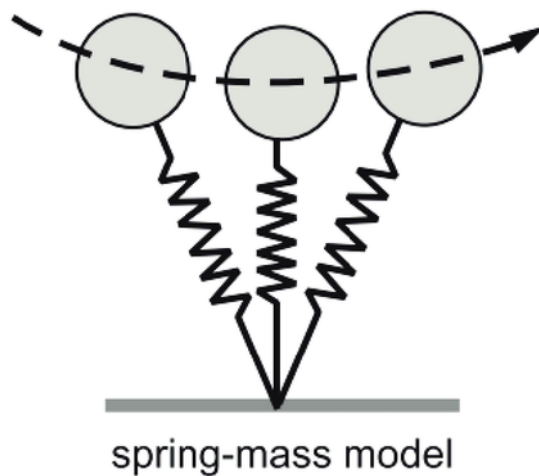


Figure 4: The spring-mass model for running (Li, 2011).

The rate of energy consumption and cost of transport for running mammals between 30 g and 140 kg within the field can be determined using the cost of supporting body mass (work done by muscles and tendons to lift and accelerate the body and limbs) and the time course of force application or ground contact time (GCT) (time the foot is in contact with the ground. The amount of energy consumed in moving a unit of body weight a unit distance decreases as step length increases with increasing body weight (Kram and Taylor, 1990).

1.5. ENERGETICS OF RUNNING AND RUNNING ECONOMY (RE)

The quantification and prediction of distance-running performance can be assessed using cardiopulmonary exercise testing (CPET)⁴ (Saunders *et al.*, 2004). During a CPET, the individual typically exercises on a stationary bike

⁴ a test used to evaluate the integrated performance of the cardiovascular (heart and blood vessels) and pulmonary (lungs) systems during exercise.

or treadmill while instruments measure physiological parameters such as heart rate, blood pressure, oxygen uptake ($\dot{V}O_2$), carbon dioxide production ($\dot{V}CO_2$), and respiratory rate. CPET provides valuable information about an individual's exercise capacity, aerobic fitness, and cardiovascular and pulmonary function. It is often used to assess exercise tolerance, diagnose cardiovascular and respiratory conditions, determine optimal exercise prescription and evaluate responses to treatment or exercise interventions. CPET expedites the objective quantification of performance indicators such the maximal rate of oxygen uptake ($\dot{V}O_{2max}$), lactate threshold⁵ and running economy (RE)⁶. RE is frequently reported as the physiological energy expenditure in terms of oxygen uptake in units of submaximal rate of oxygen uptake ($\dot{V}O_{2submax}$) in millilitres per kilogramme per minute (ml/kg/min), or mechanical energy cost, being the work required to perform a task or activity, such as overcoming friction, inertia, and gravitational forces. It is measured in Joules or Watts per kilogram per minute (J/kg/min or W/kg/min) (Novacheck, 1998; Snyder and Farley, 2011; Snyder, Kram and Gottschall, 2012; Barnes and Kilding, 2015). RE is a current research interest as it varies by up to 30% among elite runners (Table 1). Athletes with similar $\dot{V}O_{2max}$ scores but lower RE scores perform better, thus providing an additional level of performance categorisation and performance prediction (Novacheck, 1998; Barnes and Kilding, 2015, 2019; Hoogkamer *et al.*, 2016). Elite runners have stable $\dot{V}O_{2max}$, RE and lactate thresholds thus, reducing confounding variables within research. However, using only elite athletes reduces the applicability of the research to a small

⁵ utilisation of the maximal sustainable fraction of $\dot{V}O_{2max}$.

⁶ submaximal rate of oxygen uptake ($\dot{V}O_{2submax}$) at a given speed.

sect of the running population (Saunders *et al.*, 2004). At maximum running speeds, men demonstrate greater efficiency compared to women, yet at equivalent relative running intensities measured in ml/km/kg, there are no discernible gender variations. When individuals of both genders possess equal $\dot{V}O_{2\max}$, males are more economical and when both genders have equal RE, males have a greater $\dot{V}O_{2\max}$ (Daniels and Daniels, 1992).

The measurement of RE encompasses various factors that collectively represent the intricate functioning of metabolic, cardiopulmonary, biomechanical and neuromuscular systems (Figure 5). Metabolic efficiency entails the effective utilisation of energy resources to enhance performance, while cardiopulmonary efficiency pertains to minimising the energy expenditure associated with oxygen transport and utilisation processes. The neuromuscular and biomechanical attributes involve the interplay between the neural and musculoskeletal systems, impacting the conversion of power output into movement and consequently, performance.

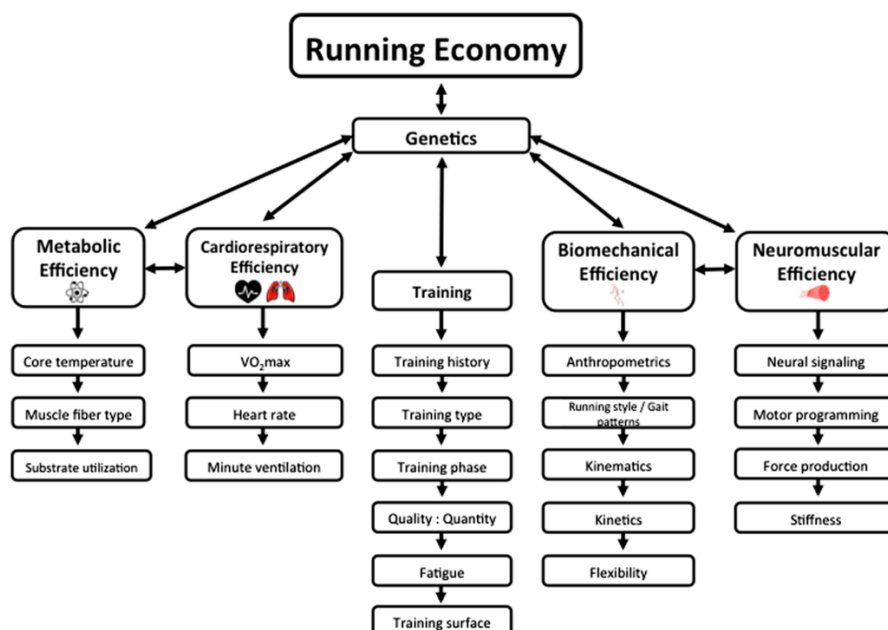


Figure 5: Factors affecting running economy (Barnes and Kilding, 2015).

Table 1: Normative Running Economy (RE) values for male and female runners of varying ability despite the challenge of accumulating this information due to varied protocols, differing gas-analysis equipment, data averaging techniques and maximal aerobic capacity categorisation (Barnes and Kilding, 2015).

		Male mean (range)		Female mean (range)	
Runner classification	Speed (km/h)	Running economy ($\dot{V}O_2$ ml/kg/min)	$\dot{V}O_{2max}$ (ml/kg/min)	Running economy ($\dot{V}O_2$ ml/kg/min)	$\dot{V}O_{2max}$ (ml/kg/min)
Recreational	10	36.7 (35.4-38.8)	54.2 (51.0-57.8)	37.7 (32.8-42.6)	49.7 (45.2-54.1)
	12	42.2 (40.4-45.3)		43.2 (38.5-48.1)	
	14	47.4 (46.0-49.5)		47.3 (40.1-51.9)	
Moderately trained	12	40.7 (37.4-48.1)	62.2 (56.6-69.1)	41.9 (28.9-41.7)	55.8 (50.5-59.4)
	14	46.8 (42.0-55.5)		47.9 (43.2-53.4)	
	16	51.4 (51.6-62.3)		52.9 (45.7-61.0)	
Highly trained	12	n/a	70.8 (65.3-80.2)	41.3 (33.3-50.2)	61.7 (56.2-72.3)
	14	45 (32.4-56.5)		48.3 (39.0-56.7)	
	16	50.6 (40.5-66.8)		54.5 (46.2-61.9)	
	18	58.1 (48.0-72.0)		58.6 (54.4-67.1)	
	20	66.5 (65.7-71.6)		n/a	
Elite	14	39.9 (36.1-44.5)	75.4 (68.2-84.1)	41.9 (38.7-46.9)	66.2 (61.1-74.2)
	16	47.9 (41.3-53.5)		48.9 (45.1-55.8)	
	18	55.9 (50.5-62.3)		56.1 (51.8-63.8)	
	20	63.9 (57.5-71.2)		n/a	

The relationship between energy cost and speed is well-researched in gait biomechanics, specifically the walk to run transition. Alexander (1992) used the work of Cavagna (1969) to produce the modelled data in Figure 6. Although this article is not available in English, the experimental procedures were published in Cavagna and Kaneko (1977) and in Rodolfo (1976) who detailed the participant descriptives for the four male subjects (28.3 ± 7.8 years, 70.3 ± 10.1 kg and height 176.8 ± 1.3 cm) included one national middle-distance runner, one national sprinter and two untrained runners.

There is a linear increase in energy expended in watts per second (W/s) with increasing speed, where walking always expends less energy than running (Figure 6A) (Alexander, 1992). These subjects walked at a preferred stride frequency at 1.3 m/s which required 300 watts (Joules per second), thus for every meter travelled approximately 230 J were utilised, approximately 140 J more than standing still. Running, on the other hand, uses 260 J/m more than standing. At higher speeds, the energy cost is lower for running compared with walking, as above certain speeds it is physically impossible to walk for mechanical, rather than energetic reasons (Margaria, 1976; Cavagna and Kaneko, 1977; Novacheck, 1998; Long and Srinivasan, 2013).

Whereas the data in Figure 6A can be converted into energy per unit distance, where metabolic power⁷ in watts is divide by speed, to produce Joules per meter. The resultant Figure 6B, depicts walking having an inverted U-shaped relationship; with the most energy efficient speed at the bottom of the U. Running, on the other hand, shows a significantly flatter relationship. Simply, this figure depicts the most energy efficient speed for walking as 1.3 m/s,

⁷ energy cost in joules per distance moved.

whereas for running it is 2.3 m/s. Below this speed, walking is more economical and above, running is more economical. Given a choice, the average adult would transition to running at approximately 2.3 m/s (Margaria, 1976; Alexander, 1992).

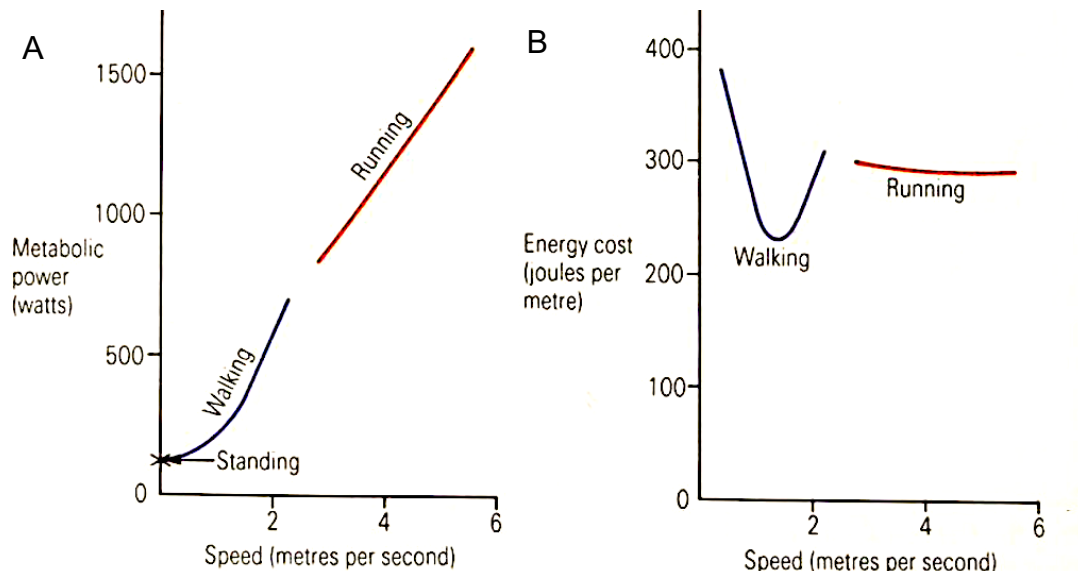


Figure 6: Example of results from cardiopulmonary exercise testing. (CPET) within the laboratory. These curves are based on a male participant locomoting at different speeds. A. When displaying metabolic power for walking and running as a function of speed. B. When displaying energy cost in joules per meter for walking and running as a function of speed (Alexander, 1992).

1.6. ENERGETICS OF RUNNING AND FOOTWEAR

Several running shoe characteristics such as; mass, cushioning, longitudinal bending stiffness (LBS) and midsole viscoelasticity influence RE thus, in turn affects running performance. When shoe mass is isolated, it determines RE with additional shoe mass increasing metabolic cost at a given workload. It is understood that for every additional 100 g in total shoe weight (50 g per shoe)

there is a 1% increase in $\dot{V}O_2$ uptake at moderate speeds (Figure 7) (Cavanagh and Kram, 1985).

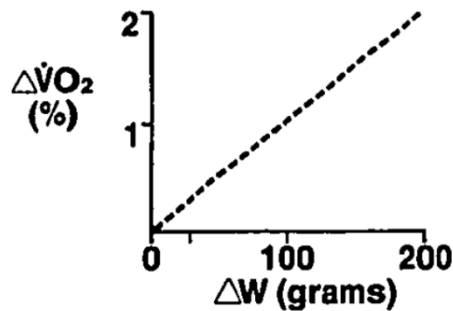


Figure 7: The effect of shoe mass on oxygen uptake ($\dot{V}O_2$ %). Where 100 g increase (per pair) in running shoe mass equates to approximately an additional 1% in $\dot{V}O_2$ uptake (Cavanagh and Kram, 1985).

According to a 14 study meta-analysis, the metabolic cost of running increases linearly with increasing shoe mass, where a combined shoe mass <440 g per pair had no detrimental effect on $\dot{V}O_2$ when compared to barefoot running (Fuller *et al.*, 2015). When extrapolated to a theoretical shoe mass of 0 g, the -0.58 standardised mean difference (SMD) in $\dot{V}O_2$ were calculated. This negative mean $\dot{V}O_2$ suggests that running barefoot or with running shoes of negligible mass, could potentially reduce oxygen uptake compared to heavier running shoes. This study provided a theoretical basis for running shoe characteristics, other than mass, being responsible for the reduction of oxygen uptake during running (Figure 8) (Fuller *et al.*, 2015).

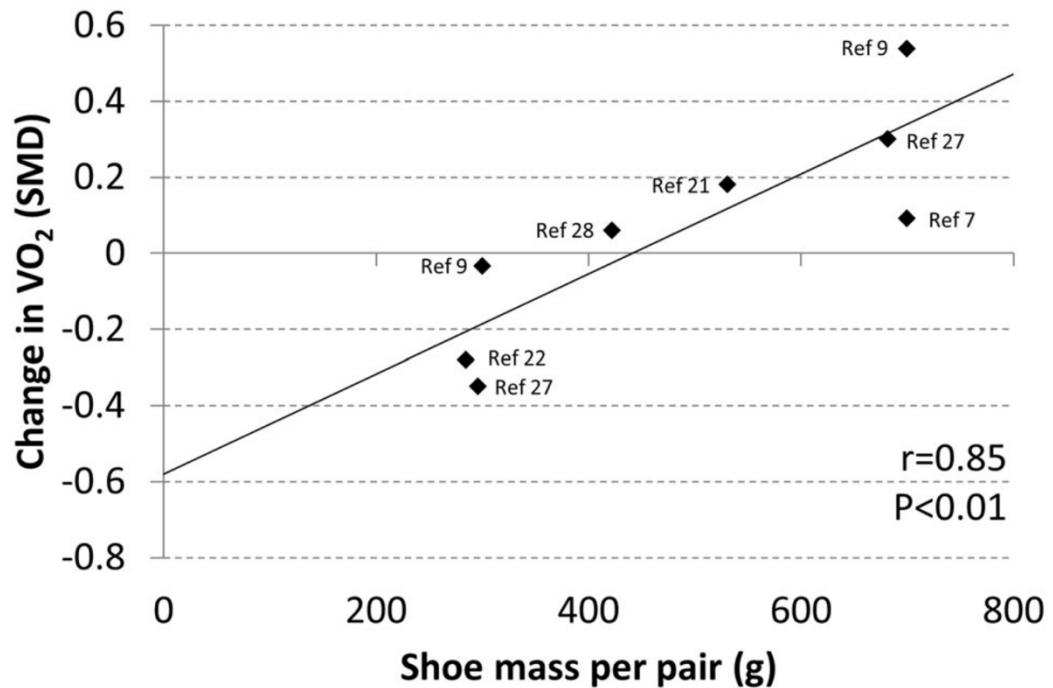


Figure 8: Change in oxygen uptake for running in shoes of different mass compared with barefoot running. Shoe mass values are the combined mass of a one shoe pair. Standardised mean difference (SMD) on the y-axis and $\dot{V}O_2$ is on the x-axis (Fuller *et al.*, 2015).

In recent years, minimalist and barefoot running was thought to be energetically optimal due to little or no shoe mass leading to higher RE benefits, however, it frequently requires greater muscular effort for the cost of cushioning the foot–ground impact (as demonstrated in Figure 8), due to the level of shock attenuation required whilst running barefoot (Fuller *et al.*, 2015; Hoogkamer *et al.*, 2018; Whiting, Hoogkamer and Kram, 2022). This is thought to be the acute, short-term changes in running gait associated with the transition from a rearfoot strike to a forefoot strike pattern, increased cadence and reduced vertical oscillation of the BCoM, that contributes to an improved RE by up to 12% (Fuller *et al.*, 2015; Hoogkamer *et al.*, 2018).

The effect of shoe cushioning on RE is less clear, where it was postulated that cushioning allowed for running with straighter legs (less knee flexion), which required less muscular effort and improved the storage and return of mechanical energy. This evidence may have facilitated the transition from minimalist running shoes to midsoles with significantly more foam (Barnes and Kilding, 2015; Hoogkamer *et al.*, 2016).

Midsole foams vary in their compliance (the amount of compression under a certain force), resilience (the percent of the stored mechanical energy that is returned) and viscoelasticity (both viscous and elastic behaviour, displaying a time-dependent response to deformation). These properties affect the energy stored and returned by the running shoe midsole, hence, act in a similar capacity to tendons. Compliance and resilience are not mutually exclusive; more compliant and resilient midsoles were known to reduce the energetic cost of running from as early as 1985 (Figure 9) (Cavanagh and Kram, 1985), however, by 2018 it was the technological developments in the entire shoe design, not just the midsole cushioning, that improved RE by 4% (Worobets *et al.*, 2014; Hoogkamer *et al.*, 2018). Further research is required to understand how these developments facilitate such significant RE benefits.



Figure 9: The effect of cushioning on running economy (RE). Two similar weighted running shoes, with shoe two having more cushioning than shoe one. Shoe two utilised less $\dot{V}O_2$ than shoe one, thus had better RE (Cavanagh and Kram, 1985).

Ethylene-vinyl acetate (EVA) foam was one of the first running shoe midsoles cushioning system innovations. EVA provides a balance of compliance and resilience with a viscoelastic response that assists running performance. EVA can be either high in compliance but low in resilience or high in resilience but low in compliance which is not conducive to consistent energy return. Thermoplastic polyurethane (TPU) and polyether block amide (PEBA) demonstrate more desirable properties due to its greater compliance and resilience simultaneously, (i.e. more linear and elastic than viscoelastic), potentially enhancing the effect of cushioning on RE, although TPU is denser than EVA so more foam is required (Worobets *et al.*, 2014; Hoogkamer *et al.*, 2018). As well as foam, manufacturers have recently embedded carbon-fibre plates into running shoe midsoles, enhancing the LBS and improving leverage, thus transmitting the force developed by the leg muscles through to the toes propelling the runner upward and forward. Such plates reduce RE by 1% through changes in the leverage of the ankle joint and the foot-toe joint (metatarsophalangeal joint) (Healey and Hoogkamer, 2021).

In 2017, Nike®, Inc., released a new series of racing shoe with many of these features which have transformed the running shoe market, providing a brand-new perspective on racing shoe design. One such shoe in the series, known as the Nike® Vaporfly (VF), where Nike® incorporated a full length, curved, carbon-fibre midsole plate to add stiffness with very little added mass. This was embedded within a thick yet lightweight and compliant PEBA based midsole being both resilient and responsive (Figure 10) (Hoogkamer *et al.*, 2018). The Nike® Vaporfly 4% weighed c. 205 g per shoe (size 10) (Barnes and Kilding, 2019). This transition instigated other large brands to produce running shoes with the same midsole characteristics.

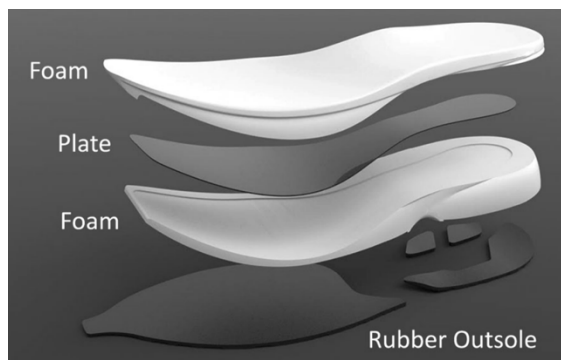


Figure 10: Exploded view of the Nike® prototype shoe that incorporates a newly developed midsole material and a full-length carbon-fibre midsole plate with forefoot curvature, embedded in the midsole (Hoogkamer *et al.*, 2018).

The prototype version of the VF shoe facilitated a reduced RE by 4% relative to the Nike® Zoom Streak 6 and the adidas® adizero Adios BOOST 2 during treadmill running at 14, 16 and 18 km/h. As a result, Nike® aptly named their first public offering the Nike® Vaporfly 4% (VF4%). The VF4% produced a 0.9% longer SL, 5.0% increase in vertical oscillations and an 8.5% decrease

in plantar flexion velocity, with no significant increase in peak vertical force (Hoogkamer *et al.*, 2018). The predicted improvement in these biomechanical variables would translate into a 0.9% faster marathon time, or a 00:01:25 (hh:mm:ss) saving at 16 km/hr, a significant performance improvement for a change of footwear (Hoogkamer, Kipp and Kram, 2019).

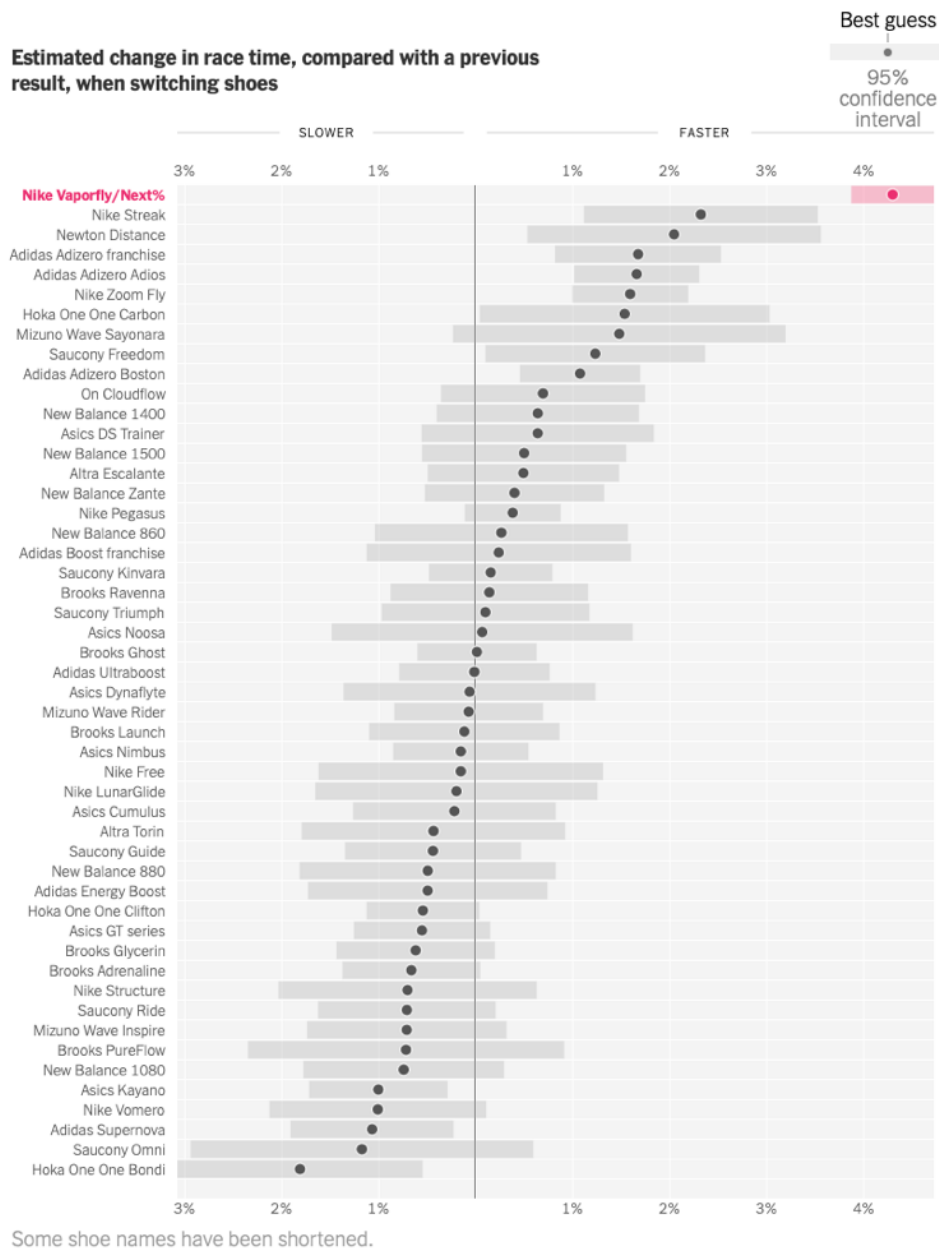


Figure 11: Estimated change in race time, compared with a previous result, when switching shoes (Quealy and Katz, 2019).

The VF series caused controversy in the running world when first released in 2017, where World Athletics were considering a total ban (O’Grady and Gracey, 2020). The limited peer-reviewed literature available concluded the VF series improved the RE of elite athletes by up to 4% (Hoogkamer *et al.*, 2018; Barnes and Kilding, 2019; Hoogkamer, Kipp and Kram, 2019; Healey

and Hoogkamer, 2021; Hunter *et al.*, 2022; Whiting, Hoogkamer and Kram, 2022). It is yet to be understood if these benefits extend to recreational runners. Quealy and Katz's (2019) conducted the most substantial analysis to date for the New York Times. This comprehensive empirical analysis used statistical models with over 100,000 data points from publicly accessed Strava records to bolster the current peer-reviewed literature. The authors pair matched runners and calculated a best guess percentage saving in completion time, with 95% confidence interval, as they switched from one model of running shoes to another. Even after controlling for potential confounding variables such as, a runners' propensity to wear a particular running shoe, runners' ability, race conditions, and race course, the outputs were similar. Those that switched to the VF series ran 4 to 5 % faster, a clear outlier at approximately 2 % faster than the next-fastest running shoe model (Figure 11) (Quealy and Katz, 2019). It appears that the culmination of publicly available evidence showing consistent performance improvements across all running abilities encouraged the switch to the VF series. To date, 41% those with a sub three-hour marathon were wearing the VF series, it is unprecedented for a single brand and model of shoe to be worn by such a high percentage of runners.

The metabolic savings of the VF were attributed to the spring-like foam midsole on energy return and the stiffness of the carbon-fibre midsole plate on ankle joint mechanics and the metatarsophalangeal (MTP) joint (Hoogkamer *et al.*, 2018). Further research is needed to understand how the RE benefit is distributed between the foam and carbon-fibre midsole plate.

1.7. INCLINE RUNNING

In level running, supporting body weight is the greatest metabolic cost, with equal measures of ESE stored and recovered during each step. However, running on an incline (uphill), the BCoM is lower at the beginning than at the end of ST, thus has a greater PE. By toe-off, net positive work must be generated by metabolically expensive concentric muscle actions such as the hip extensors to provide sufficient KE to raise the height of the BCoM to its highest point during the DF and maintain speed on the incline against gravity. This energy cost increases linearly with incline and decline compared with level running at the same speed (Figure 12).

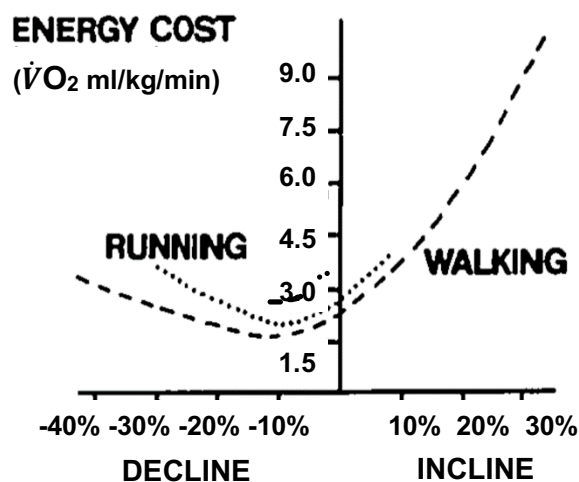


Figure 12: Optimal velocity for locomotion over several inclines. For a 65 kg participant, the most economical grade was about -10% decline, with energy cost increasing linearly with increasing incline and decline. Adapted for this project by changing the units from cal/m/kg to $\dot{V}O_2$ ml/kg/min (Cavanagh and Kram, 1985).

During level running, gravitational PE and KE of the BCoM changes are symmetrical and in-phase (Figure 3). Theoretically, all this energy could be stored elastically in the tendons and subsequently recovered. In uphill running, some mechanical energy generation is required due to the necessity of generating mechanical energy to overcome the incline. Therefore, not all the energy can be equally stored and recovered (Figure 13) (Snyder, Kram and Gottschall, 2012).

The implications of the observed changes in mechanical energy dynamics during uphill running are significant for overall running performance. Steeper inclines lead to a decrease in the Maximum Possible Elastic Stored and Returned Energy (MPESE), and runners must compensate by expending additional energy to lift the BCoM to its original height within the stride and propel it further uphill (Figure 13). This increased energy demand may have implications for endurance and efficiency during uphill segments of a run.

The MPESE undergoes changes during uphill running, reflecting the challenge of storing and retrieving energy efficiently over more energetically demanding terrains. Despite the challenges posed by steeper inclines, the stability in the percentage of Anatomically Estimated Elastic Stored Energy (AESE) suggests a consistent biomechanical adaptation calculated based on peak ground reaction force (GRF), anatomical characteristics of the foot arch and Achilles tendon implies that the body maintains a reliable mechanism for energy storage and release across various uphill grades (Snyder, Kram and Gottschall, 2012).

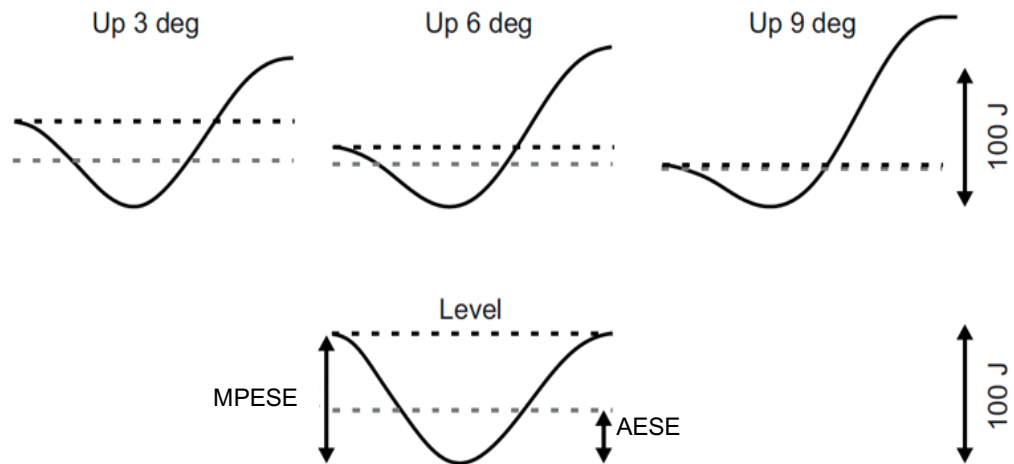


Figure 13: Elastic Stored Energy (ESE) differences with incline. The solid curves are the mechanical energy fluctuations of the BCoM throughout stance, the black dashed lines represent the maximum possible elastic stored and returned energy (MPESE), the grey dashed lines, the anatomically estimated elastic energy storage (AESE). Both mechanical energy generation and dissipation occur, with more generation occurring uphill, elastic stored energy decreases, thus the body must generate additional energy to account for this decrease. Adapted for this project from Snyder, Kram and Gottschall, (2012).

Whiting, Hoogkamer and Kram, (2022) found the VF4% is not as energy efficient on an incline compared to level running, yet Hunter et al., (2022) showed no difference on a 7% incline and decline between the VF4% and similar running shoes containing a carbon-fibre midsole plate. The precise benefits of the VF at incline require further investigation. Note that laboratory testing on a treadmill often uses a 1% incline to simulate the energetic cost of outdoor running, accounting for factors like wind resistance and surface friction (Jones and Doust, 1996).

1.8. STRIDE LENGTH (SL) AND STRIDE FREQUENCY (SF)

Runners develop either an optimal stride length (SL) (the distance covered in one gait cycle between IC and IC of the same leg), an optimal SF, or an optimal combination of SL and SF for a given running speed. Combinations of SL and SF are based on a runner's perceived exertion or desired physiological response. Preferred SL has a curvilinear relationship with RE, where the optimal SL is the most efficient at a given speed and is an important kinematic parameter for long-distance running (Figure 14) (Cavanagh and Williams, 1982; Cavanagh and Kram, 1985; Novacheck, 1998; Barnes and Kilding, 2015).



Figure 14: The curvilinear relationship between $\dot{V}O_2$ and stride length (SL). The dashed line represents the optimal SL which produces the least $\dot{V}O_2$ uptake at a given running speed. The preferred SL is close to the optimal meaning self-optimisation occurs. Adapted for this project (Cavanagh and Kram, 1985).

The stride frequency–velocity relationship shows that SF increases with increased velocity. Runners adopt lower SF to reduce the energetic cost caused by faster limb movement of unnatural and suboptimal gaits, and increased force exerted due to a shorter contact time (Whiting, Hoogkamer

and Kram, 2022). This is due to the proposition that the maximal contribution of ESE to the total work occurs at the optimal stride frequency (OSF), due to muscles performing less mechanical work, hence, consume less metabolic energy than at other SF. This notion is supported by the leg behaving like a simple spring at the preferred stride frequency (PSF) but not at lower SFs (Farley and González, 1996; Snyder and Farley, 2011).

When required to run at an incline between 0% to 7% at 15 km/h (4.17 m/s), SF increased from 2.87 Hz to 2.98 Hz to compensate and as a result SL decreased from 1.41 m to 1.35 m, validating the use of the SL calculation from speed and SF ($SL = \frac{\text{speed m/s}}{SF \text{ Hz}}$) (Padulo *et al.*, 2013).

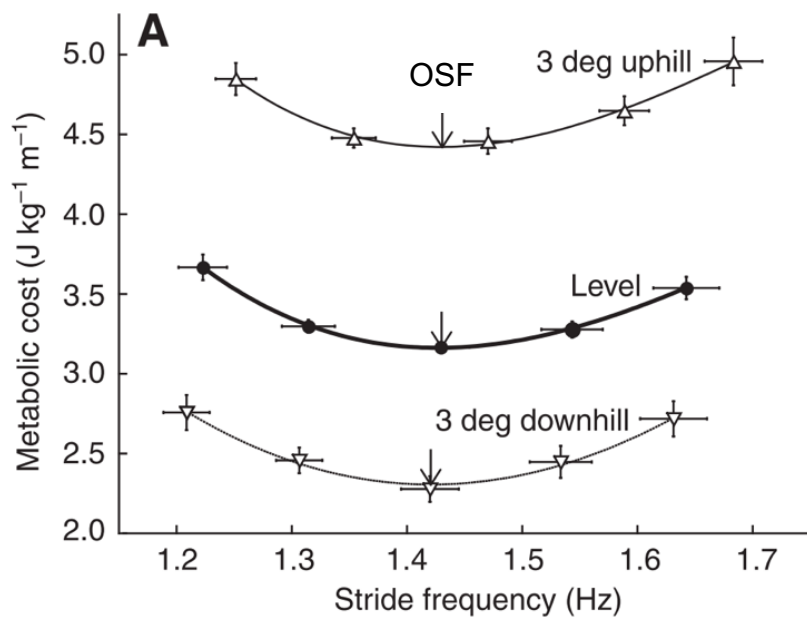


Figure 15: The relationship between stride frequency (SF) and metabolic cost. Trials were run at 2.8 m/s with SF calculated for the preferred stride frequency (PSF) then 85%, 92%, 108% and 115% of PSF. The arrow represents optimal stride frequency (OSF) where the metabolic cost is at its lowest (Snyder and Farley, 2011).

Runners travelling at a speed of 5.3, 8 and 11 km/h (1.5, 2.2 and 3 m/s) demonstrated the greatest RE benefit and maximal ESE return at an average SF 1.35 Hz or step frequency⁸ of 2.7 Hz. More recently, a U-shaped relationship was discovered for level running at 2.8 m/s between metabolic cost and SF, with the lowest metabolic cost (3.17 J/kg/m) occurring at the OSF (1.44 Hz), which increased at SF less and more than the PSF; for 85% of PSF (3.67 J/kg/m), 92% (3.30 J/kg/m), 108% (3.28 J/kg/m) and 115% (3.54 J/kg/m) (Figure 15) (Snyder and Farley, 2011).

Gender differences show women tended to have a shorter SL with a similar SF, compared to men, due to women having a smaller hip extension range possibly connected to an anatomically differing pelvis position at TO compared to males (Rueda *et al.*, 2017).

1.9. GAIT ANALYSIS

Many recreational and professional runners want a plethora of objective information about their running performance with MC being the best objective method of movement analysis to date. MC provides a quantitative assessment of running gait by recording data that when analysed can unveil a variety of kinematic gait variables (e.g. joint angles, angular velocity) and kinetic gait variables (e.g. GRF, joint moments, joint power) (Perry, 1992; Kaufman and Sutherland, 2006; Winter, 2009; Benson *et al.*, 2018).

⁸ also known as cadence, it refers to the number of steps taken per unit of time, usually measured in steps per minute (spm). It represents the rate at which the left and right feet contact the ground.

Conducting tests within a laboratory setting has inherent limitations; MC demands costly video equipment, necessitating a spacious operating environment and considerable time investment. Furthermore, the setup and data processing require specialised expertise. MC systems face challenges in collecting data from extensive participant cohorts over prolonged periods and there is a risk of influencing natural running biomechanics adversely. This influence can arise from participants having to wear cumbersome equipment and the use of treadmill running to minimise environmental variability (Fogg, 2005; Ferber *et al.*, 2016; Sejdić *et al.*, 2016; Barnes, 2017; Kluge *et al.*, 2017; Anwary, Yu and Vassallo, 2018; Reilly *et al.*, 2018; Ortega *et al.*, 2021; Ortega, 2022). These restrictions mean gait analysis outside of the research environment rely heavily on subjective tools such as, questionnaires and visual assessment scoring, over objective methods (Jenner *et al.*, no date; Barnes, 2017; Clark, 2017). There is a clear need for the development of an objective tool to quantify gait using light weight, portable and unobtrusive equipment (Jenner *et al.*, no date; Hu and Soh, 2014).

1.10. WEARABLE DEVICES

Micro-electromechanical systems (MEMS) accelerometers feature a polysilicon surface-micromachined structure positioned on top of a silicon wafer (Figure 16). This structure is suspended over the silicon wafer by polysilicon springs, offering resistance against forces induced by applied acceleration. Deflection of this structure is measured using differential capacitors, comprising of both fixed plates and plates connected to the moving

mass. Acceleration causes deflection of the mass producing a sensor output directly proportional to the applied acceleration (Analogue Devices, 2015; Clark, 2017).

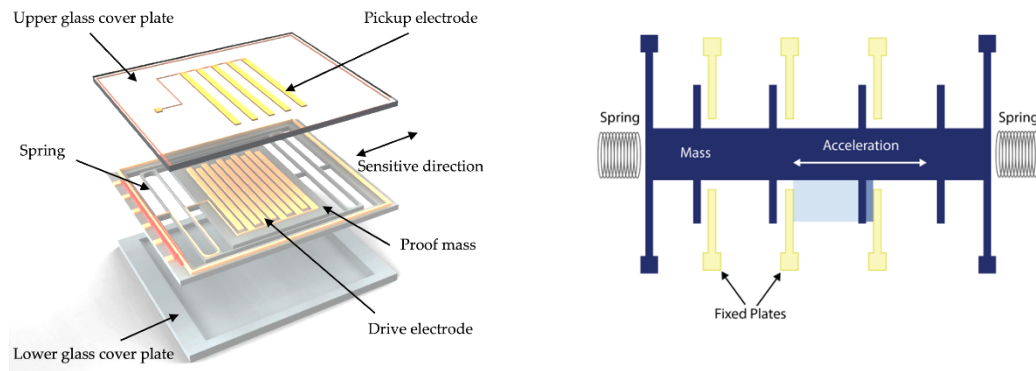


Figure 16: MEMS accelerometer (Rao et al., 2019).

The benefit of the MEMS accelerometer is that they are self-contained, require a low voltage supply, have low current drain thus can be run on batteries. They have minimal range restrictions, no line-of-sight requirements, are small, lightweight and inexpensive. They detect frequency and intensity of movements without being sensitive to external interference such as light and ferromagnetic objects. This technology can provide real-time information at relatively high sample rates which has the potential to be conducted wirelessly. The sensors typically cost less than £5, hence a huge cost advantage over the best objective gait analysis method, MC, which for a 13-camera set up costs upwards of £90,000 (Fogg, 2005).

The disadvantages of MEMS accelerometers are the captured data can contain errors caused by environmental issues such as temperature, humidity and pressure which can affect mechanical characteristics or sensitivity of the

sensor. Poor mounting or installation quality can increase mechanical stress or vibrations. External interference such as electromagnetic interference can disrupt readings. Calibration accuracy can reduce measurement accuracy this regular and accurate calibration is essential. Sensor degradation over time may reduce the sensors performance. Cross axial sensitivity can introduce magnitude error and mechanical damage from excessive shock or impact can lead to recording inconsistency or sensor failure (Fogg, 2005; Yang and Hsu, 2010; Barnes, 2017; Clark, 2017). The absolute orientation of a data point recorded by an accelerometer is impossible to calculate without integrating the data with gyroscope or magnetometer data from the same data collection period. Finally, accelerometers are sensitive to both static acceleration (due to gravity) and dynamic acceleration (caused by motion) which are difficult to separate onboard the device or post extraction, meaning data interpretation can be challenging (Yang and Hsu, 2010; Barnes, 2017).

Linear acceleration is detected along the sensitive axis of each transducer, ergo, a tri-axial sensor measures acceleration in three axes (x-, y- and z-), also known as surge, heave and sway with their corresponding angular accelerations, roll, pitch and yaw respectively (Figure 17) (Yang and Hsu, 2010).

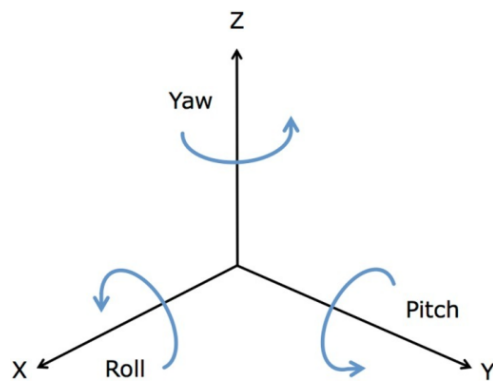


Figure 17: The x-, y- and z-axes with the corresponding angular system of roll, pitch and yaw respectively (Ellis et al., 2014).

Data captured from each axis of the accelerometer are recorded as a waveform, a graphical representation of how a signal varies with time, and will be referred to throughout this project as a movement wave. The movement wave depicts the amplitude of the signal measured using gravitational acceleration (g), with 1 g equating to approximately 9.81 m/s^2 along the sensitive axis.

In signal processing, waves can represent various types of signals, such as audio signals, radio waves, or digital signals. Understanding the characteristics of waves is fundamental to tasks like signal analysis, filtering, modulation, and many other signal processing operations. Waves play a crucial role in describing and analysing signals in both analogue and digital domains.

Commercial manufacturers have taken advantage of MEMS technology's small size, crafting multiple movement sensors, such as accelerometers, into wearable devices. The application of these devices in recent years has vastly increased, specifically enabling for objective self-monitoring and performance

analysis outside of the laboratory (Anwary, Yu and Vassallo, 2018; Brahms *et al.*, 2018; Wada *et al.*, 2018).

Nonetheless, this method does not come without limitation, commercial wearable devices include predefined processing protocols that remain the intellectual property of the developer (Benson *et al.*, 2018), meaning the raw data are not available to the end-user (Fridolfsson, Börjesson and Arvidsson, 2018). This reduction in processing transparency can lead to the deletion of important movement data points, thus the resultant feedback may not be truly representative of the activity undertaken (Jenner *et al.*, no date; Barnes, 2017; Clark, 2017), which challenges the test-retest repeatability and application of findings (Fridolfsson, Börjesson and Arvidsson, 2018). Due to this, research has transitioned to the use of custom-built wearable devices which allow for the unrestricted capture of raw data that can be extracted and processed out of the device. Some research grade wearable devices have been coined as a low-cost alternative to laboratory-based gait analysis with several methods of processing able to identify gait features and running performance outcome measures, including; spatiotemporal gait parameters (i.e., stride time, ST time, SW time, SL) (Khusainov *et al.*, 2013; Clark *et al.*, 2016a, 2016b, 2017; Barnes *et al.*, 2017; Clark, 2017; Hahn *et al.*, 2017; Kluge *et al.*, 2017; Anwary, Yu and Vassallo, 2018; Brahms *et al.*, 2018; Youn *et al.*, 2018), BCoM trajectory (Seminati *et al.*, 2013), segment centre of mass vertical displacement, angular velocity (Norris, Anderson and Kenny, 2014), physical activity behaviours (i.e., adherence) (Grant *et al.*, 2010; Barnes, 2017; Bötzel *et al.*, 2018; Fridolfsson, Börjesson and Arvidsson, 2018), and GRF (Barnes, 2017; Clark, 2017; Shahabpoor and Pavic, 2018).

1.11. ANALYTICAL TECHNIQUES

Running gait is a fundamental skill that is learned, as such, individual characteristics can overlay basic movement patterns, resulting in unique personal gait features or asymmetries, which integrate into functional gait cycles (Inman *et al.*, 2006). Many factors contribute toward movement patterns including physical, neural and mental characteristics, for instance, prosthesis, shoe type, injury and mood. The body compensates for these individual differences through the musculoskeletal system reducing energy expenditure or metabolic cost incurred because of an ineffective or asymmetrical gait (Tesio, Roi and Möller, 1991; Inman *et al.*, 2006).

Wearable devices, specifically accelerometers, have been prolifically researched for their use in gait analysis to quantify and classify pathological walking gait (Jenner *et al.*, no date; Tesio, Roi and Möller, 1991; Moe-Nilssen and Helbostad, 2004; Tao *et al.*, 2012; Norris, Anderson and Kenny, 2014; Anwary, Yu and Vassallo, 2018; Bach, Dominici and Daffertshofer, 2022) with few that look at quantifying gait in the healthy population (Malir, 2018; Soulard *et al.*, 2021; Lee *et al.*, 2023). One such study on pathological walking gait, was able to use accelerometry to identify specific gait features, such as IC and TO, and process the data to identify gait symmetry (Figure 18) (Anwary, Yu and Vassallo, 2018).

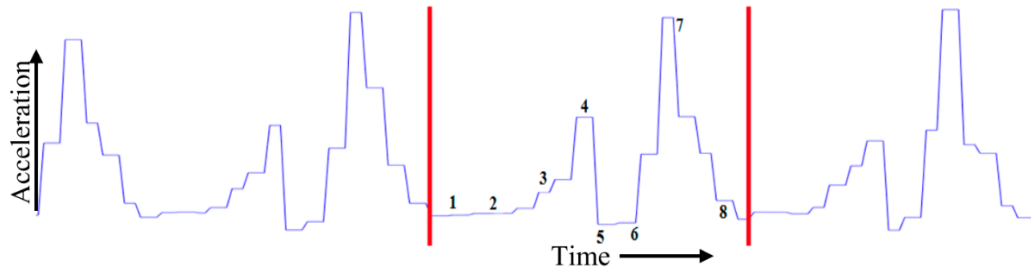


Figure 18: Eight gait features highlighted in the accelerometer movement wave. Corresponds to the walking gait events that are defined in figure 1; 1. IC, 2. Load Response (LR), 3. mid-ST, 4. Terminal-ST, 5. TO, 6. IS, 7. Mid-SW and 8. terminal-SW (Anwary, Yu and Vassallo, 2018).

Wearable accelerometers have facilitated the categorisation of children's physical performance from accelerometry and magnetometer movement data. When translating the temporal movement wave into the frequency domain using a fast Fourier Transform (FFT) (Figure 19A/ C), followed by a cumulative distribution function (CDF) (Figure 19B/ D), a measure of gait quality was derived coined Spectral Purity (SP) (discussed in more detail in 2.11). Better performers displayed a negatively skewed FFT, with more low frequency harmonics and fewer high frequency harmonics within the selected epoch⁹ (Figure 19A/ B), compared to poorer performers who displayed a wider range of harmonics and greater frequency magnitude (Figure 19C/ D) (Barnes, 2017).

⁹ a specific time interval or segment of data.

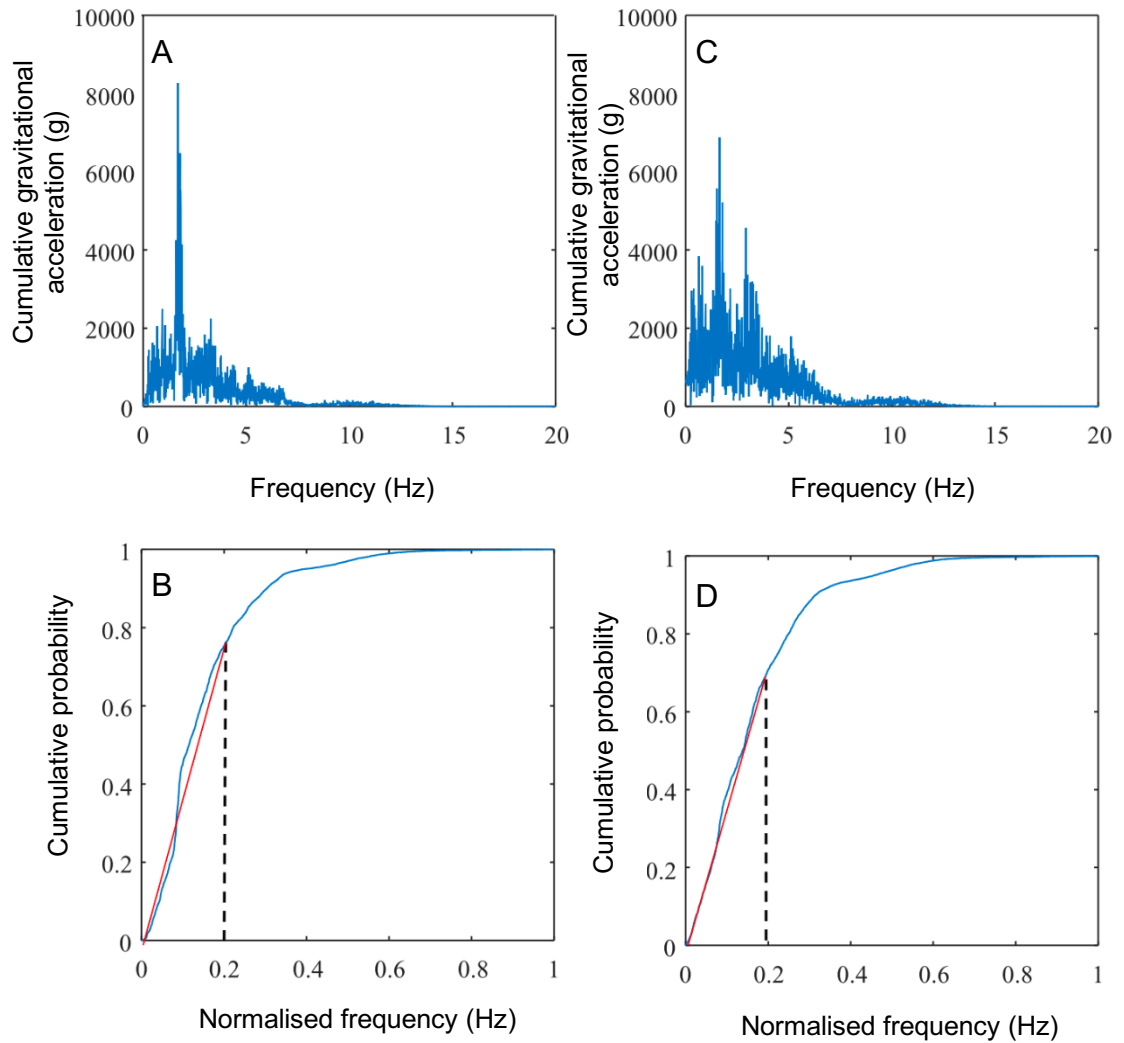


Figure 19: Fast Fourier Transform (FFT)(A and C) and Cumulative Distribution Function (CDF) (B and D) plots from which Spectral Purity (SP) is determined. Where figures A and B represent a child with low SP (higher gait quality), commonly displayed as a left (negative) skew with few, high amplitude, low frequency peaks, being classed as cleaner spectra. C and D are from a child with a high SP (low gait quality) commonly displayed as many, lower amplitude, higher frequency peaks (Barnes, 2017).

However, there are limitations of using individual gait variables to quantify gait quality as the causation of the asymmetry is challenging to distinguish and because inconsistency between measurement techniques, thus variables collected, cannot always be compared across different studies (Sadeghi *et al.*, 2000). To date, there is only one unpublished study uncovered during the

literature searches, that uses accelerometry to globally index running gait quality, captured from an athlete returning to sport from injury, over several time points (Jenner *et al.*, no date). There is a clear lack of information surrounding the objective quantification of gait quality via accelerometry, specifically surrounding running performance.

1.12. AIMS

The overarching aim of this project is to collect suitable wearable device accelerometry data to derive a series of robust processing techniques that will quantitatively measure gait quality parameters captured from runners. Secondly, to validate these processing techniques against other objective measures, such as cardiopulmonary exercise testing (CPET). Finally, to validate these processing techniques over differing inclines, replicating an outdoor environment.

1.13. OBJECTIVES

1. Investigate effect of incline on running shoe performance to establish a RE difference between types of shoes that is measurable by CPET.
2. Understand the wearable accelerometer devices sensors and their functionality.
3. Test the wearable accelerometer devices within the laboratory to ensure they are sensitive and reliable for the capture of quality movement data captured during running.

4. Formulate an accelerometer data processing technique to identify gait quality parameters that exhibit RE differences in objective 1.
5. Statistically test the processed accelerometer data to determine its suitability for use in identifying gait quality parameters that exhibit RE differences in objective 1.

CHAPTER TWO

2. FORMULATION AND OPTIMISATION OF GENERAL METHODS

SUMMARY

This chapter aimed to develop a robust method for quantitative gait assessment using accelerometry from wearable devices, offering a low-cost alternative to traditional gait analysis. Wearable devices, integrated into daily life, can capture gait data but commercial limitations hinder accessibility to raw data. Research-grade wearable devices, providing raw data access, enable transparent processing techniques for accurate gait analysis. This chapter formulates a robust method to capture, extract, calibrate and analyse accelerometry data. A novel series of analytical processing methods were coined the Global gait analysis Tool (GaiT).

2.1. INTRODUCTION

Wearable devices have become integrated into the daily lives of individuals wanting to understand more about their performance data. These devices are sensitive enough to record data in which gait variables can be extracted, such as gait cycle events and vertical acceleration (see Wearable devices - 1.10) (Jenner *et al.*, no date; Mariani *et al.*, 2010; Tao *et al.*, 2012; Barnes, 2017; Clark, 2017; Anwary, Yu and Vassallo, 2018; Wada *et al.*, 2018). Wearable devices present an opportunity to quantify the movement patterns of all types of runners in the real-world setting, not just elite athletes (Benson *et al.*, 2018). Due to this, wearable devices are currently being investigated as a low-cost and portable alternative for gait analysis offering the ability to examine performance objectively and independently of the professional research environment.

Nonetheless, there are limitations to the commercial wearable devices, having predefined processing protocols that remain the property of the manufacturer. Often, the data available to the end-user may have been processed within the device and the raw data are inaccessible. Pre-processing steps, such as filtering, can lead to the deletion of important information captured during movement. Following data processing, the resultant data may not accurately represent the activity undertaken through the specific harmonics captured within the movement wave being filtered out. As the processing techniques on board the consumer grade wearable devices are proprietary information, research grade wearable devices have instead been adopted within the gait literature due to unrestricted access to

the raw data (Jenner *et al.*, no date; Barnes, 2017; Benson *et al.*, 2017; Clark, 2017).

The lack of consensus in contextualising accelerometry-based movement data underscores the need for transparent analytical methods. This chapter aims to bridge these gaps by utilising raw data from research-grade wearable accelerometry devices. These data will build upon the research of Barnes, (2017), Clark, (2017) and Jenner *et al.*, (no date) by developing advanced processing techniques that focus on parameters such as SF to achieve the objective quantification of running gait.

2.1.1. AIM

The aim of this chapter was to develop a method to formulate and optimise a quantitative gait assessment method for wearable accelerometers, with potential utilisation outside of the laboratory. This iterative process was built up over smaller studies to form robust data collection, extraction and processing techniques with an analytical approach that proficiently contextualised running accelerometry data.

2.1.2. OBJECTIVES

1. Understand the wearable device sensors and their functionality.
2. Test the wearable devices to ensure they are sensitive enough to capture the movement patterns in runners.
3. Formulate a data processing technique to quantify running gait.

4. Statistically test the data processing technique to determine suitability for use in quantifying the running gait.

2.2. GENERAL METHODS

Uniform methods were consistently employed throughout this thesis, consolidated for clarity in the General methods section (2.2). As this chapter is focused on the optimisation of the method for potential gait analysis of accelerometry data captured whilst running, it includes some results alongside methodology.

2.2.1. WEARABLE DEVICE TECHNICAL SPECIFICATION

The research grade wearable device, previously named the SlamTracker, (Swansea University, UK) (Clark *et al.*, 2016b) (Figure 20) contained a tri-axial accelerometer (ADXL345) with a selectable dynamic range¹⁰ of ± 2 g, ± 4 g, ± 8 g, or ± 16 g, a resolution¹¹ of 4 mg/LSB (milli-g per least significant bit) for the ± 2 g range, 8 mg/LSB for the ± 4 g range, 16 mg/LSB for the ± 8 g range, and 32 mg/LSB for the ± 16 g range, an output data rate¹² from 0.1 Hz to 3200 Hz, and is powered by 2.0 V to 3.6 V making it suitable for battery-powered applications. Two SlamTrackers were used throughout this research project (one fitted to each shank) and were predefined to record at 40 Hz.

¹⁰ determines the maximum acceleration it can measure along each axis.

¹¹ the smallest detectable change in acceleration that the sensor can measure.

¹² the frequency at which acceleration data is sampled and output by the sensor.

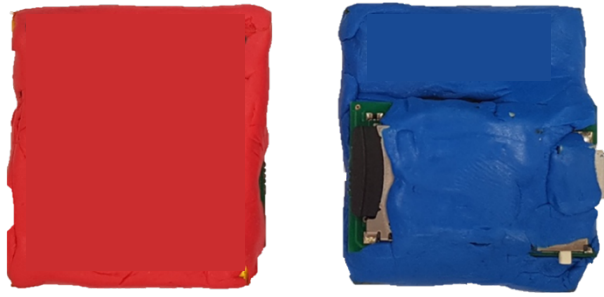


Figure 20: The two, custom made wearable devices (SlamTracker, Swansea University, UK).

Each wearable device was previously tested under static and dynamic conditions, where at lower recording frequencies it concomitantly demonstrated a small variability (<0.001 g), low coefficient of variation (CoV) and deviation from the mean, making it suitable for data collection during physical activity at 40 Hz (Clark *et al.*, 2016a, 2016b).

2.2.2. PARTICIPANT INCLUSION CRITERIA

Each participant completed a batch of questionnaires to gather personal information including; anthropometric characteristics, injury history, performance ability (whether they “yes” could or “no” could not complete 10 km in ≤ 40 minutes as a crude performance indicator), physical activity readiness questionnaire (PAR-Q) and COVID questionnaire to understand if the participants were suitable to join the study. See Ethics (2.2.3) for more details and associated appendices.

CRITERIA

No positive PAR-Q (Appendix A**Error! Reference source not found.**):

- No injuries within the last 6 months and are not currently seeing a therapist for ongoing symptoms.
- Healthy individual, with no symptomatic long-term health conditions.

A clear COVID pre-visit questionnaire (Appendix B**Error! Reference source not found.**):

- Not having had COVID-19 within the past 14 days.
- Not currently experiencing any COVID-19 symptoms.
- Not currently living with anyone who is high risk, based on the COVID-19 guidelines.
- Regular running experience with the ability to run 10 km.
- Able to maintain running on a treadmill over various inclines.

2.2.3. ETHICS

This project was granted ethical approval by the Faculty of Biological Sciences Research Ethics Committee at the University of Leeds, UK; BIOSCI-18-016 on 27/06/19 (Appendix C). Additional COVID safe procedures were implemented from December 2020 to satisfy the UK Government and University guidelines (Appendix D), the University and Faculty Health and Safety Committee, and Faculty of Biological Sciences Research Ethics Committee at the University of Leeds, UK; BIOSCI-18-016 on 15/12/20.

All participants were given an information sheet detailing the study process and that they were permitted to leave at any point (Appendix E). Each participant gave informed consent (Appendix F) before participating outlining results could only be withdrawn before entered the data analysis due to the anonymity process.

2.2.4. STATISTICAL TESTING

IBM SPSS Statistics for Macintosh, Version 28.0. (2021) (Armonk, NY: IBM Corp) was used to conduct all statistical tests.

PARTICIPANT DESCRIPTIVES

Within group differences for age, mass, height, body mass index (BMI) and performance level were investigated using an independent samples t-test to a significance of $P \leq 0.05$.

MAIN EFFECTS

Homogeneity-of-variance was tested using normally distributed histograms and Mauchly's Test of Sphericity. A non-statistically significant result ($P > 0.05$) allowed for the use of parametric measures with non-adjusted degrees of freedom, where sphericity was not met, a more conservative approach was taken by decreasing the degrees of freedom.

PARAMETRIC MEASURES

The participant testing effect stems from a participant's awareness of being studied. This can yield positive or negative effects on performance based on the individual's response. To reduce the participant testing effect, the method was repeated and crossed. Statistical testing was conducted using a two-way repeated measures ANOVA including a post-hoc pairwise comparison with Bonferroni correction to a statistical significance of $P \leq 0.05$. This was conducted for both within and between group differences, and degrees of freedom were adjusted for repeated measures.

Further investigations were conducted using the simple effects of the repeated measures ANOVA, the paired correlation coefficients and paired sample t-test to locate the root cause of the statistically significant interactions, relationships and differences with the data, respectively.

2.2.5. DATA EXTRACTION

The wearable device data were collected on a micro-SD card and imported into the programme; daily diary management (DDMT) (Wild Life Computers Inc., Redmond, WA, USA). The wearable device internal time wave (hh:mm:ss), plus three accelerometer x-, y- and z-axes waves were extracted as .txt files and imported into Igor Pro v8 (WaveMetrics, Oregon, USA). I developed a custom data processing script for this project to process the raw accelerometry data (Appendix G). A data processing summary (Appendix H) outlines the overall data extraction and processing steps taken. The initial data extraction was the same for each study unless otherwise stated. Any

additional data processing associated with a particular study was included within the respective section.

STUDY 1: WEARABLE DEVICE CALIBRATION

SUMMARY

The research centered on employing the tilt test to discern any biases and sensitivities inherent in the tri-axial accelerometers of the two wearable devices. Analysis of the results revealed the device's positioning within a right-hand coordinate system and deviations from technical specifications. The tilt test encompassed data collection across six orientations, enabling the calculation of sensitivity and bias along each accelerometer axis. These computations will inform adjustments to dynamic data acquired during testing, enhancing data integrity. To efficiently handle large volumes of data, these data processing techniques were incorporated into automated data processing scripts in Igor and MATLAB.

2.3. PREMISE

The tilt test plays a role in ensuring the accuracy and reliability of accelerometers by assessing their alignment between technical specifications and dynamic data capture (Analogue Devices, 2015; Barnes, 2017; Kieron et al., 2018). By measuring static acceleration due to gravity (g), this test provides valuable insights, particularly when the accelerometer is positioned vertically. In this orientation, the parallel axis registers 1 g, the antiparallel axis -1 g, and the perpendicular axis 0 g (Analogue Devices, 2015).

By scrutinising alignment, sensitivity, and mechanical integrity, the tilt test detects manufacturing defects and mechanical errors, ultimately providing calibration data to enhance the performance of the wearable device sensors. The obtained bias and sensitivity values from this test are indispensable for calibrating dynamic data captured by accelerometers. Additionally, the tilt test facilitates identifying the number of axes and establishing their coordinate system within the wearable devices, aligning them precisely with a known reference frame (Barnes, 2017; Clark, 2017).

2.3.1. *AIM*

The aim of this study was to assess the functionality of the accelerometer sensors embedded within each wearable device and ascertain the precise count and alignment of each axis. Furthermore, this study sought to acquire data that was able to determine sensitivity and bias. Additionally, this research aimed to develop a streamlined programming script capable of automating the calibration process of the dynamic data outside of the

wearable devices. This script was designed to ensure swift and accurate calibration during data processing, enhancing the efficiency of the overall data analysis.

2.3.2. HYPOTHESIS TESTING

Hypothesis testing has an unavoidable risk of error when accepting or rejecting the null hypothesis. There are two types of error which influence each other; a type I error or alpha (α) is a false positive conclusion, and a type II error or beta (β) is a false negative conclusion. Setting a lower significance level decreases the type I error risk but increases the type II error risk. Increasing the power of a test decreases a type II error risk but increases a type I error risk.

HYPOTHESES

1. H_0 : no difference was present between the technical specification and dynamic data captured from the accelerometers within the wearable devices.
2. H_1 : there will be a difference between the technical specification and dynamic data capture from the accelerometers within the wearable devices, enabling for the calculation of sensitivity, bias and resultant dynamic data calibration.

2.3.3. OBJECTIVES

A tilt test was conducted where both wearable devices were orientated in six different positions for one minute to capture static accelerations along each of the sensitive axes. Sensitivity, bias and dynamic accelerometry data correction equations were formulated. A data processing script was written to automate the correction of the accelerometry data.

2.4. METHOD

2.4.1. PROTOCOL

One wearable device was marked with a dot on the left corner of the front side, marked “top” and the reverse side “bottom” (Figure 24). The device was enclosed within a custom rectangular outer unit, allowing for it to stand independently for the tilt test. The outer unit was marked to identify the devices orientation. The wearable device was turned on, a vigorous shake performed to show the start of the tilt test on the resultant movement wave and then was sealed tightly within the foam filled unit to negate unwanted movement.

The unit was placed on a level surface ($0\pm0.1^\circ$), found using a BOSCH Laser Rangefinder (GLM 80 Professional, Robert Bosch Power Tools GmbH, Stuttgart, Germany), for 60 seconds in six different orientations (Figure 21). A vigorous shake was performed to mark the end of the tilt test before the device was removed from the outer unit and turned off. The procedure was conducted again for the second device.

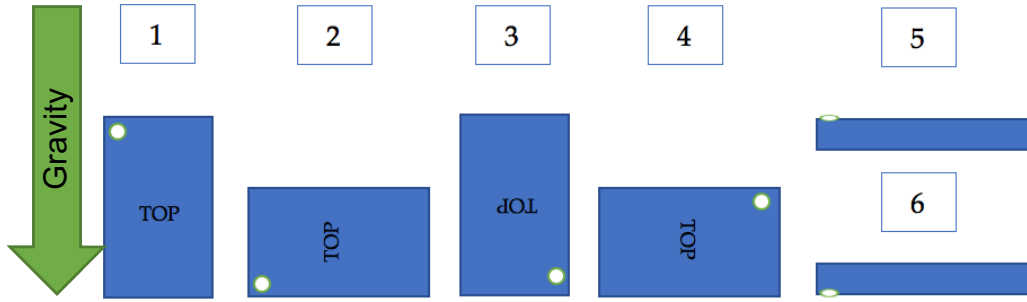


Figure 21: Orientations from 1-6 in which the wearable device was positioned for one minute each.

2.4.2. DATA EXTRACTION

Consistent data extraction methods were applied to each wearable device prior to commencing the data processing phase. For additional details, please refer to the section on Data extraction (2.2.5).

2.4.3. DATA PROCESSING

A 30 second time segment (epoch) was separated from the x-, y- and z-axis data for each of the six orientations. These epochs were sectioned 10 seconds from the orientation start time to ensure that a clean and consistent movement wave was captured. The results from each of these orientations were used to calculate the average sensitivity (S) (Equation 3) and bias (B) (Equation 4) of the tri-axial accelerometer sensors. This was conducted for both devices where the results provided the basis for the correction equation (Equation 5) used as the initial calibration step within the MATLAB script (Appendix I).

Equation 3: Sensitivity (S) equation for the x (xx), y (yy) and z (zz) axis. Where A indicates the sensor is the accelerometer, x-, y- and z- indicating the axis and the number demonstrating the orientation position of the device from **Error! Reference source not found.**

(3)

$$S_{xx} = \frac{A_{x2} - A_{x4}}{2}$$

$$S_{yy} = \frac{A_{y1} - A_{y3}}{2}$$

$$S_{zz} = \frac{A_{z5} - A_{z6}}{2}$$

Equation 4: Sensor bias (B) equation for x-, y- and z-axis all at 0 g. Where A indicates the sensor is the accelerometer, x, y and z indicating the axis and the number demonstrating the orientation position of the device from **Error! Reference source not found.**

(4)

$$B_x^{0g} = \left(\frac{A_{x1} + A_{x3} + A_{x5} + A_{x6}}{4} \right)$$

$$B_y^{0g} = \left(\frac{A_{y2} + A_{y4} + A_{y5} + A_{y6}}{4} \right)$$

$$B_z^{0g} = \left(\frac{A_{z1} + A_{z2} + A_{z3} + A_{z4}}{4} \right)$$

The smallest offset of the wearable device when mounted on a participant caused data crossover, hence, the incorrect magnitude of data was recorded in all three axes. The data were calibrated for this offset using the corrected accelerometer output equation ($A^{Static_calibrated}$) **Error! Reference source**

not found.where the bias reading (B) was deducted from the original accelerometer reading (A) during a static standing data sample, taken at the start of every testing sequency for a minimum of 10 seconds. This was divided by the sensitivity of the device (S). For instance, the $A_x^{Static_calibrated}$ was the corrected value for the data recorded via the x-axis, after recalculation the value equated to 1 g. This ultimately represented the participant standing vertically fitted with the wearable device's sensitive x-axis orientated upwards.

*Equation 5: Corrected accelerometer output reading ($A^{Static_calibrated}$) equation. Where A indicated the sensor is the accelerometer, x, y and z indicating the axis, S the sensitivity value **Error! Reference source not found.**and B indicating the sensor bias value.*

(5)

$$A_x^{Static_calibrated} = \frac{A_x - B_x^{0g}}{S_{xx}}$$

$$A_y^{Static_calibrated} = \frac{A_y - B_y^{0g}}{S_{yy}}$$

$$A_z^{Static_calibrated} = \frac{A_z - B_z^{0g}}{S_{zz}}$$

2.5. RESULTS AND DISCUSSION

There were three waves present confirming the tri-axial accelerometer was working in all three axes. Each wave was defined using a different colour; blue, green and red (Figure 22).

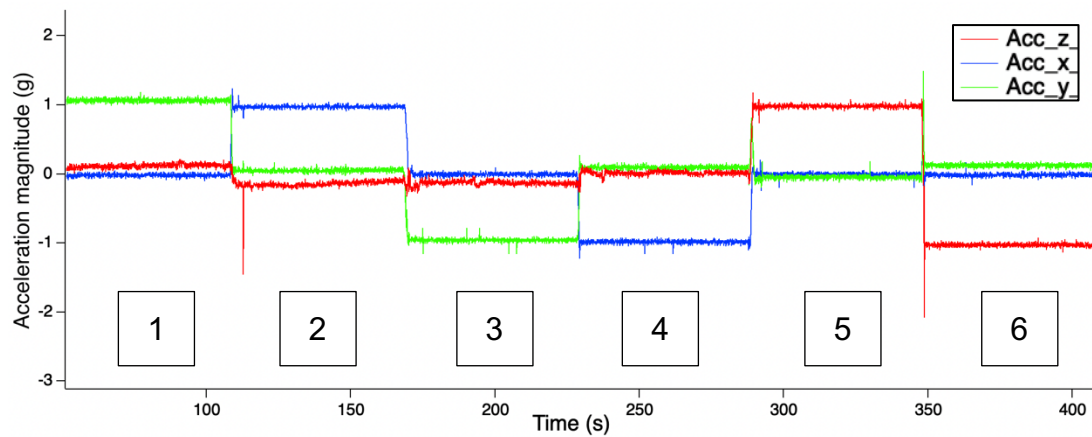


Figure 22: Tilt test gravitational effect on the each of tri-axial accelerometer axes (blue = x-axis, green = y-axis and red = z-axis) positioned in the six different orientations as noted, in **Error! Reference source not found.**

Following each movement sequence allowed for the deduction of the orientation system of the sensor within the wearable device. For instance, the green wave in position one read +1 g, position two, four, five and six 0 g, and position three -1 g (Table 2). Therefore, the sensor had a standard right-hand coordinate system, showing the device was rotated anticlockwise (Figure 22). Meaning the green wave represented the y-axis, the blue wave the x-axis and red wave the z-axis.

Table 2: tilt test results showing the gravitational (g) effect on each of the three accelerometer axes during the six orientations, performed on the red and blue wearable devices. Sensitivity (S) and the subsequent sensor bias (B) were calculated with a worked example to correct the accelerometer coordinates ($A^{Static_calibrated}$) **Error! Reference source not found..**

Device colour	Blue			Red		
Wave colour	Blue (g)	Green (g)	Red (g)	Blue (g)	Green (g)	Red (g)
Axis	x	y	z	x	y	z
Orientation 1	-0.01881	1.07949	-0.00075	0.00749	1.02039	0.14658
Orientation 2	0.98131	0.02517	-0.04105	0.94248	-0.01225	-0.02966
Orientation 3	0.02327	-0.95726	-0.04476	-0.04740	-0.98092	0.00606
Orientation 4	-0.97648	0.08687	-0.04158	-0.98519	0.04127	0.15762
Orientation 5	-0.00141	0.03688	0.99204	0.08966	-0.02065	1.12326
Orientation 6	0.00409	0.07991	-1.02920	-0.10812	0.07562	-0.94939
Sensitivity	0.97890	1.01838	1.01062	0.96384	1.00066	1.03632
Bias	0.00179	0.05721	-0.03203	-0.01459	0.02100	0.07015

The figurative representation of the wearable device with its x-, y-, z-axes coordinate system in each of the six test positions was deduced (Figure 23). This coordinate system was transferred onto the wearable devices, initially as schematic (Figure 24A) with corresponding roll (φ), pitch (ρ) and yaw (ψ) rotations established (Figure 24B). Finally, for clarity a schematic was produced depicting the placement of the wearable devices with the positive x-axis pointing superiorly along the radial axis of the participant's shank, at the point where the transverse axis converges with the tibial malleolar epicondyle (Figure 25).

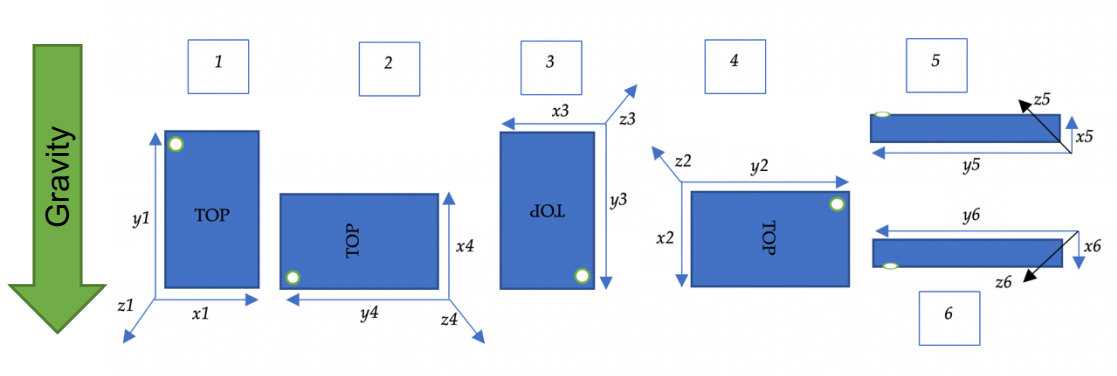


Figure 23: The resultant right-hand coordinate system is shown for the device in each of the six orientations. Gravity is demonstrated as a vertical, downward arrow.

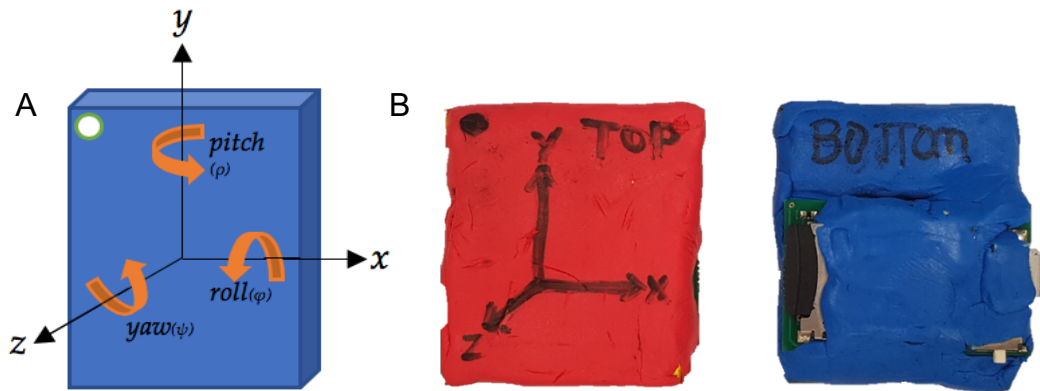


Figure 24: A. The wearable device schematic containing x-, y- and z-axes with corresponding counter clockwise rotations, roll (φ), pitch (ρ) and yaw (ψ) respectively. B. The red and blue wearable devices marked with their corresponding coordinate system, top upper left corner marker, and top and bottom orientation.

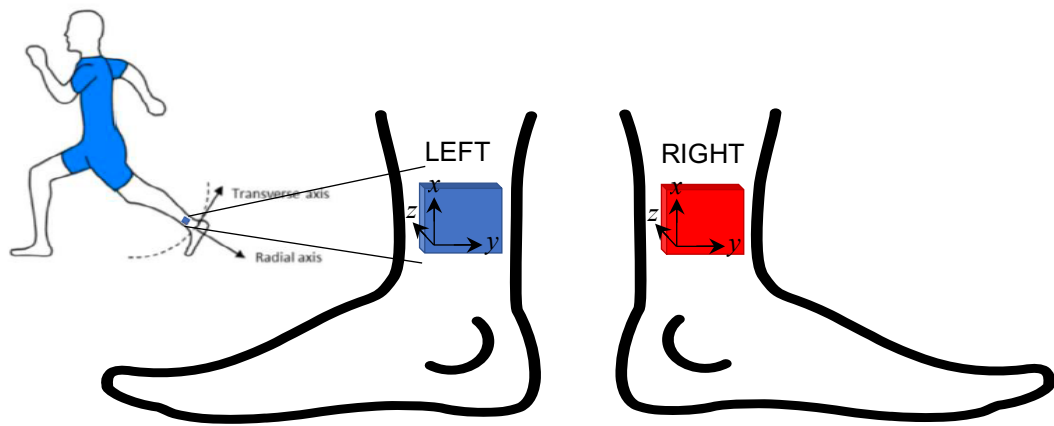


Figure 25: Image depicting the radial and transverse axis of the lower limb and converging point where the wearable device will be fitted.

The tri-axial accelerometer data were affected by the wearable device alignment, therefore, H_1 was accepted as there was a difference between the technical specification and dynamic data captured from the accelerometers. To improve the accuracy of the data recorded, the results of the tilt test were used to calculate and correct for bias and sensitivity present in each device. A worked example of a bias and sensitivity offset calibration adjustment and corrected accelerometer x-axis coordinate was conducted (Textbox 1). A calibration script in Igor Pro v8 was produced to automate the calibration process, reducing human error and saving a substantial amount of time (Appendix G).

Textbox 1: Worked example from Equation 3, Equation 4 and Equation 5 respectively using a randomly selected x-axis coordinate for Ax.

$$S_{xx} = \frac{0.98131 - -0.97648}{2}$$

$$S_{xx} = 0.97890 \text{ g}$$

$$B_x^{0g} = \left(\frac{-0.01881 + 0.02327 + -0.00141 + 0.00409}{4} \right)$$

$$B_x^{0g} = 0.00179 \text{ g}$$

$$A_x^{Static_calibrated} = \frac{7.48026 - 0.00179}{0.97890}$$

$$A_x^{Static_calibrated} = 7.63967 \text{ g}$$

2.5.1. NEXT STEPS

The subsequent phase in optimising the calibration techniques involved performing a sampling frequency test. This test has been used to identify recording discrepancies due to an imperfect manufacturing process, assessing overall wearable device performance, ensuring data capture was accurate and reliable. This is essential for valid interpretation and comparison with existing literature or standards.

STUDY 2: WEARABLE DEVICE SAMPLE FREQUENCY TEST

SUMMARY

The study addresses discrepancies with the aim of identifying and correcting manufacturing errors. The protocol involved attaching two devices, conducting synchronised movements and recording data over multiple sessions. Results indicated there was no statistically significant interaction between clock type and device colour, however, the internal clock was chosen for its lower 95% confidence interval (CI), smaller standard deviation (S.D.), and standard error (S.E.). A wave scaling calibration procedure was produced, negating the noticeable lag between the blue and red device accelerometry movement waves, improving data accuracy. The study culminated in plans to rectify rotational inaccuracies using a rotation matrix in the subsequent testing phase.

2.6. PREMISE

Sampling frequency discrepancies can be due to an imperfect manufacturing process. The actual sampling frequency¹³, can vary between the technical specification and device's ability to record. Identifying these manufacturing errors allows for raw data to be processed and corrected accordingly, minimising the impact on the processed data (Analogue Devices, 2015; Barnes, 2017; Clark, 2017).

2.6.1. *AIM*

This study aimed to identify frequency recording error between the two wearable devices using a sampling frequency test. A suitable wave scaling correction technique was formulated to correct for any error, if it occurred.

2.6.2. *HYPOTHESES*

Hypothesis testing has an unavoidable risk of error when accepting or rejecting the null hypothesis. There are two types of error which influence each other; a type I error or alpha (α) is a false positive conclusion, and a type II error or beta (β) is a false negative conclusion. Setting a lower significance level decreases the type I error risk but increases the type II error risk. Increasing the power of a test decreases a type II error risk but increases a type I error risk.

¹³ the number of samples recorded per second.

H_0 : The red and blue devices exhibited identical sampling frequencies.

H_1 : Either the red or blue devices demonstrated a disparity in sampling frequency.

2.6.3. OBJECTIVES

A sampling frequency test was used to assess for sampling error between two wearable devices. The objectives of this study were to:

1. conduct multiple sampling frequency tests of differing duration.
2. use an internal and external time point to identify which was more suitable for synchronisation of the two devices movement waves.
3. Address possible sampling frequency disparity using a wave scaling correction.

2.6.4. METHOD

2.6.5. GENERAL METHODS

Uniform methods were consistently employed throughout this thesis, consolidated for clarity in the General methods section (2.2).

2.6.6. PROTOCOL

Two wearable devices, one blue and one red, were taped together so manual synchronisation movements could be conducted to both wearable devices at the same time and orientation. A stopwatch (external time reference) was

used to note the time each wearable device was turned on. A manual vigorous shake of the wearable devices was conducted in one direction to produce large magnitude peak on the movement wave during recording and then placed down on a flat surface. This large magnitude peak was used to synchronise the blue and red device waves during the data analysis. The wearable devices were left to record between three and six hours of static data. This was repeated on three separate days at different time of the day. The wearable devices were picked up and periodically shaken throughout each test before being placed down on a flat surface again, which provided further reference and synchronisation points. At the end of the test, one final vigorous shake was conducted before the external time noted and devices turned off. The devices were used as per the manufacturer's guidelines specifically in terms of the activity frequency and temperature range.

2.6.7. DATA EXTRACTION

Consistent data extraction methods were applied to each wearable device prior to commencing the data processing phase. For additional details, please refer to the section on Data extraction (2.2.5).

2.6.8. DATA PROCESSING

The sampling frequency was calculated (Equation 6) using the wearable device time wave (internal time) and stop watch (external time) and three tri-axial accelerometer waves. Initially, the accelerometry movement wave from

the red device (intended for the right leg - RL) and blue device (intended for the left leg - LL), were cut to the same length using the large magnitude peaks from the vigorous shaking at the start and end of the test. The sampling frequency was also calculated for each of the large magnitude peaks that were conducted throughout to highlight any changes in sampling frequency during testing. See the relevant appendices for details of the data processing script (Appendix G) and data processing procedures (Appendix H).

Equation 6: Equations used to calculate frequency and wave scaling of each individual device, where Δ is change in, t is time in seconds (s), p is point number, F_t is finish time, F_p is finish point, I_t is initial time, I_p is initial point, f is frequency in hertz (Hz) and $\Delta_{t,w}$ is wave scaling.

(6)

$$\Delta_t = F_t - I_t$$

$$\Delta_p = F_p - I_p$$

$$f = \frac{\Delta_p}{\Delta_t}$$

$$\Delta_{t,w} = \frac{1}{f}$$

2.7. RESULTS AND DISCUSSION

The repeated measures ANOVA using Greenhouse-Geisser¹⁴, demonstrated that there was no statistically significant interaction between clock type

¹⁴The Greenhouse-Geisser correction is a statistical method used in repeated measures ANOVA (analysis of variance) when the assumption of sphericity is violated. Sphericity assumes that the variances of the differences between all possible pairs of within-subject

(internal or external) and device colour (red or blue) (clock*colour), ($F(1, 2) = 13.364$, $P = .067$, partial $\eta^2 = .870$) (Table 3). Meaning that the type of clock or colour of device had no statistically significant interaction on frequency of the data points recorded.

Table 3: Results of three frequency tests with $n=12$; frequency (Hz) for each test, mean and S.D. frequency for each device and clock type.

Test no.	Test duration (hh:mm)	Internal clock		External clock	
		Blue device (LL) frequency (Hz)	Red device (RL) frequency (Hz)	Blue device (LL) frequency (Hz)	Red device (RL) frequency (Hz)
1	03:04	39.99836	40.00110	39.99105	39.95726
2	06:32	39.99991	40.00013	40.10233	40.06670
3	04:33	39.99939	39.99957	40.31325	40.27142
Mean	04:23	39.99921	40.00027	40.04411	40.02018
S.D.		0.00079	0.00077	0.16365	0.15947
S.E.		0.00046	0.00045	0.09448	0.09207

A Bland-Altman plot (Figure 26 and Figure 27), also known as a difference plot or Tukey mean-difference plot, is a graphical method used to assess the agreement between two quantitative measures or methods. Ideally, most data points should cluster around the bias line, indicating good agreement. The limits of agreement (LOA) provide insight into the range of variability or disagreement between the methods, highlighting any systematic bias or variability between them (Giavarina, 2015).

conditions are equal. When this assumption is not met, the Greenhouse-Geisser correction adjusts the degrees of freedom to provide more accurate F-ratios and p-values for hypothesis testing. This correction helps to reduce the risk of Type I errors (false positives) in statistical analysis.

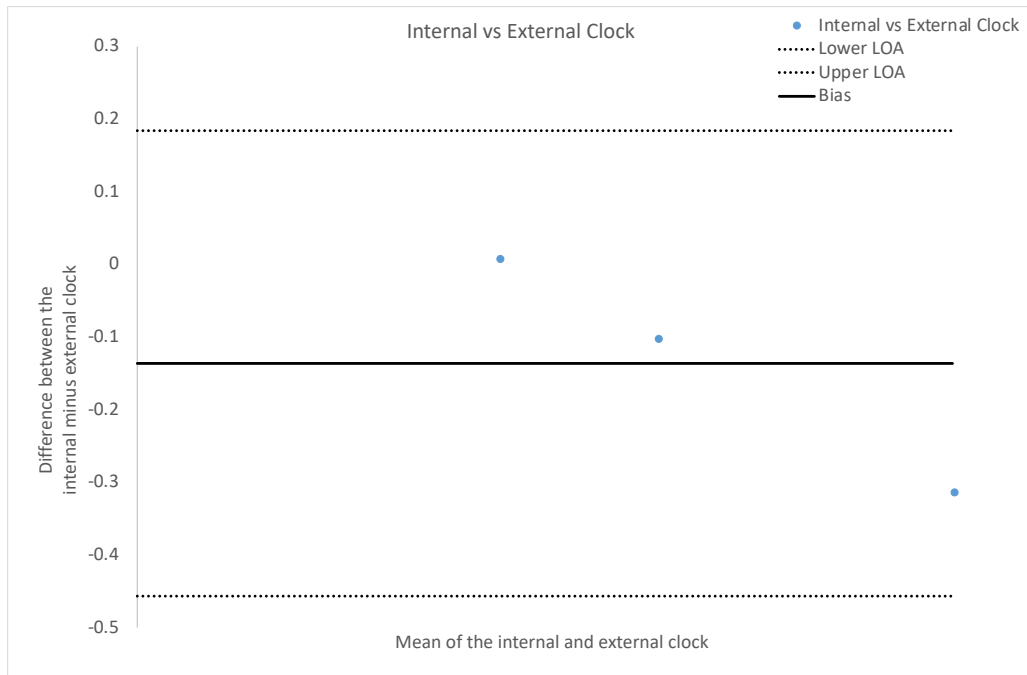


Figure 26: Bland-Altman plot of the internal versus the external clock sampling frequency results. Where the black line shows the bias, and the dashed black line the upper and lower limits of agreement (LOA).

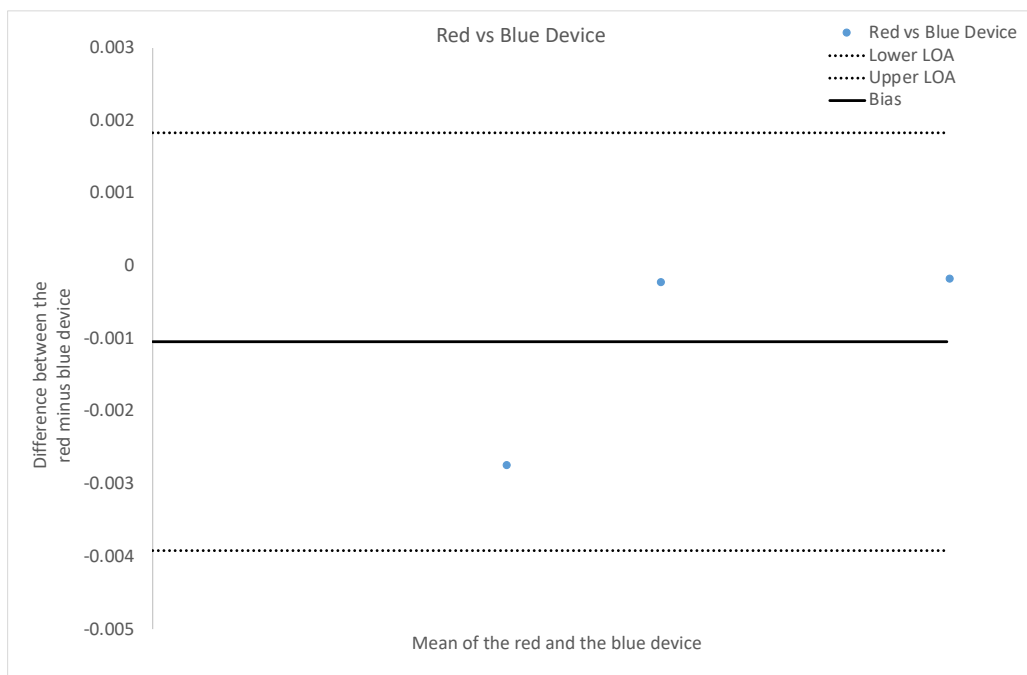


Figure 27: Bland-Altman plot of red versus the blue device sampling frequency results. Where the black line shows the bias, and the dashed black line the upper and lower limits of agreement (LOA).

Considering the plots in Figure 26 and Figure 27 the data points are scattered within the limits of agreement, meaning both the internal and external clock

and red and blue device were within the LOA. The data points also fall around the bias line, meaning both the internal and external clocks and red and blue devices produced similar results with small bias of -0.136323333 Hz and -0.001046667 Hz, respectively. As there are only three data points it is impossible to make a firm conclusion, however both figures appear to have proportional bias, meaning that the clock type or device colour methods do not agree equally through the range of measurements captured (Giavarina, 2015; Hazra and Gogtay, 2016).

The internal clock (39.99974 ± 0.00090 , 95%CI 0.00037) had a lower 95% confidence interval, smaller S.D., and S.E., over the external clock (40.11700 ± 0.14594 , 95% CI 0.05958), therefore, was selected for use during testing. This will help to negate accumulated error from several occurrences of inexact time notation between the wearable device events and the external clock during testing. It will also reduce the time discrepancies due to asynchronous human error such as, the inability to turn both devices on concurrently and physiologically being unable to press the stop watch start/stop button within 0.1 s to precisely synchronise the external clock and the wearable device.

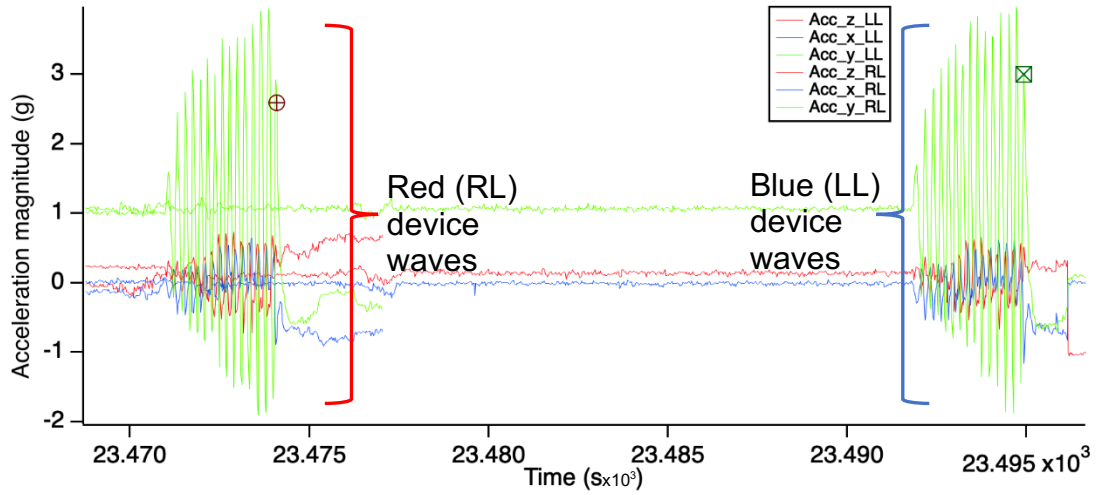


Figure 28: Graphical representation of the blue (LL) and the red (RL) devices x-, y- and z- accelerometer waves set at a 0.025 wave scaling (40 Hz). The red (RL) device waves are on the left of the figure and the blue (LL) device waves are on the right side of the figure with seconds (s) along the x-axis and gravitational acceleration (g) on the y-axis. There is an observable variation in the time and end point of the blue and red waves. This can only be corrected after the data is extracted in the Igor Pro v8 processing software by changing the wave scaling as in Equation 6.

The graphed accelerometer waves (Figure 28) show three waves for each of the two wearable devices confirming each device containing a tri-axial accelerometers. The waves are labelled blue being the x-axis, green the y-axis and red the z-axis. If Figure 17 was rotated by 90°, it would depict the orientation of the wearable devices whilst recording the data displayed in Figure 28, where the y-axis was the sensitive or vertical axis, as displayed 1g of gravitational acceleration, and the x- and z-axes were the perpendicular or the horizontal axes, as displayed 0 g.

Using Figure 28 and the Table 3, it was evident that the blue device ran faster and recorded more data points than the red device. At this point, the null hypothesis was rejected and hypothesis one accepted, concluding that the

blue device ran at a faster sampling frequency than the red device. This is a common manufacturing discrepancy for accelerometers and is rectified through calibration. The data lag between the two devices was negligible over a short time frame (1 minute), however, during the 6.5 h test the blue device recorded 835 more data points, equating to an apparent discrepancy in recording duration of 21 s at the assumed sample frequency of 40 Hz. Therefore, when overlaying both waves, the blue wave experiences a phase shift in comparison to the red wave and when capturing running data, where the LL and RL running strides would naturally occur out of phase i.e., IC on the LL and mid-SW on the RL, the phases would eventually become in phase i.e., both the LL and RL at IC together (such as during jumping) and then out of phase again and so on and so forth.

Calibrating the data at this stage was conducted by changing the wave scaling. In the context of signal processing, wave scaling refers to the process of embedding the x-points into the y-data set (Igor Pro by WaveMetrics, 2021), aligning the x-values with the corresponding y-values as shown in Equation 6. This negates lag whilst maintaining phase, something that is typically done onboard consumer grade wearable devices. The new wave scaling value for the blue device was calculated from the change in time of the red device and the number of points recorded from the blue device (Equation 7). Once the waves were rescaled, no further sample frequency processing was needed.

Equation 7: New wave scaling for the blue device based on the data collected during testing.

(7)

$$\text{Blue device } \Delta_{t,w} = \frac{\text{Red device } \Delta_t}{\text{Blue device } \Delta_p}$$

Rescaling accelerometry waves was essential for ensuring consistency, alignment, integration, and standardisation in the analysis of running data obtained from different devices. Wave scaling between devices mitigates these effects, ensuring for accurate and meaningful interpretation of the data.

2.7.1. NEXT STEPS

Finally, only rotational error remains, which can be negated using a rotation matrix; a series of equations that transposes the x-, y- and z-axes data around their respective roll, pitch and yaw rotations (Barnes, 2017). Therefore, the next study within this chapter will implement a rotation matrix to negate rotational error. This will be conducted by collecting tri-axial accelerometry data from two wearable devices whilst treadmill running in the laboratory. The study will deduce if the wearable devices are sensitive enough to capture running gait detail and whether the calibration and processing techniques will provide sufficient context to the data.

STUDY 3: FEASIBILITY STUDY - QUANTITATIVE GAIT ANALYSIS USING WEARABLE DEVICES ON RIGHT AND LEFT LOWER LIMBS

SUMMARY

The study assessed running gait using bilateral lower limb accelerometry on a treadmill at 16 km/h and a 1% incline. Wearable devices were tested for reliability, producing accelerometry movement waves from raw data, graphed to identify key protocol phases. Analytical focus was on the x-axis or radial axis whilst processing gait parameters. The FFT showed consistent Fundamental Frequency (FF) for both limbs but greater complexity in the right leg (RL). Gait complexity, measured by the CDF, indicated higher complexity in RL. Cross-correlation revealed stride-to-stride variation between limbs, with unexpected findings on placement style and gait symmetry. The analytical tools developed were termed the Global gait analysis Tool (GaiT). Strict wearable device placement showed more variation, contradicting expectations. ANOVA demonstrated that there were no statistically significant effects on FF or SP for placement style or device colour. The wearable devices were reliable for high-speed gait analysis. Future steps included assessing gait quality on various inclines and linking accelerometry data to performance.

2.8. PREMISE

A feasibility study will be conducted to investigate the use of accelerometry to quantify running gait. This previous studies within this chapter have investigated the importance of calibrating the sensors within the wearable device. This final study will combine these calibration techniques and introduce a filtering method plus a rotation matrix as the final calibration steps. These methods will reduce the number of unwanted harmonics potentially clouding important movement information, and reorientate the accelerometry data to a known reference frame using trigonometric principles to reduce the magnitude of data crossover between axes (Fogg, 2005; Steins *et al.*, 2014; Bieda and Jaskot, 2016; Anwary, Yu and Vassallo, 2018; Patonis *et al.*, 2018).

2.9. AIM

This study aimed to optimise the full data processing strategy from calibration to analytical processing, formulating a comprehensive tool that objectively quantified running performance based on the accelerometry collected via running gait (Jenner *et al.*, no date; Barnes, 2017; Benson *et al.*, 2018).

2.9.1. HYPOTHESES

1. H_0 : There was no significant difference in objective gait quality between different wearable device placement styles or device colours during treadmill running at 16 km/h on a 1% incline.

2. H₁: There is a significant difference in FF, SP and gait complexity between different wearable device placement styles or device colours treadmill running at 16 km/h on a 1% incline.

2.9.2. OBJECTIVES

A feasibility study was used to assess the use of accelerometry for quantifying running gait. The objectives of this study were to:

1. record running data at 16 km/h on a 1% incline on the wearable device tri-axial accelerometers to understand if they were sensitive enough to capture detail to show the differences between running conditions on a treadmill.
2. calibrate the treadmill running data using all techniques accumulated thus far, with the addition of a filtering and a rotation matrix to identify if the techniques selected were suitable.
3. identify how stringent the wearable device placement method needed to be to not significantly affect the treadmill running data.
4. develop several analytical techniques to process the treadmill running data in order to successfully contextualise the treadmill running data.
5. statistically determine if the effects between different wearable device placement styles and device colours during treadmill running at on the contextualised treadmill running data.

2.10. DATA PROCESSING

2.10.1. *FILTERING*

There are two arguments to filtering data in this context, one; maintaining the full range of harmonics by not filtering the data may provide a fuller picture of movement behaviour (Barnes and Kilding, 2015) Two; reducing the effects of sensor noise where low frequency vibration can limit conditions in which accelerometers can be used (Alam and Rohac, 2015). The low-pass filter, and high and low pass filter, such as the Butterworth, are commonly used on accelerometry data. A band pass range between 0.5 Hz and 12 Hz is capable of effectively detecting human movement (Puyau *et al.*, 2002; Clark *et al.*, 2016b; Barnes, 2017). Many filters depend on multiple factors including recording frequency and speed of activity. The correct filtering range is important to avoid deleting harmonics produced through human movement. For this study, a filter was applied using a high pass filter at 0.5 Hz which needed to be lower than the average recreational running cadence of 160 steps per minute (2.7 Hz), divided by two (1.35 Hz) due to using one accelerometer per limb (Clark *et al.*, 2016b). Followed by a low pass filter at the Nyquist frequency of 20 Hz which is half that of the sampling frequency of the wearable device (40 Hz) (Barnes, 2017; Barnes *et al.*, 2017; Clark, 2017; Clark *et al.*, 2017). The Nyquist frequency is the threshold above which aliasing can occur. This concept occurs when higher frequency components of a signal are indistinguishably sampled and appear as lower frequency components in the sampled data. Filtering out frequencies above the Nyquist

frequency will reduce, if not eliminate, aliasing and signal corruption (Proakis, and Manolakis, 2007).

2.10.2. *ROTATION MATRICES*

Wearable device fitting orientation affects the magnitude of acceleration received by the tri-axial accelerometer due to signal crossover. To combat the difference in the ideal alignment reading i.e., 1 g, to that of the wearable device when fitted on a participant, the data captured needs to be calibrated (as above) and then rotated using a rotation matrix (Barnes, 2017).

Secondly, accelerometers within the wearable device only be orientated to a world or laboratory frame in combination with a gyroscope or magnetometer sensor or by orientating one axis to a known direction. In this study, we chose to orientate the x-axis vertically along the radial axis of the shank, thus equating to 1 g, after the sensitivity and bias values were accounted for.

Equation 8: Rotation matrices for A. roll (φ) around x-, B. pitch (ρ) around y-, and C. yaw (ψ) around z-axis.

(8 A)

$$R_x(\varphi) = \begin{bmatrix} 1 & 0 & 0 \\ 0 & \cos(\varphi) & -\sin(\varphi) \\ 0 & \sin(\varphi) & \cos(\varphi) \end{bmatrix}$$

(8 B)

$$R_y(\rho) = \begin{bmatrix} \cos(\rho) & 0 & \sin(\rho) \\ 0 & 1 & 0 \\ -\sin(\rho) & 0 & \cos(\rho) \end{bmatrix}$$

(8 C)

$$R_z(\psi) = \begin{bmatrix} \cos(\psi) & -\sin(\psi) & 0 \\ \sin(\psi) & \cos(\psi) & 0 \\ 0 & 0 & 1 \end{bmatrix}$$

The vertical alignment of the x-axis along the shank meant that the assumption of the x-axis remained at remained at 0° meaning the transition of the y- and z- axis data around the x-axis (φ) was used to correct the data and remain within the frame of reference. This meant that Equation 8 A was not necessary for this project but could be useful for future projects where gyroscope or magnetometer data could be integrated.

Initially, the angle of transition (φ) was calculated (Equation 9) using trigonometric principles, where the difference between the average static standing accelerometer data sample required an x-, y- and z-axis reading of 1 g, 0 g and 0 g. The angle of transition (φ) was placed into the rotation matrix ($R_y(\varphi)$ Equation 8 B) to reorientate the z- and x-axes around the y-axis. The calibrated static accelerometer coordinate with sensitivity and bias removed ($A^{Static_calibrated}$) were rotated ($R_y(\varphi)$) resetting the x-axis to 1 g and the z-

axis to 0 g, forming a corrected static accelerometry coordinate ($A^{Static_corrected}$) (Equation 10). The resultant transition angles were used within a full rotation matrix to calibrate the accelerometer data recorded during running (Barnes, 2017; Clark, 2017). The corrected static accelerometry coordinate was fed forward to calculate the pitch angle of transition (ψ) (Equation 11). This angle of transition (ψ) was inserted into the corresponding pitch rotation matrix ($R_z(\psi)$) (Equation 8 C) which rotated the y- and x-axes around z-axis. The full roll and pitch rotation matrices (Equation 12) rotated the dynamic accelerometry coordinate ($A^{Dynamic}$) collected from running data to produce a resultant rotated dynamic accelerometry coordinate ($A^{Dynamic_rotated}$).

Equation 9: The calculation of the angle (φ) using the static calibrated coordinates using tangent = opposite / adjacent.

(9)

$$\rho = -\operatorname{atan}\left(\frac{A_z^{\text{Static_calibrated}}}{A_x^{\text{Static_calibrated}}}\right)$$

Equation 8 B: Rotation matrix for pitch (ρ), where the angle from Equation 9 was inserted into the rotation matrix to rotate the z-axis and x-axis about the y-axis, producing a z-axis coordinate of 0 g.

(8 B)

$$R_y (\rho) = \begin{bmatrix} \cos(\rho) & 0 & \sin(\rho) \\ 0 & 1 & 0 \\ -\sin(\rho) & 0 & \cos(\rho) \end{bmatrix}$$

Equation 10: The calculation of the static corrected accelerometer coordinate ($A^{Static_corrected}$) from a static calibrated accelerometer coordinate ($A^{Static_calibrated}$) and the pitch rotation matrix ($R_y (\rho)$)

(10)

$$A^{Static_corrected} = A^{Static_calibrated} * R_y (\rho)$$

Equation 11: The calculation of the angle (ψ) to move the y-axis and x-axis around the z-axis (yaw) from the corrected roll angle $R_z (\psi)$ using tangent = opposite / adjacent.

(11)

$$\psi = \text{atan} \left(\frac{A_y^{Static_corrected}}{A_x^{Static_corrected}} \right)$$

Equation 8 C: Rotation matrix for yaw (ψ), where the angle from Equation 11 will be inserted into the rotation matrix to rotate the y-axis and x-axis about the z-axis producing y-axis at 0 g.

(8 C)

$$R_z(\psi) = \begin{bmatrix} \cos(\psi) & -\sin(\psi) & 0 \\ \sin(\psi) & \cos(\psi) & 0 \\ 0 & 0 & 1 \end{bmatrix}$$

Equation 12: Full rotation matrix, from the calculated angles of transition from the static accelerometer data, the dynamic accelerometer data are used in the y and z rotation matrices.

(12)

$$A^{Dynamic_rotated} = A^{Dynamic} * R_y(\rho) * R_z(\psi)$$

The rotation process was translated into a custom MATLAB script (Appendix I) for automated processing of the high volumes of data.

2.11. ANALYTICAL TECHNIQUES

2.11.1. FAST FOURIER TRANSFORMATION (FFT) FOR FUNDAMENTAL FREQUENCY (FF)

The fast Fourier transform (FFT) algorithm is a fast and efficient way to compute the discrete Fourier transform (DFT), where $X(k)$ is the complex result in the frequency domain, $x(n)$ is the input sequence in the time domain, N is the number of samples in the sequence, and j is the imaginary unit.

Equation 13: Discrete Fourier Transform (DFT), where $X(k)$ is the complex result in the frequency domain, $x(n)$ is the input sequence in the time domain, e : The base of the natural logarithm, approximately equal to 2.71828, $j^2 = -1$, k : The index of the frequency component and N is the number of samples in the sequence,

(13)

$$X(k) = \sum_{n=0}^{N-1} x(n) \cdot e^{-j2\pi kn/N}$$

The FFT algorithm decomposes this computation into smaller, more manageable subproblems, which allows for a statistically significant reduction in computational complexity compared to the direct computation of the DFT which recursively breaks down the DFT computation into smaller DFTs until the base case is reached (Barnes, 2017).

The FFT can be used to describe gait complexity which can be deemed as gait smoothness, rhythm and stride-to-stride symmetry. The FFT can be used to quantify gait complexity from the magnitude and distribution of the accelerometry signal harmonics within an activity sample. In this study, the accelerometry sample time domain (x-axis) (Figure 29 A/ B) will be translated into the FFT frequency domain (x-axis) (Figure 29 C/ D) (Jenner *et al.*, no date). Each harmonic is displayed in terms of its cumulative magnitude (y-axis) accumulated throughout the movement sample (Barnes, 2017; Clark, 2017). The more harmonics present within the FFT, the higher the gait complexity and lower the gait quality, which is understood to be an inability of an individual to repeat the same motor pattern consistently over the sample period (Jenner *et al.*, no date; Clark, 2017).

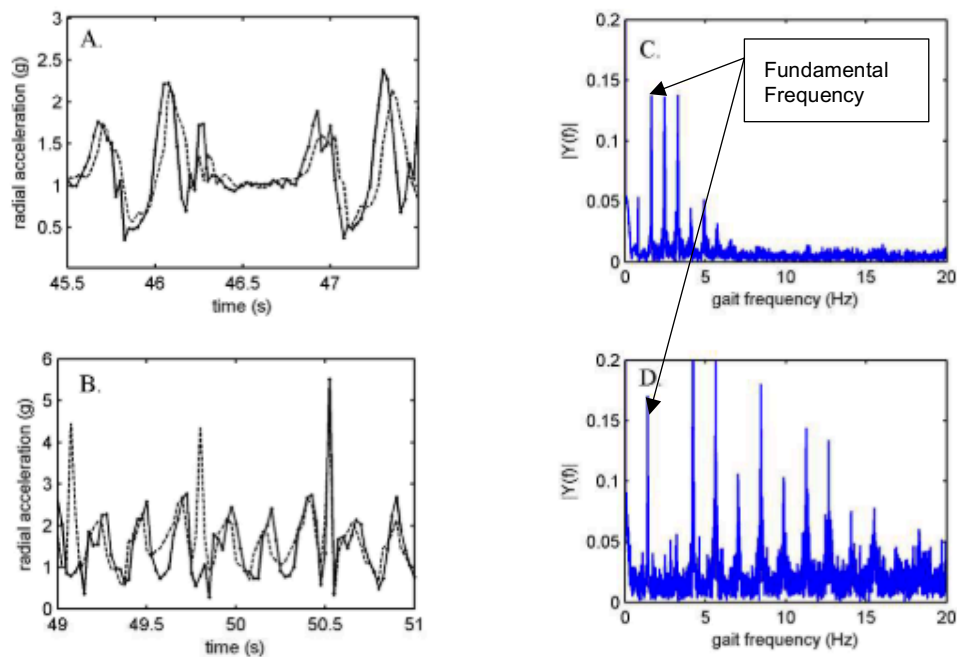


Figure 29: A. and B. show a two second radial accelerometry sample from the uninjured left leg (LL) (solid line) and injured right leg (RL) (dotted line). C. and D. show the fast Fourier transform (FFT) of the two second accelerometry sample from A. and B. respectively. A. and C. represent 4 km/h and B. and D. represent 15 km/h (Jenner *et al.*, no date).

Clark, (2017) coined the term SP to describe gait quality. Spectral Purity can be qualitatively described using the FFT where few tall, narrow low frequency harmonics and very few short, high frequency harmonics shows a less complex or cleaner movement wave, hence a lower SP score (Figure 29 A/C). Conversely, an FFT with many short, wide, low frequency harmonics and several high frequency harmonics shows a more complex movement wave, indicating lower movement quality, thus a higher SP score due to fewer duplicate movement patterns (Jenner *et al.*, no date; Barnes, 2017).

The FFT has previously been used to identify Fundamental Frequency (FF) of a movement wave, where the FF appears as the first significant low frequency component, or peak, however, it may not have the largest

amplitude (Figure 29 C/ D) (Clark, 2017). Throughout the available literature, the FFT was used to capture movement quality between an injured and uninjured limb, where the uninjured limb had fewer harmonics, thus a cleaner movement wave, compared to the injured limb having more harmonics dispersed throughout the sample. It was postulated that the additional high frequency harmonics came from changes in force distribution potentially due to compensatory motor patterns of the injured leg (Jenner *et al.*, no date). The result produced a lower symmetry index (SI) meaning there was a difference between the limbs with higher numbers being associated with larger disparity between the limbs (in this case). It is understood that fatigue, which would have affected the injured limb more so than the non-injured limb, would have negatively affected the SI thus recovery status (Jenner *et al.*, no date; Martens *et al.*, 2018).

This approach was further developed by transforming the FFT into a cumulative distribution function (CDF), providing a quantitative, objective approach to analysing the FFT data (Jenner *et al.*, no date; Barnes, 2017; Clark, 2017). This transformation may aid in contextualising running gait data by providing the platform to understand gait complexity between different runners.

2.11.2. CUMULATIVE DISTRIBUTION FUNCTION (CDF) FOR SPECTRAL PURITY (SP)

A Cumulative Distribution Function (CDF) is a mathematical function that describes the probability distribution of a random variable. $F(x)$ represents

the probability that the random variable X is less than or equal to x (Equation 14).

Equation 14: CDF is a function of x , $F(x)$, where the probability (P) that the random variable (c) is less than or equal to the variable x .

(14)

$$F(x) = P(c \leq x)$$

The CDF has previously been used to quantitate the FFT frequency spectra via quantifying gait complexity where the gradient of the CDF measured how tightly distributed the frequency components were within the gait movement wave. The gradient is determined at a probability of 0.5, or the median point, where it is established that the most common x-axis reading (in this case frequency) occurs less than or equal to 50% of the time. Spectral Purity (SP) is a term used to describe gait quality by quantifying the CDF. Qualitatively, a clean FFT movement wave with a regular repeating pattern is represented by an FFT with a high magnitude FF and few higher frequency harmonics would produce a CDF with a steeper gradient and a lower x-axis frequency reading at a probability of 0.5, equating to higher SP (Figure 30 A., C., and E.). Conversely, a less clean FFT with additional spectra randomly throughout results in a CDF demonstrating low SP through a high CDF derivative or x-axis frequency value (Figure 30 B., D., and F.). Where a one-minute epoch was taken from a movement wave from an individual with A. good motion and B. with poor motion, the corresponding FFT for C. good motion and D. poor

motion are then transformed into the equivalent CDFs for E. good motion and F. poor motion (Barnes, 2017; Clark, 2017).

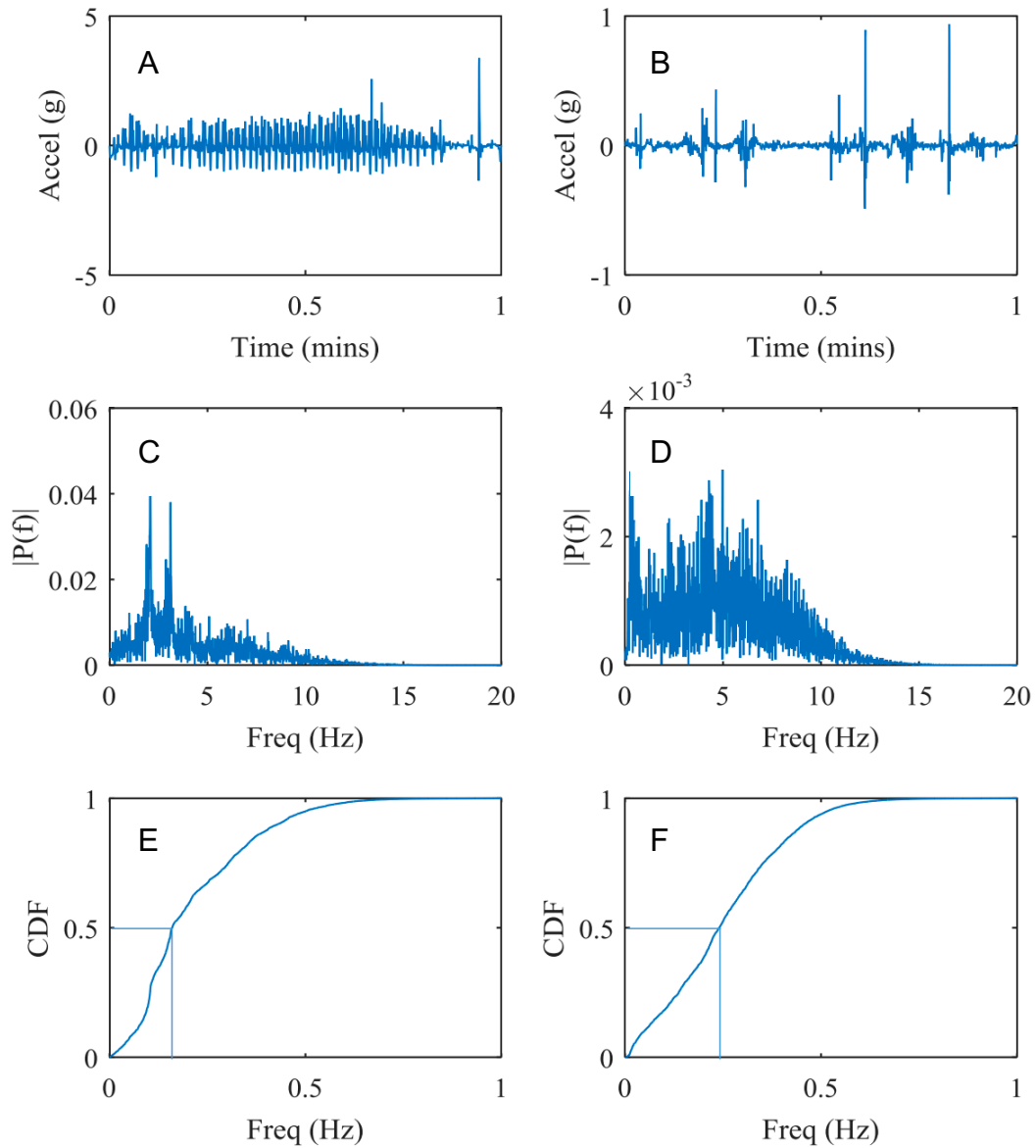


Figure 30: Sequence of the generation of a CDF: A. one-minute movement wave from an individual with good motion, B. with poor motion, C. and D. are the corresponding FFT from the movement waves, E. and F. are the corresponding CDFs from the FFT (Barnes, 2017).

The CDF has been used to link movement quality, in terms of SP, to human performance. Within this research, there was a positive relationship between

children's physical activity performance score and SP, therefore, the more skilful participants had better movement quality (Barnes, 2017).

From this information, we propose that runners who have more experience will have a cleaner movement wave, hence, better SP, demonstrated by a lower SP score. We surmise this will be due to an increased ability to repeat the same movement pattern over the sample period.

2.11.3. *CROSS-CORRELATION FOR GAIT SYMMETRY*

Correlations can be used to measure the similarity between signals. The auto-correlation function (ACF) measures the similarity of a signal with a delayed version of itself where the calculation of various lags provides information on periodicity and similarity of the signal (Equation 15). Whereas the cross-correlation function (CCF) measures the similarity between two signals at different time lags to identify time shifts and similarities between the two signals (Equation 16).

Equation 15: Auto-correlation Function (ACF) where $X[n]$ is the signal at time n , N is the total number of time points in the signal, k is the lag, \bar{X} is the mean of the signal.

(15)

$$ACF[k] = \frac{\sum_{n=1}^{N-k} (X[n] - \bar{X})(X[n+k] - \bar{X})}{\sum_{n=1}^N (X[n] - \bar{X})^2}$$

Equation 16: The Cross-correlation Function (CCF) $X_1[n]$ and $X_2[n]$ are the two signals at time n , N is the total number of time points in the signals, k is the lag, \bar{X}_1 and \bar{X}_2 are the means of the respective signals.

(16)

$$CCF[k] = \frac{\sum_{n=1}^{N-k} (X_1[n] - \bar{X}_1)(X_2[n+k] - \bar{X}_2)}{\sqrt{\sum_{n=1}^N (X_1[n] - \bar{X}_1)^2 \sum_{n=1}^N (X_2[n] - \bar{X}_2)^2}}$$

Gait symmetry measures provide further information based on the ACF and CCF. A gait symmetry index (SI) is calculated from the normalised area under the CCF curve and ranges from 0 to 1, where 0 indicates complete asymmetry and 1 perfect symmetry between the two signals (Barnes, 2017). This analytical process has been effectively utilised to identify the symmetry between the muscle mass of runners left and right lower limbs (Equation 17) (Seminati *et al.*, 2013).

Equation 17: Gait Symmetry index (SI), $X_{left}[n]$ is the signal from the left side (e.g., left leg) at time point n , $X_{right}[n]$ is the signal from the right side (e.g., right leg) at time point n , N is the total number of time points in the gait cycle.

(17)

$$Gait\ Symmetry\ Index\ (SI) = \frac{\sum_{n=1}^N |X_{left}[n] \cdot X_{right}[n]|}{\sum_{n=1}^N (|X_{left}[n]| + |X_{right}[n]|)}$$

When dealing with more than one wearable device signal at the same time, such as those representing the left and right limbs during running, both the ACF and CCF can be used. Here, the auto correlation represents the perfect stride and the value of centre peak of the auto-correlation is divided by the

mean of the two surrounding peaks of the cross-correlation and expressed as a percentage (Jenner *et al.*, no date; Barnes, 2017).

Equation 18: A recovery score (R), ranging between 0 and 100% where the percentage was calculated from the difference between the auto and cross correlation gated sequence (epoch) over the auto-correlation (Jenner et al., no date).

(18)

$$Recovery\ Score\ (R) = 100 * \left[1 - \frac{\sum_{2\Delta t} |auto_{corr} - cross_{corr}|}{\sum_{2\Delta t} |auto_{corr}|} \right]$$

Barnes, (2017) used the CCF to identify differences between the movement waves of several children during playtime. Here, social-interactions were identified as symmetrical signals and represented the same activity being undertaken during that playtime. Jenner et al., (no date) used the ACF and CCF with a customised SI to identify recovery status in an injured athlete. Differences were identified between two signals from the same individual, one signal from an injured limb and the other from a non-injured limb (Figure 31). The asymmetry between the auto and cross-correlation shows the dissimilarity between the movement profiles of left and right leg during activity. We propose the auto and cross correlation would show a more symmetrical movement pattern, therefore, a higher recovery score (R) in runners who perform better.

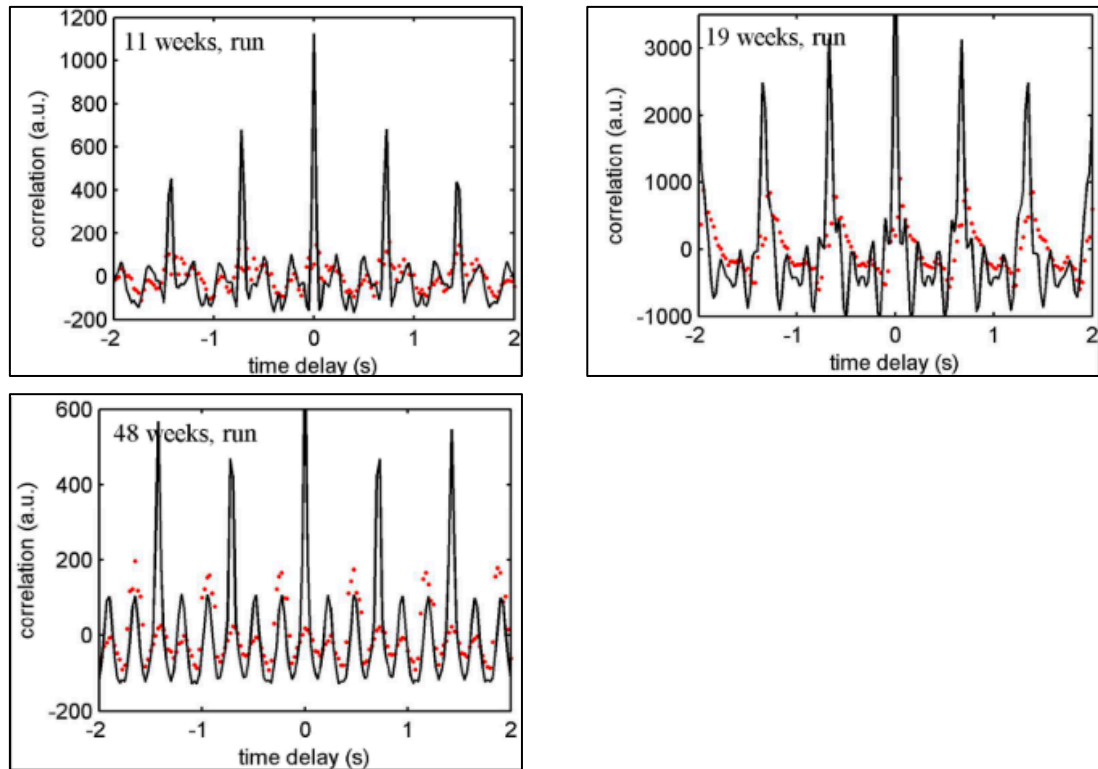


Figure 31: Auto-correlation of the non-injured leg against itself (black line) against the cross-correlation of the injured leg against the non-injured leg (dotted red line) at 11, 19 and 48-weeks post-surgery (Jenner et al., no date).

The test-retest repeatability of the wearable devices during running is of great interest. The wearable devices need to be able to collect movement data consistently and accurately within and between trials. To reduce the likelihood of type I error a feasibility study will take on a randomised element to investigate how the device fitting protocol will affect the data captured. Finally, to contextualise the accelerometry data, the analytical techniques will be explored on the test-retest running data to investigate their suitability.

2.12. PROTOCOL

Two custom-built wearable devices (red and blue) (Figure 20) were turned on and set to record at 40 Hz, then shaken simultaneously to record a discernible large magnitude peak on the movement wave to signify the start of the protocol. A stopwatch was used to capture the time the protocol events occurred to provide reference points to synchronise the two accelerometers. Two placement protocols were formulated for testing (strict and varied), where the strict placement protocol consisted of;

- calculating 10% of the shank length (the distance between the lateral tibial condyle and the tibial malleolus),
- strapping the wearable device 10% (as calculated above) above the tibial malleolar epicondyle, to avoid excess tilt if the device was placed directly on to the epicondyle,
- orientating the wearable device's positive x-axis vertically along the radial axis,
- enforcing feet directly under the hips by marching on the spot two to three times before coming to a stop. Visually assessing the final position and adjusting if necessary.

In contrast, the varied placement protocol did not measure any distance, the wearable device was strapped in approximately the correct position to the lower limb with the x-axis along the radial axis. The researcher paid little regard to the exact measurements of the shank or how the participant was standing for each fitting. The wearable device colour (blue or red) and fitting

protocol (strict or varied) was randomised, using a random number sequence, for placement on either the left or right shank.

Two male participants ($n = 2$, age = 48.1 ± 0.8 years, mass = 69.8 ± 2.5 kg, height = 184.9 ± 8.3 cm) completed eight trials for varied placement, with one participant completing eight trials for strict placement and the other participant completing seven trials for strict placement. After each wearable device was fitted, the participant completed a set number of synchronisation movements at the start and end of every trial. These created distinct patterns on the accelerometry movement wave, so the red and blue wearable device accelerometry movement waves could be synchronised to the same time point. These movements consisted of star jumps, floor based double knee lifts and chair based double knee lifts.

The participant was given operational and safety instructions for the treadmill (H/P/ cosmos sports & medical gmbh, Nussdorf-Traunstein Germany) before putting on the Nike® Vaporfly ZoomX NEXT% (VFN%) (UK 10). The participant stood still on the treadmill for 10 seconds before completing a 10-minute self-structured warm up and familiarisation period with the aim of reaching 16 km/h at a 1% incline. Eight trials at 16 km/h (4.4 m/s) were then completed where 120 seconds of running at 16 km/h was captured before the participant could stop. After the final trial, each participant was given the option to cool down before the synchronisation movements were repeated, equipment removed, wearable devices shaken then turned off, and external time noted. This was repeated for each participant.

2.12.1. *DATA EXTRACTION*

Consistent data extraction methods were applied to each wearable device prior to commencing the data processing phase. For additional details, please refer to the section on Data extraction (2.2.5).

2.13. RESULTS AND DISCUSSION

This study used bilateral lower limb (LL vs RL) accelerometry to investigate running gait on a treadmill at 16 km/h at a 1% incline. The reliability of the wearable devices was tested using a strict and varied placement protocol. The full data extraction and analytical processing techniques were tested on the resultant movement waves to contextualise the data.

The wearable devices produced a raw accelerometry movement wave in the x-, y- and z- axes. The movement waves were graphed to show the quality of the data, where the initial shake of the wearable device, the static standing position for 10 seconds, the participant building up their running speed, the 120 second segment at 16 km/h, the winding or slowing down of the runner before stopping, and then the removal and final shake of the wearable device to indicate the end of the trial could be clearly identified (Figure 32).

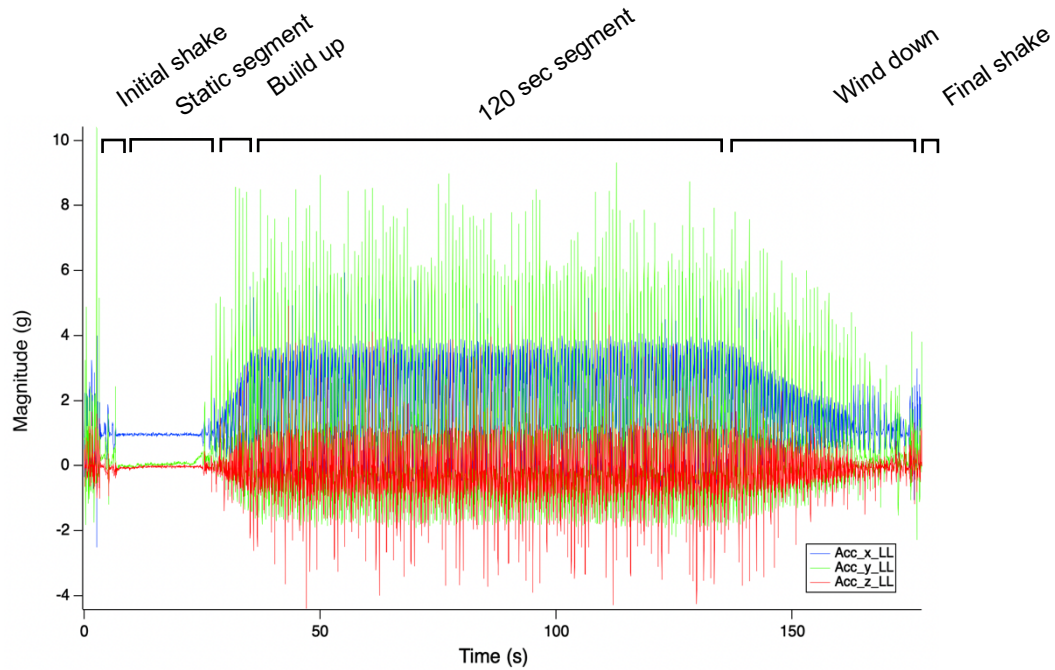


Figure 32: Raw accelerometry data graphed to show x-, y- and z-axis movement waves from one of the test-retest repeatability trials. The figure shows the protocol including the initial shaking movement of the wearable device, after fitting the participant standing in a static position, the participant building up their running speed as the treadmill was gradually increased to 16 km/h, the 120 second segment running at 16 km/h, the winding down of the runner as the treadmill was gradually decreased to 0 km/h, and the removal and final shake of the wearable devices to show the end of the trial.

To simplify the analytical process and gain an initial understanding of the data, the extraction and processing will be conducted on the radial (x-) axis only, with the intention to add the y- and z-axes data at a later date to provide a fuller picture of how the body moves in a 3-D space, rather than just vertically. Therefore, data extraction and some processing methods will be conducted on all movement waves captured to prepare for future processing and analysis, however, only the x-axis will be discussed from this point forward. The x-axis was selected as is representative of the vertical movement during running and captures the largest magnitude, therefore,

should provide a more significant opportunity to identify any gait changes throughout testing (Barnes, 2017; Clark, 2017).

The 120 second running segment (Figure 32) can be magnified so a 1.5 second epoch was visible (Figure 33). Within this epoch, two strides could be distinguished from the x-axis movement wave, which was clean enough to identify the gait parameters; push off, leg swing and maximum impact force (or the maximum GRF), based on the evidence collected by Barnes, (2017) using the same devices, which were validated against synchronous video recordings whilst treadmill running. At this point, the clarity of the data was promising enough to warrant running the analytical processing steps with the anticipation of quantifying the running gait movement wave to gain some context.

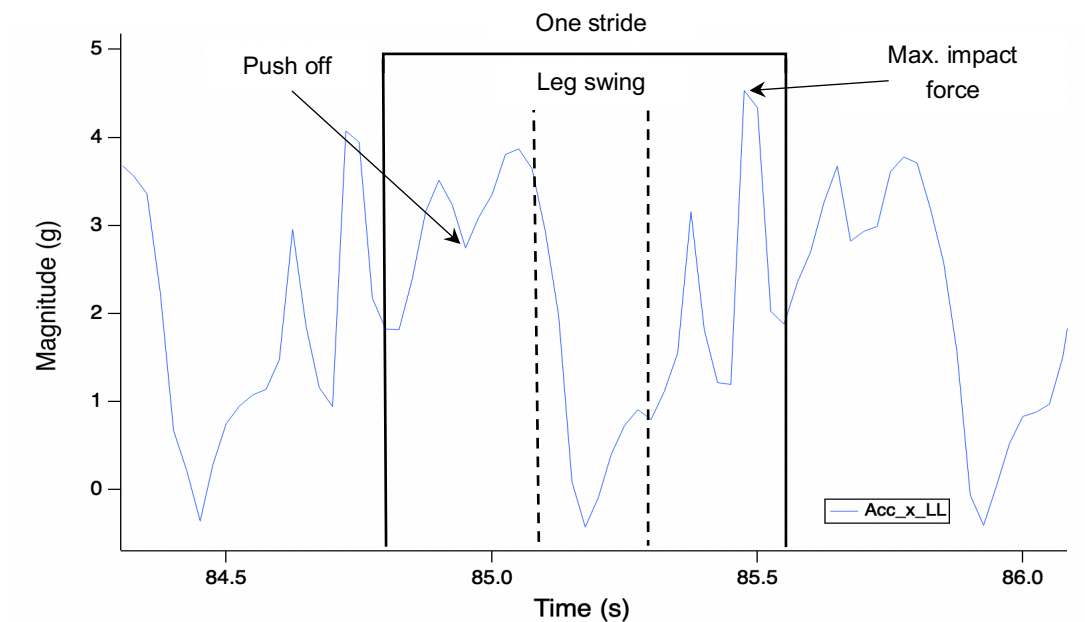


Figure 33: Two strides from the x-axis movement wave recorded via the blue accelerometer (Ac_{x_LL}) during a running trial at 16 km/h. It is possible to identifying calculable gait parameters; push off, leg swing and maximum impact force (Barnes, 2017).

As only the radial (x-) axis data were to be discussed, the two x-axis movement waves, one from each wearable device (red and blue) were extracted (General methods, 2.2). From the 120 second steady state segment at 16 km/h, a 100 second epoch was sectioned and graphed (Figure 34) for analysis using the FFT, CDF, ACF and CCF. Followed this, a statistical analysis (Statistical testing, 2.2.4) was conducted on device colour (red and blue) and placement style (strict or varied).

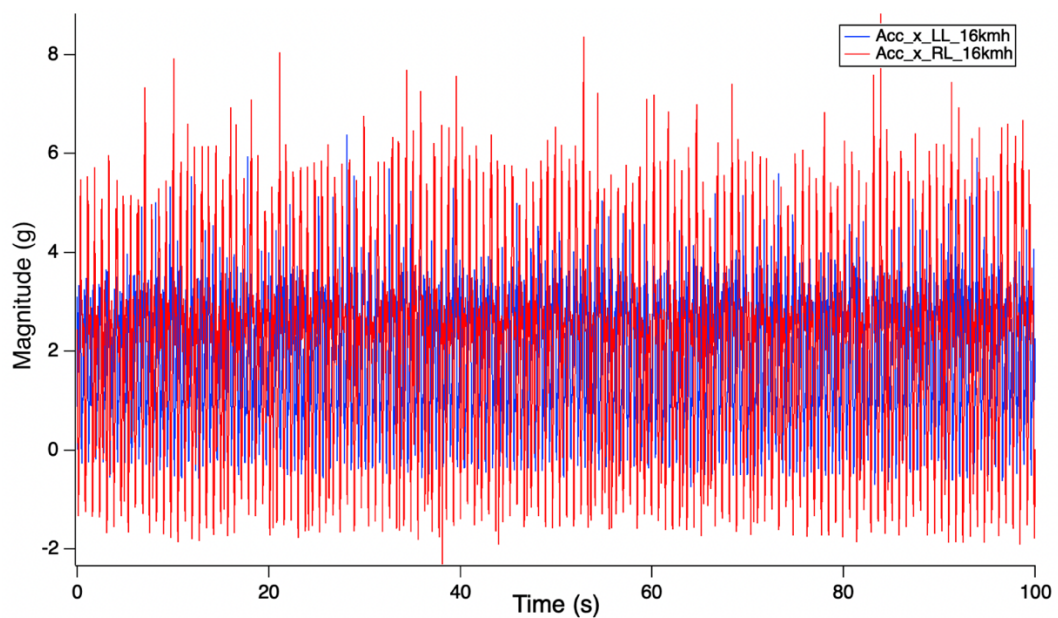


Figure 34: Raw accelerometry wave for the x-axis for a 100 second sample of running at 16 km/h from the LL and RL, where the blue Acc_x_LL wave is for the accelerometry x-axis movement wave of the left leg (LL), and red Acc_x_RL is the same for the right leg (RL) which was extracted from Figure 32.

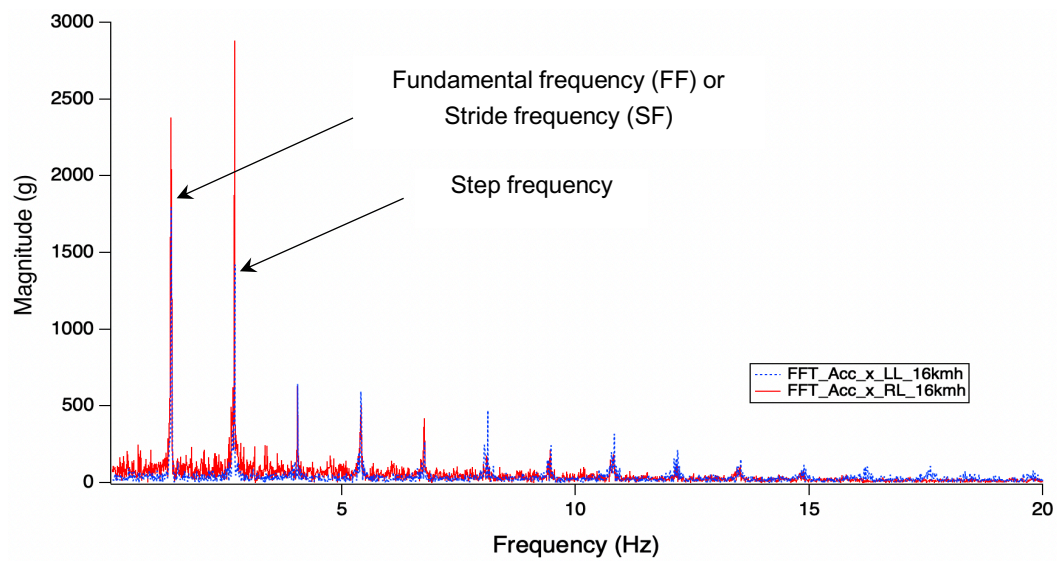


Figure 35: FFT in the frequency domain from a 100 second sample of running at 16 km/h where blue *FFT_Acc_x_LL* represents the FFT wave for the accelerometry x-axis movement wave of the left leg (LL), and red *FFT_Acc_x_RL* is the same for the right leg (RL) from Figure 34. FF is Fundamental Frequency in Hz and SF is stride frequency in Hz.

The FFT is an analytical technique used to distinguish movement data from noise through displaying separate harmonics, thus enabling for the identification of associated components of a movement pattern through their magnification. Within this study, there was always a double peak present on the FFTs. This could be attributed to the impact of the opposite leg being picked up by the accelerometer, therefore, the FF peak was half the frequency of the second peak which represented the cadence. The LL and RL FF were the same in all trials for strict 1.36 ± 0.01 Hz and varied placement 1.38 ± 0.03 Hz meaning there was an enhanced ability to repeat the same stride-to-stride pattern on the LL, whereas the RL had greater stride-to-stride variability (Figure 35).

This variability, known as gait complexity, is demonstrated through the number of harmonics present in the sample. More harmonics equate to more gait variability, ergo, increased gait complexity (Barnes, 2017). In this case, the RL showed a higher level of movement complexity than the LL. To quantify gait complexity, the FFT was analysed using the CDF.

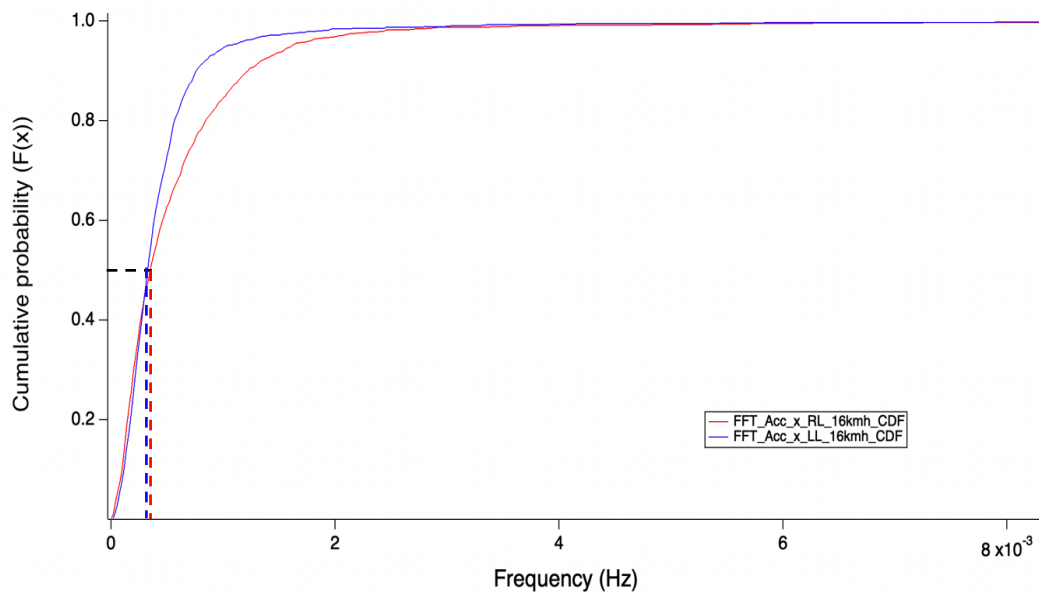


Figure 36: CDF of LL (blue) and RL (red) FFT during RE protocol at 16 km/h with black dashed line demonstrating 0.5 CDF probability and first blue dashed line representing LL normalised frequency and second red dashed line RL normalised frequency.

Gait complexity has an inverse relationship with SP. The mean SP of the RL for both placements (strict 0.0004128 ± 0.0000828 Hz, varied 0.0004021 ± 0.0000573 Hz) had a higher movement complexity equating to a higher SP score, meaning lower gait quality than the LL for both placements (strict 0.0003758 ± 0.0000472 Hz, varied 0.0003038 ± 0.0000394 Hz). The CDF from one trial (Figure 36) shows the LL (blue line) and RL (red line) cumulative probability, SP is extracted from 50% (shown by the red and blue dashed

lines). This was supported by the qualitative inspection of the FFT, where between 0-5 Hz, the RL (red) movement wave showed an excess of small magnitude peaks that are absent in the LL (blue) movement wave. This qualitative approach indicates that the participant repeated the same cadence with a similar movement pattern and magnitude per stride on the LL than the RL.

The repeated measures ANOVA using Greenhouse-Geisser (as sphericity could not be assumed) demonstrated that there was a statistically significant main effect on SP between limbs whilst using the same device ($F(1,17) = 6.953$, $P = .017$, partial $\eta^2 = .290$). This means that the movement pattern exhibited between legs is fundamentally different. Thus, it may not be possible to compare legs to one another unless using pre- and post-measurements. Moving forward, using the mean of both limbs combined will give a better approach to the analysis, however, further investigation is needed to establish firm relationships within the data. This brings the ACF and CCF into contention as in this context they are used to analyse the differences between the two wearable device movement waves to investigate gait symmetry between the LL and the RL.

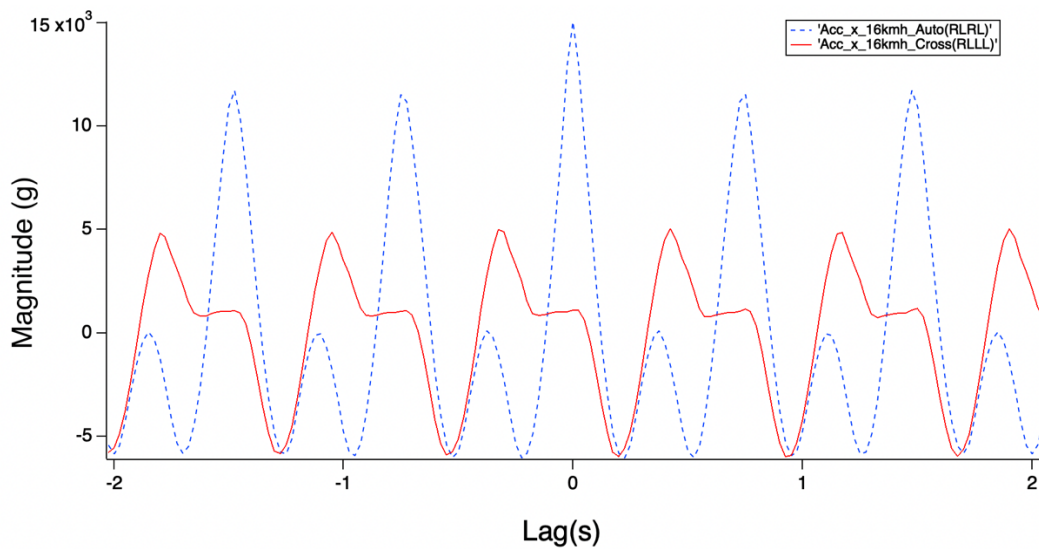


Figure 37: Auto-correlation of the RL vs RL (blue line) against the cross-correlation of the RL vs LL (red line) of x axis data during the RE protocol at 16 km/h. Where Acc_x_16kmh_Auto (RLRL) is the original 100 s epoch of the accelerometry wave for the RL that has been correlated against itself (auto-correlation) and Acc_x_16kmh_Auto (RLLL) is the original 100 s epoch of the accelerometry movement wave for the RL that has been correlated against the accelerometry wave for the LL (cross-correlation).

Gait symmetry was quantified from the stride-to-stride variation determined using the CCF and ACF. This study found that in every case, the cross-correlation two peaks magnitudes (left side 4968 g and right side 5047 g) surrounding the auto-correlation, was lower in amplitude and were dissimilar in shape compared to the central frequency peak of the auto-correlation (15054 g) demonstrating stride-to-stride variation between limbs.

The R-score for the strict placement (LL 67.5±10.3%, RL 52.2±10.8%) was lower than for varied placement (LL 74.5±8.9%, RL 61.4±11.3%) by 7% in the LL and 9.2% in the RL. This unexpectedly demonstrated the varied placement having smaller stride-to-stride variation between limbs than the strict placement, thus, better gait symmetry. A paired samples t-test show a statistically significant difference ($t(7) = 8.098$, $P \leq .001$) between the LL

(69.6%±9.5%) and RL (53.1±9.1%) R-scores captured using the blue device. This supports the notion above that the differences between the devices are significant, thus, using the cross- and auto- correlation to calculate gait symmetry is not the appropriate analytical measure for this data. Therefore, we will only continue to use the FFT for FF and the CDF for SP using the mean of both the LL and RL (Table 4).

Table 4: Descriptive statistics for the strict and varied placement of the wearable devices and the analytical processing techniques. Where N = number of participants, S.D. = standard deviation and S.E. = standard error, LL is left leg and RL is right leg. .

Placement style	Analytical technique	N	Average (Hz)	S.D.(Hz)	S.E. (Hz)
Strict	Fundamental Frequency	15	1.36	0.01	0.00
	Spectral Purity LL	15	0.0003758	0.0000472	0.0000122
	Spectral Purity RL	15	0.0004128	0.0000828	0.0000221
Varied	Fundamental Frequency	16	1.38	0.03	0.01
	Spectral Purity LL	16	0.0003038	0.0000394	0.0000099
	Spectral Purity RL	16	0.0004021	0.0000573	0.0000143

2.13.1. PLACEMENT STYLE AND DEVICE COLOUR ON

FUNDAMENTAL FREQUENCY (FF) AND SPECTRAL PURITY (SP)

The repeated measures ANOVA using Greenhouse-Geisser (as sphericity could not be assumed) demonstrated that there was no statistically significant main effect on FF for placement style or device colour (placement*colour) ($F(1, 5) = 2.597$, $P = .168$, partial $\eta^2 = .342$). This shows the blue and red wearable devices produced similar FF scores throughout the repeated trials,

therefore the FFT appears to be suitable as a measure to quantify the FF of running gait.

The repeated measures ANOVA using Greenhouse-Geisser (as sphericity could not be assumed) demonstrated that there was no statistically significant main effect on SP for placement style or device colour (placement*colour) ($F(1, 4) = 4.128$, $P = .110$, partial $\eta^2 = .511$). This shows the blue and red wearable devices produced similar SP scores when LL and RL values were combined throughout the repeated trials, therefore the CDF appears to be a suitable measure to quantify the SP of running gait.

2.14. LIMITATIONS

Some limitations of this study include a small sample size, small test-retest number, imbalanced randomisation groups and using two experienced male runners. It is understood that when testing participants, adaptations to their running technique can consciously or subconsciously occur to accommodate for the change in footwear and the impact of equipment such as fitted accelerometers and locomoting on a treadmill without forward progression. Participants wearing the VFN% for the first time may have had their running style adversely affected which we attempted to reduce with a familiarisation period. We will attempt to address some of these limitations in the next study, where possible, to broaden the applicability of the data.

2.15. CONCLUSION

Overall, the blue and red wearable devices are reliable for collecting running data in repeated trials up to 16 km/h. The movement data gained from these trials is sensitive enough to identify specific gait features at high speed. The FFT was a reliable tool for identifying FF and harmonics present within the movement wave. The CDF was a reliable tool for quantifying SP, however, only when the LL and the RL were combined. The CCF and ACF are not suitable analytical techniques for accelerometry running data collected from these wearable devices. As the novel element of this project is the combination of the analytical processing techniques to quantify gait, the tools will take a name that sums up their function, hence, the Global gait analysis Tool or GaiT. The term global defines the overall quantification of gait, rather than the segmentation and individual quantification of gait characteristics as is seen frequently throughout the literature.

2.15.1. *NEXT STEPS*

The next step in this project is to understand if GaiT can quantitate running gait quality whilst running over a variety of inclines. We intend to investigate how accelerometry and GaiT can be linked to performance.

CHAPTER THREE

3. STUDY 4: NIKE® VAPORFLY ZOOMX NEXT% RUNNING SHOES HAVE RUNNING ECONOMY BENEFITS OVER VARIOUS INCLINES COMPARED TO CONVENTIONAL RUNNING SHOES

In chapter three, study four examined the running economy (RE) benefit or penalty produced in the Nike® Vaporfly ZoomX Next% (VFN%) in comparison to a conventional running shoe, the Saucony® ProGrid Jazz 12 (JAZ) across various inclines during treadmill running at 12 km/h. Our parametric analysis confirmed the VFN% demonstrated a statistically significant RE benefits compared to the JAZ over all inclines. A novel discovery unveiled the diminishing return for RE benefit with increasing incline, as supported by the exponential decay model. The critical finding of the diminishing return was a fixed RE penalty due to mass and a fixed RE benefit due to the VFN%'s midsole technology comprising of the ZoomX foam and the carbon-fibre midsole plate. The practical application of these findings suggests a noteworthy average 3.8% RE benefit can be achieved whilst using the VFN% over a marathon course with varied elevations. Future research should explore the relationship between RE benefit, performance, and gait using accelerometry. In summary, our study not only validated the RE benefit whilst running in the VFN% over conventional running shoes but also provided nuanced insights into the impact of incline.

3.1. INTRODUCTION

This chapter will focus on capturing data that can be used to validate Gait calculated from accelerometry captured during running. A physiological measurement that can quantitate running performance will be used to explore possible relationships with running accelerometry data.

3.1.1. *RUNNING ECONOMY (RE)*

Running economy (RE) as defined by $\dot{V}O_{2\text{submax}}$, has been accepted as the universal measurement for comparing the economy of endurance activities and represents the combination of neuromuscular, biomechanical, metabolic and cardiorespiratory components of running gait without giving insight into how energy expenditure is partitioned between processes. RE provides a relative measure of overall running efficiency. It is often quantified using masked cardiopulmonary exercise testing (CPET), determined by the submaximal volume of oxygen uptake ($\dot{V}O_2$) in millilitres per kilogram of body weight per minute (ml/kg/min) at a given velocity, (often 16 km/h), or to make it comparable across any speed. A higher value of $\dot{V}O_2$ represents a lower RE. RE is also inversely related to metabolic cost, therefore, as metabolic cost increases, RE decreases (higher $\dot{V}O_2$ measurement), which in turn would lead to a slower performance time.

RE can be influenced chronically through training, or through acute interventions such as footwear, (Barnes and Kilding, 2015, 2019; Martens *et al.*, 2018; Hunter *et al.*, 2019; Senefeld *et al.*, 2021). Small changes in RE

are meaningful, where a 3% improvement in RE is expected to translate to a 1.97% faster running velocity, meaning an elite runner with a 2:04 marathon pace could achieve a 2:01:36 marathon time (Kipp, Kram and Hoogkamer, 2019).

3.1.2. *BREAKING2 CAMPAIGN*

The Nike® Breaking2 Campaign (Nike® Inc., 2016) was held on 6th May 2017, which facilitated three world-class distance runners in the pursuit of the sub two-hour marathon record using targeted performance improvement strategies and scientific innovation. In addition to an ideal formation of pacers, ad libitum fluids, ideal climate, and course, Nike® Inc., also unveiled their new Nike® Vaporfly (VF) elite running shoe. This running shoe combined a novel lightweight midsole material with an embedded carbon-fibre midsole plate with increased LBS (Healey and Hoogkamer, 2021; Hunter *et al.*, 2022).

Nike® Inc's., research team calculated a 01:59:59 (hh:mm:ss) marathon required an average speed of 21.1 km/h (5.9 m/s), being 2.56% (0.1 m/s) faster with a 2.7% reduction in RE, than Kimetto's world record marathon time of 02:02:57 (20.6 km/h or 5.7 m/s) (Hoogkamer, Kram and Arellano, 2017). At this event, Eliud Kipchoge ran an unofficial men's world record marathon time of 2:00:25. However, it was not until the Ineos challenge on 12th October 2019 when Kipchoge ran 01:59:40 in Vienna (Hoogkamer, Kipp and Kram, 2019) and only one day later, on 13th October 2019, Brigid Kosgei ran 02:14:04 at the Chicago marathon, breaking the 16-year women's marathon

world record held by Paula Radcliffe. Kipchoge and Kosgei had an important commonality, they both raced in the new Nike® series of running shoe (Nike® Vaporfly prototype (VF), Nike® Vaporfly ZoomX 4% (VF4%), Nike® Vaporfly Next% (VFN%), plus other modified models), which are known to encompass novel energy saving innovations (Burns and Tam, 2020).

The VF prototype achieve a 4.01% RE improvement through a reduction in the metabolic cost of level running compared to conventional running shoes (Hoogkamer *et al.*, 2018). Now, the VF series dominates elite and recreation running, holding the largest amount of personal best times and world records alike (Quealy and Katz, 2019; Whiting, Hoogkamer and Kram, 2022). This performance improvement is due to the embedded carbon-fibre midsole plate, the curvature of the carbon-fibre midsole plate, the midsole material, and the midsole thickness (Hoogkamer, Kipp and Kram, 2019; Healey and Hoogkamer, 2021; Senefeld *et al.*, 2021). However, there remains little understanding of the performance benefit for each component of the midsole.

3.1.3. *RUNNING ON AN INCLINE*

The biomechanical mechanisms underlying the 10-15% higher oxygen uptake during uphill running, whilst maintaining the same speed, are complex and multifactorial (Snyder and Farley, 2011; Snyder, Kram and Gottschall, 2012; Whiting, Hoogkamer and Kram, 2022). The additional energy expenditure comes from the muscular work required to lift the body uphill against gravity. Furthermore, uphill running requires alterations in running technique, including shorter SL, increased ground contact time (GCT), and

greater range of motion at the ankle, knee, and hip joints (Saunders *et al.*, 2004).

The carbon-fibre midsole plate in the VF series enhances LBS, transferring force more efficiently from IC to TO during running, therefore minimising energy expenditure and improving RE. Additionally, the heightened LBS reduces movement at the MTP joint, resulting in additional energy savings and further enhancements in RE. The carbon-fibre midsole plate appears to mimic the mechanisms experienced during uphill running, which are understood to modify running posture, prompting a forefoot IC pattern. This modification maximises the lever effect by relocating the fulcrum of the lever towards the distal end of the foot (Barnes and Kilding, 2019; Nigg, Cigoja and Nigg, 2020; Whiting, Hoogkamer and Kram, 2022, 2022).

A 1.01% RE penalty was measured to occur because of running up a 5% incline (2.82% RE benefit) compared to running on the level (3.83% RE benefit) confirming the VF4% had a negative linear relationship for RE benefit over a conventional running shoe versus increasing incline. This drop in RE benefit is thought to be associated with the decreased ESE usage and return of the VF4%, meaning the body generates additional energy to maintain performance when running up an incline (Whiting, Hoogkamer and Kram, 2022).

3.1.4. RUNNING SHOE COMPOSITION

Joubert and Jones, (2022) drew on the work of Worobets *et al.*, (2014) explaining how thermoplastic polyurethane (TPU) midsole foam found in

many of the adidas® branded models of shoes without a carbon-fibre plate improved RE by 1% compared to traditional ethylene-vinyl acetate (EVA) foam in conventional shoes. However, recent research has been directed toward a thicker foam midsole in the VFs which uses polyether block amide (PEBA), embedded with a full-length carbon-fibre midsole plate (Figure 38) (Hoogkamer *et al.*, 2018; Barnes and Kilding, 2019; Hunter *et al.*, 2019; Hébert-Losier *et al.*, 2022).

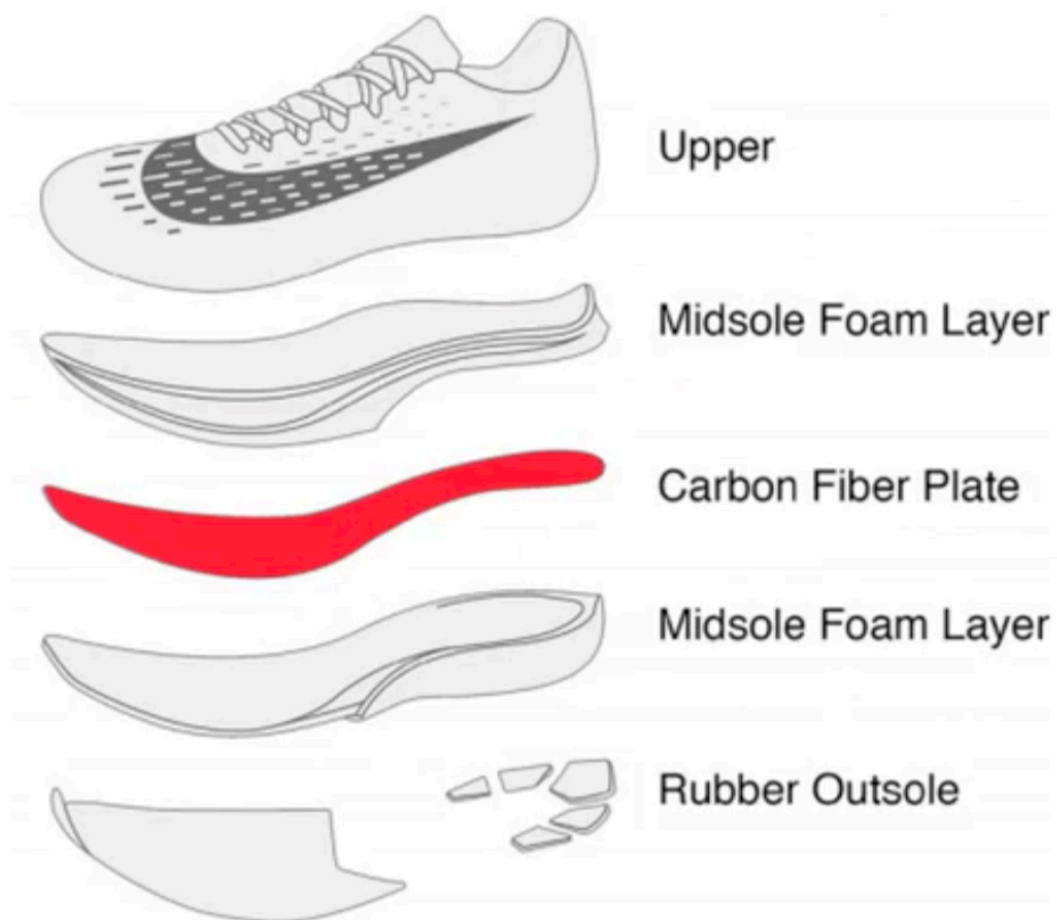


Figure 38: Breakdown of the Nike® Vaporfly (VF) running shoe build composition which contains the upper, upper midsole foam layer, carbon-fibre midsole plate, lower midsole foam layer and rubber outsole (Healey and Hoogkamer, 2021).

Many major running shoe companies have attempted to integrate such technological innovations to include a lightweight and resilient, thick midsole and a component that increases LBS, like a carbon-fibre midsole plate (Hunter *et al.*, 2019).

The ProGrid Jazz 12 (JAZ) (Figure 39) became Saucony®'s best value running shoe for the technology incorporated and weigh approximately 200 g more per pair than the VFN% (c. 300 g per JAZ running shoe vs c. 200 g per VF running shoe) (Table 5) (Colloff, 2022). This sable, neutral running shoe contains a compression moulded ethyl-vinyl acetate (EVA) midsole with a High Rebound Compound (HRC) Strobel Board with ProGrid™ at the heel and a Super Rebound Compound (SRC) impact zone with Respon-Tek™ in the forefoot linked by a midfoot support bridge. This impact deflection technology is claimed to attenuate shock ensuring a smooth heel to toe transition.



Figure 39: Saucony®'s ProGrid Jazz 12, schematic view of the running shoe construction (Saucony® Inc., 2017).

Table 5: Mass of lead weight added to the shoelaces of each shoe based on size (Colloff, 2022).

Nike® Vaporfly Next% (UK size)	Saucony® ProGrid Jazz 12 (UK size)	Mass Difference (g)
5.5	5	92
6.5	6	97
	7	100
7.5	8	109
9	9	116
10	10	101
11	11	105

Overall, although uphill running serves as a challenging and effective training method, alterations in running mechanics may amplify the energy expenditure associated with running. This, in turn, contributes to the observed decrease in RE during uphill running. A plethora of studies

demonstrated the 4.01% RE benefit of the VF4% on the level, however, there is limited evidence on an incline using the VFN%. This is despite the new running shoe having an additional 15% ZoomX midsole foam that should further facilitate ESE storage and return, providing an additional RE benefit compared to the VF4% (Hunter *et al.*, 2022). When compared to the Saucony® JAZ that is 200 g in total heavier, we would assume that there will be an additional 1% RE benefit for the VFN% over and above the conventional running shoe (JAZ).

3.1.5. *AIM*

The aim of this study will investigate the effect of various inclines on RE whilst running in the VFN% compared to a conventional running shoe (JAZ).

3.1.6. *HYPOTHESES*

A RE benefit in the VFN% compared to the JAZ when running uphill should be achieved, however, at a lesser effect than level running due to the altered mechanics of running and the running shoe, therefore:

1. The VFN% will provide a minimum 4.01% RE saving on the level (0% incline), compared to the conventional shoe.
2. The VFN% will provide a minimum 2.82% RE saving for uphill running (5% incline), compared to the conventional shoe.
3. The VFN% will have a negative linear relationship showing a decreasing RE benefit as incline increases.

4. The VFN% will provide an additional 1% RE benefit over the JAZ on all inclines because of the lower mass of the VFN%.

3.1.7. OBJECTIVES

A metabolic test was used to assess treadmill running performance via running economy (RE). The objectives of this study were to:

1. perform CPET to determine the rate of oxygen ($\dot{V}O_2$) uptake and rate of carbon dioxide ($\dot{V}CO_2$) production, enabling the calculation of gross RE.
2. conduct four treadmill inclines (0%, 1%, 3% and 5%) at 12km/h.
3. repeat objective 1. for both the VF and control running shoe (JAZ).

3.2. METHOD

3.2.1. *GENERAL METHODS*

Uniform methods were consistently employed throughout this thesis, consolidated for clarity in the General Methods section. For more comprehensive insights, consult the General methods (2.2).

3.2.2. *STATISTICAL POWER*

A standard online power calculation requiring mean and S.D., results from the test-retest study (Results and discussion, 2.13) concluded that 18 participants were needed to detect whether a statistical significance would be present within the data of the new study at the level of $P = 0.05$.

3.2.3. *PARTICIPANTS*

18 participants; $n=6$ females (age 25.68 ± 4.18 years, mass 57.68 ± 6.54 kg, height 167.97 ± 4.10 cm) and $n=12$ males (age 37.37 ± 12.26 years, mass 76.54 ± 10.95 kg, height 181.29 ± 6.12 cm). There were statistically significant differences between gender for age ($P = .009$), height ($P \leq .001$) and mass ($P \leq .001$) frequently attributed to the physiological differences in RE measurements (Barnes and Kilding, 2015) Two participants did not complete JAZ 0% and VFN% 0%, and one participant did not complete JAZ 5% and VFN% 5%. Participants fitted a UK shoe size 5.5, 6.5, 7.5, 9, 10 or 11.

Table 6: Participant descriptive statistics.

Descriptive		Mean (\pm S.D.)	S.E.
Total (n)		18	
Age (years)		33.5 \pm 11.6*	2.7
Mass (kg)		70.3 \pm 13.2*	3.1
Height (cm)		176.9 \pm 8.4*	2.0
BMI (kg/m ²)		22.4 \pm 3.3	0.8
Performance (<40 min 10 km)	Yes	10 (55.6%)	
	No	8 (44.4%)	
Order	VFN% vs JAZ	6 (33.3%)	
	JAZ vs VFN%	12 (66.7%)	

*There are statistically significant differences between gender for age ($P = 0.009$), height ($P \leq .001$) and mass ($P \leq .001$).

3.2.4. PROTOCOL

Immediately before each test session, the METAMAX 3B metabolic system (©CORTEX Biophysik GmbH, Leipzig, Germany) was calibrated with a reference gas containing known concentrations of 17% O₂ and 5% CO₂ (to ensure the concentrations of the gases in exhaled air lies in the range between the calibration gas and room air). A 3.0 L syringe (Hans Rudolph Inc., Kansas City, MO, USA) was used to calibrate the turbine to ensure accurate volume measurements. The participant's mass (*kg*) and height (*m*) were recorded before, a Polar Bluetooth smart heart rate monitor (Polar© Electro, Kempele, Finland) was fitted, resting heart rate (RHR) noted and maximal heart rate (HRM) calculated (200-age) (Sarzynski *et al.*, 2013). Finally, a breathing mask was fitted (Hans Rudolph Inc., Kansas City, MO, USA) and connected to the METAMAX 3B which was worn in a harness on the participant's torso. The METAMAX 3B calculated the volumes of O₂

inspired and CO₂ expired for every breath and averaged every 10 seconds. These data were output in real-time wirelessly to a laptop. Two running shoe types were randomly allocated; the Nike® Vaporfly ZoomX NEXT% (VFN%) and the Saucony® ProGrid Jazz 12 (JAZ) as the conventional running shoe. Immediately before the warm up, a five-minute static standing measurement was recorded.

A 10-minute self-structured warm up and familiarisation period was completed on the Pulsar treadmill (H/P/ cosmos sports & medical gmbh, Nussdorf-Traunstein Germany) with the aim of reaching 12 km/h at a 5 % incline. The warm up was followed by four intervals at 12 km/h at inclines of 0, 1, 3 or 5 % (Figure 40), where participants were blind to the randomised incline sequence by covering the incline display on the treadmill. Following the warm up, the participant ran at each incline until their $\dot{V}O_2$ plateaued. If the $\dot{V}O_2$ continued to rise and a plateau did not occur after seven minutes the interval was terminated, moving on to the next stage of the protocol. A 100 second plateaued $\dot{V}O_2$ recording with the respiratory exchange ratio (RER) (ratio of the CO₂ exhaled divided by the O₂ inhaled) remaining ≤ 1 was necessary before the interval could be terminated. This protocol was repeated on the second randomly selected running shoe type (Figure 40). At the end of the eight intervals a cool down was offered before the equipment was removed.

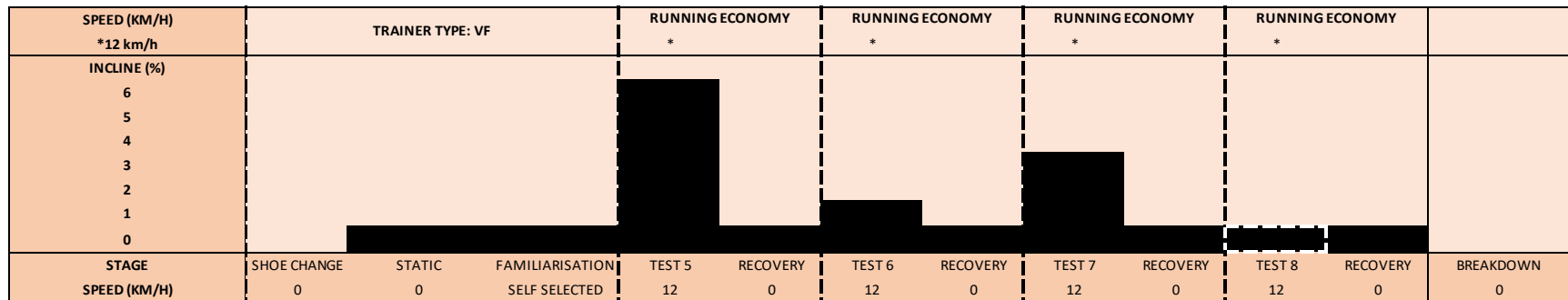
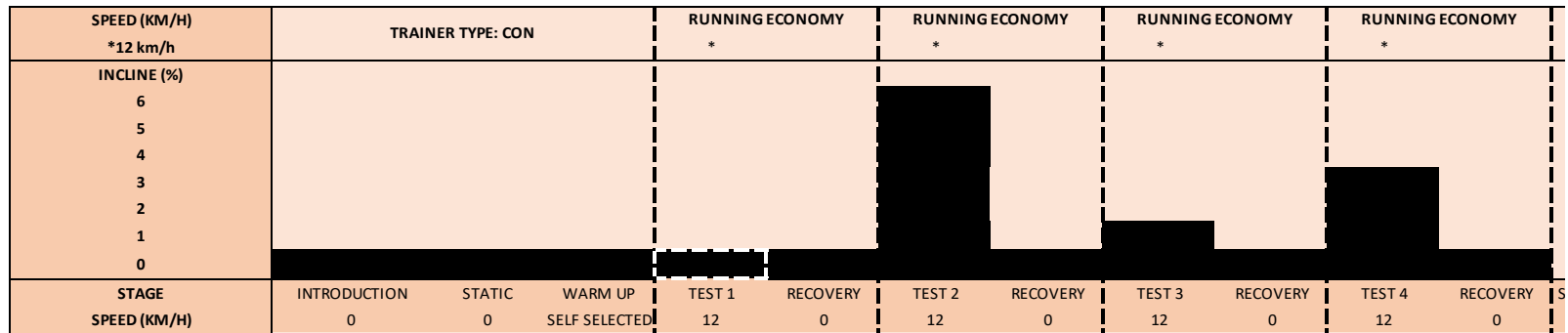


Figure 40: Incline protocol schematic. The full protocol demonstrating time spent testing the first, followed by the second randomised running shoe, at 12 km/h over four randomised intervals.

3.2.5. DATA EXTRACTION

Consistent data extraction methods were applied to each wearable device prior to commencing the data processing phase. For additional details, please refer to the section on Data extraction (2.2.5).

3.2.6. DATA PROCESSING

CALCULATION OF RUNNING ECONOMY (RE)

$\dot{V}O_2$, $\dot{V}CO_2$ and RER were imported from the METAMAX 3B into Igor Pro (v8, WaveMetrics, Oregon, USA). Outlier data points are common in breath-by-breath experiments, for example, through coughing or talking, hence, where the data point variation exceeded the local median by a value >0.1 l/min for $\dot{V}O_2$ and having a ratio >0.01 for RER, seven-point median smoothing was applied to the outlying value with the median of the neighbouring seven values (three either side of the outlier). If outliers remained, the process would be repeated with a 13-point median smooth. If the processed data still contained large amounts of visible noise (peaks) outside of the normal range, the entire interval was removed. The participant's baseline average metabolic cost was calculated from 100 seconds of static standing $\dot{V}O_2$ data, taken at an appropriate plateau at least 10 seconds from the start and end of the 100 s data sample. This was repeated for the active data recording where gross RE¹⁵ was calculated (Equation 19) when $\dot{V}O_2$ stabilised, or plateaued,

¹⁵ Gross RE takes into consideration body weight as opposed to absolute RE which does not (Barnes and Kilding, 2015).

with an RER ≤ 1 (Hoogkamer, Kram and Arellano, 2017; Hoogkamer *et al.*, 2018; Healey and Hoogkamer, 2021; Whiting, Hoogkamer and Kram, 2022).

Equation 19: Gross RE equation ($\dot{V}O_2$) in ml/kg/min.

(19)

$$\text{Gross running economy (ml/kg/min)} = \frac{(\text{Gross } \dot{V}O_2 \text{ (l/min)} * 1000)}{\text{mass (kg)}}$$

PERCENTAGE RE BENEFIT OR PENALTY

A RE benefit/ penalty (Equation 20) was used to calculate the difference between the RE benefit or penalty of the running shoe types. Expressing the data in this way provided contextualisation of the research findings to the current literature (Hoogkamer *et al.*, 2016, 2018).

Equation 20: Percentage running economy (RE) benefit/ penalty.

(20)

VF RE benefit/ penalty (%)

$$= \left(\frac{\text{JAZ gross } \dot{V}O_2 \text{ (ml/kg/min)} - \text{VF gross } \dot{V}O_2 \text{ (ml/kg/min)}}{\text{JAZ gross } \dot{V}O_2 \text{ (ml/kg/min)}} \right) * 100$$

3.3. RESULTS

3.3.1. *VARIANCE*

Homogeneity-of-variance, demonstrated through normally distributed histograms, was confirmed by Mauchly's Test of Sphericity, $X^2(5) = 3.827$, $P = .576$. Therefore, the null hypotheses were investigated using parametric testing to a statistical significance of $P = 0.05$.

3.3.2. *PARAMETRIC TESTING*

GENDER

A repeated measures ANOVA demonstrated that there was no statistically significant interaction on RE measure for running shoe and gender (running shoe*gender) ($F(1,13) = 0.047$, $P = 0.831$, $\eta^2 = 0.004$), incline and gender (incline*gender) ($F(3,39) = 2.333$, $P = 0.089$, $\eta^2 = 0.152$) and for running shoe, incline and gender (running shoe*incline*gender) ($F(3,39) = 0.358$, $p = 0.784$, $\eta^2 = 0.027$). Therefore, all results were combined and analysed using the two-way repeated measures ANOVA as one larger sample to strengthen the analysis (Appendix L).

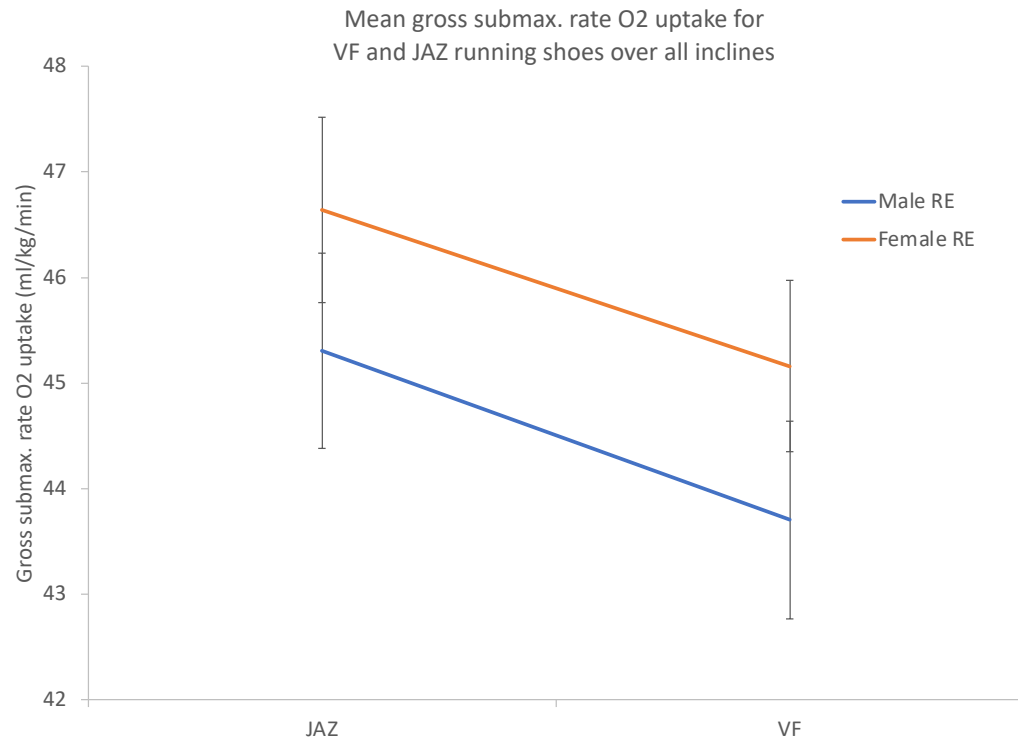


Figure 41: Mean gross rate of submaximal oxygen uptake ($\dot{V}O_2$ ml/kg/min) for the Nike® Vaporfly ZoomX NEXT% (VFN%) and Saucony® ProGrid Jazz 12 (JAZ) running shoes, averaged over all inclines, for males (blue) and females (orange) showing standard error (S.E.). On average, the JAZ had a higher $\dot{V}O_2$ uptake for both males and females than the VFN%.

Table 7: Testing results for $n = 18$ participants for gross $\dot{V}O_2$ (ml/kg/min) for running in the Nike® Vaporfly ZoomX NEXT% (VFN%) and Saucony® ProGrid Jazz 12 (JAZ) running shoes. The table shows the minimum, maximum, mean and standard deviation (S.D.) for each result.

Trainer	Incline (%)	Number of participants (n = female/ male)	Mean (\pm S.D.) ($\dot{V}O_2$ ml/kg/min)	RER (\pm S.D.)
JAZ	0	16 (5/11)	40.31 (3.16)	0.86 (0.04)
	1	18 (6/12)	42.40 (2.81)	0.89 (0.05)
	3	18 (6/12)	47.56 (2.90)	0.92 (0.04)
	5	17 (6/11)	52.72 (2.61)	0.95 (0.05)
VFN%	0	16 (5/11)	38.52 (3.03)	0.84 (0.04)
	1	18 (6/12)	40.68 (2.81)	0.86 (0.04)
	3	18 (6/12)	46.24 (3.23)	0.90 (0.05)
	5	17 (6/11)	51.28 (2.50)	0.93 (0.05)
Difference	0	16	1.79% (1.47)	
	1	18	1.71% (1.97)	
	3	18	1.31% (1.66)	
	5	17	1.44% (1.20)	

TRAINER AND INCLINE INTERACTION ON RUNNING ECONOMY (RE)

A two-way repeated-measures ANOVA demonstrated that there was no statistically significant interaction between running shoe type and incline (running shoe*incline) on RE ($F(3,42) = 0.531$, $P = 0.663$, $np^2 = 0.037$). This means that although there were clear differences in the mean $\dot{V}O_2$ ml/kg/min data (Table 7) the differences between the shoes were equal regardless of incline, hence the benefit of the VFN% was the same at each level and not

significantly better at a certain level. Therefore, the simple effects of running shoe type on RE and incline on RE were used to understand the impact on the data.

The simple effects of the two-way repeated-measures ANOVA demonstrated that there was a statistically significant interaction between mean RE and running shoe type ($F(1,14) = 30.431$, $P \leq .001$, $\eta^2 = 0.685$). To support this, a post hoc pairwise comparison with Bonferroni correction showed a statistically significant difference ($P < .001$) in mean $\dot{V}O_2$ ml/kg/min between the VFN% (44.225 ml/kg/min) and JAZ (45.748 ml/kg/min) (Figure 41). Therefore, the type of running shoe affected RE measure with the VFN% $\dot{V}O_2$ uptake being less than the JAZ.

A two-way repeated-measures ANOVA demonstrated that there was a statistically significant interaction between mean RE measure and incline ($F(3,42) = 467.784$, $P < .001$, $\eta^2 = 0.971$). To support this, a post hoc pairwise comparison with Bonferroni correction showed a statistically significant difference in mean RE measure between running shoe types for each incline (0% = 39.536 ml/kg/min, 1% = 41.434 ml/kg/min, 3% = 46.885 ml/kg/min and 5% = 52.092 ml/kg/min) thus, there was an increase in the $\dot{V}O_2$ uptake as incline increased in both the VFN% and the JAZ (Figure 42).

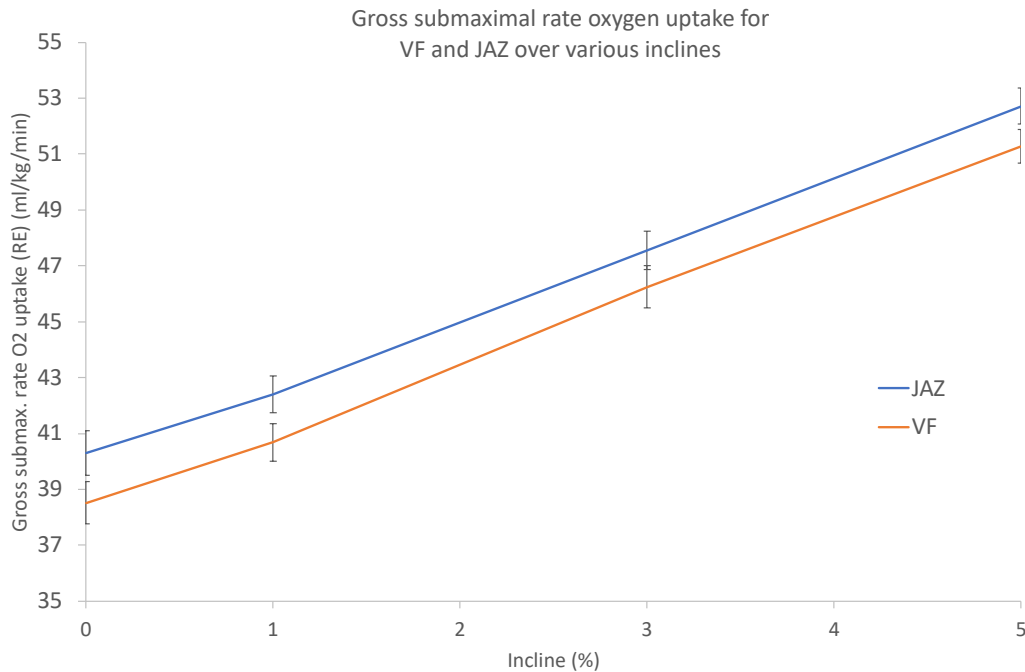
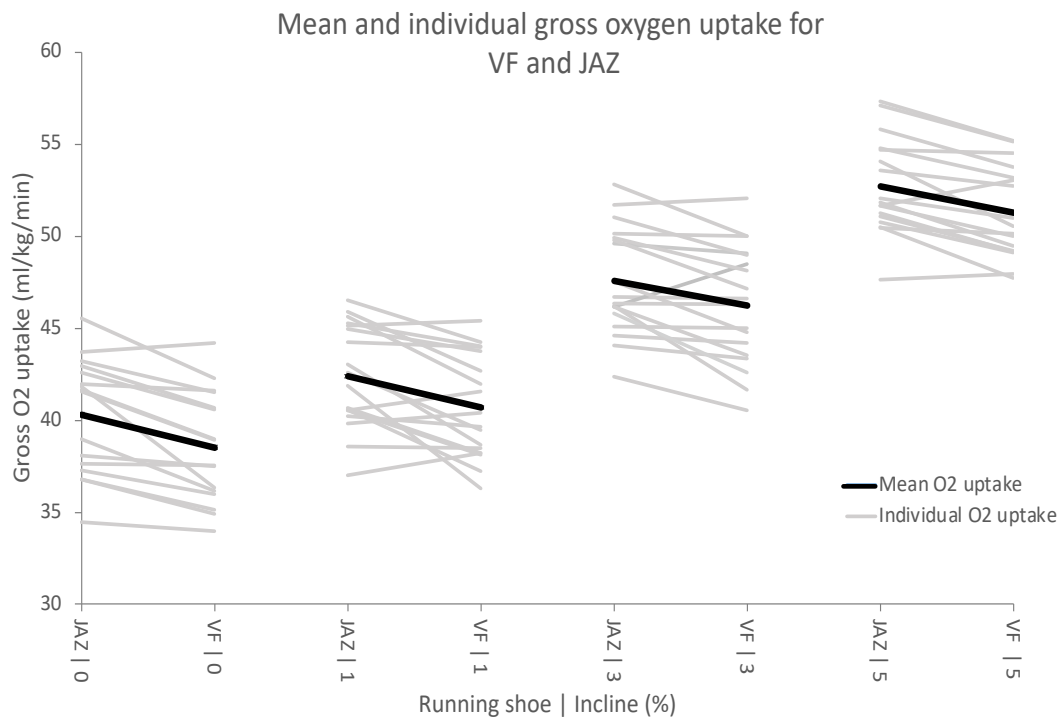


Figure 42: Gross submaximal rate oxygen uptake (ml/kg/min) at 0%, 1%, 3% and 5% incline in VFN% (orange line) and JAZ (blue line) with S.E., bars. Gross $\dot{V}O_2$ uptake was significantly less in VFN% than the JAZ ($P < 0.01$).

The paired t-test demonstrated a strong, positive correlation between the VFN% and JAZ for all inclines; 0% incline $r = .889$, $P < .001$, 1% incline $r = .753$, $P < .001$, 3% incline $r = .858$, $p < .001$, 5% incline $r = .890$, $P < .001$. There was also a statistically significant difference between mean RE measure and running shoe type (VFN% and JAZ) for all inclines; 0% incline $t_{15} = 4.878$, $P < .001$, 1% incline $t_{17} = 3.679$, $P = .002$, 3% incline $t_{17} = 3.348$, $P = .004$, 5% incline $t_{16} = 4.939$, $P < .001$ (Figure 42).



* Demonstrates a significance $p < 0.01$.

Figure 43: Mean and individual gross oxygen uptake ($\dot{V}O_2$ ml/kg/min) between the Nike® Vaporfly ZoomX NEXT% (VFN%) and Saucony® ProGrid Jazz 12 (JAZ) whilst running on a treadmill at 12 km/h at 0%, 1%, 3% and 5%. The black line reports the mean gross $\dot{V}O_2$ of all participants and the grey lines are for each individual participant.

The mean difference $\dot{V}O_2$ of the VFN% over the JAZ at 0% incline was 1.79 ml/kg/min (95% CI [1.01-2.57]), 1% incline was 1.71 ml/kg/min (95% CI [0.73-2.69]), 3% incline was 1.31 ml/kg/min (95% CI [0.48-2.14]), and 5% incline was 1.44 ml/kg/min (95% CI [0.82-2.06]) (Figure 43).

ORDER OF RUNNING SHOE INTERACTION ON RE

A two-way repeated-measures ANOVA demonstrated that there was no statistically significant interaction between mean RE measure and the order that the running shoes were tested (running shoe*order). Where 10

participants (n=10) wore JAZ first (JAZ vs VFN%) and five participants wore VFN% first (VFN% vs JAZ) ($F(1,13) = 2.886$, $P = 0.113$ $\eta^2 = 0.182$). There was no statistically significant interaction on mean RE measure between incline and order running shoes were tested (incline*order) ($F(3,39) = 0.422$, $P = 0.738$ $\eta^2 = 0.031$) meaning the changes in RE over incline was the same with either the JAZ or the VFN% worn first, or running shoe type, incline and the order of running shoe testing (running shoe*incline*order) ($F(3,39) = 0.719$, $P = 0.527$ $\eta^2 = 0.055$), meaning the changes in RE changed by a similar value between each incline, each shoe type and order of wear. To support this, a post hoc pairwise comparison with Bonferroni correction showed no statistically significant difference ($P = 0.556$) in mean RE measure between the order the running shoes were tested (JAZ followed by VFN% = 44.676 ml/kg/min and VFN% followed by JAZ = 45.608 ml/kg/min). Meaning, the randomisation of the trials for incline or running shoe type did not influence RE.

PERFORMANCE ABILITY INTERACTION ON RE

A mixed mode ANOVA demonstrated that there was no statistically significant interaction on mean RE between running shoe type and performance ability (running shoe*performance) ($F(1,13) = 0.636$, $P = 0.439$, $\eta^2 = 0.047$), incline and performance ability (incline*performance) ($F(3,39) = 0.158$, $P = 0.924$, $\eta^2 = 0.012$) (Figure 44), and running shoe type, incline and performance ability (running shoe*incline*performance) ($F(3,39) = 0.914$, $P = 0.443$ $\eta^2 = 0.066$). To support this, a post hoc pairwise comparison with Bonferroni correction showed no statistically significant difference in mean RE

measure and performance (mean “yes” measure = 44.918 ml/kg/min and “no” measure = 45.123 ml/kg/min). Although other studies have used elite athletes for the reduction of confounding variables, the applicability of the data to the real world is reduced, hence we studied a larger range of athletic abilities. Our study found no statistically significant differences in mean RE between sub-elite athletes (those that could complete 10 km in ≤ 40 minutes) and recreational runners (those that could not) over all inclines (Figure 44).

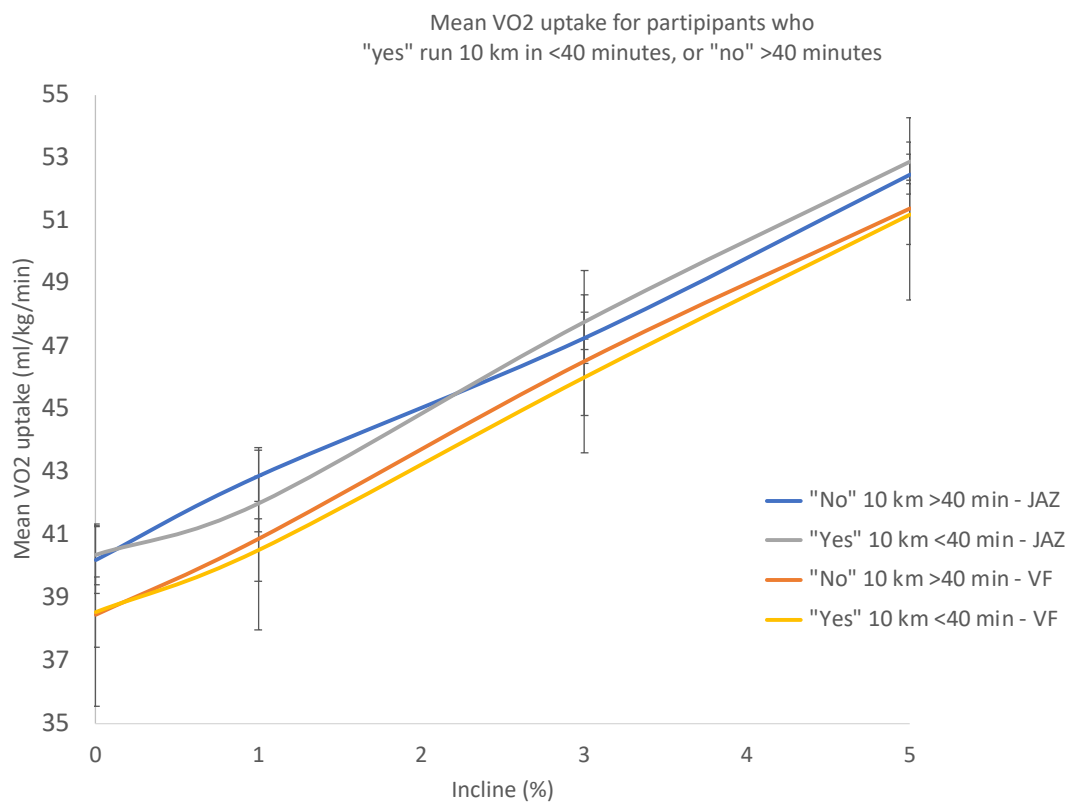


Figure 44: Mean $\dot{V}O_2$ uptake for those that "yes" can and "no" cannot run 10 km ≤ 40 -minute, against various inclines (0-5%). The JAZ and VFN% for yes and no are not significantly different..

PERCENT RE BENEFIT

The mean RE benefit (%) for the VFN% in comparison to the JAZ (thick black line) (Figure 45), demonstrates a 4.37% RE benefit at 0% incline, 3.95% RE benefit at 1% incline, 2.75% RE benefit at 3% incline and 2.70% RE benefit at 5% incline (results table provided in Appendix J). Individual participant's RE benefit or penalty (light grey lines) were plotted to visualise the range of results for each incline with variability of these results being larger than that of the current literature. We used 18 participants with a range of running abilities from -5.0% RE penalty to 13.4% RE benefit, in contrast (Hunter *et al.*, 2019) used 19 participants who showed a range of 0.0% to 6.4% RE benefit and (Hoogkamer *et al.*, 2018) used 18 participants, who achieved 2% to 6% RE benefit, all of which were high-calibre runners.

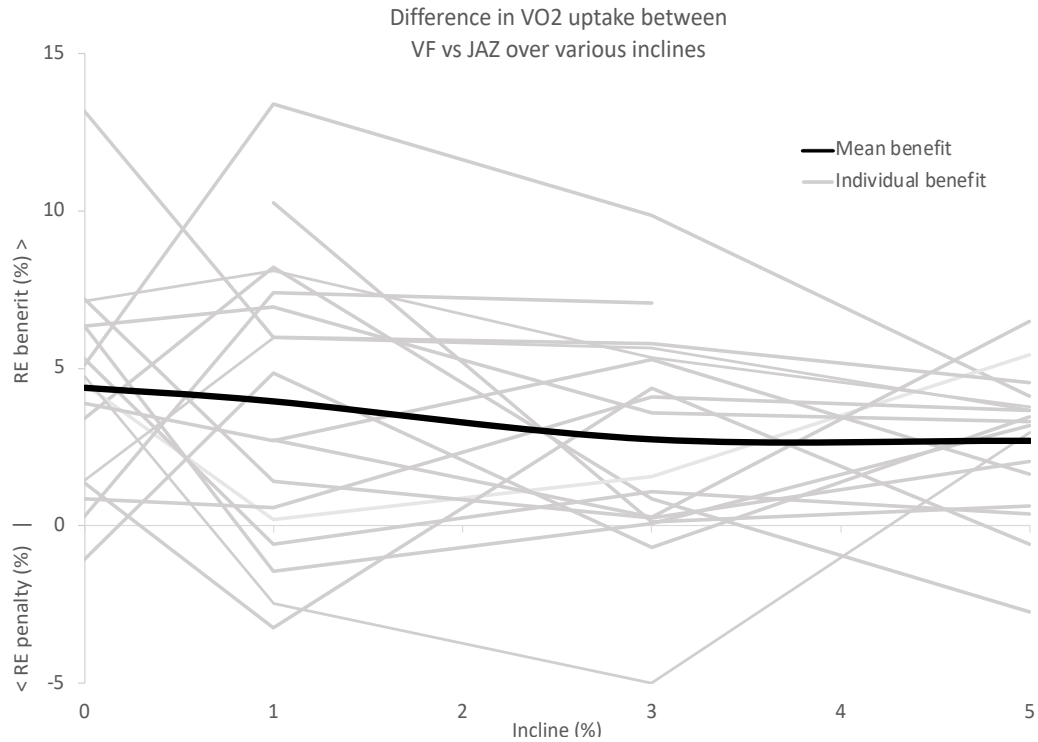


Figure 45: Running economy (RE) benefit/ penalty. The difference between $\dot{V}O_2$ uptake VFN% and JAZ divided by the JAZ to give the benefit of the VFN%. The individual grey lines are for each of the 18 participants with the thick black line being the mean result for all participants.

The RE benefit (%) between the running shoes was significantly different ($P = .01$) between each incline. There appeared to be a gradual decline in RE benefit (%) with increased incline, therefore, the data was modelled using an exponential decay fit (Equation 21) with the final iteration containing a fixed variable for y^0 (defined below) producing the best fit.

Equation 21: The exponential decay function ($F(x)$). Equation demonstrated by the variables; y^0 = fixed constant, a = is a constant ($a + y^0$ = y-intercept (RE benefit), \exp = exponential constant, x = x axis variable (incline), b = decay constant. Thus $y^0 = 2.28$ % RE benefit, $a = 2.16$ % RE benefit such that $A + y^0 = 4.45$ % (close to the measured RE benefit of 4.37 % at 0 % incline) and $b = 2.60$ (% incline).

(21)

$$F(x) = (y^0) + a * \exp^{-x/b}$$

The exponential decay curve accurately predicted RE benefit (%) at its associated incline to infinity (Figure 46). The concatenated table where the asymptote reaches 2.28% at 46% incline, however, there appears to be no further meaningful RE benefit after 16% incline (results table provided in Appendix K).

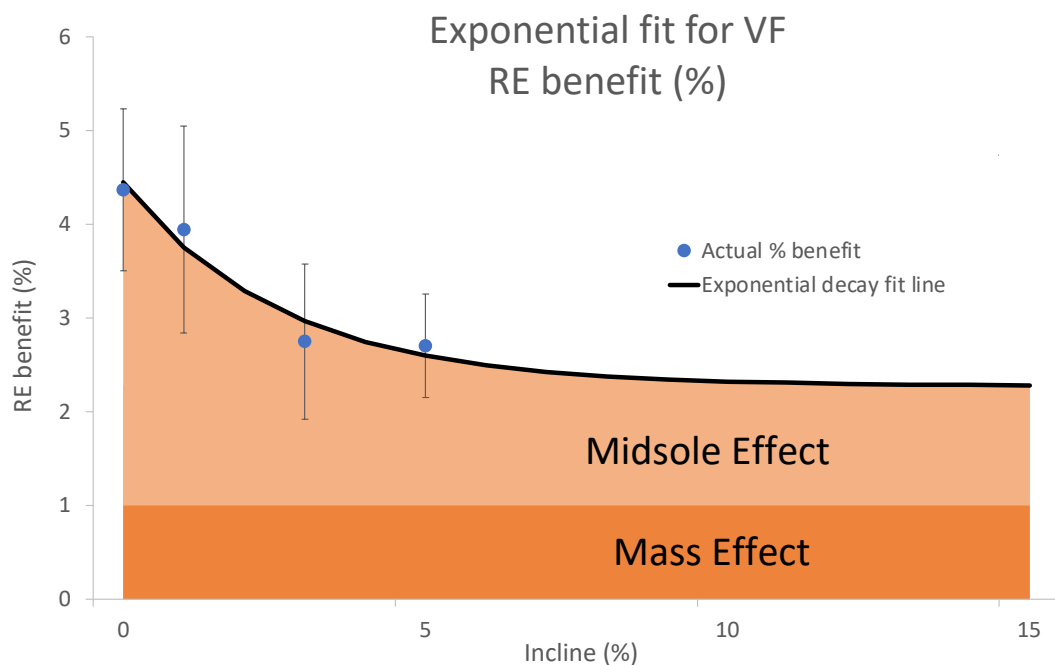


Figure 46: Gross mean $\dot{V}O_2$ uptake difference (%) (blue dots) including standard error bars. The exponential decay fit (black line), where under the fit line depicts the fixed effect of the running shoe; the mass effect being a constant 1% RE penalty per 100 g per shoe of additional running shoe mass, and the midsole effect at 1.3% benefit for the VFN% running shoe regardless of incline.

3.4. DISCUSSION

3.4.1. SUMMARY OF FINDINGS

This study investigated the gross running economy (RE) or rate of submaximal oxygen ($\dot{V}O_2$) uptake between the Nike® Vaporfly ZoomX Next% (VFN%) and the conventional running shoe, the Saucony® ProGrid Jazz 12 (JAZ) during level (0%) and incline (1, 3 and 5%) running on a treadmill at 12 km/h. For level treadmill running (0% incline) at 12 km/h, it was demonstrated that the VFN% achieved a 4.37% RE benefit compared to the JAZ, achieving a 0.36% better RE benefit than the 4.01% RE benefit achieved by the VF prototype, compared to a weight matched conventional running shoe (Hoogkamer *et al.*, 2018). At 1% incline running at 12 km/h, the VFN% achieved a 3.95% RE benefit compared to the JAZ, a 0.12% better RE benefit than the 3.83% RE benefit achieved by the VF4% (Whiting, Hoogkamer and Kram, 2022). The exponential decay model with a fixed y variable (RE benefit) provided a good and appropriate fit for the data acquired during testing, establishing a fixed 2.28% benefit up to ~1616% incline and above. The mass of the shoes contributes to 1% RE penalty out of the 2.28% RE benefit. The midsole effect contributes to 3.4545% RE benefit at 0% incline (4.4545% RE benefit – 1% RE penalty) and drops to 1.28% at ~1616% incline and above (2.28% RE benefit – 1% RE penalty).

3.4.2. *HYPOTHESIS ONE; RUNNING ON THE LEVEL (0%)*

We hypothesised that the VFN% would demonstrate at least a 4.01% RE benefit over the conventional running shoe (JAZ) during level treadmill running (0% incline) at 12 km/h. We demonstrated a 4.37% RE benefit for the VFN% (unweighted) compared to the JAZ.

The 4.01% RE benefit measured from the VF prototype which was weight matched to the adidas® adizero Adios BOOST 2 (Hoogkamer *et al.*, 2018) and a 4.20% RE benefit from the non-weight matched VF4% and a 2.9% RE benefit when weight matched to the adidas® adizero Adios BOOST 3, when tested at 14, 15, 16 and 18 km/h (Barnes and Kilding, 2019). As our study was not weight matched we can apply the 1% RE penalty for every additional 100g of additional mass per running shoe (Hoogkamer *et al.*, 2018; Hoogkamer, Kipp and Kram, 2019; Nigg, Cigoja and Nigg, 2020), meaning the RE benefit at 0% incline was 3.37% when accounting for approximately 200 g (100 g per shoe) of additional running shoe mass for the JAZ (Appendix K). This is a 0.64% lower RE benefit than the 4.01% RE benefit when compared to the adidas® adizero Adios BOOST 2 (Hoogkamer *et al.*, 2018), 0.83% lower RE benefit than the 4.20% RE benefit from the VF4% (not weight matched), and 0.47% higher RE benefit than the 2.90% RE benefit (weight matched) to the adidas® adizero Adios BOOST 3 (Barnes and Kilding, 2019). Our results support the literature for the VFN% producing a RE benefit when compared to the conventional running shoe, JAZ (Hoogkamer *et al.*, 2018; Barnes and Kilding, 2019; Hoogkamer, Kipp and Kram, 2019; Hunter *et al.*, 2019, 2022; Ortega *et al.*, 2021; Hébert-Losier *et al.*, 2022; Joubert and Jones, 2022; Whiting, Hoogkamer and Kram, 2022). However, if we do not

consider weight, our study provides an additional 0.36% RE benefit for the VFN% over the VF4% but when accounting for weight, the RE benefit for the VFN% at 0% incline is less than those reported in the literature, compared to a conventional running shoe. Our study adds to the current literature by establishing that level running in the VFN% produces a greater than 4% RE benefit, as expected, due to the advancements in technology, such as a 15% increase in ZoomX foam content in comparison to the VF4%.

It would be beneficial to have a systematic literature review on the RE differences between the various Nike® series running shoes when weight matched to the conventional running shoes to provide a true representation of the RE benefits of this running shoe series.

3.4.3. HYPOTHESIS TWO; RUNNING ON AN INCLINE (1%, 3% AND 5%)

We hypothesised that the VFN% would demonstrate at least a 2.82% RE benefit during uphill running compared to the conventional running shoe (JAZ). We accepted hypothesis two for 1% incline, with the VFN% achieving a 3.95% RE benefit (not weight matched) compared to the JAZ, a 1.13% greater RE benefit than predicted. Hypothesis two was rejected for 3% incline with a 2.75% RE benefit (not weight matched), 0.07% lower RE benefit than predicted, and finally hypothesis two was rejected for 5% incline with a 2.70% RE benefit (not weight matched), a 0.12% lower RE benefit than predicted. Although these RE benefits are close to that in the current literature, they fall below the predicted 2.82% RE benefit achieved by the VF4% when compared to the Nike® Streak 6 (approximately the same

weight) when running on an incline (Whiting, Hoogkamer and Kram, 2022). As our study tested the VFN%, we anticipated a slightly better performance than the VF4% due to the technological improvements embedded into the VF4%, however, this was not the case on this occasion (Quealy and Katz, 2019; Burns and Tam, 2020; Joubert and Jones, 2022).

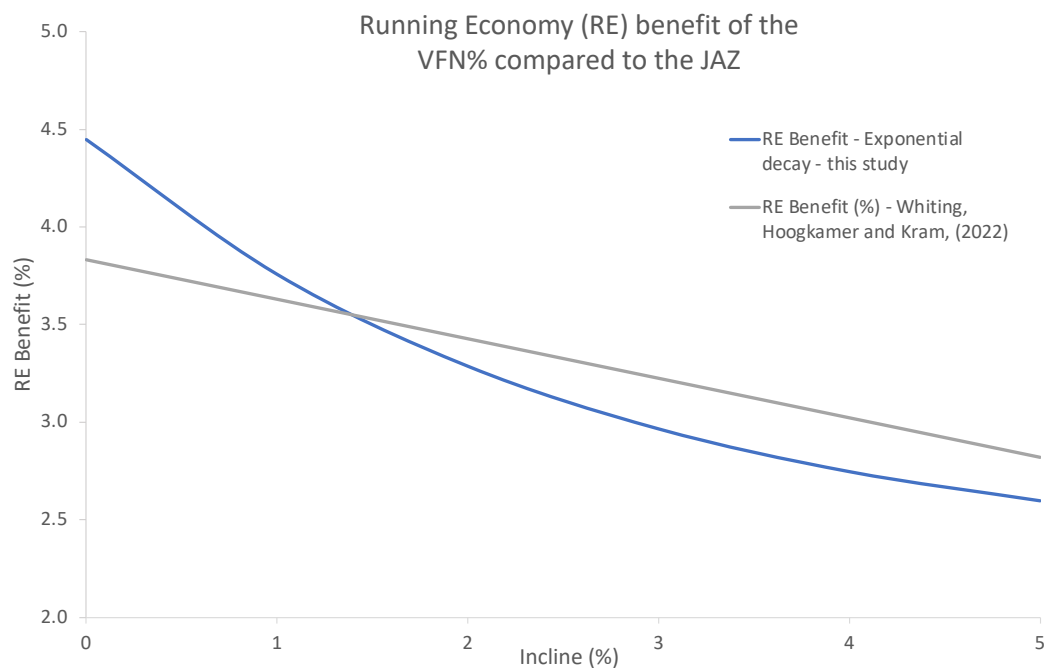


Figure 47: The RE benefit (%) of the VFN% versus the JAZ from this study (blue line) and from the VF4% versus the Nike® Streak 6 (grey line), over inclines 0-5%.

Our study showed a 4.37% RE benefit for running at 12 km/h on a 0% incline and a 3.95% RE benefit on a 1% incline meaning there was a 0.42% RE penalty for running uphill, a 2.75% RE benefit on a 3% incline meaning there was a 1.62% RE penalty and 2.70% RE benefit on a 5% incline meaning there was a 1.57% RE penalty for running uphill, when compared to the JAZ. In comparison, Whiting, Hoogkamer and Kram, (2022) showed a 3.83% RE benefit at 0% incline and 2.82% RE benefit at 5% incline, meaning there was

a 1.01% RE penalty for running uphill for VF4% when compared to the Nike® Streak 6. We hypothesised that there would be a linear relationship between RE benefit and incline based on the findings of Whiting, Hoogkamer and Kram, (2022), however, the data from our study allowed us to deduce the VFN% had a decreasing RE benefit with increasing incline, forming what appears to be an exponential decaying relationship (discussed further in the next hypothesis).

When comparing the RE penalties at a 5% incline, our study achieved 2.70% RE benefit and a 1.57% RE penalty compared to running on the level in the VFN% when compared to the JAZ. Whereas Whiting, Hoogkamer and Kram, (2022) achieved 2.82% RE benefit and a 1.01% RE penalty for VF4% when compared to the Nike® Streak 6. According to these results, VF4% had an additional 0.12% RE benefit and a 0.56% lower RE penalty when running at a 5% incline than the VFN%, meaning they were less efficient which was not anticipated. However, it is important to note that the RE penalty for the VFN% could be due to the performance differences between the conventional running shoes on an incline, or the difference in speed at which the participants were tested at.

It is unclear if Nike® Inc., anticipated that the VF series of running shoes would produce less than 4% RE benefit whilst running on an incline, in comparison to similar running shoes. Our study findings strongly support the notion that running uphill requires the generation of increased energy. This increase in energy output is essential for overcoming the gravity encountered when propelling the BCoM up an incline. Incline poses a challenge due to less effective ESE storage and return mechanisms, meaning the body must

supply additional energy to propel the BCoM uphill. As runners ascend, they generate a reduced impact force upon the ground. Diminished impact force leads to a lower ESE return from the VFN% running shoe, a consequence of the decreased impact force rather than the runner's ability to generate energy (Snyder, Kram and Gottschall, 2012).

The evidence from our study highlights that, during each step, the work done on the BCoM is an additive factor to the cyclic process of ESE storage and return. As incline increases, the work exerted on the BCoM also increases, where it becomes significantly higher than the energy being cycled. This heightened demand for mechanical energy is a compensatory mechanism required to sustain uphill momentum (Snyder, Kram and Gottschall, 2012).

3.4.4. HYPOTHESIS THREE; RELATIONSHIP OF THE DATA - EXPONENTIAL DECAY MODEL

We hypothesised a negative linear relationship between RE benefit and increasing incline. However, our third hypothesis was rejected for the discovery of a negative linear trend with a nonlinear distribution between the inclines for VFN% RE benefit compared to the JAZ.

An exponential decay model emerged as the most fitting representation for the data. This model illustrated a more accurate relationship between RE benefit and incline. A novel aspect of our study highlighted a fundamental characteristic of the data between the RE benefit of the individual components within the VFN%, where a constant y^0 , representing a 2.28% asymptote baseline which RE will never drop below. A 1% RE penalty, from

the 2.28%, was attributed to the "mass effect" of the running shoes with any RE benefit exceeding this 1% was attributed to the "midsole effect", encompassing factors such as enhanced elastic return and biomechanical advantages offered by the VFN% running shoe.

THE MASS EFFECT

The mass difference between the VFN% and the JAZ was 100 g per shoe, a lighter shoe mass provides a partial explanation for the enhanced RE benefit associated with the VFN% (Colloff, 2022). The Nike® Streak 6 is considered a streamlined variant to the VF4%, weighing 11 g less (UK size 8). This was a staple mid- to long-distance racing shoe used prolifically over the last decade. Its reduction in mass is accompanied by a thinner midsole with less EVA foam by volume, featuring a rearfoot air-cushioning unit instead of a carbon-fibre midsole plate.

In contrast to the recent literature, despite the lighter mass of the Nike® Zoom Streak 6, the VF4% demonstrated a superior 2.6% RE benefit. This outcome supports our results that the "mass effect" alone cannot dictate RE benefit, meaning the PEBA foam midsole and the carbon-fibre midsole plate significantly influence the VF series RE benefits (Whiting, Hoogkamer and Kram, 2022).

THE MIDSOLE EFFECT

The 4.01% RE benefit observed in the VFN% compared to other conventional running shoes can partly be attributed to the heightened quantity and

advanced chemical structure of the ZoomX foam. Our investigation unveiled the VFN% to exhibit a 4.37% RE benefit when compared to the JAZ, marking an additional 0.36% RE benefit compared to the VF prototype (Hoogkamer *et al.*, 2018) and an additional 0.17% RE benefit over the VF4% (Barnes and Kilding, 2019).

This improvement in RE benefit may be elucidated by the incorporation of a higher proportion (15% by volume) of the advanced ZoomX foam (Hoogkamer *et al.*, 2018; Barnes and Kilding, 2019). Whilst the teeter-totter effect attributes 6% RE benefit to midsole thickness (Nigg, Cigoja and Nigg, 2020, 2021), our results and modelled data suggest a 1.28% RE benefit from the carbon-fibre midsole plate and ZoomX midsole foam in combination, supporting the work of Whiting, Hoogkamer and Kram, (2022).

It is understood that VF series are composed of PEBA, which returns 87% of the energy under compression testing, as opposed to the traditional TPU or EVA foams which return 66% and 76% respectively (Burns and Tam, 2020; Dominy and Joubert, 2022; Joubert and Jones, 2022). It is thought that the ZoomX foam midsole increases the elasticity and deformation potential at IC facilitating the ESE storage and return mechanism during running, absorbing and transfers more ESE as the foam reforms, which is then released as additional KE and transferred into forward propulsion, thus improving RE (Hoogkamer *et al.*, 2018; Barnes and Kilding, 2019; Hoogkamer, Kipp and Kram, 2019).

The carbon-fibre midsole plate further improves RE benefit by providing a stiffer running surface for the ZoomX foam to act upon, reducing the cost per stride at IC as explained above. The carbon-fibre midsole plate acts as a

lever, creating a larger resultant moment by acting further from the point of rotation. The curvature of the carbon-fibre midsole plate has a higher LBS, which stiffens the MTP joint, reducing the MTP joint range-of-motion and angular velocity. It is postulated that the reduction in mechanical work at the MTB joint reduces muscular work, ergo improves RE. During uphill running there is a shift to a forefoot/ midfoot toe strike pattern causing additional LBS of the carbon-fibre midsole plate, improving RE benefit due to the mechanical advantage of a longer moment arm about the ankle (Stefanyshyn and Nigg, 2000; Roy and Stefanyshyn, 2006; Healey and Hoogkamer, 2021).

3.5. APPLICATION

We established a range of RE benefits for the VFN% running shoe compared to a conventional running shoe over a variety of inclines. The highest return on energy investment is during level running providing 4.37% RE benefit with a calculated exponential decay of 4.45% RE benefit to a 16% incline where after 2.28% RE benefit, no further meaningful change was seen. Translating these results into performance improvements and disseminating this evidence will facilitate bridging the gap between academia and the real-world experience, so all athletes can understand the implications of the VFN% RE benefits (Hunter *et al.*, 2022).

New York City Marathon Course Profile

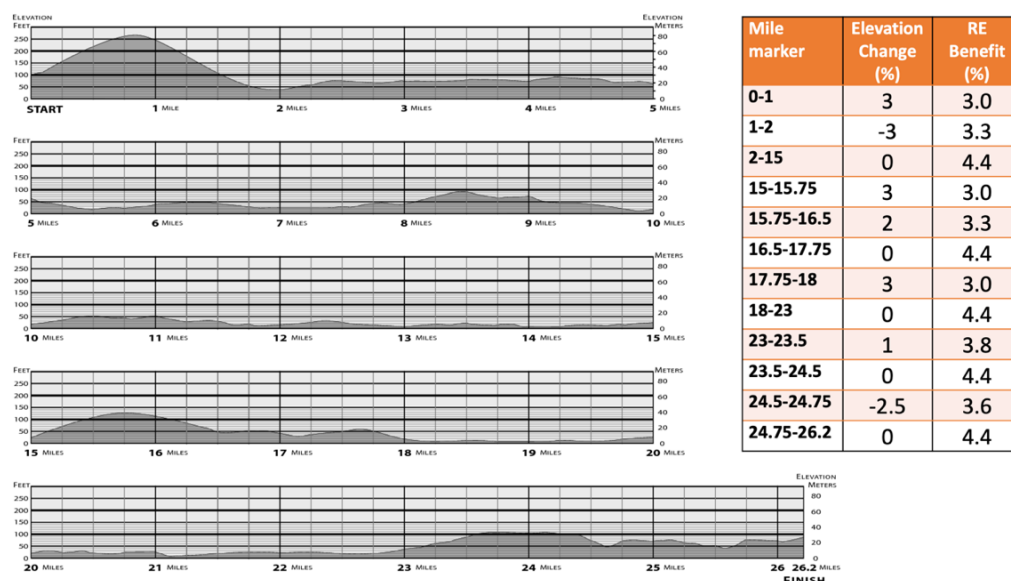


Figure 48: New York City Marathon course profile; Implication of current research on calculating VFN% RE benefits based on the exponential decay results from this study (New York Road Runners, 2024).

The exponential decay modelled data was used to produce RE benefit profile based on The New York City Marathon course with its several points of elevation (Figure 48). By providing a weighted average for elevation changes using our modelled data alongside that of Whiting, Hoogkamer and Kram, (2022), over the 26.2 miles there is a possible 3.8% RE benefit at a velocity of 12 km/h or pace of 03:30:00 hr. Using a race metrics calculator (Kipp, Kram and Hoogkamer, 2019), based on the 3.8% RE benefit, a saving of 00:07:14 hr is theoretically possible whilst running in the VFN% in comparison to wearing a traditional running shoe.

This evidence will facilitate the calculation of RE benefit in accordance with differing running course profiles, thus enabling the development of customised racing strategies for optimum energy management.

3.6. CONCLUSION

Ultimately, our study has provided an initial understanding of how the ZoomX foam and carbon-fibre midsole plate contribute to the RE benefit beyond the impact of the VFN's lighter mass. Through this evidence, we validate a synergistic relationship between the two key midsole components, coining it the "midsole effect." This novel understanding was formed using the exponential decay modelled data, enabling the identification of VFN% RE benefit at specific inclines.

FUTURE WORK

Subsequent studies should aim to offer a deeper understanding of the relationship between the carbon-fibre midsole plate and ZoomX foam in the VFN%. Emphasis should be placed on defining the exact contribution each midsole element makes toward the RE benefit observed. Specifically, research should investigate the effect of the absence of the carbon-fibre midsole plate from the ZoomX foam midsole, and finally the effect of differing quantities of ZoomX foam on RE benefit in the VFN%.

Interconnecting this study to the over-arching theme of this PhD thesis brings the next chapter of research to investigate the relationship between performance using RE benefit, and gait using accelerometry.

3.7. LIMITATIONS

PARTICIPANT ERROR

A novel element of this study explored participant performance ability; those that could and could not run 10 km in ≤ 40 minutes. The mixed mode ANOVA tested performance ability and its interaction with RE, however, there was no statistically significant interaction. Regardless, a larger participant sample, with a variety of performance abilities, distributed equally across groups may provide more insight into the effect of participant performance ability on RE over various inclines. While we observed no interaction effect on RE based on performance ability, the potential for different outcomes exists, especially with an increase in sample size. The impact of performance ability on the data may become more apparent with a larger and more diverse participant sample making the data more robust and more applicable to a broader range of runners. To make the data more robust, the “yes”, “no” element of this study can be improved by collecting an exact performance indicator such as the participants most recent 10 km race time.

GENDER DIFFERENCES

Senefeld *et al.*, (2021) highlighted in their retrospective, observational study that there was an optical gender difference with women achieving a 1.6% performance improvement compared to 0.8% for men, and for overall time with women improving by 3.7 min compared to men with 1.2 min whilst wearing the Nike® series during four major marathons. This research highlighted these gender differences as in accordance with the RE saving models due to

women's overall slower running times (Barnes and Kilding, 2015; Kipp, Kram and Hoogkamer, 2019).

Upon closer examination, the assertion holds true when discussing performance as a percentage. A more in-depth analysis of gender differences within the context of performance in the Nike® series should be considered to discern any gender-related differences. Our results indicated non-statistically significant differences warranted the combination of all data to be analysed collectively. In future studies, it would be prudent to consider both collective and separate analyses for genders to explore potential variations.

LABORATORY CONDITIONS

The absence of climate control in the laboratory environment prevented the replication of outdoor conditions, with participants often describing the setting as "warm" or "hot". To mitigate the impact of these conditions, fans were provided to enhance comfort. It is important to note that temperature is a recognised factor to negatively influence performance (Moldover and Borg-Stein, 1994; Novacheck, 1998; Saunders *et al.*, 2004; Barnes and Kilding, 2015). Despite the conditions, there was no statistically significant interaction between trial order and RE, suggesting that the performance outcomes were consistent regardless of whether it was the 1st or 8th trial completed. Regardless, the broader impact of temperature on performance remains a noteworthy consideration for future studies.

An inherent challenge in testing involves the impedance via equipment utilised, such as the gas exchange mask and treadmill. Despite efforts to mitigate this error through familiarisation periods, the extent to which RE was affected by the equipment used is crucial for accurate interpretation of results. Drawing a parallel, runners performed trials at a 1% incline to mirror the energy expenditure expected from the external environment (Ardigo, Saibene, and Avanzate, 1993; Barnes and Kilding, 2015). Future studies should explore ways to evaluate and mitigate the impact of testing equipment on performance outcomes, thus enhancing the accuracy and reliability of research findings.

CHAPTER FOUR

4. STUDY 5: THE GLOBAL GAIT ANALYSIS TOOL (GAiT) FOR THE QUANTIFICATION OF RUNNING PERFORMANCE USING ACCELEROMETRY

Study five used GaiT, an accelerometry-based tool to investigate Fundamental Frequency (FF) and Spectral Purity (SP) measures to explore the relationship between gait characteristics and running economy (RE). 23 participants ran four inclines at 12 km/h on a treadmill whilst wearing two custom-built wearable devices. Accelerometry data recorded a total of eight trials over four inclines whilst wearing the Nike® Vaporfly ZoomX NEXT% (VFN%) and the conventional running shoe, the Saucony® ProGrid Jazz 12 (JAZ). The results revealed FF increased with incline and typically SP decreased with incline, meaning gait quality improved with incline. The VFN% consistently exhibited a lower FF, suggesting a lower stride frequency (SF) and lower SP, indicating superior gait quality compared to the JAZ, typically over all inclines. The noteworthy parallel relationship between FF and running economy (RE) benefit suggests that VFN%, with lower FF values, may contribute to more economical running and potentially better performance. However, SP benefits did not exhibit a parallel relationship with RE benefit, making the direct relationship between SP and running economy less clear.

The GaiT method, particularly FF analysis, emerged as a promising predictive tool for quantifying running performance, with lower FF values potentially indicating more economical running and faster running times. SP may not directly correlate with RE benefit but it still offers insights into gait quality.

4.1. PREMISE

Along with the improvements in RE, the VFN% running shoes ability to change running mechanics over various inclines has been observed, compared to conventional running shoes. Whiting, Hoogkamer and Kram, (2022), Hoogkamer et al., (2018) and Barnes and Kilding, (2019) used MC to show that running in the VF series resulted in an increased SL and decreased SF when running at a fixed speed. Study 4: Nike® Vaporfly ZoomX NEXT% running shoes have running economy benefits over various inclines compared to conventional running shoes, determined RE benefits of running in the VFN% compared to the JAZ, over various inclines. Quantifying such benefits can be time consuming and is often confined to the laboratory, therefore, a new, cost effective and accessible long-term approach is desirable to make gait analysis available to a larger remit. Accelerometry has been investigated as a potential tool to quantify gait outside of the laboratory (Fogg, 2005; Tao *et al.*, 2012; Barnes, 2017). In the previous chapter we produced GaiT, a novel tool that quantified FF and SP as a measure of running gait quality using accelerometry (Analytical techniques, 2.11). It is crudely accepted that those with better skill levels are better performers (Barnes, 2017), therefore, using similar accelerometry techniques we propose to investigate the feasibility of linking RE, as a performance measure, to FF and/ or SP as a gait quality measure. The product of this investigation will be a tool that not only quantifies gait quality but can also predict performance within the laboratory, with the ultimate aim of extending these findings outside of the laboratory.

4.1.1. AIM

The aim of this chapter is to relate GaiT measures; FF and SP from accelerometry to a running performance measure; RE from CPET. A feasibility study will examine these measures from data collected during treadmill running at 12 km/h whilst wearing the VFN% and the JAZ over various inclines. By correlating FF and SP with RE data from the previous study, we will explore the potential of predicting performance using GaiT. The future work from the previous study recommended to split the data for gender and analyse as two separate groups which will be conducted for this study.

4.1.2. HYPOTHESES

For both males and females:

1. The VFN% will produce a lower FF than the JAZ over all inclines, thus lower SF.
2. FF will increase with increasing incline in both running shoes.
3. Lower RE values will be associated with lower FF values.
4. The VFN% will produce lower SP levels than the JAZ over all inclines, ergo have better gait quality.
5. Higher SP values will be seen with increasing incline.
6. Lower RE values will be associated with lower SP values.

4.1.3. OBJECTIVES

Several treadmill running trials were conducted to contextualise gait quality via accelerometry. The objectives were to:

1. Conduct four treadmill running trials to collect accelerometry data at inclines (0%, 1%, 3% and 5%), at 12km/h for the VFN% and JAZ.
2. Utilise the package of calibration, processing and analytical techniques developed in chapter three to contextualise the accelerometry data captured.
3. Statistically test the data to determine if GaiT variables FF and SP are suitable to quantify running gait.
4. Explore any relationships between VFN% and JAZ, and the GaiT measures FF and SP.
5. Explore any relationships between GaiT measures; FF, SP and RE with the aim of using GaiT as a predictive tool for running performance.

4.2. GENERAL METHODS

Uniform methods were consistently employed throughout this thesis, consolidated for clarity in the General Methods section. For more comprehensive insights, consult the General methods (2.2).

4.2.1. STATISTICAL POWER

A standard online power calculation requiring mean and S.D., results from Study 4: Nike® Vaporfly ZoomX NEXT% running shoes have running

economy benefits over various inclines, compared to conventional running shoes (Results, 3.3) concluded that 23 participants were needed to detect whether a statistical significance would be present within the data at the level of $P = 0.05$.

4.2.2. PARTICIPANTS

23 participants; $n=6$ females and $n=17$ males volunteered to participate within the study (Table 8). There were statistically significant differences between gender for age ($P = .012$), mass ($P \leq .001$) and height ($P \leq .001$) therefore the data was grouped by gender and analysed separately. Two male and one female participant did not complete JAZ 0% and VFN% 0% due to a late protocol addition, one male did not complete VFN% 0%, 1%, 3% or 5%, one male participant and one female did not complete JAZ 3% due to a wearable device malfunction, and finally one male participant did not complete JAZ 5% or VFN% 5% due to fitness. Participants fitted a UK shoe size 5.5, 6.5, 7.5, 9, 10 or 11.

Table 8: Participant descriptive statistics.

Gender	Descriptive	Category	Value (%)	Mean (±S.D.)
Male	Total (n)			17
	Age (years)			35.3 ± 12.7*
	Mass (kg)			74.6 ± 9.1
	Height (cm)			180.9 ± 6.4
	BMI (kg/m ²)			22.9 ± 3.1
	Performance (<40 min 10 km)	Yes	13 (76.5%)	
		No	4 (23.5%)	
	Order	VFN% vs JAZ	4 (23.5%)	
		JAZ vs VFN%	13 (76.5%)	
Female	Total (n)			6
	Age (years)			25.7 ± 4.2*
	Mass (kg)			57.7 ± 6.5*
	Height (cm)			168.0 ± 4.1*
	BMI (kg/m ²)			20.4 ± 1.9
	Performance (<40 min 10 km)	Yes	2 (33.3%)	
		No	4 (66.7%)	
	Order	VFN% vs JAZ	2 (33.3%)	
		JAZ vs VFN%	4 (66.7%)	

*There are statistically significant differences between gender for age ($P = .012$), mass ($P \leq .001$) and height ($P \leq .001$).

4.2.3. PROTOCOL

Additionally, to the Protocol (3.2.4), two custom-built wearable devices (red and blue) were turned on and set to record at 40 Hz, then shaken simultaneously to record a discernible large magnitude peak on the movement wave to signify the start of the protocol. A stopwatch was used to capture protocol events providing reference points for synchronisation. The red wearable device was fitted to the right shank and the blue to the left shank using the strict placement protocol;

- calculating the shank length (the distance between the lateral tibial condyle and the tibial malleolus),
- strapping the wearable device 10% above the tibial malleolar epicondyle in comparison to total shank length, to avoid excess tilt if the device was placed directly on to the epicondyle,
- orientating the wearable device's positive x-axis vertically along the radial axis,
- enforcing feet directly under the hips.

After each wearable device was fitted, the participant completed five small feet together jumps as they were distinct on the accelerometry wave. These jumps were repeated before and after each trial as they facilitated the synchronisation of the red and blue accelerometer movement waves to each other.

The participant was given operational and safety instructions for the treadmill (H/P/ cosmos sports & medical gmbh, Nussdorf-Traunstein Germany) before putting on the a pair of running shoes as directed by the randomisation protocol (see Protocol, 3.2.4 for further details). The participant stood statically on the treadmill for 10 seconds before completing a 10-minute self-structured warm up and familiarisation period with the aim of reaching 12 km/h at a 5% incline. Following this, four trials were completed where the inclines 0%, 1%, 3% and 5% were randomised, each lasting 120 seconds at 12 km/h (3.3 m/s). The participants were blinded to the incline sequence by covering the incline display on the treadmill. After the final trial, each participant was given the option to cool down before the synchronisation movements were

repeated. This was conducted for the VFN% and JAZ and repeated for each participant.

4.2.4. DATA EXTRACTION

Consistent data extraction methods were applied to each wearable device prior to commencing the data processing phase. For additional details, please refer to the section on Data extraction (2.2.5).

4.2.5. DATA PROCESSING AND ANALYTICAL TECHNIQUES

Additionally, to the method above, the data processing has been summarised for ease (Appendix H). The analytical measures were developed in an iterative process resulting in:

- The FFT; instead of quantifying the first FF peak, the first four FF peaks will be quantified to understand how gait may vary over a larger range of harmonics.
- The CDF; the function in its current format provided very small frequency readings across the x-axis which were not relatable to this project. To transform to a CDF, the FFT was integrated using the rectangular method (Equation 22). The median (50%) y-axis SP value was retained.
- The CCF and ACCF; were removed as these were ineffective at providing consistent quantification of gait symmetry (see Conclusion (3.6) for detail).

Equation 22: Rectangular integration method of the FFT. A. the calculation of the intensity or height (h) of each rectangle under the FFT within the area to be calculated, where a is the initial point and b is the final of the base of the area along x (frequency domain). This is then divided by n being the number of sections the distance between a-b was divided into. B. is the function of the integration equation of b-a where n is the repeating unit for the number of rectangles within the area to be integrated giving the total area under the FFT at each frequency harmonic i.e. the CDF of the FFT.

(22 A)

$$h = \frac{b - a}{n}$$

(22 B)

$$I = \int_a^b f(x) dx \approx h[f(x_1^*) + f(x_2^*) + \dots + f(x_n^*)]$$

PERCENTAGE FF AND SP BENEFIT OR PENALTY

FF and SP benefit (%) (Equation 23) was created and calculated between the VFN% and JAZ running shoes, with the emphasis toward the VFN% benefit the provided compared to the JAZ. The data were portrayed in this way to be comparable to the RE data produced in Study 4: Nike® Vaporfly ZoomX NEXT% running shoes have running economy benefits over various inclines compared to conventional running shoes that used Percentage RE benefit.

(23)

$$\begin{aligned} & \text{FF/ SP benefit/ penalty (\%)} \\ &= \left(\frac{\text{FF/ SP JAZ (Hz)} - \text{FF/ SP VF (Hz)}}{\text{FF/ SP JAZ (Hz)}} \right) * 100 \end{aligned}$$

4.3. RESULTS

4.3.1. VARIANCE

Homogeneity-of-variance, was demonstrated through normally distributed histograms and confirmed by Mauchly's Test of Sphericity that sphericity was not met for the males for SP $X^2(5) = 6.794$, $P = .239$, and for the females for; FF peak 1 $X^2(5) = 3.882$, $P = .621$, FF peak 2 $X^2(5) = 7.644$, $P = .238$, FF peak 3 $X^2(5) = 3.637$, $P = .654$, FF peak 4 $X^2(5) = 3.612$, $P = .657$ and SP $X^2(5) = 11.379$, $P = .076$. Due to this, a repeated measures ANOVA with the Greenhouse-Geisser correction was used. Where sphericity was met (males FF Peak 1-4 only) the hypotheses were tested using the repeated measures ANOVA with sphericity assumed to a statistical significance of $P = 0.05$.

4.3.2. STATISTICAL TESTING

DETERMINING FF PEAK

A paired samples t-test was conducted to determine if the FF peaks 1-4 were significantly different from one another between running shoe types. The results indicated that for males; there was a non-statistically significant

difference between FF peak 1 and 2 (0.040 ± 0.150); [$t(13) = 0.998$, $P = .337$], peak 1 and 3 (-0.037 ± 0.144); [$t(13) = 0.962$, $P = .354$], peak 1 and 4 (-0.757 ± 2.95); [$t(13) = -0.959$, $P = .355$], peak 2 and 3 (-0.003 ± 0.158); [$t(13) = -0.067$, $P = .947$], peak 2 and 4 (-0.797 ± 2.92); [$t(13) = -1.02$, $P = .326$], peak 3 and 4 (-0.794 ± 2.95); [$t(13) = -1.008$, $P = .332$]. With larger non-statistically significant differences for the females equalling; $P = .936$, $.852$, $.731$, $.884$, $.640$ and $.498$, respectively.

Therefore, the null hypothesis was accepted as there was no statistically significant difference between FF peaks 1-4, thus only FF peak 1 will be discussed from this point forward.

DETERMINING PERFORMANCE ABILITY

The data were grouped by performance ability (those that could and could not complete 10 km in ≤ 40 minutes). As the data did not satisfy the requirements of an ANOVA, an independent samples t-test was used to determine there were no statistically significant differences in FF or SP for the inclines 0%, 1%, 3% and 5%. Therefore, the results were not grouped for performance ability throughout the statistical analysis.

FUNDAMENTAL FREQUENCY (FF)

For males and females, the two-way repeated-measures ANOVA demonstrated that there was no statistically significant interaction on FF for running shoe type ($F(6,6) = 1.892$, $P = .229$, $\eta^2 = 0.654$), ($F(1,3) = 4.545$, $P = .123$, $\eta^2 = 0.602$) respectively, indicating that the effect of trainer type on

FF was independent of incline. Each running shoe type had the same effect of FF at each incline.

For males, there was a statistically significant interaction between FF and incline ($F(3,33) = 13.420$, $p < .001$, $\eta^2 = .550$). This implied the statistically significant interaction for incline and FF was due to each incline having a different effect on FF.

To support this, a post hoc pairwise comparison with Bonferroni correction showed a statistically significant difference for the FF of the JAZ between inclines 0% and 5% ($P = .004$) and 1% and 5% ($P = .002$), and the FF of the VFN% between inclines 0% and 5% ($P = .027$), 1% and 5% ($P = .049$), 3% and 5% ($P = .038$) (

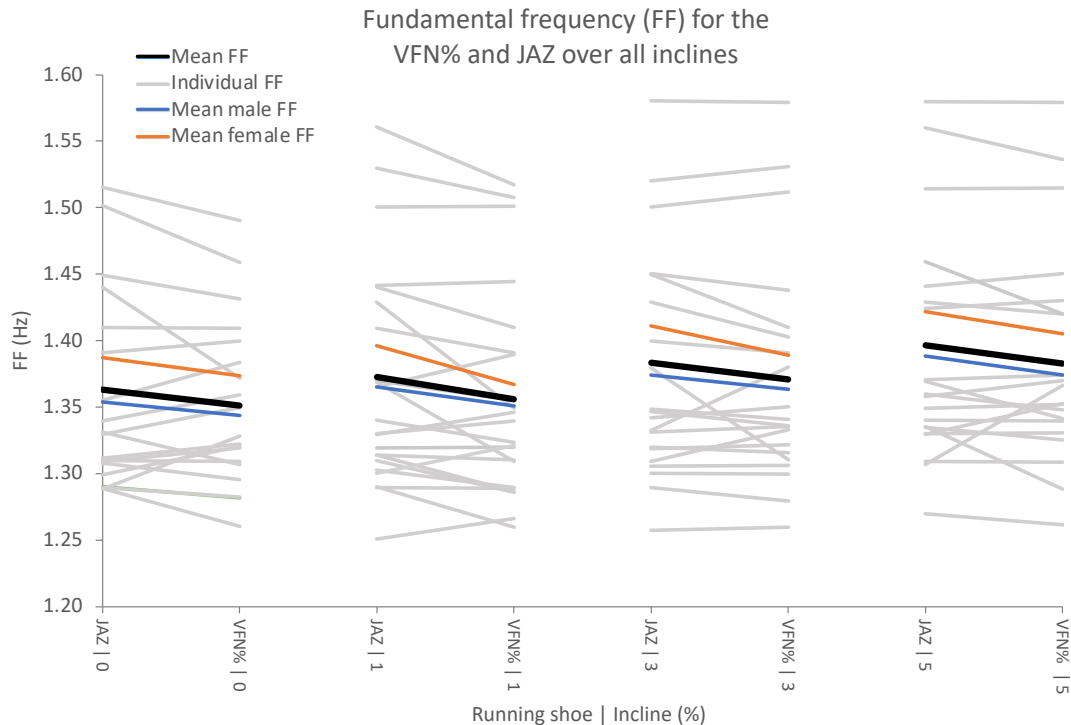


Figure 49). Ergo, each incline had a different effect on FF.

For males and females, the VFN% FF was consistently lower than the JAZ FF over all inclines (Figure 50, Table 9). For the females, there was a statistically significant interaction for FF and incline ($F(1.523,4.570) = 11.214$, $P = .019$, $\eta^2 = .789$). To inspect the causality, a post hoc pairwise comparison with Bonferroni correction showed a statistically significant difference between males and females for the FF of the JAZ and the VFN% at 1% incline ($P = .041$) (Figure 50), however, the differences at other inclines are non-significant.

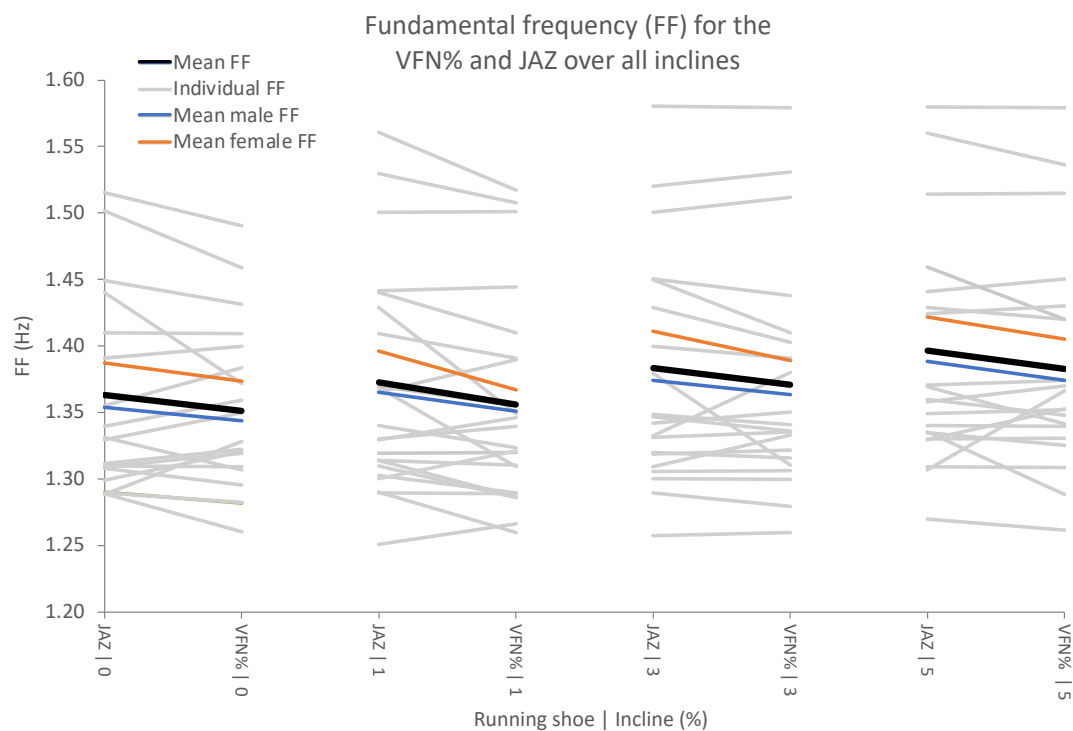


Figure 49: Fundamental Frequency (FF) for the VFN% and the JAZ running shoe over incline 0%, 1%, 3% and 5%. Mean FF for all participants (black line), mean FF for females (orange line), mean FF for males (blue line) and FF for each individual participant (grey line). Mean FF is lower for the VFN% than the JAZ over all inclines.

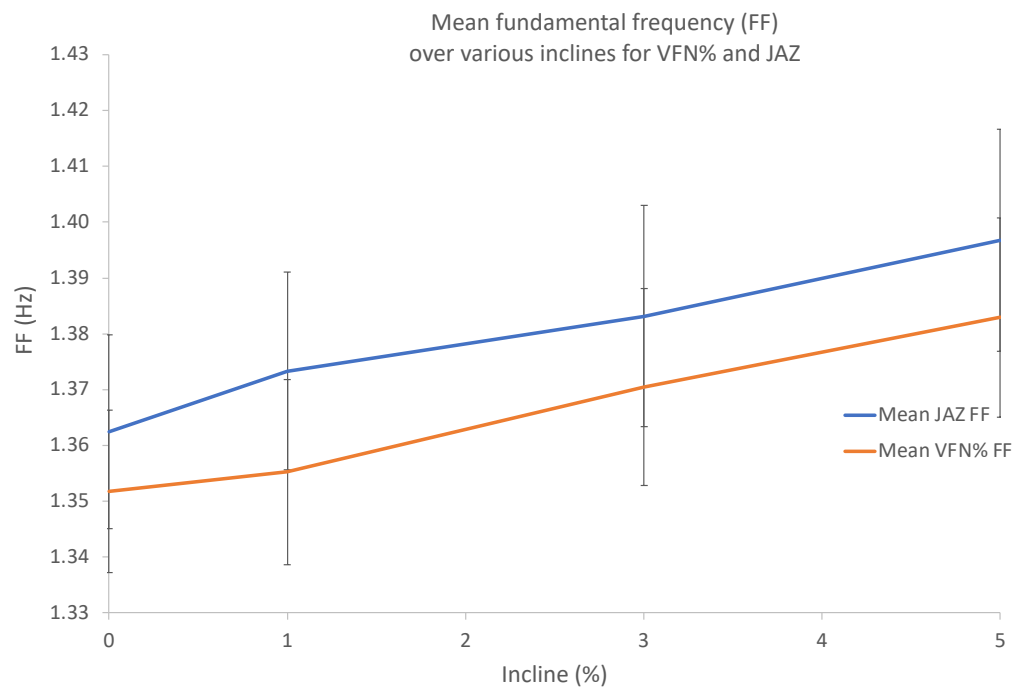


Figure 50: Mean Fundamental Frequency (FF) for the VFN% (orange) and the JAZ (blue) running shoes, where the VFN% facilitated a lower FF, thus SF than the JAZ whilst treadmill running over all inclines.

Table 9: Results for Fundamental Frequency (FF) for the VFN% and JAZ running shoes over 0%, 1%, 3% and 5% incline, including the N, mean, S.D., and mean difference.

Gender	Incline (%)	Measure	N	Mean (Hz)	S.D. (Hz)	Mean difference (Hz)
Male	0	JAZ	17	1.35	0.08	0.01
	0	VFN%	17	1.34	0.05	
	1	JAZ	17	1.37	0.09	0.02
	1	VFN%	17	1.35	0.08	
	3	JAZ	17	1.37	0.09	0.01
	3	VFN%	17	1.36	0.09	
	5	JAZ	17	1.39	0.09	0.02
	5	VFN%	17	1.37	0.09	
Female	0	JAZ	6	1.39	0.04	0.02
	0	VFN%	6	1.37	0.04	
	1	JAZ	6	1.40	0.03	0.03
	1	VFN%	6	1.37	0.04	
	3	JAZ	6	1.41	0.04	0.02
	3	VFN%	6	1.39	0.03	
	5	JAZ	6	1.42	0.04	0.01
	5	VFN%	6	1.41	0.03	

CONTEXTUALISING FUNDAMENTAL FREQUENCY (FF) USING PERCENTAGE BENEFIT

To explore the relationship between FF and RE, the data were transformed into percentage benefit (Equation 20) before being statistically analysed.

A two-way repeated-measures ANOVA demonstrated that there was no statistically significant interaction between FF benefit and incline ($F(3,33) = .584$, $P = .630$, $\eta^2 = .050$). Meaning the RE benefit achieved over all inclines was statistically similar. A post hoc pairwise comparison with Bonferroni correction showed there was no statistically significant difference between the

FF benefit over all inclines. Although the differences were not statistically different, according to the mean difference between the FF benefit of the VFN% compared to the JAZ, the VFN% produced a FF benefit (positive results), rather than a penalty (negative results), over all inclines; 0% incline (0.78 ± 1.93 Hz), 1% (1.32 ± 1.87 Hz), 3% (0.92 ± 1.70 Hz) and 5% (0.99 ± 1.66 Hz) (Table 10, Figure 51). The females (orange line) received a larger FF benefit compared to the males (blue line) at every incline (Table 10, Figure 52).

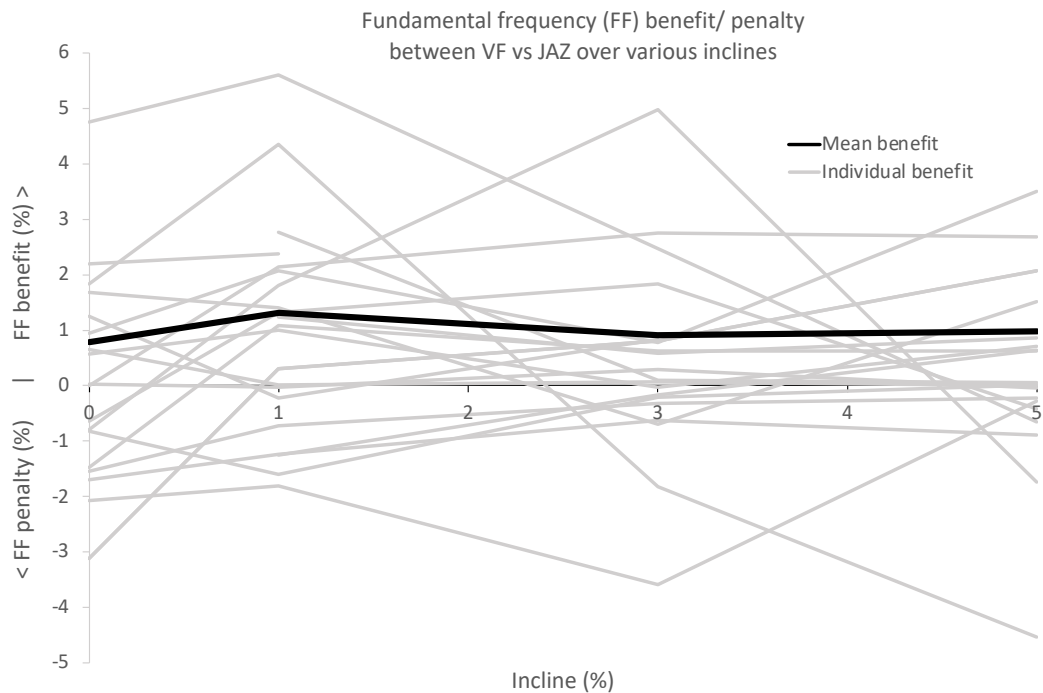


Figure 51: Fundamental Frequency (FF) benefit/ penalty. The difference between FF in the VFN% and the JAZ divided by the FF in JAZ, times 100 to give the benefit of the FF in the VFN% (Equation 23). The individual grey lines are for each of the male and female participants, with the thick black line being the combined mean result for all participants.

Table 10: Results for Fundamental Frequency (FF) benefit for the VFN% over 0%, 1%, 3% and 5% incline, including the N, mean and S.D.

Gender	Incline (%)	N	Mean (%)	S.D. (%)
Male	0	17	0.75	2.09
	1	17	1.05	1.91
	3	17	0.80	1.71
	5	17	1.06	1.23
Female	0	6	1.00	1.25
	1	6	2.12	1.18
	3	6	1.56	1.85
	5	6	1.19	2.78
Both	0	23	0.78	1.93
	1	23	1.32	1.87
	3	23	0.92	1.70
	5	23	0.99	1.66

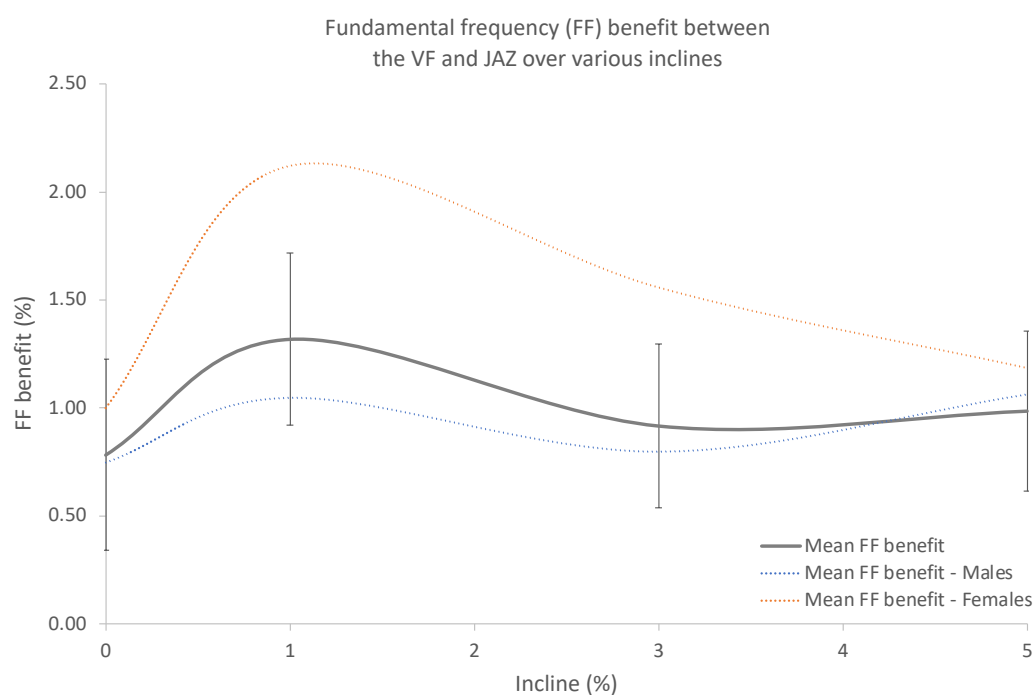


Figure 52: Fundamental Frequency (FF) benefit expressed as a percentage between the VFN% and the JAZ running shoe. The mean benefit of all participant data (black), female data (orange) and male data (blue) over all inclines tested. This shows that at 1% incline there is a different response that at any other incline. The females have a greater FF benefit that the males, on average.

RUNNING ECONOMY (RE) AND FUNDAMENTAL FREQUENCY (FF)

A Pearson correlation coefficient quantifies the strength and direction of a linear relationship between two variables. It ranges from -1 to +1, where $r = 1$ indicates a perfect, strong positive linear relationship where, $r = -1$ indicates a perfect, strong negative linear relationship, values between 0.3 and 0.7 have a moderate relationship, between 0.1 and 0.2 have a weak relationship, and $r = 0$ indicates no linear relationship. A Pearson correlation coefficient was computed to determine the relationship between the percentage difference (benefit or penalty) between the VFN% and the JAZ for FF and RE across inclines 0%, 1%, 3% and 5%.

At 0% incline, the males had a statistically significant moderate, positive relationship between FF JAZ and RE JAZ [$r(15) = .562$, $P = .029$] (Figure 53). The females had a strong, negative relationship between FF JAZ and RE JAZ, [$r(6) = -.874$, $P = .023$], and FF VFN% and RE VFN%, [$r(6) = -.817$, $P = .047$] (Figure 54). At 5% incline, the females had a strong negative relationship between FF JAZ and RE JAZ, [$r(5) = -.929$, $P = .023$].

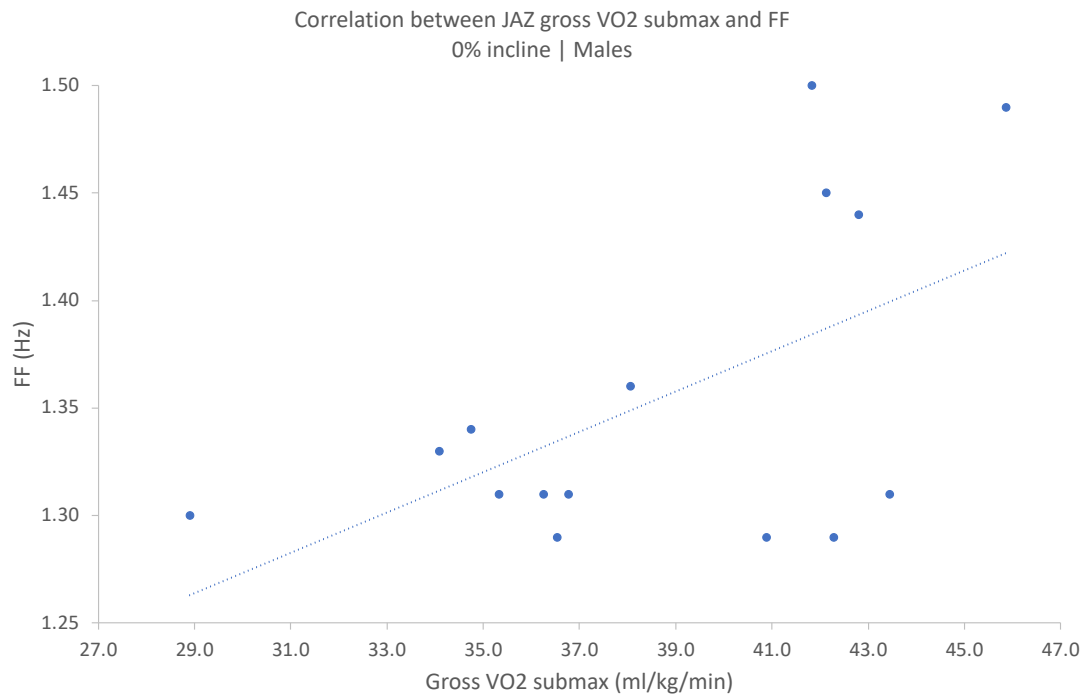


Figure 53: Correlation for male running data at 0% incline for $\dot{V}O_2$ uptake (ml/kg/min) vs FF (Hz) whilst treadmill running in the JAZ running shoes. This figure shows a statistically significant strong, positive relationship, where $\dot{V}O_2$ uptake increases, FF increases.

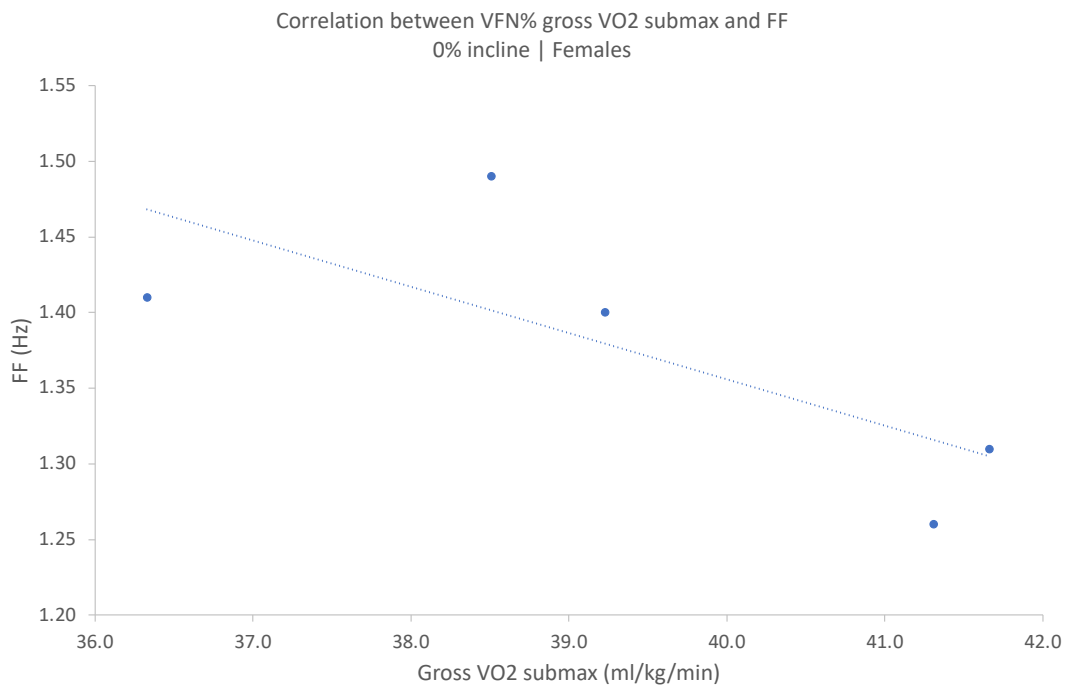


Figure 54: Correlation for female treadmill running data at 0% incline for $\dot{V}O_2$ uptake (ml/kg/min) vs FF (Hz) for VFN% running shoes. This figure shows a statistically significant strong, negative relationship, where when $\dot{V}O_2$ uptake increases, FF decreases.

CONTEXTUALISING FUNDAMENTAL FREQUENCY (FF) USING PERCENTAGE BENEFIT

Due to the lack of consensus in the data, it was not possible to model FF benefit as conducted for RE in the previous chapter. However, the data for FF benefit (Figure 55) has been superimposed with the RE benefit and RE exponential decay fit modelled data to provide a brief understanding of how these data may be interpreted together.

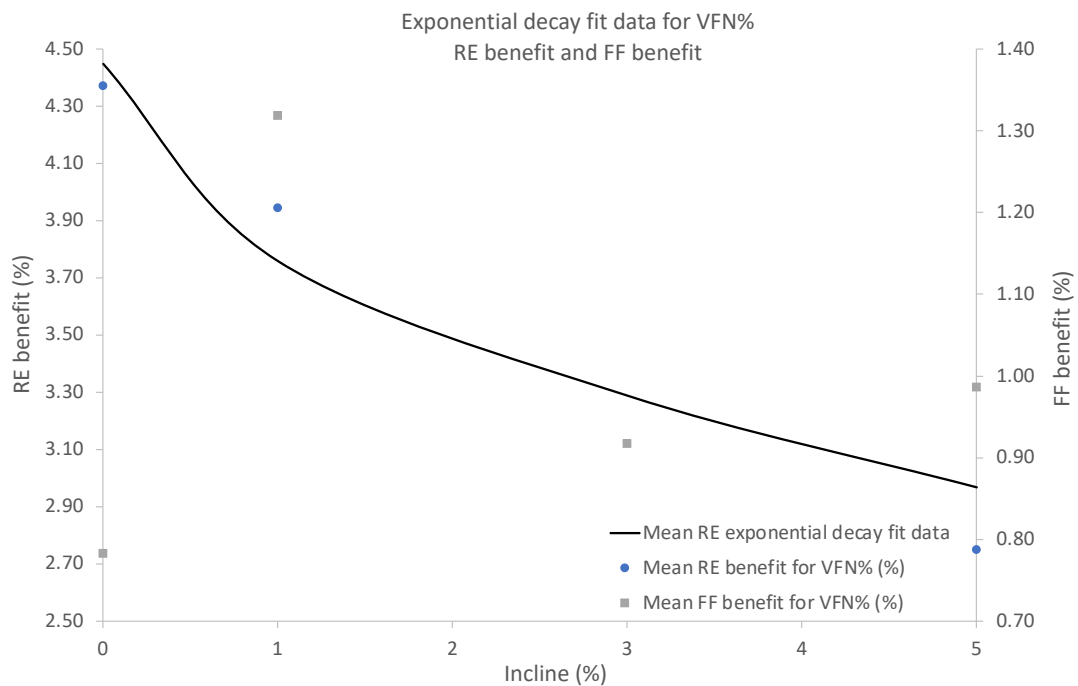


Figure 55: Running Economy (RE) benefit versus Fundamental Frequency (FF) benefit. The difference between FF in the VFN% and the JAZ divided by the FF in JAZ times 100 to give the percentage benefit of the FF in the VFN% (Equation 23). The black line is the exponential decay fitted data, the blue dots are the mean RE benefit and the grey squares are the FF benefit.

FF benefit parallels RE benefit above 1% incline (Figure 55), with a statistical significance at 0% incline. This means that as FF benefit decreases with increasing incline, it mirrors the decrease in RE with increasing incline. This

provides a novel solution for predicting performance from accelerometry data by using FF benefit as a marker of RE benefit, which we have established up to a 5% incline and modelled using the exponential decay fit to calculate anticipated RE benefit based on incline.

SPECTRAL PURITY (SP)

For the males, the two-way repeated-measures ANOVA demonstrated that there was a statistically significant interaction between SP and incline ($F(2.28,25.05) = 6.559$, $P = .004$, $\eta^2 = .374$) suggesting the effect of incline on SP varied. There was no statistically significant interaction between SP and running shoe type ($F(1.00,11.00) = .978$, $P = .344$, $\eta^2 = .082$), hence SP was consistent between running shoes.

A post hoc pairwise comparison with Bonferroni correction showed there was a statistically significant difference between the SP values at 1% and 3% incline ($P = .012$) (Figure 56).

For females, the two-way repeated-measures ANOVA demonstrated that there was no statistically significant interaction between SP and incline ($F(1.659,4.978) = 1.326$, $P = .335$, $\eta^2 = 0.307$), or SP and running shoe type ($F(1.000,3.000) = 0.050$, $P = .838$, $\eta^2 = 0.016$). The absence of a statistically significant interaction indicates that the effect of incline on SP and the effect of running shoe on SP was the same at each level.

For males and females, the VFN% had significantly superior SP over the JAZ over almost all inclines for both males and females (Table 11, Figure 56).

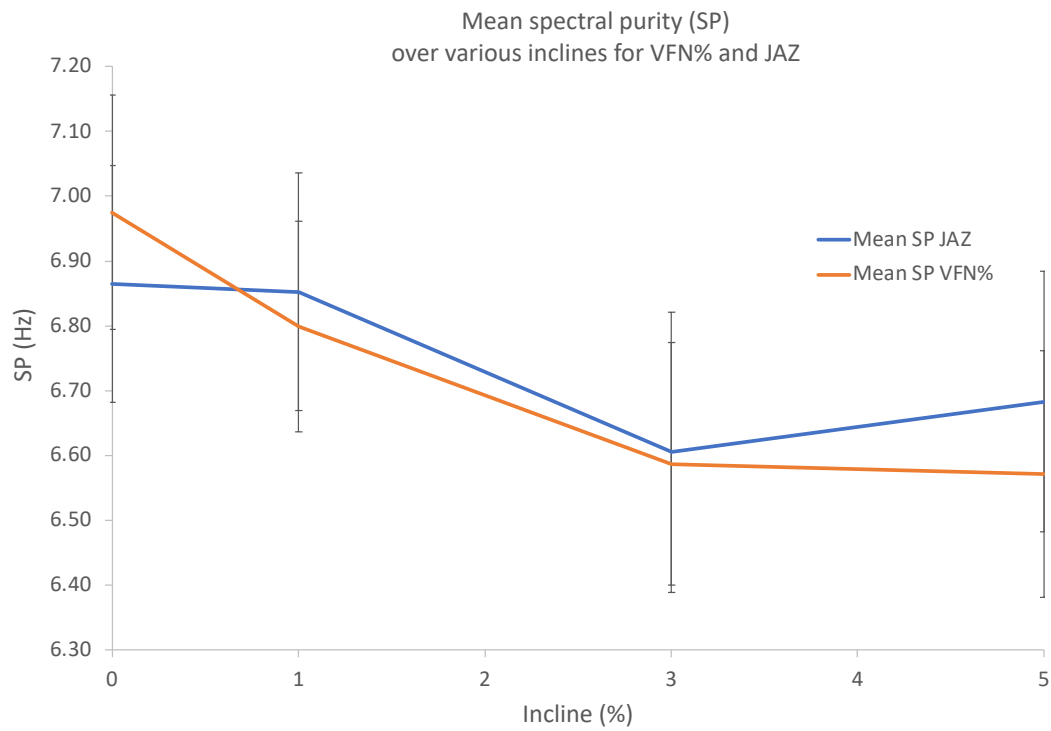


Figure 56: Mean Spectral Purity (SP) for the VFN% (orange) and the JAZ (blue) running shoe, where on average the VFN% facilitated lower SP, compared to the JAZ, over all inclines but 0%. This means that typically the VFN% has superior gait quality.

Table 11: Results for Spectral Purity (SP) for the VFN% and the JAZ running shoes over 0%, 1%, 3% and 5% incline, including the N, mean, S.D., and mean difference.

Gender	Incline (%)	Measure	N	Mean (Hz)	S.D. (Hz)	Mean difference (Hz)
Male	0	JAZ	12	6.83	0.75	0.02
	0	VFN%	12	6.81	0.72	
	1	JAZ	12	6.97	0.78	0.16
	1	VFN%	12	6.81	0.74	
	3	JAZ	12	6.65	0.89	0.02
	3	VFN%	12	6.63	0.74	
	5	JAZ	12	6.72*	0.83	0.09
	5	VFN%	12	6.64	0.66	
Female	0	JAZ	4	7.34	1.19	-0.22
	0	VFN%	4	7.56	1.04	
	1	JAZ	4	7.53	1.07	0.16
	1	VFN%	4	7.38	0.97	
	3	JAZ	4	7.29	1.15	-0.02
	3	VFN%	4	7.30	1.16	
	5	JAZ	4	7.45	1.12	0.20
	5	VFN%	4	7.25	1.15	

CONTEXTUALISING SPECTRAL PURITY (SP) USING PERCENTAGE

BENEFIT

To explore the relationship between SP and RE, the data were transformed into percentage benefit (Equation 20) before being statistically analysed.

A two-way repeated-measures ANOVA demonstrated that there was no statistically significant interaction between SP benefit and incline ($F(3,33) = 1.035$, $P = .390$, $\eta^2 = .086$).

A post hoc pairwise comparison with Bonferroni correction showed there was no statistically significant difference between SP benefit over all inclines.

There was a SP benefit for the VFN% compared to the JAZ over almost all inclines; 1% ($.79 \pm 5.38$ Hz), 3% ($.27 \pm 4.86$ Hz) and 5% (1.66 ± 7.11 Hz) with the JAZ producing a SP benefit at 0% incline compared to the VFN% (-1.61 ± 6.33 Hz). The males (blue line) received a larger SP benefit compared to the females (orange line) over incline 0%, 1% and 3% incline but not at 5% incline (Table 12, Figure 58). Meaning the amount of SP benefit achieved between and within each incline was similar.

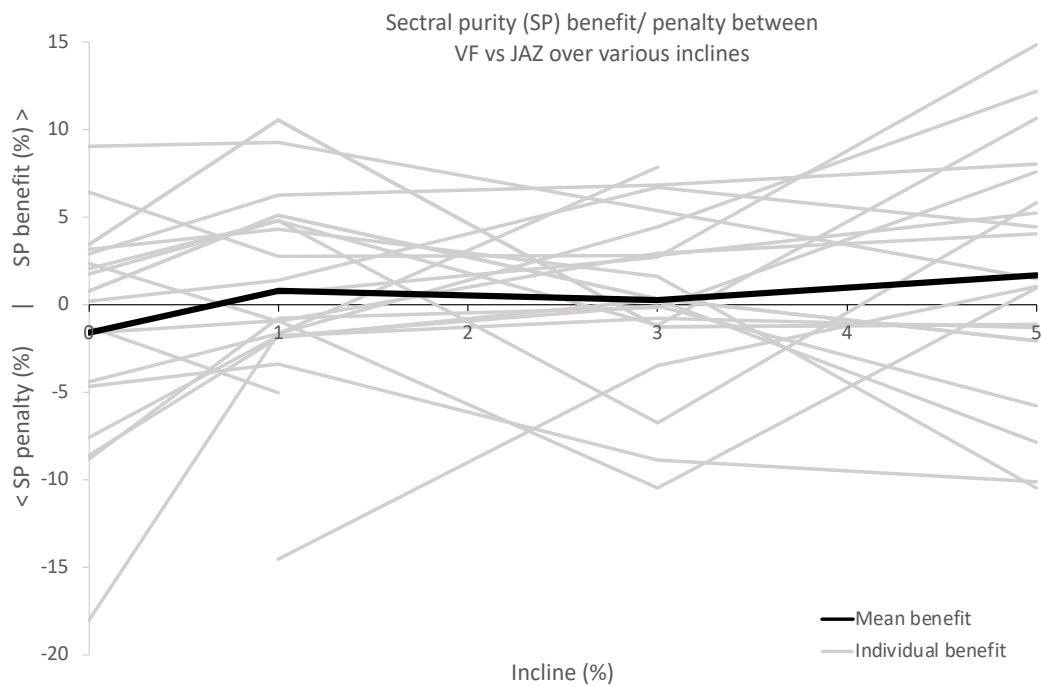


Figure 57: Spectral Purity (SP) benefit/ penalty. The difference between SP in the VFN% and the JAZ divided by the SP in JAZ, times 100 to give the SP percentage benefit of the VFN%. The individual grey lines are for each participant, with the thick black line being the mean for all participants.

Table 12: Results for Spectral Purity (SP) benefit or penalty for the VFN% over 0%, 1%, 3% and 5% incline, including the N, mean and S.D.

Gender	Incline (%)	N	Mean (%)	S.D. (%)
Male	0	17	-1.09	6.81
	1	17	1.49	4.25
	3	17	0.67	5.55
	5	17	1.58	7.44
Female	0	6	-2.68	4.87
	1	6	-1.03	7.27
	3	6	-0.13	1.53
	5	6	3.11	6.77
Both	0	23	-1.61	6.33
	1	23	0.79	5.38
	3	23	0.27	4.86
	5	23	1.66	7.11

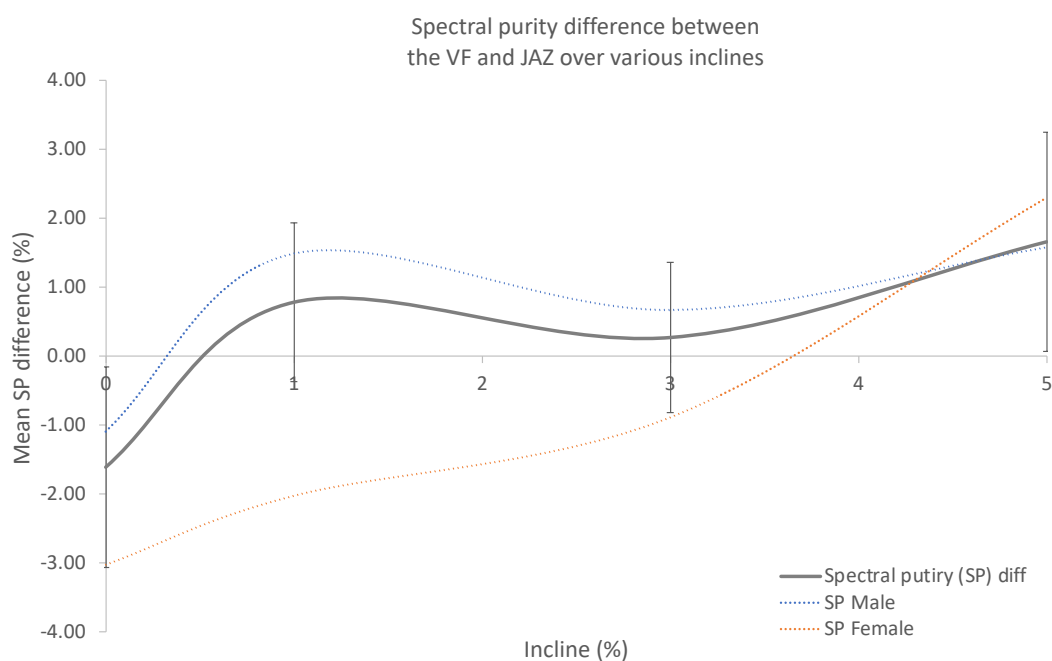


Figure 58: Spectral Purity (SP) expressed as the percentage benefit or penalty between the VFN% and the JAZ running shoes, where the mean difference of all participant data (black line) showing S.E., bars, SP difference for the females (orange dashed line) and male data (blue dashed line) over all inclines tested.

RUNNING ECONOMY (RE) AND SPECTRAL PURITY (SP)

A Pearson correlation coefficient was computed to determine the relationship between the percentage difference between the VFN% and the JAZ for variables SP and RE across inclines 0%, 1%, 3% and 5%.

At 0%, the males and the females had a strong positive relationship between SP VFN% and SP JAZ, [$r(16) = .908$, $P < .001$], [$r(6) = .971$, $P = .001$], respectively. At 1% incline, the males had a moderate, positive relationship between SP VFN% and SP JAZ, [$r(14) = .792$, $P < .001$]. The females had a strong, positive relationship between SP VFN% and SP JAZ, [$r(5) = .954$, $P = .012$]. At 3% incline, the males and the females had a strong positive relationship between SP VFN% and SP JAZ, [$r(15) = .915$, $P < .001$] and [$r(5) = .999$, $P < .001$], respectively. At 5% incline, the males and females had a strong, positive relationship between SP VFN% and SP JAZ, [$r(15) = .830$, $P < .001$] and [$r(5) = .908$, $p = .033$], respectively. The females demonstrated a strong negative relationship between SP JAZ and RE JAZ, [$r(5) = -.902$, $P = .036$] (Figure 59).

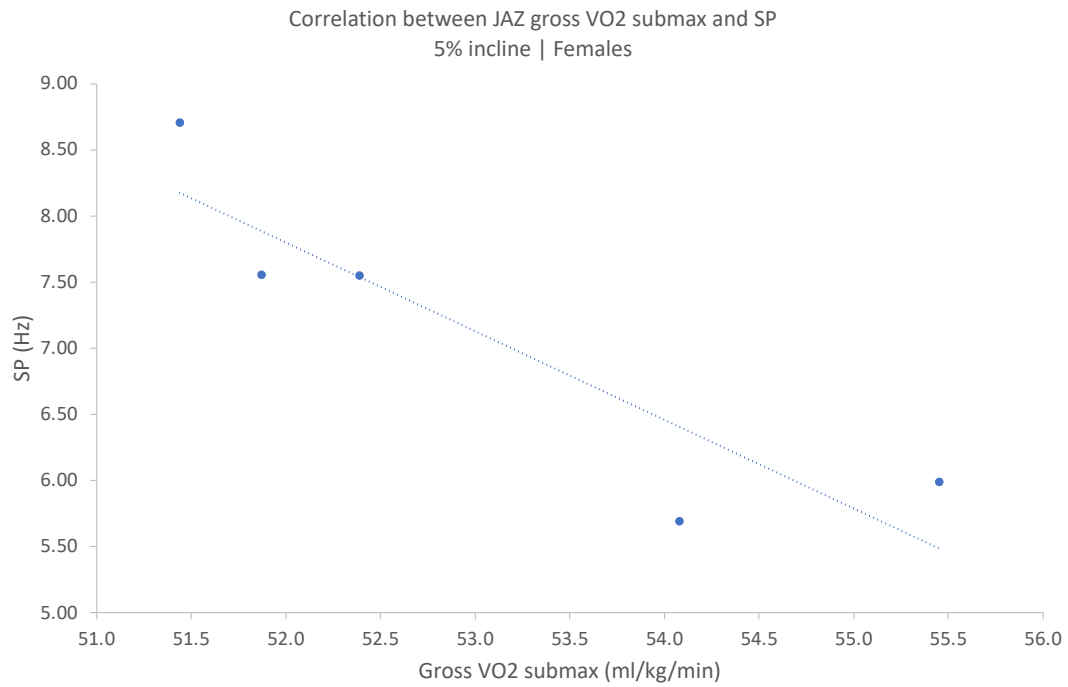


Figure 59: Females treadmill running at 5% incline; gross $\dot{V}O_2$ uptake (ml/kg/min) vs SP (Hz) for JAZ running shoes. A statistically significant strong, negative relationship, where when gross $\dot{V}O_2$ uptake increases, SP decreases.

Overall, due to the lack of consensus in the data, it was not possible to model SP benefit as conducted for RE in the previous chapter. However, the data for SP benefit (Figure 60) has been superimposed with the RE benefit and RE exponential decay fit modelled data to provide a qualitative understanding of how these data may be interpreted together.

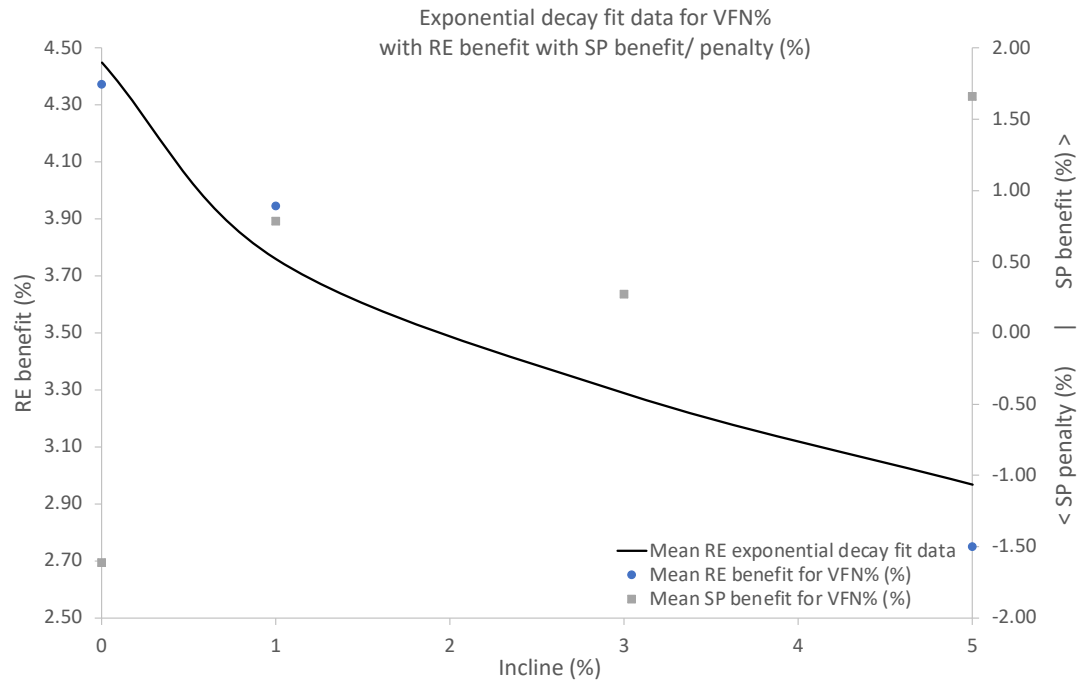


Figure 60: Running Economy (RE) benefit versus Spectral Purity (SP) benefit imposed over VFN% exponential decay modelled data for RE benefit. The difference between SP in the VFN% and the JAZ divided by the SP in JAZ to give the percentage benefit of the SP in the VFN% (Equation 23). The black line is the exponential decay fitted data, the blue dots are the mean RE benefit and the grey squares are the superimposed mean SP benefit.

SP benefit does not parallel RE benefit as well as FF benefit (Figure 60) and due to having very limited statistically significant information, a direct relationship cannot be drawn. Regardless, there appears to be potential for developing a novel solution for predicting gait quality using accelerometry data. Here, lower SP scores would equate to cleaner FFT movement waves, thus a general loss of higher frequency components at increasing inclines, with a link between better performing runners yet to be established.

4.4. DISCUSSION

4.4.1. HYPOTHESIS ONE; FOR MALES AND FEMALES THE VFN% WILL PRODUCE A LOWER FUNDAMENTAL FREQUENCY (FF) THAN THE JAZ OVER ALL INCLINES, THUS LOWER STRIDE FREQUENCY (SF).

For hypothesis one, we predicted that for both genders, the VFN% would produce a lower FF than the JAZ over all inclines, thus lower SF based on the work of Hoogkamer et al., (2018); Barnes and Kilding, (2019); Hoogkamer, Kipp and Kram, (2019). We accepted hypothesis one as the VFN% FF was lower than the JAZ FF for both males and females over all inclines (Table 9). This translated to VFN% facilitating a lower SF than the JAZ over all inclines. This study demonstrated a reduction in VFN% FF as incline increased, therefore, because speed was constant, SL must have increased to compensate whilst wearing the VFN% than when wearing the JAZ (Hunter *et al.*, 2022). Our study evidenced the VFN% provided a small but significant decrease in SF of 0.03 Hz, which supports the finding of Ortega *et al.*, (2021), who noted that running shoes containing a carbon-fibre midsole plate, known to increase LBS and decrease SF. Yet, in a different study it was reported that there was no statistically significant difference in SL whilst running over various inclines in a running shoe containing a carbon-fibre midsole plate (Hunter *et al.*, 2022).

A lower SF is associated with a more energy-efficient running pattern as longer contact times during each stride allow the muscles and tendons to cycle energy more efficiently, potentially reducing the metabolic cost of running. A longer SL at the same SF implies a greater horizontal displacement per stride.

This can result in a more effective conversion of PE into forward motion, contributing to improved running economy (Cavanagh and Williams, 1982; Snyder and Farley, 2011; Snyder, Kram and Gottschall, 2012).

The females received a larger FF benefit compared to the males at every incline (Table 10, Figure 52). It is unclear why there is an additional FF benefit at 1% incline, however, it is possibly due to the composition of the VFN%, where the ZoomX foam and carbon fibre footplate work more effectively at 1% incline than at any other incline tested. These gender differences in FF benefit could be attributed to variations in biomechanics between genders. Females often exhibit different running mechanics, including differences in joint kinematics and muscle activation patterns which may lead to differing responses to certain shoe features, resulting in a more pronounced FF benefit for females. Further analysis of the VFN% running shoe design and its interaction with incline-specific demands may provide a deeper understanding.

4.4.2. HYPOTHESIS TWO; FOR MALES AND FEMALES FUNDAMENTAL FREQUENCY (FF) WILL INCREASE WITH INCREASING INCLINE IN BOTH RUNNING SHOES.

For hypothesis two, we predicted that for both genders, FF would increase with increasing incline in both running shoes (Snyder and Farley, 2011; Snyder, Kram and Gottschall, 2012; Whiting, Hoogkamer and Kram, 2022). We accepted hypothesis two, where FF values increased with increasing incline (Table 9, Figure 50). These findings are in line with the current literature, with reference to Padulo et al., (2013) who observed a 2.0%

increase in SF between 0% and 2% incline, and a 4.8% increase in SF between 0% and 7% incline, with similar relative decreases in SL. The statistically significant interaction for incline and FF implied each incline had a different effect on FF, with 5% incline having a distinct impact over the other inclines. Steeper inclines require greater muscular work and may necessitate a more significant adjustment in SF to maintain running velocity, specifically when treadmill running. The 5% incline appeared to pose a unique challenge, forcing significant alterations in FF. Additionally, there was a statistically significant difference found between the FF of the JAZ and the VFN% at 1% incline (Figure 50), however, it is not understood why this incline is different to the others. When using percentage benefit to contextualise the data, a meaningful difference for FF benefit at 1% incline for both genders was also present. Despite the lack of statistical significance, the mean differences in FF benefit between VFN% and JAZ suggest a consistent FF benefit rather than a penalty across all inclines. The VFN% running shoe design, such as cushioning and stiffness, could play a role in how runners regulate FF on an incline. Further investigation into the interaction between the VF series midsole components and incline specific adaptations may provide a deeper insight.

*4.4.3. HYPOTHESIS THREE; FOR MALES AND FEMALES LOWER
RUNNING ECONOMY (RE) VALUES WILL BE ASSOCIATED WITH
LOWER FUNDAMENTAL FREQUENCY (FF) VALUES.*

For hypothesis three, we predicted that runners who have lower RE values will be associated with lower FF values. We accepted hypothesis three for the males only at 0% incline, with the females displaying the inverse relationship at 0% and 5% incline.

The positive relationship in the male data suggests that, at 0% incline, higher FF values in the JAZ are associated with better RE, implying that, for males, a slightly higher SF in JAZ is correlated with a more economical running pattern. Conversely, the negative relationship in female data indicated that lower FF values in both the JAZ and VFN% are associated with better RE at 0% incline. This suggests that females select lower SFs to achieve an improvement in RE regardless of running shoe at moderate inclines, however, at higher inclines, females benefit from even lower SFs, specifically in the JAZ, to achieve an improvement in RE.

The different relationships between the males and females for the FF vs RE shows that the more economical females (those with a better RE thus lower mean $\dot{V}O_2$ uptake) increased their FF to accommodate, meaning they would have had to reduce their SL to maintain the same speed. However, the male participants behaved on the contrary, where the more economical runners decreased their FF, thus having to increase their SL to maintain the same speed. The current literature shows that male athletes increase SL in VFN% when running at a fixed speed (Hoogkamer *et al.*, 2018; Barnes and Kilding,

2019), interestingly there is not current evidence to support the case in female athletes. At the time of this thesis, female athletes are yet to be studied in the VF research and this warrants further investigation.

Existing literature indicates that RE is not impacted when shortening SL by up to 3 % compared to the preferred SL, however, deviations greater than 6 % negatively affected RE (Moore, 2016). The female participants derived greater benefits from the shortening of SL, in contrast to the male participants in our study. Our findings highlight the adaptability of runners, who dynamically adjust their SL and SF in response to exertion intensity, with a multitude of potential combinations, highlighting the emergence of personal gait features (Cavanagh and Williams, 1982; Inman *et al.*, 2006). There should be particular attention paid to gender differences as highlighted by our study findings.

4.4.4. HYPOTHESIS FOUR; FOR MALES AND FEMALES THE VFN% WILL PRODUCE LOWER SPECTRAL PURITY (SP) LEVELS THAN THE JAZ, ERGO HAVE BETTER GAIT QUALITY.

For hypothesis four, we predicted that the VFN% would produce lower SP values than the JAZ. We accepted this hypothesis for both males and females as the VFN% had significantly lower SP, thus superior gait quality over the JAZ over almost all inclines (Table 11). The males received a larger SP benefit compared to the females over incline 0%, 1% and 3% incline but not at 5% incline (Table 12, Figure 58). It is unclear why there is an additional SP benefit for the JAZ at 0% incline for both genders and additionally at 1% and 3% incline for females.

It is well known that increased effort leads to elements of physiological and neurological fatigue, where runners become less competent in the positioning of the foot and leg at foot-strike. More experienced runners have an improved capacity to delay the effects of increased muscular effort and peripheral fatigue associated with increased step frequency. Therefore, experienced runners can maintain a consistent locomotion pattern for longer, leading to higher levels of gait symmetry (Seminati *et al.*, 2013). In relation to our research, the more experience runners would demonstrate a cleaner FFT, leading to lower SP values, hence higher gait quality compared to the inexperienced runners. This may clarify why the phenomenon where increases in FF lead to increases in SP can be associated with more experienced runners. Clark (2017) also demonstrated statistically significant differences in movement quality in young children between motor competence classifications, thus, for our research, the runners who were classified as better performers should have achieved higher levels of gait quality through having advanced neural control. However, we determined no statistically significant differences for those who could and could not perform 10 km in ≤ 40 minutes. By deduction, this means the VFN% must have an independent effect on RE regardless of experience level. We postulated that the VFN% facilitated a delay in the onset of neurological fatigue, thus providing more time for economical running, ergo additional RE benefit. Fatigue would be an interesting addition to this work, including exploring the relationship between fatigue and GaiT.

4.4.5. *HYPOTHESIS FIVE; FOR MALES AND FEMALES HIGHER*

SPECTRAL PURITY (SP) VALUES WILL BE SEEN WITH INCREASING INCLINE.

For hypothesis five, we predicted that higher SP values will be seen with increasing incline, meaning gait quality will diminish. We rejected hypothesis five because SP improved with incline (Table 11). These results may have been due to the large number of experienced athletes within the sample, where running experience is an important elements of gait symmetry (Seminati *et al.*, 2013). Running on an incline requires greater activation of the triceps surae, hamstrings and gluteal muscles, contributing to a more comprehensive and efficient distribution of workload, potentially enhancing overall gait quality (Seminati *et al.*, 2013).

There was a statistically significant difference between the SP values at 1% and 3% incline ($P = .012$), indicating that running on a 1% incline compared to a 3% incline had different effect on gait quality (Figure 56). Regardless of overall significance, SP has a negative relationship with incline; where increasing incline yields decreasing SP until reaching a plateau. This implies that the complexity of the harmonic components within the FFT decrease as incline increases, thus, running gait quality increases with incline.

The current literature has evidenced the VFN% during uphill running attenuates shock by having a lower GRF and shorter GCT than other comparative running shoes (Fuller *et al.*, 2015; Hoogkamer *et al.*, 2018; Whiting, Hoogkamer and Kram, 2022). Therefore, as the VFN% lower GRFs with increasing incline this would ultimately reduce the quantity and magnitude

of higher frequency components recorded within the accelerometry running wave, which are ultimately expressed in the FFT.

Therefore, we propose a plausible connection between GaiT; FF and the improved RE benefits facilitated by the VFN% compared to conventional running shoes (Hoogkamer *et al.*, 2018). Our study contributes novel evidence, endorsing the use of accelerometer-based gait analysis which aligns with the VFN% RE literature, allowing for a quantitative evaluation of running performance, thus fulfilling the central premise of this thesis. While the current data may not support comprehensive modelling and understanding of these research findings, the observed enhancement in gait quality during incline running merits further exploration for its potential application to quantitatively assess running performance. This invites validation of GaiT; FF and SP for accelerometer-based gait analysis within and beyond laboratory confines.

4.4.6. HYPOTHESIS SIX; FOR MALES AND FEMALES LOWER RUNNING ECONOMY (RE) VALUES WILL BE ASSOCIATED WITH LOWER SPECTRAL PURITY (SP) VALUES.

For hypothesis six, we predicted that for males and females lower RE values would be associated with lower SP values. We accepted hypothesis six for the females at a 5% incline only as they demonstrated a negative relationship between RE and SP. This means that the more efficient female runners had lower SP values, meaning those with lower RE values (better performers) had better quality gait. This concept was discussed earlier in this chapter, where

better performers demonstrate an improved capacity to maintain movement patterns (Jenner *et al.*, no date; Barnes, 2017; Clark, 2017).

Thus, as $\dot{V}O_2$ uptake increased, the SP value decreased, meaning the movement wave was cleaner and running gait quality higher. Additionally, these results show that SP of the VFN% and JAZ behave in the same way. The distinction is that the VFN% consistently demonstrated a lower SP value, providing better gait quality than the JAZ over all inclines (Figure 59).

The VFN% during uphill running consistently demonstrated a higher RE benefit, lower GRF and shorter GCT than other comparative running shoes (Hoogkamer *et al.*, 2018). These RE benefits are thought to be due to the increased ZoomX foam and increased LBS from the carbon fibre plate. We are postulating that the construction of the VFN% may be providing the foundation for improved movement quality via a smoother heel-to-toe transition. This transition could occur due to altered biomechanics at the foot, reducing movement variability, thus fulfilling our definition of improved gait quality through reduced SP values (Padulo *et al.*, 2013; Hoogkamer *et al.*, 2018; Healey and Hoogkamer, 2021; Ortega *et al.*, 2021; Hunter *et al.*, 2022; Whiting, Hoogkamer and Kram, 2022).

4.5. CONCLUSION AND NEXT STEPS

4.5.1. SUMMARY OF FINDINGS

This study investigated the feasibility of the calibration and analytical processing techniques to produce a novel gait analysis tool (GaiT) applicable

over various inclines to contextualise running data from accelerometry. The GaiT used FF and SP to identify gait variations between the Nike® Vaporfly ZoomX NEXT% (VFN%) and a conventional running shoe the Saucony® ProGrid Jazz 12 (JAZ) using runners of various abilities. In addition to predicting performance using accelerometry, the intersection of GaiT; FF and SP data, with RE data was explored. 18 participants; n=6 females and n=12 males volunteered in the cardiopulmonary exercise testing protocol and 23 participants; n=6 females and n=17 males volunteered in the accelerometry protocol.

Hypothesis one was accepted as the GaiT measure FF decreased with increasing incline meaning SF increased at a fixed speed. Hypothesis two was accepted as the VFN% FF was lower than the JAZ FF over all inclines leading to an increase in SL at a fixed speed. Hypothesis three was accepted for males, with lower RE values being associated with lower FF values, ergo, lower SF values equated to increased SL to maintain the same speed. The females displayed the inverse behaviour, where the better performers had higher FF values and a shorter SL. Hypothesis four was accepted as the VFN% produced lower SP values than the JAZ, meaning the VFN% had superior gait quality (fewer high frequency harmonics) for almost all inclines. Hypothesis five was rejected as the GaiT measure SP decreased in value with increasing incline, meaning gait quality improved with incline. Hypothesis six was accepted for the females where a negative relationship existed between RE and SP, meaning better performers (lower RE values) had better gait quality with increasing incline.

For the most part, FF benefit parallels RE benefit which provides a novel solution for predicting performance from accelerometry data; lower FF values equate to more economical performances (lower RE), ergo better performance times, whilst treadmill running at a fixed speed up to a 5% incline. SP benefit does not parallel RE benefit so clearly.

In summary, the GaiT for FF, calculated from the FFT frequency-domain analytics, has the potential to bridge the gap between quality and quantity measures for gait analysis. Ultimately, we have provided a novel method to quantitate running gait and provided a solid foundation toward understanding the use of FF from accelerometry to predict RE from CPET. We are providing an inexpensive, portable and accurate method to calculate treadmill running gait quality and performance over various inclines within the laboratory. We believe with further testing and optimisation, GaiT will be a beneficial tool for all runners to understand their gait quality and predict performance outside of the laboratory.

4.5.2. FUTURE WORK

To strengthen the data, the randomisation and grouping procedures need to be balanced. Additionally, only one speed and one attempt at each incline was tested, even though this method is frequently conducted throughout the literature. It is understood that test-retest methods at two to five days to reduce fatigue and minimises within-subject RE variation by 90–98% respectively, thus this method could be repeated two to three times effectively (Roy and Stefanyshyn, 2006). Avoiding convenience samples and balancing participant

characteristics may influence the results, although the current literature rationalises gender differences for RE with females exhibiting higher $\dot{V}O_2$ uptake (Barnes and Kilding, 2015).

CHAPTER FIVE

5. GENERAL DISCUSSION

5.1. PROJECT AIM

The aim of this thesis was to bridge the gap between laboratory and real-world gait analysis by addressing the critical need for a portable and quantitative method for running gait analysis. Using a series of studies within the controlled laboratory environment, a research grade wearable accelerometry device was validated as sensitive enough to capture robust running gait data. A collection of data processing techniques yielded several running gait variables which were able to quantitatively capture running gait quality, particularly the frequency of a runner's foot strike as measured by the Fourier transform of an acceleration-time wave. These data processing techniques were used to contextualise the acceleration-time wave data, unveiling a relationship between these gait variables and running performance.

5.2. CHAPTER 1: GENERAL INTRODUCTION

Traditionally, quantitative running gait analysis has been confined to laboratories that have specialised measurement equipment. Motion capture (MC), the best objective method for gait analysis, requiring a considerable level of expertise and proficiency in equipment operation and data analysis (Jenner *et al.*, no date; Norris, Anderson and Kenny, 2014; Barnes, 2017; Caldas *et al.*, 2017; Anwar, Yu and Vassallo, 2018). Most research focused on understanding gait variables in their isolated form, particularly within

clinical populations where gait patterns were compromised. There were few studies (Jenner *et al.*, no date; Barnes, 2017; Clark, 2017) investigating gait in a global sense where specific analytical techniques were used to contextualise gait parameters, much like statistical analyses.

This project set out to assess whether a wearable device had a sufficiently sensitive accelerometer to capture high-quality, unprocessed accelerometer-time wave running data. Using these data a series of robust data processing techniques were developed to quantitatively measure running gait quality. This work was driven by the distinct need for a portable solution to make quantitative gait analysis more accessible outside of traditional laboratory testing options.

5.3. CHAPTER 2: FORMULATION AND OPTIMISATION OF GENERAL METHODS

Chapter two formulated and investigated the suitability of the data processing method and analytical techniques selected to move from a simple accelerometer-time wave to quantifiable measures of running gait. The specifically selected and optimised calibration techniques successfully maintained the detail required, enabling for the differentiation of protocol events within the movement wave (Analogue Devices, 2015; Barnes, 2017; Kieron *et al.*, 2018). Prior to analysis of the data, the calibration process consisted of; amending the sampling frequency of one device (blue) to match the other (red), adjusting for sensitivity and bias in both devices, applying a high and low pass filter (0.5 Hz/ 20 Hz) to all acquired data, and implementing

a rotation matrix to correct for misalignment of the devices when fitting them to the participant's limb (Barnes, 2017; Clark, 2017). Hence, the wearable devices were shown to be reliable at collecting treadmill running data from a participant, whilst treadmill running up to 16 km/h during repeated trials.

The formulation and optimisation of the analytical tool; the Global gait analysis Tool (GaiT) was iterative and evolved based on the findings of the several studies reported throughout the chapter. This novel analytical tool contained three measures; the fast Fourier transformation (FFT) of the accelerometer-time data to the frequency domain established the Fundamental Frequency (FF) of the runner's foot strike; the cumulative distribution function (CDF) of the FFT established Spectral Purity (SP); and the cross-correlation function (CCF) and auto-correlation function (ACF) of the accelerometer-time waves calculated gait symmetry using a symmetry index (SI). These measures previously contextualised physical activity in young children, highlighting skill level as a measure of performance (Barnes, 2017; Clark, 2017), and as a tool to objectify the return to sport from injury (Jenner *et al.*, no date). Contextualising running gait quality using accelerometer-time waves was a novel aspect of this project. The strict fitting protocol plus two GaiT measures (FFT and CDF) developed in this chapter were shown to have the potential for measuring running gait on a treadmill at speeds of up to 16 km/h, however, further optimisation and benchmarking against quantified levels of running performance were needed to validate these measures.

This novel approach has the potential to be developed into a running gait quality feedback tool, appealing to coaches, runners and researchers alike.

From a clinical perspective this objective tool could be used in healthcare, rehabilitation and monitoring to gather a global perspective on lifestyle data where treatment can be adapted accordingly.

5.4. CHAPTER 3: NIKE® VAPORFLY ZOOMX NEXT% RUNNING SHOES HAVE RUNNING ECONOMY BENEFITS OVER VARIOUS INCLINES COMPARED TO CONVENTIONAL RUNNING SHOES

Chapter three established that Nike® Vaporfly ZoomX NEXT% running shoes have running economy benefits over various inclines compared to conventional running shoes, using cardiopulmonary exercise testing (CPET) in synchronisation with accelerometry. The interval protocol tested runners on several treadmill inclines (from 0 – 5 %) at 12 km/h whilst wearing the Nike® Vaporfly ZoomX Next% (VFN%) and when wearing a conventional running shoe, the Saucony® ProGrid Jazz 12 (JAZ). At 0% incline, the VFN% achieved a 4.37% RE benefit over the JAZ in line with the 4.01% previously reported by Hoogkamer et al., (2018) and the 3.83% reported by Whiting, Hoogkamer and Kram, (2022). At 3% incline the VFN% achieved a 2.75% RE benefit and at 5% incline a 2.70% RE benefit, in line with the 2.82% measured by Whiting, Hoogkamer and Kram, (2022) when compared to conventional running shoes. The novel element of this chapter was establishing the VFN% had an exponential decay of RE benefit on an incline rather than a linear decline of RE benefit as suggested by Whiting, Hoogkamer and Kram, (2022). In addition, fitting of RE benefit against incline to an exponential decay model we isolated the mass benefit from the midsole benefit. No further meaningful

decline of RE benefit was seen after 16% incline, leaving a fixed 2.28% RE benefit thereafter. Translation of these benefits into race gains was illustrated by taking the incline profile of the New York Marathon course and applying an average 3.8% RE benefit across the course to suggest that more than 7-minutes could be saved by wearing the Nike® Vaporfly ZoomX NEXT% compared to wearing a conventional running shoe.

These novel findings could influence the consumer fitness market increasing interest in the Nike® Vaporfly running shoe series and other similar performance-enhancing footwear. Strategically directing awareness of the research generated from this project could potentially influence public health by encouraging more people to try running, specifically through the interest in testing some performance enhancing footwear. Additionally, the attention directed toward the research generated from this project has the potential to influence other footwear manufacturers to invest further in their technological research and even adapt their current running shoe offering. Finally, researchers may be interested in continuing this line of inquiry to understand more around the limitations of these performance enhancing running shoes and incline.

5.5. CHAPTER 4: THE GLOBAL GAIT ANALYSIS TOOL (GaiT) FOR THE QUANTIFICATION OF PERFORMANCE DIFFERENCES BETWEEN RUNNING WEARING VFN% AND JAZ SHOES USING ACCELEROMETRY

Chapter four explored the validation of GaiT using running accelerometry data acquired alongside the RE data whilst wearing the VFN% and JAZ running shoes during cardiopulmonary exercise testing (CPET) over various treadmill inclines (Chapter 3). GaiT measures, FF and SP, identified movement variations within and between runners whilst wearing the VFN% and JAZ running shoes. The GaiT measure FF increased with increasing incline, thus stride frequency (SF) increased (as expected for incline running), thus SL had to decrease as a consequence. SP decreased in value with increasing incline, suggesting gait quality improved. The VFN% running shoe had consistently lower FF values when compared to the JAZ, thus facilitating a longer stride length (SL), over all inclines. The VFN% running shoes produced consistently lower SP values, suggesting these running shoes have superior gait quality, when compared to the JAZ running shoe, over almost all inclines.

These novel findings cannot be directly equated to the RE benefits measured in this chapter but a qualitative comparison suggests that FF benefit follows the same profile as RE benefit of the VFN%. This enabled a parallel to be drawn between RE and FF as a predictor of physiological performance, even though this differed between genders. Barnes, (2017) reported a positive relationship between higher skill level, as measured by SP, to better performance, whereas the SP data from runners wearing the VFN% and JAZ

shoes requires more participants before a clear link to RE benefit can be identified.

For males, a negative relationship existed between RE and FF, and RE and SP, indicated that better performers had lower SF and better gait quality. The females displayed the inverse of this relationship for RE and FF but the same relationship for RE and SP. These findings support those reported by Clark, (2017); Hoogkamer et al., (2018) and Barnes and Kilding, (2019).

A novel solution for predicting treadmill running performance was established between GaiT's FF benefit by its parallel relationship to RE benefit. GaiT therefore has the potential to bridge the gap between quality and quantity measures for gait analysis by being able to predict performance based on FF inside of the laboratory when running at a fixed speed. With further testing of running at a fixed speed when fresh and when fatigued, there is the potential for development and application outside of the laboratory where running speed is not fixed, such as seen in Hunter et al., (2022). This novel analytical tool therefore has the potential to provide access to affordable and objective performance prediction based on gait measures in real-world athletic experiences.

The impact of this evidence on the sport of running could be significant, with the novel ability to assess and improve running performance through the utilisation of a wearable device is astounding and could change the face of laboratory based biomechanical gait analysis globally. From a healthcare and rehabilitation perspective, formulating an app housing the GaiT feature that

could contextualise return to wellness would allow clinicians to easily monitor and update patient rehabilitation programmes.

5.6. PHILOSOPHICAL AND SPECULATIVE IMPACTS

5.6.1. *REVOLUTIONISING SPORTS AND ATHLETIC TRAINING*

Beyond Performance, these research findings could lead to a new era in athletic training where data-driven insights that are not just about understanding the individual aspects of the biomechanics of movement but about looking at the human body in a global perspective and taking a novel understanding of how to enhance performance. This could foster a deeper connection between athletes and their bodies, promoting a more mindful approach to training.

Democratising elite training by making advanced gait analysis tools accessible to athletes at all levels, not just elites. This democratisation could provide an opportunity for more athletes to reach their full potential.

5.6.2. *TRANSFORMING HEALTHCARE AND REHABILITATION*

Portable gait analysis tools could become integral in preventive healthcare, where regular gait analysis could help detect early signs of musculoskeletal issues or other health problems, enabling early intervention and even promoting preventative healthcare.

A wearable device with the addition of an app containing the GaiT tool could contribute to personalised medicine by providing detailed data that could be used to tailor rehabilitation programs to individual needs, enhancing recovery outcomes.

5.6.3. CONSUMER FITNESS MARKET

GaiT if integrated into an app can be seamlessly utilised by many types of fitness trackers or even mobile phones, thus can be integrating seamlessly into daily life and providing continuous feedback to help individuals maintain optimal physical health using a unique wellness score. Additionally, by incorporating gamification elements, GaiT could make fitness more engaging and fun, encouraging more people to stay active and healthy.

5.6.4. PUBLIC HEALTH INITIATIVES

On a larger scale, aggregated GaiT data from populations could be used to monitor public health trends and inform public health policies. This data could help identify areas with high incidences of gait-related issues and target interventions more effectively.

If marketed correctly, GaiT integrated into an app could influence public health campaigns, where insights from this global gait analysis could be used to promote active lifestyles, reducing the prevalence of sedentary-related health problems.

5.6.5. SCIENTIFIC RESEARCH AND TECHNOLOGICAL ADVANCEMENTS

The novel method in addition to GaiT produced from this research could open new research avenues in biomechanics, sports science and even cognitive science, as gait can reflect neurological health. The large datasets generated by these devices could be used to train AI models, leading to advancements in predictive analytics and personalised recommendations for both athletes and the general public.

5.6.6. PRODUCT DEVELOPMENT AND INNOVATION

Shoe and sports equipment manufacturers could use gait analysis data to design products tailored to individual needs, enhancing performance and reducing injury risks.

The development of new wearable technologies could provide more detailed insights into running performance and gait. Potentially integrating other physiological measures like heart rate variability and muscle activity could provide a more holistic view to gait quality and performance.

5.6.7. CONCLUSION

This evidence has the potential to impact not only the academic field but also various aspects of daily life, healthcare and technology. Speculating on these broader impacts highlights the far-reaching implications of the applicability of

this evidence and emphasises its significance beyond the confines of the laboratory.

5.7. LIMITATIONS

Although all care was taken to minimise the bias and errors within this research, there will always be further optimisation required to better the method. Additionally, further validation of the findings is necessary and will need development. The limitations of this work are discussed throughout this thesis, however several overarching limitations need to be acknowledged and addressing these limitations in future work will strengthen the validity and applicability of the findings.

5.7.1. *SAMPLES SIZE AND REPRESENTATION*

The study would benefit from a more powerful and balanced sample size that accurately represents the running community at all experience levels. The current sample may not adequately capture the diversity within the running population, which could limit the generalisability of the results. Future research should aim to include a broader and more representative sample to enhance the robustness of the conclusions.

5.7.2. *RANDOMISATION PROCESS*

Ensuring a balanced randomisation process, particularly in terms of the order of running shoe testing, is crucial. Although the imbalance seen in some of the studies throughout this thesis were not significant. Future studies should implement a more stringent randomisation protocol to minimise potential biases related to testing order.

5.7.3. GENDER DIFFERENCES

The current research has highlighted the need to explore gender differences more thoroughly. Examining gender groups separately and in combination is essential to uncover any variations in the results. Future work should focus on stratifying data by gender to provide more detailed insights and ensure that findings are applicable to both male and female runners.

5.7.4. METHODOLOGICAL CONSTRAINTS

The research design and methodologies used in this thesis have their inherent limitations. For instance, the reliance on specific data collection techniques (e.g., laboratory-based treadmill testing) may introduce biases or limitations in the type of data collected. Future research could benefit from employing a mixed-method approaches such as including subjective data on participation experience or incorporating additional data sources such as incorporating a systematic review to provide a more comprehensive understanding of the phenomena studied.

5.7.5. TECHNOLOGICAL AND INSTRUMENTATION LIMITATIONS

The tools and technologies used for data collection and analysis, such as CPET and accelerometry, have limitations regarding accuracy, reliability and sensitivity. These limitations could impact the validity of the findings. Future work could involve the use of more advanced or alternative technologies to

enhance data accuracy and reliability such as live data streaming and the use of AI with its advanced predictive capacity.

5.7.6. LONGITUDINAL CONSIDERATIONS

The cross-sectional nature of the current study limits the ability to infer causal relationships. Longitudinal studies, which follow participants over time, would provide more robust insights into the long-term effects and causal relationships within the studied variables. In this project, it is important to understand the long-term implications of GaiT and how the data collected using this tool may be effective at supporting runners in the future. Future research should consider longitudinal designs to address this limitation. With injury being an important aspect of health, wellness and longevity within the running community.

By addressing these areas, future research can build on the findings of this thesis, offering more comprehensive and generalisable insights into the factors influencing running performance, running shoe effectiveness. The links with this research and injury are significant and has great research importance with causal relationships posing a significant global influence on the sport of running, the wearable technology industry, and injury prevention and rehabilitation.

5.8. FUTURE WORK

Due to the impact of COVID on this project, additional data were collected but time restraints meant they could not be included within this body of work. The

logical next step would be to fully process and analyse the data collected from this additional work: Study 6: The impact of fatigue on GaiT.

CIBA Foundation Symposium (1981) (Moldover and Borg-Stein, 1994) defined fatigue as the moment when a participant is unable to maintain the required muscle contraction or performed workload. Fatigue affects biomechanical gait variables by; altering neuromuscular function, slowing muscle reaction times, reducing energy transfer between concentric and eccentric muscle contractions (Dierks, Davis and Hamill, 2010), increasing/ decreasing stride length, decreasing/ increasing stride frequency (Verbitsky *et al.*, 1998; Barnes and Kilding, 2015), and attenuating peak dynamic loads and acceleration patterns (Verbitsky *et al.*, 1998; García-Pérez *et al.*, 2014). Fatigue is a known risk factor for injury, where the prolonged accumulation of these sub-optimal biomechanics can lead to overuse injuries (McGrath *et al.*, 2017; Martens *et al.*, 2018). Martens *et al.*, (2018) demonstrated that running biomechanics alter shortly before exhaustion, specifically the heterogenous nature of stride biomechanics during test-retest intervals.

We believe that GaiT, the bespoke quantitative analytical tool, can identify the development of fatigue in treadmill running data. A fatigue inducing protocol was conducted (n=12) to establish if the accelerometry running data recorded on the wearable devices was sensitive enough to identify gait changes during the development of fatigue. The data would be analysed as in the previous chapter using GaiT with the hypothesis that FF will increase and SP will decrease with the onset of fatigue due to the breakdown of the participants movement pattern (Jenner *et al.*, no date; Clark, 2017). Processing this sample of data would enable for the exploration of any possible significance

or relationship between fatigue and GaiT and would provide another step towards validating the tool for testing outdoor running performance.

Additionally, future work could investigate a longitudinal data collection to provide a fatigue data set big enough to identify the onset of injury. The data processed with GaiT would provide a relationship between FF and fatigue, thus aiming to quantify the level of fatigue responsible for the onset of overuse injuries. There is an excellent opportunity here to produce a live feedback system to a coach or runner, where objective information regarding an athlete's fatigue status and injury likelihood score is available during a training session. Such a novel system has the potential to eliminate the subjectivity behind some of the current methods of injury prevention.

The next step for developing this technique as a tool to be used outside of the laboratory could be achieved by using a protocol, similar to that of the test-retest repeatability study (Protocol 2.12) but conducted on a running track with a pacing watch to control for speed variability. To validate GaiT outdoors with this protocol, 25 participants would be needed to detect a statistical significance at $P = 0.05$.

This information would be incredibly useful for coaches and athletes, where reducing the likelihood of injury will have a global impact on time away from sport at every level, improving mental health, improving long term athletic career prospects, improving national/ global ranking through athlete retention, plus other positive benefits associated with reduced injury. A tool like this could change the face of sport.

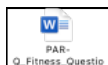
5.9. CONCLUSION

In conclusion running in the Nike® Vaporfly ZoomX NEXT% (VFN%) running shoe was shown here to produce more economical running by lowering RE by up to 4 % than when running in a conventional running shoe and this benefit declined as incline increased. There appeared to be no further meaningful RE penalty below 2.8 % incline or above a 16% incline. We were able to isolate the mass benefit from the midsole benefit due to the carbon fibre plate and ZoomX foam in the VFN% running shoe. The Global gait analysis Tool (GaiT) highlighted Fundamental Frequency (FF) of the Fourier transformed accelerometry-time wave acquired during running as an indicator of RE whilst treadmill running at 12 km/h over various inclines. However, Spectral Purity (SP) of the Fourier transformed accelerometry wave needs further exploration with additional cardiopulmonary exercise data to identify any solid relationships. There is the potential to use GaiT to identify fatigue in running data and with longitudinal data collection to investigate the link with overuse injuries.

We are confident that GaiT can be explored for its potential for predicting performance from running accelerometry data and to investigate a potential link with injury, however, there needs to be further data collection to conclude its suitability for use outside of the laboratory.

APPENDICES

Appendix A: Participant PAR-Q



UNIVERSITY OF LEEDS

PAR-Q Form

(Physical Activity Readiness Questionnaire)

Forename: _____ **Surname:** _____

For most people physical activity should not pose any problem or hazard. PAR-Q is designed to identify the small number of adults for whom physical activity might be inappropriate or those who should have medical advice concerning the type of activity most suitable for them.

Please read the questions below carefully

Has your doctor ever said that you have a heart condition **OR** a family history of heart disease **OR** high blood pressure **OR** high cholesterol **OR** diabetes/prediabetes **OR** elevated cholesterol?

- 1) Do you feel pain in your chest at rest, during your daily activities of living, **OR** when you do physical activity?
- 2) Do you lose balance because of dizziness **OR** have you lost consciousness in the last 12 months? Please answer **NO** if your dizziness was associated with over-breathing (including during vigorous exercise).
- 3) Have you ever been diagnosed with another chronic medical condition (other than heart disease or high blood pressure)?
- 4) Are you currently taking prescribed medications for a medical condition?
- 5) Do you have a bone or joint problem that could be made worse by becoming more physically active? Please answer **NO** if you had a joint problem in the past, but it does not limit your current ability to be physically active. For example, knee, ankle, shoulder or other.

Has your doctor ever said that you should only do medically supervised physical activity?

If any one or more of the above applies, please check the box:

☐

DECLARATION AND AUTHORISATION

I confirm that the information given is a true and accurate statement. I understand that if I have declared any of the conditions listed, further information may be requested and I will not be able to participate in this study.

Please be aware that it is your responsibility to inform us if there is a change to any of your answers on the PAR-Q.

Signature:

Date:

Appendix B: Pre-visit COVID questionnaire



UNIVERSITY OF LEEDS

School of Biomedical Sciences
FACULTY OF BIOLOGICAL SCIENCES

Pre-visit COVID-19 Participant Screening Questionnaire

Prior to any research visit to the university, please complete this questionnaire and bring a copy with you.

If you answer 'YES' to any of the questions below please contact a member of the research team *before* you leave your home to attend the scheduled session. Please circle your responses below.

1. Would you classify yourself as being 'vulnerable' in relation to COVID-19 risk?

YES

NO

2. Is anyone in your household or social bubble classified as vulnerable in relation to COVID-19 risk?

YES

NO

3. Have you in the last 14-days had any (even if mild) COVID-19 symptoms:

A. A new continuous cough:

YES

NO

B. A high temperature – you feel hot to touch on your chest or back:

YES

NO

C. A loss or change to your sense of smell or taste:

YES

NO

4. To your knowledge, have you had any contact with anyone (both within and outside your household or social bubble) who has had any COVID-19

symptoms (even if mild) in the last 14-days (see question 3 A, B, C for details of COVID-19 symptoms):

YES

NO

5. To your knowledge, have you been in contact with anyone who has tested positive for COVID-19 in the last 14-days:

YES

NO

6. Have you been contacted by NHS track-and-track and told to self-isolate in the last 14-days:

YES

NO

7. If you have been to the lab before, has there been any change in your health status since you last visited the lab?

YES

NO

Note to researcher: Please insert participant SID below, and attach to the datasheet for today's experiment.

Participant SID: _____

Date: _____

Appendix C: Ethical clearance



UNIVERSITY OF LEEDS

University Research Ethics Committee - application for ethical review

Please email your completed application form along with any relevant supporting documents to ResearchEthics@leeds.ac.uk (or to FMHUniEthics@leeds.ac.uk if you are based in the Faculty of Medicine and Health) at least 6 weeks before the research/ fieldwork is due to start. Dentistry and Psychology applicants should follow their School's procedures for submitting an application.

Ethics reference (leave blank if unknown)	Student number (if a student application)	Grant reference (if externally funded)	Module code (if applicable)
Faculty or School Research Ethics Committee to review the application (put a 'X' next to your choice)		Arts, Humanities and Cultures (PVAR)	
	x	Biological Science (BIOSCI)	
		ESSL, Environment and LUBS (AREA)	
		MaPS and Engineering (MEEC)	
		School of Dentistry (DREC)	
		School of Healthcare (SHREC)	
		School of Medicine (SoMREC)	
		School of Psychology (SoPREC)	
Indicate what type of ethical review you are applying for:	x	Student project (PhD, Masters or Undergraduate)	
		Staff project (externally or internally funded)	

SECTION 1: BASIC PROJECT DETAILS

1.1	Research title	Accelerometer-based gait analysis for quantitative assessment of physical activity outside the laboratory		
1.2	Research start date (dd/mm/yy)	Proposed fieldwork start date (dd/mm/yy)	Proposed fieldwork end date (dd/mm/yy)	Research end date (dd/mm/yy)
	07/01/19	01/04/19	30/06/2022	30/09/2022
Yes	No			
x		<p>1.3 I confirm that I have read and understood the current version of the University of Leeds Research Ethics Policy.</p> <p><i>The Policy is available at http://ris.leeds.ac.uk/ResearchEthicsPolicies.</i></p>		
x		<p>1.4 I confirm that I have read and understood the current version of the University of Leeds Research Data Management Policy.</p> <p><i>The policy is available at https://library.leeds.ac.uk/info/14062/research_data_management/68/research_data_management_policy.</i></p>		
x		<p>1.5 I confirm that I have read and understood the current version of the University of Leeds Information Protection Policy.</p> <p><i>The policy is available at http://it.leeds.ac.uk/info/116/policies/249/information_protection_policy</i></p>		
x		<p>1.6 I confirm that NHS ethical review is not required for this project.</p> <p><i>Refer to http://ris.leeds.ac.uk/NHSEthicalreview for guidance in identifying circumstances which require NHS review</i></p>		
	x	<p>1.7 Will the research involve NHS staff recruited as potential research participants (by virtue of their professional role) or NHS premises/ facilities?</p> <p><i>Please note: If yes, NHS R&D management permission or local management permission may also be needed. Refer to http://ris.leeds.ac.uk/NHSEthicalreview.</i></p>		

SECTION 2: CONTACT DETAILS

2.1 Name of applicant	Dr Graham Askew
2.2 Position (eg PI, Co-I, RA, student)	PI
2.3 Department/School	School of Biomedical Sciences
2.4 Faculty	Faculty of Biological Sciences
2.5 Work address (usually at the University of Leeds)	School of Biomedical Sciences Faculty of Biological Sciences University of Leeds Leeds LS2 9JT
2.6 Telephone number	01133432897
2.7 University of Leeds email address	g.n.askew@leeds.ac.uk

SECTION 3: SUMMARY OF THE RESEARCH

3.1 In plain English provide a brief summary of the aims and objectives of the research.

(max 300 words). The summary should briefly describe

- the background to the research and why it is important,
- the questions it will answer and potential benefits,
- the study design and what is involved for participants.

Your answers should be easily understood by someone who is not experienced in the field you are researching, (eg a member of the public) - otherwise it may be returned to you. Where technical terms are used they should be explained. Any acronyms not generally known should be described in full.

Running economy accounts for a large proportion of variation in distance running performance, and is linked to a variety of factors including the biomechanical characteristics of the runner's gait. In injured runners, rehabilitation state is also characterised by gait. Gait can be readily measured

in the laboratory using multi-camera motion capture systems. However, such systems are expensive and tend to be limited to specialist laboratories; the activities that can be quantified tend to be limited to steady state conditions (such as constant velocity treadmill locomotion); laboratory setups may result in unnatural gait; and setup and processing time means that the approach is unsuitable for assessing large numbers of individuals. These limitations mean that the rehabilitation state of runners is largely assessed by observation and palpation. Commercially available inertial measurement units (IMUs), that measure body accelerations for example, could provide a cheaper solution to characterising movement that can be deployed in an everyday setting. However, a major limitation of these devices is that the outputs represent an average over a specific time period and much of the information available in the raw acceleration wave is irretrievably lost. Thus, these devices are unable to give detailed information about activity levels over short timescales (sub-second) and are inadequate to describe the quality of activity, an area that is of growing interest in the sport and exercise science arena. We have developed a customised device and analytical approach that allows gait to be quantified in the appropriate time and frequency domains and offers the potential of providing meaningful meta-analysis for activity levels of large populations as well as of individuals.

The main aim of this project is to derive a series of robust measures from accelerometry, validated in the laboratory against 3D movement data, that can give accurate information of an individual's physical activity and metabolic energy expenditure. This will be done in healthy and rehabilitating endurance runners. Once validated in the laboratory, we will assess the devices under field-based conditions.

The following methods will be used:

- (1) Motion capture. Anatomical markers will be placed bilaterally on anatomical landmark positions and their 3D position captured using a twelve-camera Qualisys system. These data will be used to compute the 3D trajectory of the body centre of mass (represented as a Lissajous plot) and the dynamical symmetry indices of locomotion in the three spatial axes computed.
- (2) Accelerometry. Custom-built IMUs will be attached to the test subject. Raw signals will be processed using Fast Fourier Transforms, and auto and cross-correlations to extract a range of gait parameters and determine an index of gait symmetry. The extracted values from the IMU will be validated against the motion capture data.
- (3) Electromyography. In some participants, lower-limb muscle activity patterns will be recorded using surface electromyography.
- (4) Energy Cost Measurement. In some participants, oxygen consumption will be measured using mask respirometry to measure metabolic cost of transport or running economy (i.e. the oxygen consumed to move 1 kg of body mass 1 m distance). The duration of the exercise bouts will be dictated by the time taken for oxygen consumption and carbon dioxide production to reach a steady level

(typically five minutes).

Laboratory studies: subjects will attend the laboratory, usually on up to two occasions, for 1-2 hours per session. Subjects will be asked to complete one of a number of possible protocols (when participants are recruited, it will be for testing under a specific protocol). For example:

- (1) *Treadmill running at a range of speeds.* Runners will have markers and IMUs attached to the body and their gait recorded using motion capture. Heart rate will be recorded. In some runners, (a) metabolic energy expenditure will be determined using respirometry, or (b) muscle activity patterns will be determined using electromyography. The aim is to determine whether running performance (assessed by measuring running economy) is related to gait and whether differences in running economy are related to muscle activation patterns.

Speeds will cover the range 10-18 km/h (2 km/h increments) and are expected to elicit <90% max. heart rate); for the metabolic measurements speeds will not exceed those at which respiratory exchange ratio >1. The protocol duration will be approximately 15 mins (without respirometry) – 60 mins (with respirometry), excluding warm-up/cool-down.

- (2) *Treadmill running at a range of speeds with asymmetrical limb loading.* As in (1), but runners will additionally wear a load on one limb (either upper or lower limb) to induce gait asymmetry. Loads will not exceed 5% (foot/ shank) or 10% (thigh) of body mass. The aim is to determine whether gait asymmetries that will be quantified using motion capture can be detected using the IMUs. The selected speeds are likely to induce 80-85% max. heart rate.

The protocol duration will be approximately 15 mins, excluding warm-up/cool-down.

- (3) *Incremental treadmill running to induce fatigue.* As in (1), but the running protocol will involve incremental increases in speed until the subject reaches voluntary exhaustion. This protocol is likely to elicit a heart rate close to maximum by the end of the test, but will be of relatively short duration (>90% max. heart rate for ~5 mins). The aim is to determine whether fatigue affects gait (especially gait symmetry) that can be detected using the IMU.

Speeds will cover the range 10-18 km/h. The protocol duration will be approximately 30 mins, excluding warm-up/cool-down.

Field studies: subjects will be asked to attend an athletics track on up to two occasions for approximately 1 hour. Subjects will be asked to complete one of a number of possible protocols. For example:

<p>(1) <i>Gait analysis during track running.</i> Runners will have IMUs attached to the body. They will run at a specified pace for approximately 1.2-1.6 km. In some runners, metabolic energy expenditure will be determined using respirometry. The aim is to determine whether running performance (assessed by measuring running economy) is related to gait as detected using an IMU in the field. The selected speeds are likely to induce 80-85% max. heart rate.</p> <p>The protocol duration will be approximately 6 mins, excluding warm-up/cool-down.</p> <p>(2) <i>Interval session.</i> Runners will have IMUs attached to the body and will perform an interval session as per their normal training routine (i.e. we will not dictate the session, however, we may target specific types of session by liaising with the runners' coaches). The aim is to determine whether fatigue during an interval session affects gait (especially gait symmetry) that can be detected using an IMU in the field.</p>	
3.2 Where will the research be undertaken?	<p>Laboratory research will be carried out at the University of Leeds.</p> <p>Field work will be carried out in a variety of locations, usually athletics tracks (e.g. Leeds Beckett University, University Academy Keighley).</p>
3.3 Who is funding the research?	University of Leeds studentship.
<p><i>NB: If this research will be financially supported by the US Department of Health and Human Services or any of its divisions, agencies or programmes please ensure the additional funder requirements are complied with. Further guidance is available at http://ris.leeds.ac.uk/FWAcompliance and you may also contact your FRIO for advice.</i></p>	
<p>SECTION 4: RESEARCH DATA AND IMPACT</p> <p>You may find the following guidance helpful:</p> <ul style="list-style-type: none"> • Research data management guidance • Advice on planning your research project • Dealing with issues relating to confidentiality and anonymisation • Funder requirements and University of Leeds Research Data Management Policy 	
4.1 What is the data source? (Indicate with an 'X' all that apply)	
x	New data collected for this research

x	Data previously collected for other research
	Data previously collected for non-research purposes
	Data already in the public domain
	Other, _____ please _____ state: _____.
4.2 How will the data be collected? (Indicate with an 'X')	
	Through one-to-one research interviews
	Through focus groups
x	Self-completion (e.g. questionnaires, diaries)
	Through observation
	Through autoethnographic research
x	Through experiments/ user-testing involving participants
	From external research collaborators
	Other, _____ please _____ state: _____.
4.3 How will you make your research data available to others in line with: the University's, funding bodies' and publishers' policies on making the results of publicly funded research publicly available (in compliance with UK data protection legislation)? (max 200 words)	
<p>The project will generate anatomical, physiological and biomechanical data on each subject, including locomotor energetics, patterns of muscle activity and 3D kinematics of the body. These data, the metadata that describe these data and the parameters derived from the data that are used in subsequent analyses will be collected and managed in accordance with the University of Leeds policy on Good Research Practice. These comply with the Joint Code of Practice on Research. All original data will be retained for at least 10 years and will remain the property of the University of Leeds. All data will be managed in accordance with the current UK data protection policy. Electronic data also being backed up and archived at the University of Leeds.</p> <p>These data have many potential uses in biomechanics. Accordingly, data will be made available to colleagues and interested parties upon request (anonymised raw and analysed data as appropriate) but normally after publication or presentation at conferences via talks and poster presentations. Publications will be announced, made available through specific web sites (such as the repository) and within journals as appropriate. Supplementary</p>	

files associated with publications will be used wherever possible to ensure critical data and analysis can be best shared.	
4.4 How do you intend to share the research data, both within and outside the research team? (Indicate with an 'X')	
x	Depositing in a specialist data centre or archive
x	Submitting to a journal to support a publication
x	Depositing in a self-archiving system or an institutional repository
	Dissemination via a project or institutional website
	Informal peer-to-peer exchange
	No plans to report or disseminate the data
	Other, please state: _____.
4.5 How do you intend to report and disseminate the results of the study? (Indicate with an 'X')	
x	Peer reviewed journals
x	Internal report
x	Conference presentation
x	Publication on website
	Other publication
	Submission to regulatory authorities
	No plans to report or disseminate the results
x	Other, please state: _potential patent application or IP protection_____.
4.6 Give details of the expected impact of the research. Further guidance is available at https://www.ukri.org/innovation/excellence-with-impact . (max words 200)	

Development of a tool that allows gait quality to be assessed in the field will be of interest to athletic coaches and recreational runners. The research may also lead to improved assessment of rehabilitation status of injured runners. The research will also be of interest to those involved in health care with an interest in assessing and rehabilitating gait – e.g. prosthetists working with lower-limb amputees, stroke patients, etc. The research will be used to inspire audiences to take an interest in science by informing people about technological advances in science and the applications of biological research. We will engage with the people through open source publication, local and national media and open lectures. We will remain aware of the possibilities of patenting our research findings by making use of the Research and Innovation Service, a facility set up specifically to identify and secure potential technology transfer in research output. They deal with patents, licensing, and spinout companies, and provide staff with support in these endeavours. If either a potential patent application or IP protection was required, the appropriate internal reports will be filed.

SECTION 5: PROTOCOLS

Which [protocols](#) will be complied with? (Indicate with an 'X').

There may be circumstances where it makes sense not to comply with a protocol, this is fine but should be clarified in your application.

x

Data protection, anonymisation and storage and sharing of research data

x

Informed consent

Verbal consent

Reimbursement of research participants

Low risk observation

SECTION 6: ADDITIONAL ETHICAL ISSUES

6.1 Indicate with an 'X' in the left-hand column whether the research involves any of the following:

	Discussion of sensitive topics, or topics that could be considered sensitive
	Prolonged or frequent participant involvement
	Potential for adverse environmental impact
x	The possibility of harm to participants or others (including the researcher(s))

	Participants taking part in the research without their knowledge and consent (eg covert observation of people in non-public places)
	The use of drugs, placebos or invasive, intrusive or potentially harmful procedures of any kind
	Food substances or drinks being given to participants (other than refreshments)
	Vitamins or any related substances being given to participants
	Acellular blood, urine or tissue samples obtained from participants (ie no NHS requirement)
x	Members of the public in a research capacity (participant research)
	Participants who are particularly vulnerable (eg children, people with learning disabilities, offenders)
	People who are unable to give their own informed consent
	Researcher(s) in a position of authority over participants, eg as employers, lecturers, teachers or family members
	Financial inducements (other than reasonable expenses and compensation for time) being offered to participants
	Cooperation of an intermediary to gain access to research participants or material (eg head teachers, prison governors, chief executives)
	Potential conflicts of interest
	Internet participants or other visual/ vocal methods where participants may be identified
	Scope for incidental findings, ie unplanned additional findings or concerns for the safety or wellbeing of participants.
	The sharing of data or confidential information beyond the initial consent given
	Translators or interpreters
	Research conducted outside the UK
	An international collaborator
	The transfer of data outside the European Economic Area

	Third parties collecting data
	Other ethical clearances or permissions
6.2 For the ethical issues indicated in 6.1 provide details of any additional ethical issues the research may involve and explain how these issues will be addressed. (max 200 words)	
<p>Potential harm to the participants</p> <p>A risk assessment has been completed for the type of testing to be carried out (covers the potential risks to the both participants and the researchers). A summary of the following potential hazards has been identified:</p> <ol style="list-style-type: none"> 1. <i>Treadmill operation.</i> Hazards are: (i) tripping/falling as a result of sudden acceleration/ deceleration; (ii) injuries resulting from the high-speed running belt. Controls are: (i) use of safety equipment (e.g. harness, emergency stop cord), (ii) briefing participants on safety; (iii) proper equipment training and supervision of users; (iv) wearing of covered shoes; (v) observers not standing too close to moving belt. 2. <i>Respirometry</i> (analysis of exhaled gases). Hazards are: (i) exchange of biological fluids and the transmission of disease (e.g. COVID-19). Controls are: (i) soaking and thorough disinfection of face masks, breathing tubes and mouth pieces; (ii) limiting the period where participant and experimenter are <2 m to <15 mins; (iii) experimenter and participant to wear PPE (experimenter to wear FFP3 facemask, visor, gloves, apron; participant to wear facemask until respirometry equipment must be attached); (iv) storage of contaminated equipment in bag prior to disinfection/sterilisation). 3. <i>Exercise testing.</i> Hazards are overexertion leading to nausea, sprains, muscle pulls, cardiac arrest, exertional heat illness etc. Controls are: (i) subjects will be briefed on pre-exercise preparation (e.g. no food); (ii) participants will properly warm up/ cool down; (iii) subjects will complete a pre-exercise questionnaire (e.g. PAR-Q) that will allow researchers to assess the subject's ability to participate in the physical activity; (iv) heart rate will be monitored as an index of exercise intensity; (v) CPR trained person will be present during test. 4. <i>General laboratory access.</i> Hazards are: (i) bruising, fractures, concussion, etc resulting from slips, trips or falls. Controls are: (i) thoroughfares through area to be clearly identified; (ii) thoroughfare routes to not have cables laid across them (or to be laid in cable protectors); (iii) spills to be cleaned up immediately; (iv) reporting of damaged flooring; (v) wearing of suitable footwear. 5. <i>Outdoor testing.</i> Hazards are: (i) exposure to adverse environmental conditions; (ii) bruising, fractures, concussion, etc resulting from slips, trips or falls; (iii) injury from handling equipment; (v) injury from vehicles. Controls are: (i) consultation of weather forecast, wearing 	

suitable clothing, carrying water and use of suncream, insect repellent as appropriate; (ii) wearing suitable footwear, use of lit paths; researchers undertake manual handling training, equipment carried in stages.

6. *Electromyography*. Hazards are: (i) irritation and (ii) transmission of disease. Controls are: (i) use of hypoallergenic electrodes; (ii) use of PPE during electrode attachment (experimenter to wear FFP3 facemask, visor, gloves, apron; participant to wear facemask); (iii) limiting the period where participant and experimenter are <2 m to <15 mins.
7. COVID-19 Transmission. Hazards are: (i) transmission of disease. Controls are: (i) access to lab booked via ARIA; (ii) pre-testing questionnaire; (iii) avoidance of public transport; (iv) wearing of PPE (experimenter to wear FFP3 facemask, visor, gloves, apron; participant to wear facemask); (v) limiting the period where participant and experimenter are <2 m to <15 mins; (vi) storage of contaminated equipment in bag prior to disinfection/sterilisation).

SECTION 7: RECRUITMENT AND CONSENT PROCESS

For guidance refer to <http://ris.leeds.ac.uk/InvolvingResearchParticipants> and the [research ethics protocols](#).

7.1 State approximately how much data and/ or how many participants are going to be involved.

The number of participants will vary for the different experiment types. For all participants, anthropomorphic data and running history will be collected. For the laboratory-based measurements we anticipate a sample size of up to 25 individuals. Each individual will have their whole-body biomechanics assessed by measuring the 3D movements of their body segments; some will additionally have metabolic and muscle activity recorded. These data will be collected at a range of walking and running speeds. For each of the field-based measurements we anticipate collecting data on approximately 100 individuals. These data will consist of acceleration recordings, running speed and in some instances metabolic, motion or EMG data or video recordings.

7.2 How was that number of participants decided upon? (max 200 words)
Please note: The number of participants should be sufficient to achieve worthwhile results but should not be so high as to involve unnecessary recruitment and burdens for participants. This is especially pertinent in research which involves an element of risk. Describe here how many participants will be recruited, and whether this will be enough to answer the research question. If you have received formal statistical advice then please indicate so here, and describe that advice.

In the experiments aimed at quantifying 3D body kinematics, our experiments are designed to detect a 10% difference with a 5% significance level and a statistical power of 90%. The sample size calculation is based on data on the symmetry indices from Seminati et al. (2013) who reported a standard deviation of 5-8%: we will therefore require approximately 16 participants.

Where the principal outcome is metabolic energy expenditure. Our experiments are designed to detect a 10% difference with a 5% significance level and a statistical power of 90%. Our sample size calculation is based on data from Askew et al. (2011: doi:10.1098/rspb.2011.0816) who reported a standard deviation of 10% for walking metabolic rate: we will therefore require approximately 22 participants. A sample of 25 subjects will be used with a buffer of 15% to account for incomplete measures. Since accelerometry will be performed simultaneously with the metabolic data, the group size exceeds the minimum needed for the accelerometry data set.

Insufficient data are currently available to calculate sample size for either the laboratory- or field-based accelerometry measurements. However, based on the work of Barnes (2018) we expect that the sample size noted above will suffice (note that accelerometry data are collected simultaneously with metabolic/ kinematics data). For the population profiling study (field-based) we expect to use approximately 100 participants based on the number used by Barnes et al. (2016), which was 103. There simply are not any suitable data to enable us to assess this in a more precise manner. The number will be reviewed throughout the study as we collect and analyse the data, at which time we will have a better understanding of the likely variation in our measurements.

7.3 How are the participants and/ or data going to be selected? List the inclusion and exclusion criterial. (max 200 words)

Recruitment could occur in a variety of forms including the use of emails and advertisements (flyers distributed in appropriate locations around the University) or via local contacts (e.g. through running club coaches and/or committee members). Recruitment materials will inform participants that they will be participating in a research study. A general description of the purpose of the study will be given together with an outline of what participation in the study will entail written in lay language. Details of how to enrol will be given as well as inclusion/ exclusion criteria (if appropriate).

Inclusion criteria:

- (i) informed consent must have been obtained;
- (ii) must complete a pre-exercise questionnaire and be fit to undertake exercise;
- (iii) must be capable of running at a predetermined pace for a predetermined distance

(iv) must be an experienced runner, familiar with endurance running training and racing.

Exclusion criteria:

- (i) unable to provide informed consent (e.g. individuals who do not have a good understanding and command of English);
- (ii) participant's pre-exercise questionnaire highlights areas of concern.

7.4 For each type of methodology, describe the process by which you will obtain and document freely given informed consent for the collection, use and reuse of the research data. Explain the storage arrangements for the signed consent forms.

Guidance is available at <http://ris.leeds.ac.uk/InvolvingResearchParticipants>. The relevant documents (information sheet and consent form) need to be attached to the end of this application. If you are not using an information sheet and/ or seeking written consent, please provide an explanation.

Participants will initially be given an information sheet explaining the purpose of the study and what participation in it will involve. They will be given at least 48 hours before the study commences. A member of the research team will then talk to them about taking part. At this stage they will be given an overview of the research process and any questions they have will be answered. Once the volunteer fully understands what is expected of them, they will be asked to sign a form to indicate they give their informed consent to take part in the study. Consent will be given by the participant signing the consent form in the presence of a member of the research team and counter-signed by a member of the research team in the presence of the participant (see submitted consent form).

Signed consent forms will be archived in a lockable room with controlled access, or kept in a locked filing cabinet, or kept in a locked drawer. These documents will be scanned in so can be stored electronically within a password protected computer/ archive, with controlled access, at the University of Leeds. All documentation will be treated in accordance with the appropriate data protection act and GDPR policy. All applicable information will be discarded after 10 years.

7.5 Describe the arrangements for withdrawal from participation and withdrawal of data/ tissue. *Please note: It should be made clear to participants in advance if there is a point after which they will not be able to withdraw their data.* See also <http://ris.leeds.ac.uk/ResearchDataManagement>. (max 200 words)

The "informed consent" form will explain to the participant that their involvement in the study is voluntary and without any specific benefits and that they are free to withdraw from the study at any time until their anonymised data is pooled for analysis, at which point it will not be possible to withdraw their data from the study.

<p>7.6 Provide details of any incentives you are going to use and explain their purpose. (max 200 words)</p> <p><i>Please note: Payment of participants should be ethically justified. The FREC will wish to be reassured that research participants are not being paid for taking risks or that payments are set at a level which would unduly influence participants. A clear statement should be included in the participant information sheet setting out the position on reimbursement of any expense incurred.</i></p>	
N/A	
<p>SECTION 8: DATA PROTECTION, CONFIDENTIALITY AND ANONYMISATION</p> <p>Guidance is available at http://ris.leeds.ac.uk/ConfidentialityAnonymisation</p>	
8.1 How identifiable will the participants be? (Indicate with an 'X').	
	Fully identifiable
x	Identity of subject protected by code numbers/ pseudonyms
	Fully anonymised
x	Anonymised but potentially identifiable
	Data only in aggregated form
	Other
8.2 Describe the measures you will take to deal with issues of anonymity. (max 200 words)	
<p>Confidentiality will be maintained by keeping research data anonymous. All personal data will be accessible only to those who need it (i.e. PI and the research team). Sensitive data will be kept in a lockable room with controlled access, or kept in a locked filing cabinet, or kept in a locked drawer, or stored on password-protected computers with controlled access. Personal data will be kept separate from the research data. All research data will be anonymised by attributing a subject code (e.g. subject 1, subject 2, subject A etc) to all data collected of the participants, and data will be stored on a password-protected computer with controlled access. Video recordings and images from which participants could be visually identified will only be accessible to those who need it (i.e. PI and the research team).</p>	
8.3 Describe the measures you will take to deal with issues of confidentiality, including any limits to confidentiality. (Please note that research data which appears in reports or other publications is not confidential, even if it is fully	

<p>anonymised. For a fuller explanation see http://ris.leeds.ac.uk/ConfidentialityAnonymisation). (max 300 words)</p>
<p>All personal data will be accessible only to those who need it (i.e. PI and the research team). Sensitive data will be kept in a lockable room with controlled access, or kept in a locked filing cabinet, or kept in a locked drawer, or stored on password-protected computers with controlled access. Personal data will be kept separate from the research data. All research data will be anonymised by attributing a subject code (e.g. subject 1, subject 2, subject A etc.) for each participant, and data will be stored on a password-protected computer with controlled access. Video files containing images from which participants could be identified made during the research study will only be accessible to those who need it (i.e. PI and the research team).</p>
<p>8.4 Who will have access to the research data apart from the research team (e.g. translators, authorities)? (max 100 words)</p>
<p>No one apart from the research team. Data may be made available upon request, however will be anonymised and coded to protect participants identity in accordance with the University of Leeds's confidentiality and anonymisation policy.</p>
<p>8.5 Describe the process you will use to ensure the compliance of third parties with ethical standards. (max 100 words)</p>
<p>N/A.</p>
<p>8.6 Where and in what format(s) will research data, consent forms and administrative records be retained? (max 200 words)</p> <p><i>Please note: Mention hard copies as well as electronic data. Electronic data should be stored securely and appropriately and in accordance with the University of Leeds Data Protection Policy available at http://www.leeds.ac.uk/secretariat/data_protection_code_of_practice.html.</i></p>
<p>Research data will be in the following formats:</p> <ul style="list-style-type: none"> (i) hardcopies (e.g. consent forms, lab books) (ii) electronic copies (e.g. 3D positional data, metabolic data, muscle activity data, video recordings) <p>Hard copies will be stored in a lockable room with controlled access, or kept in a locked filing cabinet, or kept in a locked drawer, or stored on password-protected computers with controlled access, as outlined in the Universities Data Protection Policy. Electronic copies of data will be stored (temporarily) on password-protected, encrypted laptops during data collection in the laboratory and field. Electronic copies of data, the metadata that describe these data and the parameters derived from the data that are used in subsequent analyses will be backed up electronically on our laboratory computers, which are mirrored every 2 hours onto multiple disc systems in separate locations on campus. Our University computing networks are</p>

protected from viruses and data piracy by various virus checkers and firewalls. This will help to ensure the security of the data held on project PCs.		
8.7 If online surveys are to be used, where will the responses be stored? (max 200 words)		
Refer to: http://it.leeds.ac.uk/info/173/database_and_subscription_services/206/bristol_online_survey_accounts and http://ris.leeds.ac.uk/SecuringResearchData for guidance.		
N/A.		
8.8 Give details and outline the measures you will take to assess and to mitigate any foreseeable risks (other than those already mentioned) to the participants, the researchers, the University of Leeds or anyone else involved in the research? (max 300 words)		
<p>The risks to the participants are those associated with participating in the study (covered in risk assessment and in section 6.2). Risks to the researchers are those associated with carrying out the research (covered in section 6.2). The risks to the University are the potential for harm resulting from someone's negligence. The following statement will be added to the "Information Sheet":</p> <p><i>"If you are harmed by taking part in this research project, there are no special compensation arrangements. If you are harmed due to someone's negligence then you may have grounds for legal action, but you may have to pay for it. Regardless of this, if you have any concerns about any aspect of the way in which you have been approached or treated during the course of this study, you may complain to the University Secretary."</i></p>		
SECTION 9: OTHER ETHICAL ISSUES		
Yes	No	(Indicate with an 'X')
x		<p>9.1 Is a health and safety risk assessment required for the project?</p> <p><i>Please note: Risk assessments are a University requirement for all fieldwork taking place off campus. The risk assessment forms and further guidance on planning for fieldwork in a variety of settings can be found on the University's Health & Safety website along with further information about risk assessment: http://www.leeds.ac.uk/safety/fieldwork/index.htm. Contact your Faculty Health and Safety Manager for</i></p>


		further advice. See also http://ris.leeds.ac.uk/HealthAndSafetyAdvice .
	x	9.2 Is a Disclosure and Barring Service check required for the researcher? <i>Please note: It is the researcher's responsibility to check whether a DBS check is required and to obtain one if it is needed.</i>
9.3 Any other relevant information		
Risk assessments covering this research are provided with this form. Questionnaires and a PAR-Q that will be used to pre-screen participants and researchers for underlying health problems or COVID-19 are provided.		
9.4 Provide details of any ethical issues on which you would like to ask the Committee's advice.		
SECTION 10: FURTHER DETAILS FOR STUDENT PROJECTS (COMPLETE IF APPLICABLE)		
Your supervisor is required to provide email confirmation that they have read, edited and agree with the form above. It is a good idea to involve your supervisor as much as possible with your application. If you are unsure how to answer any of the questions do ask your supervisors for advice.		
10.1 Qualification working towards (indicate with an 'X')		
x	Bachelor's degree	Module code: SPSC3061; SPSC3389
x	Master's degree (including PgCert, PgDip)	
x	Research degree (i.e. PhD)	
10.2 Primary supervisor's contact details		
Name (title, first name, last name)		Dr. Graham Askew
Department/ School/ Institute		School of Biomedical Sciences, University of Leeds
Telephone number		0113-34-32897

University of Leeds email address		G.N.Askew@leeds.ac.uk
10.3 Second supervisor's contact details		
Name (title, first name, last name)		Dr. Andy Brown
Department/ School/ Institute		School of Chemical & Process Engineering, University of Leeds
Telephone number		0113-34-32382
University of Leeds email address		A.P.Brown@leeds.ac.uk
Yes	No	10.4 To be completed by the student's supervisor
X		The topic merits further research
X		I believe that the student has the skills to carry out the research
<p>SECTION 11: OTHER MEMBERS OF THE RESEARCH TEAM</p> <p>(COMPLETE IF APPLICABLE)</p>		
Name (title, first name, last name)		Danielle Charles
Role (eg PI, Co-I)		PhD student
Department/ School/ Institute		School of Biomedical Sciences, University of Leeds
Telephone number		
University of Leeds email address		bsdc@leeds.ac.uk
Name (title, first name, last name)		
Role (eg PI, Co-I)		
Department/ School/ Institute		

Telephone number		
University email address		
Name (title, first name, last name)		
Role (eg PI, Co-I)		
Department/ School/ Institute		
Telephone number		
University of Leeds email address		
<p align="center">SECTION 12: SUPPORTING DOCUMENTS</p>		
<p>Indicate with an 'X' which supporting documents have been included with your application.</p> <p>Wherever possible the research title on consent forms, information sheets, other supporting documentation and this application should be consistent. The title should make clear (where appropriate) what the research is about. There may be instances where a different title is desirable on information to participants (for example – in projects which necessarily involve an element of deception or if giving the title might skew the results of the research). It is not imperative that the titles are consistent, or detailed, but where possible then they should be.</p>	x	<p>Information sheet(s)</p> <p><i>Please note: Include different versions for different groups of participants eg for children and adults if applicable. Refer to http://ris.leeds.ac.uk/InvolvingResearchParticipants for guidance in producing participant information sheets.</i></p>
	x	<p>Consent form(s)</p> <p><i>Please note: Include different versions for different groups of participants eg for children and adults if applicable. Refer to http://ris.leeds.ac.uk/InvolvingResearchParticipants for guidance in producing participant consent forms.</i></p>
		<p>Recruitment materials</p> <p><i>Please note: Eg poster, email etc used to invite people to participate in your research project.</i></p>
	x	<p>Letter/ email seeking permission from host/ gatekeeper</p>

Supporting documents should be saved with a meaningful file name and version control, eg 'Participant_Info_Sheet_v1' or 'Parent_Consent_From_v2'. Refer to the examples at http://ris.leeds.ac.uk/InvolvingResearchParticipants .		Questionnaire/ interview questions
	x	Health and safety risk assessment <i>Please note: Risk assessments are a University requirement for all fieldwork taking place off campus. The risk assessment forms and further guidance on planning for fieldwork in a variety of settings can be found on the University's Health & Safety website along with further information about risk assessment: http://www.leeds.ac.uk/safety/fieldwork/index.htm. Contact your Faculty Health and Safety Manager for further advice. Also refer to http://ris.leeds.ac.uk/HealthAndSafetyAdvice.</i>
		Data management plan <i>Refer to https://library.leeds.ac.uk/info/14062/research_data_management/62/data_management_planning</i>
SECTION 13: SHARING INFORMATION FOR TRAINING PURPOSES		
Yes	No	(Indicate with an 'X')
x		I would be content for information in the application to be used for research ethics and research data management training purposes within the University of Leeds. All personal identifiers and references to researchers, funders and research units would be removed.
SECTION 14: DECLARATION		
1. The information in this form is accurate to the best of my knowledge and belief and I take full responsibility for it. 2. I undertake to abide by the University's ethical and health & safety policies and guidelines, and the ethical principles underlying good practice guidelines appropriate to my discipline.		

3. If the research is approved I undertake to adhere to the study protocol, the terms of this application and any conditions set out by the Research Ethics Committee.
4. I undertake to ensure that all members of the research team are aware of the ethical issues and the contents of this application form.
5. I undertake to seek an ethical opinion from the REC before implementing any [amendments](#) to the protocol.
6. I undertake to submit progress/ [end of project reports](#) if required.
7. I am aware of my responsibility to be up to date and comply with the requirements of the law and relevant guidelines relating to security and confidentiality of personal data.
8. I understand that research records/ data may be subject to inspection for [audit](#) purposes if required in future.
9. I understand that personal data about me as a researcher in this application will be held by the relevant FRECs and that this will be managed according to the principles established in the Data Protection Act.

	Applicant	Student's supervisor (if applicable)
Signature		
Name	Dr Graham Askew	
Date	30 th November 2020	

Appendix D: Additional COVID measures



COVID-19 SAFE WORKING PROTOCOL: Miall 4.08 (Lab 4B) (Biomechanics Lab)

Use of the biomechanics lab will be by booking only (*via* the ARIA system). If more than one participant is to be tested at the same time, arrival times will be staggered to minimise risk of multiple people in the lab corridor at the same time. **The timing of participant arrival will be scheduled to avoid times when large numbers of students may be entering or leaving the building – i.e. avoid the period 10 minutes before and after the hour.** Testing performed in these labs cannot be done following social distancing guidelines. This protocol has also been written assuming that exercise and associated measures are aerosol generating procedures (AGPs), therefore full PPE will be required, with a station to put this on set up inside the lab. Depending upon the testing to be completed, there will be up to four experimenters (this can be anybody: staff, technician, postdoc, PhD, Undergrad, where appropriate) in the room along with the participant (maximum of 5 people in each lab in total). A member of staff who is ILS trained will also need to be on site, and close by (e.g. in a nearby office), or alternative arrangements made with the H&S team (e.g. notifying an identified H&S contact on site by phone when we start and then finish testing).

All experimenters and participants will be asked to complete a COVID-19 symptoms screening questionnaire before leaving home to travel to the lab (in the 24 hr before) the first visit to the labs to confirm the absence of any COVID-19 symptoms (see attached). They will then be asked to confirm prior to each subsequent visit before leaving to travel to the lab (in the preceding 24 hr) that there has been no change in the details submitted (e.g. no change in personal symptom status, or symptom status of people in their household). If any symptoms are reported, the individual will be advised to stay home, and to get a test as soon as possible.

<https://www.nhs.uk/conditions/coronavirus-covid-19/testing-and-tracing/get-a-test-to-check-if-you-have-coronavirus/>

Anyone reporting COVID-19 symptoms will initiate our protocol as described in the section below.

All experimenters and participants will download and activate the NHS COVID-19 app and have their mobile phones turned on during the testing and follow advice from the NHS if alerted.

Experimenters will arrive before the participant to set up the lab area. Before entering the lab, experimenters will use hand sanitising gel and then put on a mask (FFP3). Once inside the lab they will additionally use hand sanitising gel and put on a visor and gloves at the PPE station. Experimenters will set up as

much of the equipment as can be done in advance. Experimenters will arrange to meet participants at a specific time at the Miall building entrance on level 4 (off Clarendon Way). When leaving the lab to meet the participant at this time, the experimenter will remove their gloves in the lab (but keep their mask and visor on), they will then leave the lab, sanitise their hands and exit the building. Participants will be asked to wear a mask to the university, and keep this on until the start of testing. Participants will be asked to arrive dressed in suitable clothing for the testing, and advised that no shower facilities will be available after testing at the present time. Participants will also be asked to bring as little of their personal belongings as possible with them, but to bring a water bottle so they have access to drinking water. Once the experimenter has met the participant at the Miall level 4 entrance, they will be invited to leave any personal belongings in a locker (situated outside the laboratory on Miall level 4) and sanitise their hands before entering the lab. They will be invited to take a seat within the lab while the experimenter follows behind, sanitising their hands, and putting on the necessary PPE at the PPE station (i.e. gloves and apron). Once the experimenters and participant are all in the lab, the sign indicating that testing is taking place will be put on the door. All doors have to remain closed as they are fire doors.

There are three main steps in the experiment. The first involves the attachment of devices (e.g. motion capture markers, respirometry equipment and accelerometers) to the participant and/or respirometry equipment (mask and portable analyser). This *would* require the experimenter and participant to be closer than 1 m for a period up to 30-35 minutes (attaching accelerometers takes approximately 2-3 minutes; attaching motion capture markers approximately 25 minutes, respirometry equipment approximately 5 minutes). However, to reduce the risk of COVID-19 infection, the participant will be asked to attach the markers themselves, demonstrated by one of the experimenters at a distance of >2 m. Once this has been completed, the experimenter will check the marker placement, adjusting positioning where necessary, and attach the accelerometers in a period not longer than 15 minutes. Accelerometers will be attached by the experimenter. During this step, both the participant and experimenters will wear PPE (FFP3 mask, visor and apron for the researcher and facemask and visor for participant). In tests where respirometry is performed, the participant will remove their facemask and visor prior to attachment of the respirometry mask – this will always be the last step before testing commences; the experimenter will continue to wear (FFP3 mask, visor and apron). The experimenter will attach the respirometry mask. Once devices have been attached, the second step is the testing/data collection (including warm up and cool down). Testing will be undertaken as normal using all the standard equipment (e.g. motion capture reflective markers, exercise testing with ECG/EMG, accelerometers, respirometry). During the exercise test, participants will be asked to remove their mask and visor (placing this on a trolley) just prior to starting, after which the test will proceed as normal. During this step the experimenters and participant maintain social distancing > 2 m and the experimenters will continue to wear PPE. In the third step, following completion of the test, the participant will be helped off the treadmill, invited to wash their hands, and asked that as soon as they feel comfortable to put their mask back on. Any attached research

equipment (accelerometers, reflective markers, respirometry equipment etc) will then be removed. Accelerometers and markers will be removed first by the experimenter (this takes ~1 min). When used, the respirometry mask will be removed last by the experimenter and immediately placed inside a single use plastic bag, taking care not to contaminate the outside of the bag. The experimenter will then remove their gloves, sanitise their hands and apply new gloves. Equipment removal requires the experimenter and participant to be closer than 1 m for a period up to 5 minutes. Once the participant feels fully recovered, they will be allowed to leave. The participant will be asked to use the hand-sanitiser as they leave the lab, exiting via the Miall level 4 entrance.

Once the participant has left, experimenters will remove PPE. During removal, the outside of PPE will be considered to be contaminated and immediately placed in clinical waste bags. The experimenters will then sanitise their hands, lock the lab and leave a red sign on the door to highlight that the area is currently 'contaminated'. They will then return after 1 hour to disinfect the lab, all lab equipment and the lab door handles. When leaving the lab after cleaning, the red 'contaminated' sign will be changed to a green 'clean' sign on the door. Respirometry equipment and visor will be disinfected during the 1hr the lab is left empty, and then sterilised (e.g. using ethylene oxide). The bag used to transport the contaminated respirometry equipment will be disposed of in clinical waste.

General

1. Experimenters will have read and understood the relevant sections of the general guidelines around interaction during the COVID-19 pandemic at <https://www.gov.uk/guidance/working-safely-during-coronavirus-covid-19/labs-and-research-facilities>, and this SWP to ensure they understand the protocol for work in this area.
2. Experimenters will confirm they are not considered clinically extremely vulnerable and that members of their family units they live with do not fall into this category (as detailed under point 2 in the above guidelines)
3. Experimenters will consider their symptom status, and check that of the participant before either leave home to travel to the lab.
4. Experimenters will inform their PI (Graham Askew/ Andy Brown) or Jackie Goodall if their PI cannot be reached immediately if they have any COVID-19 symptoms including a high temperature, a new, continuous cough and/ or a loss or change to sense of smell or taste. As described above, this will be recorded for each visit to the lab (<https://www.nhs.uk/conditions/coronavirus-covid-19/check-if-you-have-coronavirus-symptoms/>)

Arriving at and leaving University

1. Experimenters will only be in the lab area when necessary. All work that can be done from home will be done from home.
2. All lab visits will be booked in using the ARIA booking system.
3. On arrival, the first person will wipe down communal areas in the lab corridor (e.g. door handles). The green 'clean' sign on the door will confirm that the lab area is clean.

4. Any security and H&S issues will be reported to the PI.
5. Before setting up the lab, a precautionary clean of the area will be conducted.
6. When testing is finished the lab and all equipment will be cleaned using the appropriate solutions (e.g. commercial anti-viral cleaning sprays) and green signs indicating the labs are clean will be put on the doors so this is clear to other users of the area.
7. We will clean the lab areas ourselves. This will minimise the number of users entering the space, and ensure that our Green and Red sign system works. Any rubbish (clinical and domestic waste) will be put in a designated spot for pick-up.
8. Spirometry equipment and visor will be disinfected during the 1hr the lab is left empty, and then sterilised (e.g. using ethylene oxide). Any rubbish (clinical and domestic waste) will be put in a designated spot for pick-up.

Protocol for when notified of positive COVID-19 symptoms

If any symptoms are reported testing will be cancelled, the individual reporting symptoms (experimenter/ researcher or participant) will be advised to get a test as soon as possible and stay home until the results of this test are known.

Participant (prior to visit 1): If symptoms are reported or the participant tested positive for COVID-19 prior to the first test, the experiment will be cancelled. The participant will be advised that they must stay at home and follow the government advice to book a test through the [NHS Test and Wave](#) service. If this is prior to the first visit, no further action will be taken. The participant will be allowed to take part if more than 14-days have passed since the onset of symptoms and/ or positive test result, and they are fit to do so.

Participant (if test positive after first visit): If a participant tests positive, they will be advised to follow NHS guidance and self-isolate for 14-days. The researcher (or PI) will also inform all participants who have been involved in the lab testing in the previous 14-days that there has been a positive COVID-19 test in those that have used the facility, but testing within the labs will be allowed to continue. The participant who tested positive will be allowed to restart/continue the study if more than 14-days have passed since the positive test result, and they are fit to do so.

Experimenter/ Researcher: A researcher who is self isolating or tests positive for COVID-19, must inform the University of Leeds in the following ways: (i) inform their line manager (PI (Graham Askew/ Andy Brown/ Jackie Goodall); (ii) report the positive test to the University *via* the website (<https://coronavirus.leeds.ac.uk/>) email (reportcovid@leeds.ac.uk) or phone (0113 343 8777); (iii) The Faculty H&S manager (Katherine Wilson k.m.wilson1@leeds.ac.uk). The individual must not attend campus if they have any symptoms or tested positive for COVID-19. They must stay at home and follow the government advice to book a test through the [NHS Test and Wave](#) service. If the researcher received a negative test result for COVID-19, they should advise their line manager/PI and discuss the circumstances with them. If they experienced symptoms, took a covid test and received a negative result, then they will be free to return to work when they feel well enough to do so. But if the researcher was required to self-isolate as a close contact of a

person who had tested positive, then a negative test result does not change the self-isolation period and they must continue to self-isolate. The researcher (or PI) will also inform all participants who have been involved in the lab testing in the previous 14-days that there has been a positive COVID-19 test in those that have used the facility, but testing within the labs will be allowed to continue.

While working at University

1. Typically, there will be no lone working. However, the following procedures will be followed to cover both lone, and small group working:
 - a. When 2 or more users are in the building users will check the wellbeing of their colleagues at least hourly (typically researchers will be working together, so this is not a concern).
 - b. When only 1 user is in the building they will contact their PI, or another delegated person, on a regular basis (hourly) to confirm all is well.
2. Miall Level 4 has 2 communal toilets in close proximity, all users of this facility will observe strict hygiene procedures at all times.
3. Experimenters will bring in their own drinking water and snacks/food, and will consume this in the office area (Garstang 5.61) while observing a safe distance of at least 2 m. Users of this space must ensure that occupancy does not exceed the agreed capacity.
4. Equipment in labs will be used at the same time by multiple people, but while in the lab researchers will wear gloves and a mask.
5. As a general principle, standard government hygiene guidelines will be followed while in the university: wash hands regularly for 20 s with soap, coughs and sneezes should be into a tissue (or elbow), followed by handwashing. Hands will also be washed when taking off gloves before leaving the lab.
6. Face coverings will be worn in lab areas, but is not at present required when working inside buildings on University campus – social distancing guidelines will be followed. Experimenters can, however, wear a mask if they choose.
7. Levels of hand sanitiser, hand wash etc. will be monitored, and reported to building services if levels fall too low.
8. All standard emergency procedures will be followed – e.g. in case of the fire alarm going off, standard procedures to leave immediately will be followed, along with social distancing where possible. We will ask experimenters to carry a small bottle of hand sanitiser with them, so that if they have to leave immediately, they will still have the ability to sanitise their hands.
9. All first aid facilities (e.g. first aid box, automatic defibrillator, oxygen) remain in place, along with the standard protocols – for emergencies, dial 9-999 (if dialling from a university phone) for an ambulance followed by 32222 to inform security.
10. If there are any concerns about safety, everyone is encouraged to discuss there with: the designated area PI, HR contact, or a member of the Health and Safety Team (safety@leeds.ac.uk).

Ordering and receiving goods

1. Orders will be placed from home.
2. Consumables will be delivered to FBS Goods Inwards is opened ALL deliveries will be arranged for Goods Inwards, Level 5 Roger Stephens Building. Social Distancing guidelines will be followed when picking up orders.

Any physical problems with Building / Infrastructure / Fire / First Aid:

Contact security 0113 343 2222, Security@Leeds.ac.uk

Any problems with equipment, ordering, lab issues etc:

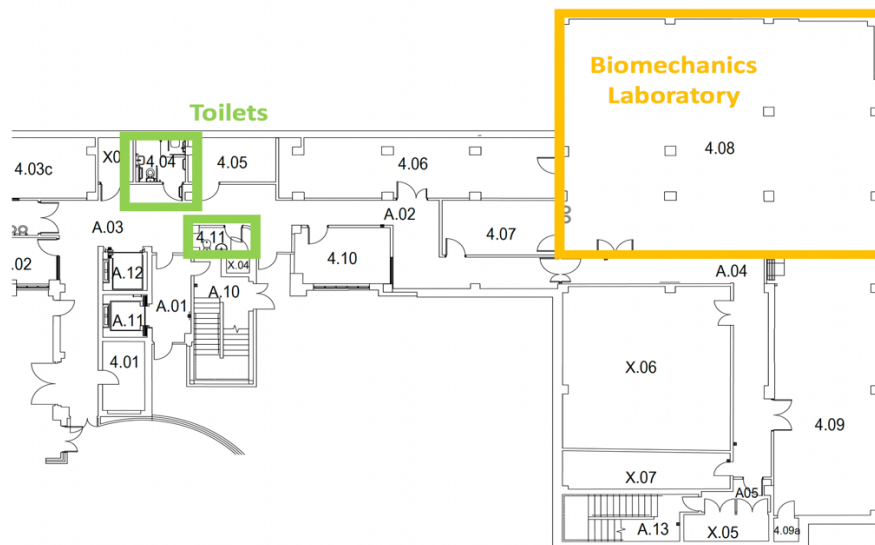
Contact PI

Any other problems:

Contact Graham Askew: 07904 165783,
g.n.askew@leeds.ac.uk

Area specific details

Biomechanics Laboratory Miall 4.08 (Lab 4B)



Appendix E: Participant information sheet



Participant Information Sheet **Accelerometer-based gait analysis**

You are being invited to take part in a research project. Before you decide to participate, it is important for you to understand why the research is being done and what it will involve. Please take time to read the following information carefully and discuss it with others if you wish. Ask a member of the research team if there is anything that is not clear or if you would like more information. Take time to decide whether or not you wish to take part.

What is the purpose of the project?

To understand how wearable activity monitors, known as inertial measurement units (IMU) can be used to characterise gait during running. By doing so, we hope to provide a tool that can help with training and rehabilitation of runners.

Why have I been chosen?

You have been chosen because you are healthy and have not been advised against participating in physical activity. You are willing and able to participate in our study and are an experienced runner.

What do I have to do?

Prior to visiting the laboratory, you are asked to maintain your usual diet and activity level and refrain from drinking alcohol. You should bring with you appropriate clothing in which to exercise. Females participants will need to wear tight-fitting shorts and a vest/ crop top; male participants, tight-fitting shorts and running vest/ tight-fitting top (male participants may elect to run without a top). Note that tight-fitting shorts are required to prevent obstruction of markers that will be attached to your body – see below. You can also bring something warm to wear after the study. You will need to wear your usual clean running shoes. Note that changing and showering facilities are available at the laboratory.

You will be asked to visit the Biomechanics Laboratory (Miall Building) at the University of Leeds at a pre-arranged time, on up to two occasions, for 1-2 hours per session. A member of the research team will attach an activity monitor to each ankle, light-weight markers to your body (e.g. ankles, knee, hip, shoulder, etc) using double sided tape and a heart rate monitor. The member of the research team may be male or female – if you do not wish the member of the research team to attach the activity monitor or markers to your body, you may withdraw from the study and there will not be any negative consequences. Your movements will be recorded using a motion capture system and activity monitor; a video camera may also be used.

***Optional statements that *may* be included for some participants:**

Whilst you are exercising, you will wear a mask which will be used to collect your expired air for analysis.

The activity of some of your leg muscles will be recorded using electrodes attached to your skin. To attach the electrodes we may shave hair at the electrode attachment site and cleanse the skin.

Weights will be attached to one of your ankles or thigh.

****One of the following two statements will be included:**

You will run on a treadmill at a range of speeds, covering the range 10-18 km/h; the speeds will be presented in a random order. At each speed you will run for up to, approximately, 5 minutes with recovery periods in between each speed.

You will run on a treadmill at incrementally increasing speeds until you reach voluntary exhaustion.

What are the possible disadvantages and risks of taking part?

There is a small chance that you could trip or fall or of over-exertion during the exercise testing. There is a small chance that you may experience an injury, such as a muscle pull, sprain, tendonitis or post-exercise muscle soreness. There is also a small risk of cardiac arrest or sudden death (0.54 incidents per 100,000 participants in long distance running races). To minimise this risk, we will ask you to complete a pre-exercise questionnaire to assess your suitability to participate in the study. We will also give you time to familiarise yourself with running on the treadmill. We will ask you to perform warm-up and cooling-down exercises at the start and end of the tasks. At least one person trained in resuscitation (CPR) will be present during each test, and an automated external defibrillator will be available.

If you are harmed by taking part in this research project, there are no special compensation arrangements. If you are harmed due to someone's negligence then you may have grounds for legal action, but you may have to pay for it. Regardless of this, if you have any concerns about any aspect of the way in which you have been approached or treated during the course of this study, you may complain to the University Secretary.

What are the possible benefits of taking part?

Whilst there are no immediate benefits for those people participating in the project, it is hoped that this work will lead to the development of a tool that allows gait quality to be assessed in the field, and will be of interest to athletic coaches and runners.

Do I have to take part?

It is up to you to decide whether or not to take part. If you do decide to take part you will be given this information sheet to keep and be asked to sign a consent form. You can still withdraw at any time and you do not have to give a reason. If you do decide to withdraw or not participate in the study, there will not be any negative consequences, however, once your anonymised data are pooled for analysis it will not be possible to withdraw your data from the study.

Your participation in this study is entirely voluntary and without any specific benefits.

Will my taking part in this project be kept confidential?

If it is possible to identify you from the data, either directly or indirectly, the data is classified as personal data. This means the storage and use of your data will be handled in accordance with the Data Protection Act (2018), General Data Protection Regulation (GDPR), the Human Rights Act (1998), and the University's Code of Practice and Data Protection policies.

All of your data will be anonymised, which means that you will not be identifiable in any reports or publications. Some images and video recordings may be used to publicise the research (e.g. scientific publication, internal reports, at scientific conferences, on University website or for use by the media). In these recordings it may be possible to identify you, however, it will not be possible to link you with the specific research data that relates to you.

Research participants privacy notice

For more information on how and why the University uses personal data for research – see <https://dataprotection.leeds.ac.uk/wp-content/uploads/sites/48/2019/02/Research-Privacy-Notice.pdf>

Ethics

This study has been reviewed and given a favourable opinion by BIOSCI Faculty Research Ethics Committee on 27.06.2019, ethics reference BIOSCI 18-016.

Contact for further information

If you would like further information about the study and what is being asked of you, please contact a member of the research team:

Danielle Charles

Faculty of Biological Sciences, University of Leeds, LS2 9JT,
email: bsdc@leeds.ac.uk

Dr. Graham Askew

Faculty of Biological Sciences, University of Leeds, LS2 9JT,
email: g.n.askew@leeds.ac.uk, tel: 0113-343-2897

Thank you for taking the time to read through this information

Appendix F: Participant consent form



Consent to take part in Accelerometer-based gait analysis for quantitative assessment of physical activity outside the laboratory	Add your initials next to the statement if you agree
I confirm that I have read and understand the information sheet dated explaining the above research project and I have had the opportunity to ask questions about the project.	
I understand that my participation is voluntary and that I am free to withdraw** at any time without giving any reason and without there being any negative consequences. In addition, should I not wish to answer any question(s) I am free to decline.	
I give permission for members of the research team to have access to my anonymised responses. I understand that my name will not be linked with the research materials, and I will not be identified or identifiable in the report or reports that result from the research. I understand that my responses will be kept strictly confidential.	
I agree for the data (including motion capture/ video data) collected from me to be stored and used in relevant future research in an anonymised form. All data collected may be used for different purposes in the future.	
I understand that from the video data and images it may be possible to identify me, however, it will not be possible to link me with my specific research data.	
I agree that images and video recordings may be used to publicise the research (e.g., in scientific publication, internal reports, at scientific conferences, on the University website or for use by the media)	
I understand that other genuine researchers will have access to this data only if they agree to preserve the confidentiality of the information as requested in this form.	
I understand that relevant sections of the data collected during the study, may be looked at by auditors from the University of Leeds where it is relevant to my taking part in this research. I	

give permission for these individuals to have access to my records.		
I agree to take part in the above research project and will inform the lead researcher should my contact details change during the project and, if necessary, afterwards.		
Name of participant		
Participant's signature		
Date		
Name of lead researcher [or person taking consent]		
Signature		
Date*		
Ethics Reference	Committee	BIOSCI-18-016 approved on 27.06.2019

*To be signed and dated in the presence of the participant.

** Should you choose to withdraw from the study, data not yet pooled for analysis will not be used. If any further information is needed, please contact Danielle Charles (bsdc@leeds.ac.uk).

Once this has been signed by all parties the participant should receive a copy of the signed and dated participant consent form, the letter/ pre-written script/ information sheet and any other written information provided to the participants. A copy of the signed and dated consent form should be kept with the project's main documents which must be kept in a secure location.

Appendix G: Full Igor code for accelerometry processing

Igor v8 script for accelerometry data.

```
#pragma TextEncoding = "UTF-8"
#pragma rtGlobals=3 // Use modern global access method
and strict wave access.

//Load waves LL
macro load_data_Acc_LL()
•Print date()
•Rename Acc_x,Acc_x_LL; Rename Acc_y,Acc_y_LL; Rename
Acc_z,Acc_z_LL; Rename
Time_dd_hh_mm_ss_sss,Time_dd_hh_mm_ss_sss_Acc_LL;
•SetScale/P x 0,0.025,"",
Acc_z_LL,Acc_x_LL,Acc_y_LL,Time_dd_hh_mm_ss_sss_Acc_LL
end

//Load waves RL
macro load_data_Acc_RL()
•Print date()
•Rename Acc_x,Acc_x_RL; Rename Acc_y,Acc_y_RL; Rename
Acc_z,Acc_z_RL; Rename
Time_dd_hh_mm_ss_sss,Time_dd_hh_mm_ss_sss_Acc_RL;
•SetScale/P x 0,0.025,"",
Acc_z_RL,Acc_x_RL,Acc_y_RL,Time_dd_hh_mm_ss_sss_Acc_RL
•Display Acc_z_LL,Acc_x_LL,Acc_y_LL, Acc_z_RL,Acc_x_RL,Acc_y_RL as
"Full Wave for acc xyz axes waves from the left leg (LL) (blue) and
right leg (RL) (red)"
•ModifyGraph lsize=0.25,rgb(Acc_x_RL)=(1,16019,65535);DelayUpdate
•ModifyGraph rgb(Acc_y_RL)=(32792,65535,1);DelayUpdate
•ModifyGraph lsize=0.25,rgb(Acc_x_LL)=(1,16019,65535);DelayUpdate
•ModifyGraph rgb(Acc_y_LL)=(32792,65535,1);DelayUpdate
•Label bottom "Time (s)"; DelayUpdate
•Label left "Radial (x axis) acceleration (g)"
•Legend/C/N=text0/A=MC
•ShowInfo
end

//Segment - Full wave LL (MUST BE PRECISE ON THE END OF THE WAVE
PLACEMENT DUE TO LL/RL DIFFERENCES)
macro Segment_Fullwave_LL ()
•Print date()
•Duplicate/R=[pcsr(A),pcsr(B)] Acc_x_LL Acc_x_LL_Fullwave;
DelayUpdate
•Duplicate/R=[pcsr(A),pcsr(B)] Acc_y_LL Acc_y_LL_Fullwave;
DelayUpdate
•Duplicate/R=[pcsr(A),pcsr(B)] Acc_z_LL Acc_z_LL_Fullwave;
DelayUpdate
end

//Segment - Full wave RL
macro Segment_Fullwave_RL()
•Print date()
•Duplicate/R=[pcsr(A),pcsr(B)] Acc_x_RL Acc_x_RL_Fullwave;
DelayUpdate
•Duplicate/R=[pcsr(A),pcsr(B)] Acc_y_RL Acc_y_RL_Fullwave;
DelayUpdate
•Duplicate/R=[pcsr(A),pcsr(B)] Acc_z_RL Acc_z_RL_Fullwave;
DelayUpdate
```

```

•Display Acc_x_LL_Fullwave,Acc_y_LL_Fullwave,Acc_z_LL_Fullwave as
"Fullwave segment for acc xyz axes waves from the left leg (LL)
(blue) and right leg (RL) (red)"; DelayUpdate
•AppendToGraph Acc_x_RL_Fullwave, Acc_y_RL_Fullwave,
Acc_z_RL_Fullwave; DelayUpdate
•ModifyGraph
lsize=0.25,rgb(Acc_x_LL_Fullwave)=(1,16019,65535);DelayUpdate
•ModifyGraph
lsize=0.25,rgb(Acc_x_RL_Fullwave)=(1,16019,65535);DelayUpdate
•ModifyGraph rgb(Acc_y_LL_Fullwave)=(32792,65535,1);DelayUpdate
•ModifyGraph rgb(Acc_y_RL_Fullwave)=(32792,65535,1);DelayUpdate
•Label bottom "Time (s)";DelayUpdate
•Label left "Acceleration (g)"
•Legend/C/N=text0/A=MC
•ShowInfo
end

//Set start point and scaling LL Blue & INTERPOLATE
//change number of points and scaling for LL
macro Set_start_point_scaling_interpolate_LL_blue()
•Print date()
•SetScale/P x 0,0.025,"",
Acc_x_RL_Fullwave,Acc_y_RL_Fullwave,Acc_z_RL_Fullwave; Delayupdate
SetScale/P x 0,0.0249776521,"",
Acc_x_LL_Fullwave,Acc_y_LL_Fullwave,Acc_z_LL_Fullwave

//Interpolate points LL Blue
//The number needs to be filled in here at exactly the same start
and last points i.e. fit the LL (longer wave) into the RL wave
length (shorter wave)
//Put in number points of RL wave
MACRO Interpolate_LL_Fullwave()
•Interpolate2/T=1/N=384478/Y=Acc_x_LL_Fullwave_I Acc_x_LL_Fullwave;
Delayupdate
•Interpolate2/T=1/N=384478/Y=Acc_y_LL_Fullwave_I Acc_y_LL_Fullwave;
Delayupdate
•Interpolate2/T=1/N=384478/Y=Acc_z_LL_Fullwave_I Acc_z_LL_Fullwave;
Delayupdate
DeletePoints 384478,1,
Acc_x_RL_Fullwave,Acc_y_RL_Fullwave,Acc_z_RL_Fullwave
•Display Acc_x_LL_Fullwave_I, Acc_y_LL_Fullwave_I,
Acc_z_LL_Fullwave_I, Acc_x_RL_Fullwave, Acc_y_RL_Fullwave,
Acc_z_RL_Fullwave as "Fullwave segment interpolated for acc xyz
axes waves from the left leg (LL) (blue) and right leg (RL) (red)"
•ModifyGraph
lsize=0.25,rgb(Acc_x_LL_Fullwave_I)=(1,16019,65535);DelayUpdate
•ModifyGraph
lsize=0.25,rgb(Acc_x_RL_Fullwave)=(1,16019,65535);DelayUpdate
•ModifyGraph rgb(Acc_y_LL_Fullwave_I)=(32792,65535,1);DelayUpdate
•ModifyGraph rgb(Acc_y_RL_Fullwave)=(32792,65535,1);DelayUpdate
•Label bottom "Time (s)"; DelayUpdate
•Label left "Acceleration (g)"
•Legend/C/N=text0/A=MC
•ShowInfo
//Fullwave Segment tables to transfer into Matlab
•Edit/K=0 root:Acc_x_LL_Fullwave_I, root:Acc_y_LL_Fullwave_I,
root:Acc_z_LL_Fullwave_I, root:Acc_x_RL_Fullwave,
root:Acc_y_RL_Fullwave, root:Acc_z_RL_Fullwave
end

//Static Segment LL Blue - average section to paste into Matlab

```

```

macro Segment_Static_LLRL()
•Print date()
•Duplicate/R=[pcsr(A),pcsr(B)] Acc_x_LL_Fullwave_I
Acc_x_LL_STATIC;Delayupdate
•Duplicate/R=[pcsr(A),pcsr(B)] Acc_y_LL_Fullwave_I
Acc_y_LL_STATIC;Delayupdate
•Duplicate/R=[pcsr(A),pcsr(B)] Acc_z_LL_Fullwave_I
Acc_z_LL_STATIC;Delayupdate
•Duplicate/R=[pcsr(A),pcsr(B)] Acc_x_RL_Fullwave
Acc_x_RL_STATIC;Delayupdate
•Duplicate/R=[pcsr(A),pcsr(B)] Acc_y_RL_Fullwave
Acc_y_RL_STATIC;Delayupdate
•Duplicate/R=[pcsr(A),pcsr(B)] Acc_z_RL_Fullwave
Acc_z_RL_STATIC;Delayupdate
Display
Acc_x_RL_STATIC,Acc_y_RL_STATIC,Acc_z_RL_STATIC,Acc_x_LL_STATIC,Acc
_y_LL_STATIC,Acc_z_LL_STATIC as "Static segment for acc xyz axes
waves from the left leg (LL) (blue) and right leg (RL)
(red)";Delayupdate
•ModifyGraph
lsize=0.25,rgb(Acc_x_LL_STATIC)=(1,16019,65535);DelayUpdate
•ModifyGraph
lsize=0.25,rgb(Acc_x_RL_STATIC)=(1,16019,65535);DelayUpdate
•ModifyGraph rgb(Acc_y_LL_STATIC)=(32792,65535,1);DelayUpdate
•ModifyGraph rgb(Acc_y_RL_STATIC)=(32792,65535,1);DelayUpdate
•Label bottom "Time (s)";DelayUpdate
•Label left "Acceleration (g)";DelayUpdate
•Legend/C/N=text0/A=MC
•Edit/K=0 Acc_x_RL_STATIC, Acc_y_RL_STATIC, Acc_z_RL_STATIC,
Acc_x_LL_STATIC, Acc_y_LL_STATIC, Acc_z_LL_STATIC
end

```

//Rescale waves from matlab - name them Acc_x_LL_Rotated, etc.

```

macro Rescale_filter_rotated_waves_from_matlab()
•Print date()
•SetScale/P x 0,0.025,"", Acc_x_RL_Rotated, Acc_y_RL_Rotated,
Acc_z_RL_Rotated,Acc_x_LL_Rotated, Acc_y_LL_Rotated,
Acc_z_LL_Rotated; Delayupdate

```

//IIR (direct from I) filter 3rd order low pass (20 Hz) and high pass (1 Hz) AO 19/06/23

//IIR (direct from I) filter 3rd order low pass (20 Hz) and high pass (0.5 Hz) AO 02/05/23

//Filter 1st order high and low pass AO 250123

//1st order low pass being 20Hz (Nyquist frequency), high pass being 0.5 Hz (0.05 smallest detectable frequency using 40Hz)

```

•Duplicate/O Acc_x_LL_Rotated, Acc_x_LL_Filtered; DelayUpdate
•Duplicate/O Acc_y_LL_Rotated, Acc_y_LL_Filtered; DelayUpdate
•Duplicate/O Acc_z_LL_Rotated, Acc_z_LL_Filtered; DelayUpdate
•Duplicate/O Acc_x_RL_Rotated, Acc_x_RL_Filtered; DelayUpdate
•Duplicate/O Acc_y_RL_Rotated, Acc_y_RL_Filtered; DelayUpdate
•Duplicate/O Acc_z_RL_Rotated, Acc_z_RL_Filtered; DelayUpdate
•FilterIIR/LO=0.5/HI=0.0249766/ORD=3 Acc_x_LL_Filtered
•FilterIIR/LO=0.5/HI=0.0249766/ORD=3 Acc_y_LL_Filtered
•FilterIIR/LO=0.5/HI=0.0249766/ORD=3 Acc_z_LL_Filtered
•FilterIIR/LO=0.5/HI=0.0249766/ORD=3 Acc_x_RL_Filtered
•FilterIIR/LO=0.5/HI=0.0249766/ORD=3 Acc_y_RL_Filtered
•FilterIIR/LO=0.5/HI=0.0249766/ORD=3 Acc_z_RL_Filtered
•Display Acc_x_LL_Filtered, Acc_y_LL_Filtered, Acc_z_LL_Filtered,
Acc_x_RL_Filtered, Acc_y_RL_Filtered, Acc_z_RL_Filtered as "Full

```

```

Wave filtered for acc xyz axes waves from the left leg (LL) (blue)
and right leg (RL) (red)"
•ModifyGraph
lsize=0.25,rgb(Acc_x_LL_Filtered)=(1,16019,65535);DelayUpdate
•ModifyGraph
lsize=0.25,rgb(Acc_x_RL_Filtered)=(1,16019,65535);DelayUpdate
•ModifyGraph rgb(Acc_y_RL_Filtered)=(32792,65535,1);DelayUpdate
•ModifyGraph rgb(Acc_y_LL_Filtered)=(32792,65535,1);DelayUpdate
•Label bottom "Time (s)";DelayUpdate
•Label left "Acceleration (g)"
•Legend/C/N=text0/A=MC
•ShowInfo
end

//SPLIT FILTERED WAVES
MACRO Split_filtered_wave_LL()
•Duplicate/R=[pcsr(A),pcsr(B)] Acc_x_LL_Filtered
Acc_x_LL_Filtered1; DelayUpdate
•Duplicate/R=[pcsr(A),pcsr(B)] Acc_y_LL_Filtered
Acc_y_LL_Filtered1; DelayUpdate
•Duplicate/R=[pcsr(A),pcsr(B)] Acc_z_LL_Filtered
Acc_z_LL_Filtered1; DelayUpdate
END

MACRO Split_filtered_wave_RL()
•Duplicate/R=[pcsr(A),pcsr(B)] Acc_x_RL_Filtered
Acc_x_RL_Filtered1; DelayUpdate
•Duplicate/R=[pcsr(A),pcsr(B)] Acc_y_RL_Filtered
Acc_y_RL_Filtered1; DelayUpdate
•Duplicate/R=[pcsr(A),pcsr(B)] Acc_z_RL_Filtered
Acc_z_RL_Filtered1; DelayUpdate
•Display Acc_x_LL_Filtered1,Acc_y_LL_Filtered1,Acc_z_LL_Filtered1
as "Filtered segment for acc xyz axes waves from the left leg (LL)
(blue) and right leg (RL) (red)"; DelayUpdate
•AppendToGraph Acc_x_RL_Filtered1, Acc_y_RL_Filtered1,
Acc_z_RL_Filtered1; DelayUpdate
•ModifyGraph
lsize=0.25,rgb(Acc_x_LL_Filtered1)=(1,16019,65535);DelayUpdate
•ModifyGraph
lsize=0.25,rgb(Acc_x_RL_Filtered1)=(1,16019,65535);DelayUpdate
•ModifyGraph rgb(Acc_y_LL_Filtered1)=(32792,65535,1);DelayUpdate
•ModifyGraph rgb(Acc_y_RL_Filtered1)=(32792,65535,1);DelayUpdate
•Label bottom "Time (s)";DelayUpdate
•Label left "Acceleration (g)"
•Legend/C/N=text0/A=MC
•ShowInfo
END

//Delete ...filtered waves

//Rename and rescale filtered waves from filtered 1 > filtered to
the code works again
MACRO Rename_and_rescale_filtered1_waves()
Rename Acc_x_LL_Filtered1,Acc_x_LL_Filtered
Rename Acc_y_LL_Filtered1,Acc_y_LL_Filtered
Rename Acc_z_LL_Filtered1,Acc_z_LL_Filtered
Rename Acc_x_RL_Filtered1,Acc_x_RL_Filtered
Rename Acc_y_RL_Filtered1,Acc_y_RL_Filtered
Rename Acc_z_RL_Filtered1,Acc_z_RL_Filtered

```

```

SetScale/P x 0,0.025,"",
Acc_x_LL_Filtered,Acc_y_LL_Filtered,Acc_z_LL_Filtered
SetScale/P x 0,0.025,"",
Acc_x_RL_Filtered,Acc_y_RL_Filtered,Acc_z_RL_Filtered
END

```

```

//ANALYSIS
//INCLINE_1_16kmh
//Segment and rename waves VF 1% incline testing LL and RL
macro INC_1_16kmh_segment_LLRL()
•Print date()
•Duplicate/R=[pcsr(A),pcsr(B)] Acc_x_LL_Filtered
Acc_x_LL_INC_1_16kmh
•Duplicate/R=[pcsr(A),pcsr(B)] Acc_y_LL_Filtered
Acc_y_LL_INC_1_16kmh
•Duplicate/R=[pcsr(A),pcsr(B)] Acc_z_LL_Filtered
Acc_z_LL_INC_1_16kmh
•Duplicate/R=[pcsr(A),pcsr(B)] Acc_x_RL_Filtered
Acc_x_RL_INC_1_16kmh
•Duplicate/R=[pcsr(A),pcsr(B)] Acc_y_RL_Filtered
Acc_y_RL_INC_1_16kmh
•Duplicate/R=[pcsr(A),pcsr(B)] Acc_z_RL_Filtered
Acc_z_RL_INC_1_16kmh
•SetScale/P x 0,0.025,"",
Acc_x_RL_INC_1_16kmh,Acc_y_RL_INC_1_16kmh,Acc_z_RL_INC_1_16kmh,
Acc_x_LL_INC_1_16kmh,Acc_y_LL_INC_1_16kmh,Acc_z_LL_INC_1_16kmh
•Display Acc_x_LL_INC_1_16kmh, Acc_x_RL_INC_1_16kmh as "VF 1%
incline testing at 16 km/h for acc x axis wave from the left leg
(LL) (blue) and right leg (RL) (red)"
•ModifyGraph rgb(Acc_x_LL_INC_1_16kmh)=(1,16019,65535)
•Label bottom "Time (s)"
•Label left "Radial (x axis) acceleration (g)"
•Legend/C/N=text0/A=MC
•ShowInfo

//FFT of VF 1% incline testing left leg (LL) and right leg (RL) -
must be an even number of rows selected i.e. 0-3999
MACRO INC_1_16kmh_FFT_INT_acc_x_LLRL()
•FFT/OUT=3/RP=[0,3999]/DEST=FFT_Acc_x_RL_INC_1_16kmh
Acc_x_RL_INC_1_16kmh;DelayUpdate
•FFT/OUT=3/RP=[0,3999]/DEST=FFT_Acc_y_RL_INC_1_16kmh
Acc_y_RL_INC_1_16kmh;DelayUpdate
•FFT/OUT=3/RP=[0,3999]/DEST=FFT_Acc_z_RL_INC_1_16kmh
Acc_z_RL_INC_1_16kmh;DelayUpdate
•FFT/OUT=3/RP=[0,3999]/DEST=FFT_Acc_x_LL_INC_1_16kmh
Acc_x_LL_INC_1_16kmh;DelayUpdate
•FFT/OUT=3/RP=[0,3999]/DEST=FFT_Acc_y_LL_INC_1_16kmh
Acc_y_LL_INC_1_16kmh;DelayUpdate
•FFT/OUT=3/RP=[0,3999]/DEST=FFT_Acc_z_LL_INC_1_16kmh
Acc_z_LL_INC_1_16kmh;DelayUpdate
•Display FFT_Acc_x_LL_INC_1_16kmh as "Fast Fourier Transform (FFT)
of the VF 1% incline testing at 16 km/h for acc x axis waves from
the left leg (LL) (blue) and right leg (RL) (red)"
•AppendtoGraph FFT_Acc_x_RL_INC_1_16kmh
•ModifyGraph rgb(FFT_Acc_x_LL_INC_1_16kmh)=(1,16019,65535)
•ModifyGraph lstyle(FFT_Acc_x_LL_INC_1_16kmh)=2
•Label bottom "Frequency (Hz)"
•Label left "Cumulative Magnitude (g)"
•Legend/C/N=text0/A=MC

```

```

•ShowInfo

//Run multipeak fitting

//Integration of the FFT for VF 1% incline testing at 16 km/h.
•Integrate
FFT_Acc_x_LL_INC_1_16kmh/D=FFT_Acc_x_LL_INC_1_16kmh_CDF;DelayUpdate
•Integrate
FFT_Acc_x_RL_INC_1_16kmh/D=FFT_Acc_x_RL_INC_1_16kmh_CDF;DelayUpdate
•CurveFit/TBOX=1017 Sigmoid FFT_Acc_x_LL_INC_1_16kmh_CDF /D
•CurveFit/TBOX=1017 Sigmoid FFT_Acc_x_RL_INC_1_16kmh_CDF /D
•Display FFT_Acc_x_LL_INC_1_16kmh_CDF,
FFT_Acc_x_RL_INC_1_16kmh_CDF, fit_FFT_Acc_x_LL_INC_1_16kmh_CDF,
fit_FFT_Acc_x_RL_INC_1_16kmh_CDF as "CDF of the FFT for VF 1%
incline testing at 16 km/h for acc x axis wave from the left leg
(LL) (blue) and right leg (RL) (red)";DelayUpdate
•ModifyGraph
rgb(FFT_Acc_x_RL_INC_1_16kmh_CDF)=(65535,0,0);DelayUpdate
•ModifyGraph
rgb(fit_FFT_Acc_x_RL_INC_1_16kmh_CDF)=(65535,0,0);DelayUpdate
•ModifyGraph
rgb(FFT_Acc_x_LL_INC_1_16kmh_CDF)=(1,16019,65535);DelayUpdate
•ModifyGraph
rgb(fit_FFT_Acc_x_LL_INC_1_16kmh_CDF)=(1,16019,65535);DelayUpdate
•Label bottom "Frequency (Hz)"
•Label left "Cumulative Magnitude (g)"
•Legend/C/N=text0/A=MC

//Find CDF level at 25% LL/RL
•findLevel fit_FFT_Acc_x_LL_INC_1_16kmh_CDF,
(Wavemax(fit_FFT_Acc_x_LL_INC_1_16kmh_CDF)*.25)
•findLevel fit_FFT_Acc_x_RL_INC_1_16kmh_CDF,
(Wavemax(fit_FFT_Acc_x_RL_INC_1_16kmh_CDF)*.25)

//Find CDF level at 50% LL/RL
•findLevel fit_FFT_Acc_x_LL_INC_1_16kmh_CDF,
(Wavemax(fit_FFT_Acc_x_LL_INC_1_16kmh_CDF)*.5)
•findLevel fit_FFT_Acc_x_RL_INC_1_16kmh_CDF,
(Wavemax(fit_FFT_Acc_x_RL_INC_1_16kmh_CDF)*.5)

//Find CDF level at 75% LL/RL
•findLevel fit_FFT_Acc_x_LL_INC_1_16kmh_CDF,
(Wavemax(fit_FFT_Acc_x_LL_INC_1_16kmh_CDF)*.75)
•findLevel fit_FFT_Acc_x_RL_INC_1_16kmh_CDF,
(Wavemax(fit_FFT_Acc_x_RL_INC_1_16kmh_CDF)*.75)

//Run multipeakfit2

//Show table from multipeakfit2
macro Table_multipeakfit2()
•Edit/K=0
root:Packages:MultiPeakFit2:MPF_SetFolder_1:W_AutoPeakInfo
end

//ANALYSIS
//INCLINE_0
//Segment and rename waves VF 0% incline testing LL and RL
macro INC_0_segment_LLRL()
•Print date()
•Duplicate/R=[pcsr(A),pcsr(B)] Acc_x_LL_Filtered Acc_x_LL_INC_0
•Duplicate/R=[pcsr(A),pcsr(B)] Acc_y_LL_Filtered Acc_y_LL_INC_0

```



```

•Duplicate/R=[pcsr(A),pcsr(B)] Acc_z_LL_Filtered Acc_z_LL_INC_0
•Duplicate/R=[pcsr(A),pcsr(B)] Acc_x_RL_Filtered Acc_x_RL_INC_0
•Duplicate/R=[pcsr(A),pcsr(B)] Acc_y_RL_Filtered Acc_y_RL_INC_0
•Duplicate/R=[pcsr(A),pcsr(B)] Acc_z_RL_Filtered Acc_z_RL_INC_0
•SetScale/P x 0,0.025,"",
Acc_x_RL_INC_0,Acc_y_RL_INC_0,Acc_z_RL_INC_0,
Acc_x_LL_INC_0,Acc_y_LL_INC_0,Acc_z_LL_INC_0
•Display Acc_x_LL_INC_0, Acc_x_RL_INC_0 as "VF 0% incline testing
at 12 km/h for acc x axis wave from the left leg (LL) (blue) and
right leg (RL) (red)"
•ModifyGraph rgb(Acc_x_LL_INC_0)=(1,16019,65535)
•Label bottom "Time (s)"
•Label left "Radial (x axis) acceleration (g)"
•Legend/C/N=text0/A=MC
•ShowInfo

//FFT of VF 0% incline testing left leg (LL) and right leg (RL) -
must be an even number of rows selected i.e. 0-3999
//INC_0_FFT_INT_acc_x_LLRL()
•Print date()
•FFT/OUT=3/RP=[0,3999]/DEST=FFT_Acc_x_RL_INC_0
Acc_x_RL_INC_0;DelayUpdate
•FFT/OUT=3/RP=[0,3999]/DEST=FFT_Acc_y_RL_INC_0
Acc_y_RL_INC_0;DelayUpdate
•FFT/OUT=3/RP=[0,3999]/DEST=FFT_Acc_z_RL_INC_0
Acc_z_RL_INC_0;DelayUpdate
•FFT/OUT=3/RP=[0,3999]/DEST=FFT_Acc_x_LL_INC_0
Acc_x_LL_INC_0;DelayUpdate
•FFT/OUT=3/RP=[0,3999]/DEST=FFT_Acc_y_LL_INC_0
Acc_y_LL_INC_0;DelayUpdate
•FFT/OUT=3/RP=[0,3999]/DEST=FFT_Acc_z_LL_INC_0
Acc_z_LL_INC_0;DelayUpdate
•Display FFT_Acc_x_LL_INC_0 as "Fast Fourier Transform (FFT) of the
VF 0% incline testing at 12 km/h for acc x axis waves from the left
leg (LL) (blue) and right leg (RL) (red)"
•Appendtograph FFT_Acc_x_RL_INC_0
•ModifyGraph rgb(FFT_Acc_x_LL_INC_0)=(1,16019,65535)
•ModifyGraph lstyle(FFT_Acc_x_LL_INC_0)=2
•Label bottom "Frequency (Hz)"
•Label left "Magnitude (g)"
•Legend/C/N=text0/A=MC
•ShowInfo

//Run Analysis> multipeak fitting

//Integration of the FFT for VF 0% incline testing at 12 km/h.
MACRO INT_0()
•Print date()
•Integrate FFT_Acc_x_LL_INC_0/D=FFT_Acc_x_LL_INC_0_CDF;DelayUpdate
•Integrate FFT_Acc_x_RL_INC_0/D=FFT_Acc_x_RL_INC_0_CDF;DelayUpdate
•CurveFit/TBOX=1017 Sigmoid FFT_Acc_x_LL_INC_0_CDF /D
•CurveFit/TBOX=1017 Sigmoid FFT_Acc_x_RL_INC_0_CDF /D
•Display FFT_Acc_x_LL_INC_0_CDF, FFT_Acc_x_RL_INC_0_CDF,
fit_FFT_Acc_x_RL_INC_0_CDF, fit_FFT_Acc_x_LL_INC_0_CDF as "CDF of
the FFT for VF 0% incline testing at 12 km/h for acc x axis wave
from the left leg (LL) (blue) and right leg (RL) (red)";DelayUpdate
•ModifyGraph rgb(FFT_Acc_x_RL_INC_0_CDF)=(65535,0,0);DelayUpdate
•ModifyGraph
rgb(fit_FFT_Acc_x_RL_INC_0_CDF)=(65535,0,0);DelayUpdate
•ModifyGraph
rgb(FFT_Acc_x_LL_INC_0_CDF)=(1,16019,65535);DelayUpdate

```

```

•ModifyGraph
rgb(fit_FFT_Acc_x_LL_INC_0_CDF)=(1,16019,65535);DelayUpdate
•Label bottom "Frequency (Hz)"
•Label left "Cumulative Magnitude (g)"
•Legend/C/N=text0/A=MC

//Find CDF level at 25% LL/RL
•findLevel fit_FFT_Acc_x_LL_INC_0_CDF,
(Wavemax(fit_FFT_Acc_x_LL_INC_0_CDF)*.25)
•findLevel fit_FFT_Acc_x_RL_INC_0_CDF,
(Wavemax(fit_FFT_Acc_x_RL_INC_0_CDF)*.25)

//Find CDF level at 50% LL/RL
•findLevel fit_FFT_Acc_x_LL_INC_0_CDF,
(Wavemax(fit_FFT_Acc_x_LL_INC_0_CDF)*.5)
•findLevel fit_FFT_Acc_x_RL_INC_0_CDF,
(Wavemax(fit_FFT_Acc_x_RL_INC_0_CDF)*.5)

//Find CDF level at 75% LL/RL
•findLevel fit_FFT_Acc_x_LL_INC_0_CDF,
(Wavemax(fit_FFT_Acc_x_LL_INC_0_CDF)*.75)
•findLevel fit_FFT_Acc_x_RL_INC_0_CDF,
(Wavemax(fit_FFT_Acc_x_RL_INC_0_CDF)*.75)

//Print area under CDF LL
•Print area(fit_FFT_Acc_x_LL_INC_0_CDF)
//Print area under CDF RL
•Print area(fit_FFT_Acc_x_RL_INC_0_CDF)
end

//Run multipeakfit2

//Show table from multipeakfit2
//Table_multipeakfit2_0()
//•Edit/K=0
root:Packages:MultiPeakFit2:MPF_SetFolder_1:W_AutoPeakInfo

//ANALYSIS
//INCLINE_1
//Segment and rename waves VF 1% incline testing LL and RL
macro INC_1_segment_LLRL()
•Print date()
•Duplicate/R=[pcsr(A),pcsr(B)] Acc_x_LL_Filtered Acc_x_LL_INC_1
•Duplicate/R=[pcsr(A),pcsr(B)] Acc_y_LL_Filtered Acc_y_LL_INC_1
•Duplicate/R=[pcsr(A),pcsr(B)] Acc_z_LL_Filtered Acc_z_LL_INC_1
•Duplicate/R=[pcsr(A),pcsr(B)] Acc_x_RL_Filtered Acc_x_RL_INC_1
•Duplicate/R=[pcsr(A),pcsr(B)] Acc_y_RL_Filtered Acc_y_RL_INC_1
•Duplicate/R=[pcsr(A),pcsr(B)] Acc_z_RL_Filtered Acc_z_RL_INC_1
•SetScale/P x 0,0.025,"",
Acc_x_RL_INC_1,Acc_y_RL_INC_1,Acc_z_RL_INC_1,
Acc_x_LL_INC_1,Acc_y_LL_INC_1,Acc_z_LL_INC_1
•Display Acc_x_LL_INC_1, Acc_x_RL_INC_1 as "VF 1% incline testing
at 12 km/h for acc x axis wave from the left leg (LL) (blue) and
right leg (RL) (red)"
•ModifyGraph rgb(Acc_x_LL_INC_1)=(1,16019,65535)
•Label bottom "Time (s)"
•Label left "Radial (x axis) acceleration (g)"
•Legend/C/N=text0/A=MC
•ShowInfo

```

```

//FFT of VF 1% incline testing left leg (LL) and right leg (RL) -
must be an even number of rows selected i.e. 0-3999
//INC_1_FFT_INT_acc_x_LLRL()
•FFT/OUT=3/RP=[0,3999]/DEST=FFT_Acc_x_RL_INC_1
Acc_x_RL_INC_1;DelayUpdate
•FFT/OUT=3/RP=[0,3999]/DEST=FFT_Acc_y_RL_INC_1
Acc_y_RL_INC_1;DelayUpdate
•FFT/OUT=3/RP=[0,3999]/DEST=FFT_Acc_z_RL_INC_1
Acc_z_RL_INC_1;DelayUpdate
•FFT/OUT=3/RP=[0,3999]/DEST=FFT_Acc_x_LL_INC_1
Acc_x_LL_INC_1;DelayUpdate
•FFT/OUT=3/RP=[0,3999]/DEST=FFT_Acc_y_LL_INC_1
Acc_y_LL_INC_1;DelayUpdate
•FFT/OUT=3/RP=[0,3999]/DEST=FFT_Acc_z_LL_INC_1
Acc_z_LL_INC_1;DelayUpdate
•Display FFT_Acc_x_LL_INC_1 as "Fast Fourier Transform (FFT) of the
VF 1% incline testing at 12 km/h for acc x axis waves from the left
leg (LL) (blue) and right leg (RL) (red)"
•Appendtograph FFT_Acc_x_RL_INC_1
•ModifyGraph rgb(FFT_Acc_x_LL_INC_1)=(1,16019,65535)
•ModifyGraph lstyle(FFT_Acc_x_LL_INC_1)=2
•Label bottom "Frequency (Hz)"
•Label left "Magnitude (g)"
•Legend/C/N=text0/A=MC
•ShowInfo

//Integration of the FFT for VF 1% incline testing at 12 km/h.
macro INT_1()
•Print date()
•Integrate FFT_Acc_x_LL_INC_1/D=FFT_Acc_x_LL_INC_1_CDF;DelayUpdate
•Integrate FFT_Acc_x_RL_INC_1/D=FFT_Acc_x_RL_INC_1_CDF;DelayUpdate
•CurveFit/TBOX=1017 Sigmoid FFT_Acc_x_LL_INC_1_CDF /D
•CurveFit/TBOX=1017 Sigmoid FFT_Acc_x_RL_INC_1_CDF /D
•Display FFT_Acc_x_LL_INC_1_CDF, FFT_Acc_x_RL_INC_1_CDF,
fit_FFT_Acc_x_LL_INC_1_CDF, fit_FFT_Acc_x_RL_INC_1_CDF as "CDF of
the FFT for VF 1% incline testing at 12 km/h for acc x axis wave
from the left leg (LL) (blue) and right leg (RL) (red)";DelayUpdate
•ModifyGraph rgb(FFT_Acc_x_RL_INC_1_CDF)=(65535,0,0);DelayUpdate
•ModifyGraph
rgb(fit_FFT_Acc_x_RL_INC_1_CDF)=(65535,0,0);DelayUpdate
•ModifyGraph
rgb(FFT_Acc_x_LL_INC_1_CDF)=(1,16019,65535);DelayUpdate
•ModifyGraph
rgb(fit_FFT_Acc_x_LL_INC_1_CDF)=(1,16019,65535);DelayUpdate
•Label bottom "Frequency (Hz)"
•Label left "Cumulative Magnitude (g)"
•Legend/C/N=text0/A=MC

//Find CDF level at 25% LL/RL
•findLevel fit_FFT_Acc_x_LL_INC_1_CDF,
(Wavemax(fit_FFT_Acc_x_LL_INC_1_CDF)*.25)
•findLevel fit_FFT_Acc_x_RL_INC_1_CDF,
(Wavemax(fit_FFT_Acc_x_RL_INC_1_CDF)*.25)

//Find CDF level at 50% LL/RL
•findLevel fit_FFT_Acc_x_LL_INC_1_CDF,
(Wavemax(fit_FFT_Acc_x_LL_INC_1_CDF)*.5)
•findLevel fit_FFT_Acc_x_RL_INC_1_CDF,
(Wavemax(fit_FFT_Acc_x_RL_INC_1_CDF)*.5)

```

```

//Find CDF level at 75% LL/RL
•findLevel fit_FFT_Acc_x_LL_INC_1_CDF,
(Wavemax(fit_FFT_Acc_x_LL_INC_1_CDF)*.75)
•findLevel fit_FFT_Acc_x_RL_INC_1_CDF,
(Wavemax(fit_FFT_Acc_x_RL_INC_1_CDF)*.75)

//Print area under CDF LL
•Print area(fit_FFT_Acc_x_LL_INC_1_CDF)
//Print area under CDF RL
•Print area(fit_FFT_Acc_x_RL_INC_1_CDF)
end
//Run multipeakfit2

//Show table from multipeakfit2
macro Table_multipeakfit2_1()
•Edit/K=0
root:Packages:MultiPeakFit2:MPF_SetFolder_1:W_AutoPeakInfo
end

//ANALYSIS
//INCLINE_3
//Segment and rename waves VF 3% incline testing LL and RL
macro INC_3_segment_LLRL()
•Print date()
•Duplicate/R=[pcsr(A),pcsr(B)] Acc_x_LL_Filtered Acc_x_LL_INC_3
•Duplicate/R=[pcsr(A),pcsr(B)] Acc_y_LL_Filtered Acc_y_LL_INC_3
•Duplicate/R=[pcsr(A),pcsr(B)] Acc_z_LL_Filtered Acc_z_LL_INC_3
•Duplicate/R=[pcsr(A),pcsr(B)] Acc_x_RL_Filtered Acc_x_RL_INC_3
•Duplicate/R=[pcsr(A),pcsr(B)] Acc_y_RL_Filtered Acc_y_RL_INC_3
•Duplicate/R=[pcsr(A),pcsr(B)] Acc_z_RL_Filtered Acc_z_RL_INC_3
•SetScale/P x 0,0.025,"",
Acc_x_RL_INC_3,Acc_y_RL_INC_3,Acc_z_RL_INC_3,
Acc_x_LL_INC_3,Acc_y_LL_INC_3,Acc_z_LL_INC_3
•Display Acc_x_LL_INC_3, Acc_x_RL_INC_3 as "VF 3% incline testing
at 12 km/h for acc x axis wave from the left leg (LL) (blue) and
right leg (RL) (red)"
•ModifyGraph rgb(Acc_x_LL_INC_3)=(1,16019,65535)
•Label bottom "Time (s)"
•Label left "Radial (x axis) acceleration (g)"
•Legend/C/N=text0/A=MC
•ShowInfo

//FFT of VF 3% incline testing left leg (LL) and right leg (RL) -
must be an even number of rows selected i.e. 0-3999
//INC_3_FFT_INT_acc_x_LLRL()
•FFT/OUT=3/RP=[0,3999]/DEST=FFT_Acc_x_RL_INC_3
Acc_x_RL_INC_3;DelayUpdate
•FFT/OUT=3/RP=[0,3999]/DEST=FFT_Acc_y_RL_INC_3
Acc_y_RL_INC_3;DelayUpdate
•FFT/OUT=3/RP=[0,3999]/DEST=FFT_Acc_z_RL_INC_3
Acc_z_RL_INC_3;DelayUpdate
•FFT/OUT=3/RP=[0,3999]/DEST=FFT_Acc_x_LL_INC_3
Acc_x_LL_INC_3;DelayUpdate
•FFT/OUT=3/RP=[0,3999]/DEST=FFT_Acc_y_LL_INC_3
Acc_y_LL_INC_3;DelayUpdate
•FFT/OUT=3/RP=[0,3999]/DEST=FFT_Acc_z_LL_INC_3
Acc_z_LL_INC_3;DelayUpdate
•Display FFT_Acc_x_LL_INC_3 as "Fast Fourier Transform (FFT) of the
VF 3% incline testing at 12 km/h for acc x axis waves from the left
leg (LL) (blue) and right leg (RL) (red)"
•Appendtograph FFT_Acc_x_RL_INC_3

```

```

•ModifyGraph rgb(FFT_Acc_x_LL_INC_3)=(1,16019,65535)
•ModifyGraph lstyle(FFT_Acc_x_LL_INC_3)=2
•Label bottom "Frequency (Hz)"
•Label left "Magnitude (g)"
•Legend/C/N=text0/A=MC
•ShowInfo

//Integration of the FFT for VF 3% incline testing at 12 km/h.
macro INT_3()
•Print date()
•Integrate FFT_Acc_x_LL_INC_3/D=FFT_Acc_x_LL_INC_3_CDF;DelayUpdate
•Integrate FFT_Acc_x_RL_INC_3/D=FFT_Acc_x_RL_INC_3_CDF;DelayUpdate
•Display FFT_Acc_x_LL_INC_3_CDF, FFT_Acc_x_RL_INC_3_CDF as "CDF of
the FFT for VF 3% incline testing at 12 km/h for acc x axis wave
from the left leg (LL) (blue) and right leg (RL) (red)";DelayUpdate
•CurveFit/TBOX=1017 Sigmoid FFT_Acc_x_LL_INC_3_CDF /D
•CurveFit/TBOX=1017 Sigmoid FFT_Acc_x_RL_INC_3_CDF /D
•ModifyGraph rgb(FFT_Acc_x_RL_INC_3_CDF)=(65535,0,0);DelayUpdate
•ModifyGraph
rgb(fit_FFT_Acc_x_RL_INC_3_CDF)=(65535,0,0);DelayUpdate
•ModifyGraph
rgb(FFT_Acc_x_LL_INC_3_CDF)=(1,16019,65535);DelayUpdate
•ModifyGraph
rgb(fit_FFT_Acc_x_LL_INC_3_CDF)=(1,16019,65535);DelayUpdate
•Label bottom "Frequency (Hz)"
•Label left "Cumulative Magnitude (g)"
•Legend/C/N=text0/A=MC

//Find CDF level at 25% LL/RL
•findLevel fit_FFT_Acc_x_LL_INC_3_CDF,
(Wavemax(fit_FFT_Acc_x_LL_INC_3_CDF)*.25)
•findLevel fit_FFT_Acc_x_RL_INC_3_CDF,
(Wavemax(fit_FFT_Acc_x_RL_INC_3_CDF)*.25)

//Find CDF level at 50% LL/RL
•findLevel fit_FFT_Acc_x_LL_INC_3_CDF,
(Wavemax(fit_FFT_Acc_x_LL_INC_3_CDF)*.5)
•findLevel fit_FFT_Acc_x_RL_INC_3_CDF,
(Wavemax(fit_FFT_Acc_x_RL_INC_3_CDF)*.5)

//Find CDF level at 75% LL/RL
•findLevel fit_FFT_Acc_x_LL_INC_3_CDF,
(Wavemax(fit_FFT_Acc_x_LL_INC_3_CDF)*.75)
•findLevel fit_FFT_Acc_x_RL_INC_3_CDF,
(Wavemax(fit_FFT_Acc_x_RL_INC_3_CDF)*.75)

//Print area under CDF LL
•Print area(fit_FFT_Acc_x_LL_INC_3_CDF)
//Print area under CDF RL
•Print area(fit_FFT_Acc_x_RL_INC_3_CDF)
end
//Run multipeakfit2

//Show table from multipeakfit2
macro Table_multipeakfit2_3()
•Edit/K=0
root:Packages:MultiPeakFit2:MPF_SetFolder_1:W_AutoPeakInfo
end

//ANALYSIS

```

```

//INCLINE_5
//Segment and rename waves VF 5% incline testing LL and RL
macro INC_5_segment_LLRL()
•Print date()
•Duplicate/R=[pcsr(A),pcsr(B)] Acc_x_LL_Filtered Acc_x_LL_INC_5
•Duplicate/R=[pcsr(A),pcsr(B)] Acc_y_LL_Filtered Acc_y_LL_INC_5
•Duplicate/R=[pcsr(A),pcsr(B)] Acc_z_LL_Filtered Acc_z_LL_INC_5
•Duplicate/R=[pcsr(A),pcsr(B)] Acc_x_RL_Filtered Acc_x_RL_INC_5
•Duplicate/R=[pcsr(A),pcsr(B)] Acc_y_RL_Filtered Acc_y_RL_INC_5
•Duplicate/R=[pcsr(A),pcsr(B)] Acc_z_RL_Filtered Acc_z_RL_INC_5
•SetScale/P x 0,0.025,"",
Acc_x_RL_INC_5,Acc_y_RL_INC_5,Acc_z_RL_INC_5,
Acc_x_LL_INC_5,Acc_y_LL_INC_5,Acc_z_LL_INC_5
•Display Acc_x_LL_INC_5, Acc_x_RL_INC_5 as "VF 5% incline testing
at 12 km/h for acc x axis wave from the left leg (LL) (blue) and
right leg (RL) (red)"
•ModifyGraph rgb(Acc_x_LL_INC_5)=(1,16019,65535)
•Label bottom "Time (s)"
•Label left "Radial (x axis) acceleration (g)"
•Legend/C/N=text0/A=MC
•ShowInfo

//FFT of VF 5% incline testing left leg (LL) and right leg (RL) -
must be an even number of rows selected i.e. 0-3999
//INC_5_FFT_INT_acc x LLRL()
•FFT/OUT=3/RP=[0,3999]/DEST=FFT_Acc_x_RL_INC_5
Acc_x_RL_INC_5;DelayUpdate
•FFT/OUT=3/RP=[0,3999]/DEST=FFT_Acc_y_RL_INC_5
Acc_y_RL_INC_5;DelayUpdate
•FFT/OUT=3/RP=[0,3999]/DEST=FFT_Acc_z_RL_INC_5
Acc_z_RL_INC_5;DelayUpdate
•FFT/OUT=3/RP=[0,3999]/DEST=FFT_Acc_x_LL_INC_5
Acc_x_LL_INC_5;DelayUpdate
•FFT/OUT=3/RP=[0,3999]/DEST=FFT_Acc_y_LL_INC_5
Acc_y_LL_INC_5;DelayUpdate
•FFT/OUT=3/RP=[0,3999]/DEST=FFT_Acc_z_LL_INC_5
Acc_z_LL_INC_5;DelayUpdate
•Display FFT_Acc_x_LL_INC_5 as "Fast Fourier Transform (FFT) of the
VF 5% incline testing at 12 km/h for acc x axis waves from the left
leg (LL) (blue) and right leg (RL) (red)"
•Appendtograph FFT_Acc_x_RL_INC_5
•ModifyGraph rgb(FFT_Acc_x_LL_INC_5)=(1,16019,65535)
•ModifyGraph lstyle(FFT_Acc_x_LL_INC_5)=2
•Label bottom "Frequency (Hz)"
•Label left "Magnitude (g)"
•Legend/C/N=text0/A=MC
•ShowInfo

//Integration of the FFT for VF 5% incline testing at 12 km/h.
macro INT_5()
•Print date()
•Integrate FFT_Acc_x_LL_INC_5/D=FFT_Acc_x_LL_INC_5_CDF;DelayUpdate
•Integrate FFT_Acc_x_RL_INC_5/D=FFT_Acc_x_RL_INC_5_CDF;DelayUpdate
•Display FFT_Acc_x_LL_INC_5_CDF, FFT_Acc_x_RL_INC_5_CDF as "CDF of
the FFT for VF 5% incline testing at 12 km/h for acc x axis wave
from the left leg (LL) (blue) and right leg (RL) (red)";DelayUpdate
•CurveFit/TBOX=1017 Sigmoid FFT_Acc_x_LL_INC_5_CDF /D
•CurveFit/TBOX=1017 Sigmoid FFT_Acc_x_RL_INC_5_CDF /D
•ModifyGraph rgb(FFT_Acc_x_RL_INC_5_CDF)=(65535,0,0);DelayUpdate
•ModifyGraph
rgb(fit_FFT_Acc_x_RL_INC_5_CDF)=(65535,0,0);DelayUpdate

```

```

•ModifyGraph
rgb(FFT_Acc_x_LL_INC_5_CDF)=(1,16019,65535);DelayUpdate
•ModifyGraph
rgb(fit_FFT_Acc_x_LL_INC_5_CDF)=(1,16019,65535);DelayUpdate
•Label bottom "Frequency (Hz)"
•Label left "Cumulative Magnitude (g)"
•Legend/C/N=text0/A=MC

//Find CDF level at 25% LL/RL
•findLevel fit_FFT_Acc_x_LL_INC_5_CDF,
(Wavemax(fit_FFT_Acc_x_LL_INC_5_CDF)*.25)
•findLevel fit_FFT_Acc_x_RL_INC_5_CDF,
(Wavemax(fit_FFT_Acc_x_RL_INC_5_CDF)*.25)

//Find CDF level at 50% LL/RL
•findLevel fit_FFT_Acc_x_LL_INC_5_CDF,
(Wavemax(fit_FFT_Acc_x_LL_INC_5_CDF)*.5)
•findLevel fit_FFT_Acc_x_RL_INC_5_CDF,
(Wavemax(fit_FFT_Acc_x_RL_INC_5_CDF)*.5)

//Find CDF level at 75% LL/RL
•findLevel fit_FFT_Acc_x_LL_INC_5_CDF,
(Wavemax(fit_FFT_Acc_x_LL_INC_5_CDF)*.75)
•findLevel fit_FFT_Acc_x_RL_INC_5_CDF,
(Wavemax(fit_FFT_Acc_x_RL_INC_5_CDF)*.75)

//Print area under CDF LL
•Print area(fit_FFT_Acc_x_LL_INC_5_CDF)
//Print area under CDF RL
•Print area(fit_FFT_Acc_x_RL_INC_5_CDF)
end

//Run multipeakfit2

//Show table from multipeakfit2
macro Table_multipeakfit2_5()
•Edit/K=0
root:Packages:MultiPeakFit2:MPF_SetFolder_1:W_AutoPeakInfo
end

```

Appendix H: Summary of the data processing and analytical techniques.

1. Load raw accelerometry waves into Igor Pro v8 as .txt files.
2. Segment the entire wave into clean activity epochs.
3. Synchronise starting point on both the red and blue wearable device waves.
4. Change wave scaling and start point on the blue device to match the red device.
5. Interpolate the number of points on the blue device to match that of the red device by deleting points.
6. Segment a 10 second static wave epoch and record the average x, y and z wave reading.
7. Export the full x, y and z waves as .txt files.
8. Load waves into MATLAB.
9. Enter the static data average into the MATLAB code.
10. Perform a sensitivity and bias offset calibration on the raw x, y and z waves.
11. Rotate the three waves.
12. Export waves as .txt files.
13. Load waves into Igor Pro v8 as .txt files.
14. Re-set the wave scaling and the starting point.
15. Run the filter.
16. Run the analytical processing script in Igor;
 - 16.1. Fast Fourier Transform (FFT),
 - 16.2. Cumulative Distribution Function (CDF),
 - 16.3. Cross- and auto-correlation (CCF & ACF).

Appendix I: Custom MATLAB calibration script for sensitivity, bias adjustment, coordinate correction and rotation.

A custom script was produced in MATLAB R2019a (The MathWorks, Inc., Natick, Massachusetts, USA) which was used to apply the pitch R_y (ρ) and R_z (ψ) rotation equations, translating the vector angles from the static data when it was re-orientate it to 1, 0, 0 and use this to feed these angles to re-orientate the dynamic accelerometry data whilst fitted on the shank collected during running.

```
[filenames,pathnames]=uigetfile('*.txt','Select txt file');
load(fullfile(pathnames,filenames));

i=1;
%Using a static section to rotate the data to form 1, 0 , 0. From
here the Final angles will be applied to the dynamic data using the
loop below.
AccelCoordStaticLL = [0.922693798    0.164624478 0.112014727];
AccelCoordStaticRL = [0.952107378    0.228172796 0.149110598];
BiasLL = [0.0017852162 0.0572094130 -0.0320330048];
BiasRL = [-0.0145921833 0.0209972119 0.0701501689];
SensitivityLL = [0.9788961978 1.0183770637 1.0106186978];
SensitivityRL = [0.9638366628 1.0006589858 1.0363233118];
AccelCoordStaticLL(i,1) = (AccelCoordStaticLL(i,1)-
BiasLL(1))/SensitivityLL(1);
AccelCoordStaticLL(i,2) = (AccelCoordStaticLL(i,2)-
BiasLL(2))/SensitivityLL(2);
AccelCoordStaticLL(i,3) = (AccelCoordStaticLL(i,3)-
BiasLL(3))/SensitivityLL(3);
AccelCoordStaticRL(i,1) = (AccelCoordStaticRL(i,1)-
BiasRL(1))/SensitivityRL(1);
AccelCoordStaticRL(i,2) = (AccelCoordStaticRL(i,2)-
BiasRL(2))/SensitivityRL(2);
AccelCoordStaticRL(i,3) = (AccelCoordStaticRL(i,3)-
BiasRL(3))/SensitivityRL(3);

%Gives new z and x values (zeroes out z) LL
ZaboutYangleLL = -
atan(AccelCoordStaticLL(i,3)/AccelCoordStaticLL(i,1));
ZaboutYLL = [cos(ZaboutYangleLL) 0 sin(ZaboutYangleLL); 0 1 0; -
sin(ZaboutYangleLL) 0 cos(ZaboutYangleLL)];
CorrectedZangleLL = AccelCoordStaticLL*ZaboutYLL;

%Gives new z and x values (zeroes out z) RL
ZaboutYangleRL = -
atan(AccelCoordStaticRL(i,3)/AccelCoordStaticRL(i,1));
ZaboutYRL = [cos(ZaboutYangleRL) 0 sin(ZaboutYangleRL); 0 1 0; -
sin(ZaboutYangleRL) 0 cos(ZaboutYangleRL)];
CorrectedZangleRL = AccelCoordStaticRL*ZaboutYRL;

%Gives new y and x (zeroes out y) LL
```

```

YaboutZangleLL =
atan(CorrectedZangleLL(i,2)/CorrectedZangleLL(i,1));
YaboutZLL = [cos(YaboutZangleLL) -sin(YaboutZangleLL) 0;
sin(YaboutZangleLL) cos(YaboutZangleLL) 0; 0 0 1];

%Gives new y and x (zeroes out y) RL
YaboutZangleRL =
atan(CorrectedZangleRL(i,2)/CorrectedZangleRL(i,1));
YaboutZRL = [cos(YaboutZangleRL) -sin(YaboutZangleRL) 0;
sin(YaboutZangleRL) cos(YaboutZangleRL) 0; 0 0 1];

%Gives x = 1, y = 0, z = 0 for static data LL
Corrected_Coordinates_LL =
AccelCoordStaticLL(i,:)*ZaboutYLL*YaboutZLL;

%Gives x = 1, y = 0, z = 0 for static data RL
Corrected_Coordinates_RL =
AccelCoordStaticRL(i,:)*ZaboutYRL*YaboutZRL;

%Rotate Data
RotatedDataLL = (DYNAMIC_FILENAME) (:,1:3);
RotatedDataRL = (DYNAMIC_FILENAME) (:,4:6);

%This produces a new data set which is a copy of itself
"RotatedData" is the new object and "Data" is the original that is
being copied into

%RotatedData
% length(RotatedData) is the total number of data points, so this
will apply to all data - 1:length = from 1 to all data points in
table

%For loop LL/RL
for i = 1:length(RotatedDataLL)
    RotatedDataLL(i,:) = RotatedDataLL(i,:)*ZaboutYLL*YaboutZLL;
    RotatedDataRL(i,:) = RotatedDataRL(i,:)*ZaboutYRL*YaboutZRL;
end

%save files and rename Acc_x_LL_Rotated Acc_y_LL_Rotated
Acc_z_LL_Rotated, Acc_x_RL_Rotated, Acc_y_RL_Rotated,
Acc_z_RL_Rotated

```

Appendix J: Table for gross metabolic usage of oxygen uptake (ml/kg/min) between the VF and the JAZ over 0, 1, 3 and 5% incline.

Gross metabolic usage of oxygen uptake (ml/kg/min) of the Nike® Vaporfly NEXT% (VFN%) and Saucony® ProGrid Jazz 12 (JAZ) running shoe over inclines 0%, 1%, 3% and 5% whilst running on a treadmill at 12 km/h. The DIFF being the absolute difference between the VFN% and JAZ oxygen uptake (ml/kg/min) and % DIFF being calculated using (Equation 23). This table also displays the mean oxygen uptake (ml/kg/min), S.D. = standard deviation, CoV = coefficient of variation and S.E. = standard error of the mean.

Trainer		JAZ GROSS ($\dot{V}O_2$ ml/kg/min)				VFN% GROSS $\dot{V}O_2$ ($\dot{V}O_2$ ml/kg/min)				Difference GROSS ($\dot{V}O_2$ ml/kg/min)				Difference (%)			
Incline (%)		0	1	3	5	0	1	3	5	0	1	3	5	0	1	3	5
Participant no.	1		43.06	46.68	50.45		38.64	46.63	50.14		4.42	0.05	0.31		10.26	0.11	0.62
	2	36.78	41.90	46.22	51.27	34.91	36.28	41.66	49.16	1.87	5.62	4.56	2.11	5.09	13.40	9.86	4.12
	3	37.26	40.56	44.59	51.64	35.99	37.23	44.21	53.05	1.27	3.33	0.38	-1.41	3.40	8.21	0.85	-2.73
	4	36.78	38.57	44.05	50.47	35.13	38.49	43.36	47.73	1.65	0.08	0.69	2.74	4.48	0.21	1.56	5.43
	5	34.46	37.01	42.39	47.65	34.00	38.21	40.53	47.93	0.47	-1.20	1.85	-0.28	1.35	-3.24	4.37	-0.59
	6	42.93	45.14	49.59	54.70	40.65	45.40	49.06	54.49	2.28	-0.26	0.53	0.21	5.31	-0.58	1.07	0.38
	7	43.73	46.51	51.68	57.11	44.19	44.25	52.04	55.15	-0.47	2.26	-0.35	1.97	-1.07	4.85	-0.69	3.45

	8	45.52	45.64	52.81	57.35	42.27	41.95	49.99	55.18	3.25	3.70	2.82	2.16	7.13	8.10	5.34	3.77
	9	42.60	40.56	46.17	54.78	40.58	41.56	48.47	53.16	2.02	-1.00	-2.30	1.63	4.73	-2.48	-4.99	2.97
	10	38.06	40.53	46.15	51.06	37.51	38.11	43.55	49.19	0.55	2.42	2.61	1.87	1.45	5.97	5.65	3.66
	11	41.83	40.67	47.53	51.81	36.32	38.23	44.78	49.45	5.51	2.44	2.75	2.36	13.16	6.00	5.78	4.56
	12	37.64	42.61	45.81		37.53	39.45	42.57		0.11	3.16	3.24		0.30	7.41	7.07	
	13		44.96	50.14	54.05		43.74	50.00	50.54		1.22	0.14	3.51		2.72	0.28	6.50
	14	38.97	40.22	45.10	52.04	36.16	39.65	44.99	50.98	2.81	0.57	0.11	1.07	7.21	1.42	0.25	2.05
	15	41.63	45.89	49.92	50.77	38.99	42.70	48.14	49.09	2.64	3.19	1.79	1.68	6.34	6.94	3.58	3.31
Participant no.	16	41.98	44.22	51.04	55.81	41.62	43.97	48.96	53.76	0.36	0.26	2.08	2.04	0.86	0.58	4.08	3.66
	17	41.57	39.84	46.33	51.65	38.94	40.42	46.30	50.01	2.63	-0.58	0.03	1.65	6.33	-1.45	0.06	3.19
	18	43.19	45.26	49.79	53.59	41.52	44.04	47.16	52.72	1.68	1.22	2.62	0.88	3.88	2.69	5.27	1.64
Mean		40.31	42.40	47.56	52.72	38.52	40.68	46.25	51.28	1.79*	1.71*	1.31*	1.44*	4.37*	3.95*	2.75*	2.70*
S.D.		3.16	2.81	2.90	2.61	3.03	2.81	3.23	2.50	1.47	1.97	1.66	1.20	3.46	4.68	3.52	2.28
CoV		0.08	0.07	0.06	0.05	0.08	0.07	0.07	0.05	0.82	1.15	1.27	0.83	0.79	1.19	1.28	0.84
S.E.		0.79	0.66	0.68	0.63	0.76	0.66	0.76	0.61	0.37	0.47	0.39	0.29	0.87	1.10	0.83	0.55

* Significance to p=0.01.

Appendix K: RE benefit (%) predicted from the exponential decay equation.

RE benefit (%) predicted from the exponential decay equation shown from inclines 1 to 15 with a split data table to incline 46 showing the asymptote of 2.2781% rounded up to 2.28% which depicts the fixed effect of the VFN% running shoe.

Incline (%)	Actual results (%)	Weight adjusted RE benefit (%)	Exponential decay RE benefit (%)	Weight adjusted RE benefit (%)
0	4.37	2.37	4.45	3.45
1	3.95	1.95	3.76	2.76
2			3.29	2.29
3	2.75	0.75	2.97	1.97
4			2.75	1.75
5	2.70	0.70	2.60	1.60
6			2.50	1.50
7			2.43	1.43
8			2.38	1.38
9			2.35	1.35
10			2.33	1.33
11			2.31	1.31
12			2.30	1.30
13			2.29	1.29
14			2.29	1.29
15			2.29	1.29
16			2.28	1.28
50			2.28	1.28

Appendix L: Testing results for n = 23 participants for analytical measures calculated from the wearable device accelerometry wave. The table shows the mean, standard deviation (S.D.) and standard error (S.E.) for each result.

Male	Trainer	Analytical measure	Peak no.	Incline (%)	Mean	S.E.	S.D.
	JAZ	FF	1	0	1.35	0.02	0.08
			2		2.71	0.04	0.15
			3		4.06	0.06	0.23
			4		5.46	0.11	0.41
			1	1	1.36	0.02	0.09
			2		2.73	0.04	0.17
			3		4.10	0.06	0.26
			4		5.46	0.08	0.34
			1	3	1.37	0.02	0.09
			2		2.75	0.05	0.18
			3		4.12	0.07	0.28
			4		5.50	0.10	0.38
			1	5	1.39	0.02	0.09
			2		2.78	0.05	0.18
			3		4.16	0.07	0.27
			4		5.60	0.12	0.50
		SP		0	6.76	0.18	0.72
				1	6.83	0.17	0.71
				3	6.53	0.22	0.88
				5	6.55	0.20	0.80
	VFN%	FF	1	0	1.34	0.01	0.05
			2		2.69	0.03	0.10
			3		4.03	0.04	0.16
			4		5.38	0.06	0.22
			1	1	1.35	0.02	0.08
			2		2.70	0.04	0.16
			3		4.06	0.06	0.24
			4		5.41	0.08	0.32
			1	3	1.36	0.02	0.09
			2		2.73	0.04	0.17
			3		4.09	0.06	0.26
			4		5.49	0.09	0.36

			1	5	1.37	0.02	0.08
			2		2.75	0.04	0.17
			3		4.12	0.07	0.25
			4		5.50	0.09	0.34
		SP		0	6.83	0.18	0.69
				1	6.73	0.17	0.67
				3	6.48	0.19	0.74
				5	6.45	0.20	0.77
	Difference (%)	FF	1	0	-0.03	0.56	2.09
			2		-0.07	0.54	2.03
			3		-0.07	0.55	2.06
			4		0.72	1.03	3.85
			1	1	0.49	0.48	1.91
			2		0.39	0.44	1.76
			3		0.38	0.46	1.84
			4		0.43	0.45	1.80
			1	3	0.19	0.44	1.71
			2		0.18	0.44	1.70
			3		0.21	0.44	1.70
			4		-0.64	0.95	3.68
			1	5	0.25	0.32	1.23
			2		0.20	0.32	1.25
			3		0.22	0.33	1.28
			4		0.97	0.77	2.97
		SP		0	-0.49	1.82	6.81
				1	2.04	1.06	4.26
				3	0.55	1.43	5.53
				5	1.61	1.92	7.44
Female	JAZ	FF	1	0	1.39	0.04	0.09
			2		2.77	0.08	0.17
			3		4.16	0.12	0.26
			4		5.55	0.15	0.34
		FF	1	1	1.40	0.03	0.08
			2		2.79	0.07	0.17
			3		4.19	0.10	0.25
			4		5.58	0.14	0.34
		FF	1	3	1.41	0.04	0.08
			2		2.82	0.08	0.17
			3		4.23	0.11	0.25

			4		5.64	0.15	0.34
		FF	1	5	1.42	0.04	0.10
			2		2.84	0.09	0.20
			3		4.26	0.13	0.29
			4		5.69	0.17	0.39
		SP		0	7.18	0.49	1.09
				1	6.91	0.55	1.34
				3	6.86	0.62	1.38
				5	7.10	0.56	1.25
	VFN%	FF	1	0	1.37	0.04	0.09
			2		2.75	0.08	0.18
			3		4.12	0.12	0.27
			4		5.49	0.16	0.36
		FF	1	1	1.37	0.04	0.09
			2		2.73	0.07	0.17
			3		4.10	0.11	0.26
			4		5.46	0.14	0.35
		FF	1	3	1.39	0.03	0.08
			2		2.78	0.07	0.16
			3		4.17	0.10	0.24
			4		5.56	0.13	0.32
		FF	1	5	1.41	0.03	0.08
			2		2.81	0.06	0.15
			3		4.22	0.09	0.22
			4		5.62	0.12	0.30
		SP		0	7.37	0.44	0.99
				1	6.98	0.42	1.02
				3	6.86	0.49	1.21
				5	6.88	0.45	1.11
	Difference between (%)	FF	1	0	1.27	0.65	1.29
			2		0.97	0.55	1.22
			3		0.97	0.51	1.13
			4		1.00	0.55	1.22
		FF	1	1	2.14	0.48	1.18
			2		2.10	0.47	1.14
			3		2.08	0.47	1.14
			4		2.10	0.49	1.20
		FF	1	3	0.53	0.83	1.85
			2		0.37	0.85	1.91

			3		0.33	0.84	1.87
			4		0.34	0.82	1.82
		FF	1	5	0.03	1.24	2.78
			2		0.04	1.23	2.76
			3		-0.02	1.22	2.73
			4		0.08	1.22	2.72
		SP		0	-3.02	2.17	4.86
				1	-2.03	2.96	7.26
				3	-0.92	0.69	1.55
				5	2.30	3.04	6.79

REFERENCES

1. Alam, M. and Rohac, J. (2015) 'Adaptive data filtering of inertial sensors with variable bandwidth', *Sensors (Switzerland)*, 15(2), pp. 3282–3298. Available at: <https://doi.org/10.3390/s150203282>.
2. Alexander, R.M. (1991) 'Energy-saving mechanisms in walking and running', *Journal of Experimental Biology*, (160), pp. 55–69.
3. Alexander, R.M. (1992) 'Running. The human machine', in: London: Natural History Museum Publications, pp. 74–87.
4. Analogue Devices (2015) 'Digital Accelerometer'.
5. Anwary, A.R., Yu, H. and Vassallo, M. (2018) 'An Automatic gait feature extraction method for identifying gait asymmetry using wearable sensors', *Sensors (Switzerland)*, 18(2). Available at: <https://doi.org/10.3390/s18020676>.
6. Ardigo, L.P., Saibene, F. and Avanzate, B. (1993) 'Mechanical determinants of gradient walking energetics in man', *Journal of Physiology*, (471), pp. 725–735.
7. Bach, M.M., Dominici, N., and Daffertshofer, A., (2022) 'Predicting vertical ground reaction forces from 3D accelerometry using reservoir computers leads to accurate gait event detection', *Frontiers in Sports and Active Living*, (4), pp. 1–12. Available at: <https://doi.org/10.3389/fspor.2022.1037438>.
8. Barnes, C. et al. (2017) 'Quantitative Time Profiling of Children's Activity and Motion', *Medicine and Science in Sports and Exercise*, 49(1), pp. 183–190. Available at: <https://doi.org/10.1249/MSS.0000000000001085>.

9. Barnes, C.M. (2017) Group-based analysis of human exercise, performance and health. University of Swansea.
10. Barnes, K.R. and Kilding, A.E. (2015) 'Running economy: measurement, norms, and determining factors', *Sports Medicine - Open*, 1(1), pp. 1–15. Available at: <https://doi.org/10.1186/s40798-015-0007-y>.
11. Barnes, K.R. and Kilding, A.E. (2019) 'A Randomized Crossover Study Investigating the Running Economy of Highly-Trained Male and Female Distance Runners in Marathon Racing Shoes versus Track Spikes', *Sports Medicine*, 49(2), pp. 331–342. Available at: <https://doi.org/10.1007/s40279-018-1012-3>.
12. Benson, A.P. et al. (2017) 'Data collection, handling, and fitting strategies to optimize accuracy and precision of oxygen uptake kinetics estimation from breath-by-breath measurements', *Journal of Applied Physiology*, 123(1), pp. 227–242. Available at: <https://doi.org/10.1152/jappphysiol.00988.2016>.
13. Benson, L.C. et al. (2018) 'The use of wearable devices for walking and running gait analysis outside of the lab: A systematic review', *Gait and Posture*, 63(April), pp. 124–138. Available at: <https://doi.org/10.1016/j.gaitpost.2018.04.047>.
14. Bieda, R. and Jaskot, K. (2016) 'Determining of an object orientation in 3D space using direction cosine matrix and non-stationary Kalman filter', *Archives of Control Sciences*, 26(2), pp. 223–244. Available at: <https://doi.org/10.1515/acsc-2016-0013>.

15. Bötzel, K. et al. (2016) 'Gait recording with inertial sensors--How to determine initial and terminal contact.', *Journal Of Biomechanics*, 49(3), pp. 332–337. Available at: <https://doi.org/10.1016/j.jbiomech.2015.12.035>.
16. Bötzel, K. et al. (2018) 'Quantification of gait parameters with inertial sensors and inverse kinematics.', *Journal of Biomechanics*, 72, pp. 207–214. Available at: <https://doi.org/10.1016/j.jbiomech.2018.03.012>.
17. Brahms, C.M. et al. (2018) 'Stride length determination during overground running using a single foot-mounted inertial measurement unit.', *Journal of Biomechanics*, 71, pp. 302–305. Available at: <http://search.ebscohost.com/login.aspx?direct=true&db=sph&AN=128695436&site=ehost-live>.
18. Bramble, D.M. and Lieberman, D.E. (2004) 'Endurance running and the evolution of Homo', *Nature*, 432(7015), pp. 345–352. Available at: <https://doi.org/10.1038/nature03052>.
19. Burns, G.T. and Tam, N. (2020) 'Is it the shoes? A simple proposal for regulating footwear in road running', *British Journal of Sports Medicine*. BMJ Publishing Group, pp. 439–441. Available at: <https://doi.org/10.1136/bjsports-2018-100480>.
20. Caldas, R. et al. (2017) 'A systematic review of gait analysis methods based on inertial sensors and adaptive algorithms', *Gait and Posture*, 57(February), pp. 204–210. Available at: <https://doi.org/10.1016/j.gaitpost.2017.06.019>.

21. Cavagna, G.A. and Kaneko, M. (1977) 467 With 3 text-figure8 Printed in Great Britain MECHANICAL WORK AND EFFICIENCY IN LEVEL WALKING AND RUNNING, J. Physiol.
22. Cavanagh, P.R. and Kram, R. (1985) 'Mechanical and muscular factors affecting the efficiency of human movement', *Medicine and science in sports and exercise*, 17(3), pp. 326–331.
23. Cavanagh, P.R. and Williams, K.R. (1982) 'The effect of stride length variation on oxygen uptake during distance running', *Medicine and science in sports and exercise*, 14(1), pp. 30–35.
24. Clark (2017) Profiling Movement and Gait Quality in Children's Physical Activity. Swansea University. Available at: <https://doi.org/10.13140/RG.2.2.16110.51524>.
25. Clark, C. et al. (2016a) 'A Kinematic Analysis of Fundamental Movement Skills', *Sport Science Review*, 25(3–4), pp. 261–275. Available at: <https://doi.org/10.1515/ssr-2016-0014>.
26. Clark, C. et al. (2016b) 'SlamTracker Accuracy under Static and Controlled Movement Conditions', *Sport Science Review*, 25(5–6), pp. 374–383. Available at: <https://doi.org/http://dx.doi.org/10.1515/ssr-2016-0020>.
27. Clark, C. et al. (2017) 'Profiling Movement Quality Characteristics of Children (9-11y) During Recess', *European Journal of Human Movement*, 39, pp. 143–160. Available at: <https://www.researchgate.net/publication/322508890>.
28. Colloff, P. (2022) The implication of Nike Vaporflys on the energetic cost of running, including the influence of incline and shoe mass. Leeds.

29. Daniels, J. and Daniels, N. (1992) 'Running economy of elite male and elite female runners', *Medicine and Science in Sports and Exercise*, 24(4), pp. 483–489. Available at: <http://journals.lww.com/acsm-msse> by BhDMf5ePHKav1zEoum1tQfN4a+kJLhEZgbslHo4XMi0hCywCX1AWnYQp/IIQrHD3i3D0OdRyi7TvSFI4Cf3VC4/OAVpDDa8KKGKV0Ymy+78= (Accessed: 8 May 2024).
30. DeJong, A.F., Fish, P.N. and Hertel, J. (2021) 'Running behaviors, motivations, and injury risk during the COVID-19 pandemic: A survey of 1147 runners', *PLoS ONE*, 16(2 February). Available at: <https://doi.org/10.1371/journal.pone.0246300>.
31. Dierks, T.A., Davis, I.S. and Hamill, J. (2010) 'The effects of running in an exerted state on lower extremity kinematics and joint timing', *Journal of Biomechanics*, 43(15), pp. 2993–2998. Available at: <https://doi.org/10.1016/j.jbiomech.2010.07.001>.
32. Dominy, T.A. and Joubert, D.P. (2022) 'Effects Of A Carbon-Plated Racing Shoe On Running Economy At Slower Running Speeds', *Medicine & Science in Sports & Exercise*, 54(9S), pp. 624–624. Available at: <https://doi.org/10.1249/01.mss.0000882908.08780.07>.
33. Ellis, K. et al. (2014) 'Identifying Active Travel Behaviors in Challenging Environments Using GPS, Accelerometers, and Machine Learning Algorithms.', *Frontiers in public health*, 2, p. 36. Available at: <https://doi.org/10.3389/fpubh.2014.00036>.
34. Farley, C.T. and González, O. (1996) 'Leg stiffness and stride frequency in human running', *Journal of Biomechanics*, 29(2), pp. 181–186. Available at: [https://doi.org/10.1016/0021-9290\(95\)00029-1](https://doi.org/10.1016/0021-9290(95)00029-1).

35. Ferber, R. et al. (2016) 'Gait biomechanics in the era of data science.', *Journal Of Biomechanics*, 49(16), pp. 3759–3761. Available at: <https://doi.org/10.1016/j.jbiomech.2016.10.033>.
36. Fogg, E.J. (2005) 'An inertial sensor system for analysing human movement', U211490. Available at: <http://search.proquest.com/docview/301655398?accountid=37552>.
37. Fridolfsson, J., Börjesson, M. and Arvidsson, D. (2018) 'A Biomechanical Re-Examination of Physical Activity Measurement with Accelerometers.', *Sensors (Basel, Switzerland)*, 18(10), p. 3399. Available at: <https://doi.org/10.3390/s18103399>.
38. Fuller, J.T. et al. (2015) 'The Effect of Footwear on Running Performance and Running Economy in Distance Runners', *Sports Medicine*, 45(3), pp. 411–422. Available at: <https://doi.org/10.1007/s40279-014-0283-6>.
39. García-Pérez, J.A. et al. (2014) 'Effects of treadmill running and fatigue on impact acceleration in distance running', *Sports Biomechanics*, 13(3), pp. 259–266. Available at: <https://doi.org/10.1080/14763141.2014.909527>.
40. Giavarina, D. (2015) 'Understanding Bland Altman analysis', *Biochemia Medica*, 25(2), pp. 141–151. Available at: <https://doi.org/10.11613/BM.2015.015>.
41. Grant, P.M. et al. (2010) 'Analyzing free-living physical activity of older adults in different environments using body-worn activity monitors', *Journal of Aging and Physical Activity*, 18(2), pp. 171–184.

42. Hahn, H. et al. (2017) 'Biomechanical, metabolic and cardiopulmonary responses of masters recreational runners during running at different speeds.', *Research in Sports Medicine*, 25(2), pp. 118–131. Available at: <https://doi.org/10.1080/15438627.2017.1282359>.
43. Hazra, A. and Gogtay, N. (2016) 'Biostatistics series module 6: Correlation and linear regression', *Indian Journal of Dermatology*, 61(6), pp. 593–601. Available at: <https://doi.org/10.4103/0019-5154.193662>.
44. Healey, L.A. and Hoogkamer, W. (2021) 'Longitudinal bending stiffness does not affect running economy in Nike Vaporfly Shoes', *Journal of Sport and Health Science*, 11(3), pp. 285–292. Available at: <https://doi.org/10.1016/j.jshs.2021.07.002>.
45. Hébert-Losier, K. et al. (2022) 'Metabolic and performance responses of male runners wearing 3 types of footwear: Nike Vaporfly 4%, Saucony Endorphin racing flats, and their own shoes', *Journal of Sport and Health Science*, 11(3), pp. 275–284. Available at: <https://doi.org/10.1016/j.jshs.2020.11.012>.
46. Hoogkamer, W. et al. (2016) 'Altered running economy directly translates to altered distance-running performance', *Medicine and Science in Sports and Exercise*, 48(11), pp. 2175–2180. Available at: <https://doi.org/10.1249/MSS.0000000000001012>.
47. Hoogkamer, W. et al. (2018) 'A Comparison of the Energetic Cost of Running in Marathon Racing Shoes', *Sports Medicine*, 48(4), pp. 1009–1019. Available at: <https://doi.org/10.1007/s40279-017-0811-2>.

48. Hoogkamer, W., Kipp, S. and Kram, R. (2019) 'The Biomechanics of Competitive Male Runners in Three Marathon Racing Shoes: A Randomized Crossover Study', *Sports Medicine*, 49(1), pp. 133–143. Available at: <https://doi.org/10.1007/s40279-018-1024-z>.
49. Hoogkamer, W., Kram, R. and Arellano, C.J. (2017) 'How Biomechanical Improvements in Running Economy Could Break the 2-hour Marathon Barrier', *Sports Medicine*, 47(9), pp. 1739–1750. Available at: <https://doi.org/10.1007/s40279-017-0708-0>.
50. Hu, X. and Soh, G.S. (2014) 'A study on estimation of planar gait kinematics using minimal inertial measurement units and inverse kinematics.', *Conference Proceedings: ... Annual International Conference Of The IEEE Engineering In Medicine And Biology Society. IEEE Engineering In Medicine And Biology Society. Annual Conference*, 2014, pp. 6911–6914. Available at: <https://doi.org/10.1109/EMBC.2014.6945217>.
51. Hunter, I. et al. (2019) 'Running economy, mechanics, and marathon racing shoes', *Journal of Sports Sciences*, 37(20), pp. 2367–2373. Available at: <https://doi.org/10.1080/02640414.2019.1633837>.
52. Hunter, I. et al. (2022) 'Energetics and Biomechanics of Uphill, Downhill and Level Running in Highly-Cushioned Carbon Fiber Midsole Plated Shoes', *Journal of Sports Science and Medicine*, 21(1), pp. 127–130. Available at: <https://doi.org/10.52082/jssm.2022.127>.
53. Igor Pro by WaveMetrics (2021) Wave Scaling, WaveMetrics. Available at: <https://www.wavemetrics.com/forum/general/wave-scaling-0#> (Accessed: 16 November 2023).

54. Inman, V.T. et al. (2006) 'Human Locomotion', in J. Rose and James.G. Gamble (eds) Human Walking. Third Edit. Philadelphia: Lippincott Williams and Wilkins, pp. 1–18.
55. Jenner, O.R. et al. (no date) 'Quantifying return to fitness after knee injury using gait accelerometry', International Journal of Sports Physiology and Performance [Preprint].
56. Jones, A.M. and Doust, J.H. (1996) 'A 1% treadmill grade most accurately reflects the energetic cost of outdoor running', Journal of Sports Sciences, 14(4), pp. 321–327. Available at: <https://doi.org/10.1080/02640419608727717>.
57. Joubert, D.P. and Jones, G.P. (2022) 'A comparison of running economy across seven highly cushioned racing shoes with carbon-fibre plates', Footwear Science, 14(2), pp. 71–83. Available at: <https://doi.org/10.1080/19424280.2022.2038691>.
58. Joukov, V., Karg, M. and Kulic, D. (2014) 'Online tracking of the lower body joint angles using IMUs for gait rehabilitation.', Conference Proceedings: ... Annual International Conference Of The IEEE Engineering In Medicine And Biology Society. IEEE Engineering In Medicine And Biology Society. Annual Conference, 2014, pp. 2310–2313. Available at: <https://doi.org/10.1109/EMBC.2014.6944082>.
59. Kaufman, K.R. and Sutherland, D.H. (2006) 'Kinematics of Normal Human Walking', in J. Rose and J.G. Gamble (eds) Human Walking. Third. Philadelphia, USA: Lippincott Williams and Wilkins, pp. 33–51.
60. Khusainov, R. et al. (2013) 'Real-time human ambulation, activity, and physiological monitoring: taxonomy of issues, techniques, applications,

- challenges and limitations.’, *Sensors* (Basel, Switzerland), (13), pp. 12852–12902. Available at: <https://doi.org/10.3390/s131012852>.
61. Kieron, D.C. et al. (2018) ‘Estimating running spatial and temporal parameters using an inertial sensor.’, *Sports Engineering* (Springer Science & Business Media B.V.), 21(2), pp. 115–122. Available at: <https://doi.org/10.1007/s12283-017-0255-9>.
62. Kipp, S., Kram, R. and Hoogkamer, W. (2019) ‘Extrapolating metabolic savings in running: Implications for performance predictions’, *Frontiers in Physiology*, 10(FEB), pp. 1–8. Available at: <https://doi.org/10.3389/fphys.2019.00079>.
63. Kluge, F. et al. (2017) ‘Towards mobile gait analysis: Concurrent validity and test-retest reliability of an inertial measurement system for the assessment of spatio-temporal gait parameters’, *Sensors* (Switzerland), 17(7). Available at: <https://doi.org/10.3390/s17071522>.
64. Kram, R. and Taylor, C.R. (1990) ‘Energetics of running: A new perspective’, *Nature*, 346(6281), pp. 265–267. Available at: <https://doi.org/10.1038/346265a0>.
65. Lee, H.J. et al. (2023) ‘A normative study of the gait features measured by a wearable inertia sensor in a healthy old population’, *Gait and Posture*, 103(May 2022), pp. 32–36. Available at: <https://doi.org/10.1016/j.gaitpost.2023.04.006>.
66. Li, C. (2011) BIOLOGICAL, ROBOTIC, AND PHYSICS STUDIES TO DISCOVER PRINCIPLES OF LEGGED LOCOMOTION ON GRANULAR MEDIA.

67. Lissiana, T. et al. (2017) 'Do subjective assessments of running patterns reflect objective parameters?', *European Journal of Sport Science*, 17(7), pp. 847–857. Available at: <http://search.ebscohost.com/login.aspx?direct=true&db=sph&AN=125985626&site=ehost-live>.
68. Long, L.L. and Srinivasan, M. (2013) 'Walking, running, and resting under time, distance, and average speed constraints: Optimality of walk-run-rest mixtures', *Journal of the Royal Society Interface*, 10(81). Available at: <https://doi.org/10.1098/rsif.2012.0980>.
69. Malir, G. (2018) *The Use of Biomechanical Characteristics of Gait, Detected by Accelerometers, as an Index of Running Economy in Trained, Female, Endurance Athletes*. University of Leeds.
70. Margaria, R. (1976) *Biomechanics and energetics of muscular exercise*. Oxford: Clarendon Press.
71. Mariani, B. et al. (2010) '3D gait assessment in young and elderly subjects using foot-worn inertial sensors', *Journal of Biomechanics*, 43(15), pp. 2999–3006. Available at: <https://doi.org/10.1016/j.jbiomech.2010.07.003>.
72. Martens, G. et al. (2018) 'Reproducibility of the Evolution of Stride Biomechanics During Exhaustive Runs', *Journal of Human Kinetics*, 64(1), pp. 57–69. Available at: <https://doi.org/10.1515/hukin-2017-0184>.
73. McGrath, D. et al. (2017) 'Frontal-Plane Variability in Foot Orientation During Fatiguing Running Exercise in Individuals With Chronic Ankle

- Instability.’, *Journal of Athletic Training* (Allen Press), 52(11), pp. 1019–1027. Available at: <https://doi.org/10.4085/1062-6050-52.11.20>.
74. Menolotto, M. et al. (2020) ‘Motion capture technology in industrial applications: A systematic review’, *Sensors* (Switzerland). MDPI AG, pp. 1–25. Available at: <https://doi.org/10.3390/s20195687>.
75. Moe-Nilssen, R. and Helbostad, J.L. (2004) ‘Estimation of gait cycle characteristics by trunk accelerometry’, *Journal of Biomechanics*, 37(1), pp. 121–126. Available at: [https://doi.org/10.1016/S0021-9290\(03\)00233-1](https://doi.org/10.1016/S0021-9290(03)00233-1).
76. Moldover, J.R. and Borg-Stein, J. (1994) ‘Exercise and Fatigue’, *The Physiological Basis of Rehabilitation Medicine*, 39(5), pp. 393–411. Available at: <https://doi.org/10.1016/b978-1-4831-7818-9.50021-6>.
77. Moore, I. S. (2016) Is There an Economical Running Technique? A Review of Modifiable Biomechanical Factors Affecting Running Economy. *Sports Medicine*, 46(6), 793–807. Available at: <https://doi.org/10.1007/s40279-016-0474-4>.
78. Nigg, B.M., Cigoja, S. and Nigg, S.R. (2020) ‘Effects of running shoe construction on performance in long distance running’, *Footwear Science*, 12(3), pp. 133–138. Available at: <https://doi.org/10.1080/19424280.2020.1778799>.
79. Nigg, B.M., Cigoja, S. and Nigg, S.R. (2021) ‘Teeter-totter effect: A new mechanism to understand shoe-related improvements in long-distance running’, *British Journal of Sports Medicine*. BMJ Publishing Group, pp. 462–463. Available at: <https://doi.org/10.1136/bjsports-2020-102550>.

80. Nike Inc. (2016) Breaking2 Campaign. Available at:
<https://www.nike.com/gb/running/breaking2>.
81. Norris, M., Anderson, R. and Kenny, I.C. (2014) 'Method analysis of accelerometers and gyroscopes in running gait: A systematic review', *Proceedings of the Institution of Mechanical Engineers, Part P: Journal of Sports Engineering and Technology*, 228(1), pp. 3–15. Available at:
<https://doi.org/10.1177/1754337113502472>.
82. Novacheck, T.F. (1998) *The biomechanics of running, Gait and Posture*.
83. O'Grady, T.J. and Gracey, D. (2020) 'An Evaluation of the Decision by World Athletics on Whether or Not to Ban the Nike Vapor Fly Racing Shoe in 2020', *Entertainment and Sports Law Journal*, 18(1). Available at: <https://doi.org/10.16997/eslj.257>.
84. Ortega, J.A. et al. (2021) 'Energetics and Biomechanics of Running Footwear with Increased Longitudinal Bending Stiffness: A Narrative Review', *Sports Medicine*, 51(5), pp. 873–894. Available at:
<https://doi.org/10.1007/s40279-020-01406-5>.
85. Ortega, J.A. (2022) *The Effects of Footwear Longitudinal Bending Stiffness on the Energetics and Biomechanics of Uphill Running*, ScholarWorks @ UMass Amherst. University of Massachusetts Amherst. Available at: <https://doi.org/10.7275/31019592>.
86. Padulo, J. et al. (2013) 'A Paradigm of Uphill Running', *PLoS ONE*, 8(7), pp. 1–8. Available at:
<https://doi.org/10.1371/journal.pone.0069006>.

87. Patonis, P. et al. (2018) 'A fusion method for combining low-cost IMU/magnetometer outputs for use in applications on mobile devices', *Sensors* (Switzerland), 18(8). Available at: <https://doi.org/10.3390/s18082616>.
88. Perry, J. (1992) *Gait Analysis: Normal and Pathological Function*. USA: Slack Inc.
89. Plymire, D.C. (2002) 'Running, Heart Disease, and the Ironic Death of Jim Fixx', *Research Quarterly for Exercise and Sport*, 73(1), pp. 38–46. Available at: <https://doi.org/10.1080/02701367.2002.10608990>.
90. Proakis, J.G. and Manolakis, D.G., (2007) *Digital Signal Processing: Principles, Algorithms, and Applications*. 4th ed. Upper Saddle River, NJ: Prentice Hall.
91. Puyau, M.R. et al. (2002) 'Validation and calibration of physical activity monitors in children', *Obesity Research*, 10(3), pp. 150–157. Available at: <https://doi.org/10.1038/oby.2002.24>.
92. Quealy, K. and Katz, J. (2019) 'Nike's Fastest Shoes May Give Runners an Even Bigger Advantage Than We Thought', *The New York Times*, 13 December, pp. 1–15.
93. Rao, K. et al. (2019) 'A MEMS Micro-g Capacitive Accelerometer Based on Through-Silicon-Wafer-Etching Process', *Micromachines*, 10(6). Available at: <https://doi.org/10.3390/mi10060380>.
94. Reilly, M.O. et al. (2018) 'Wearable Inertial Sensor Systems for Lower Limb Exercise Detection and Evaluation: A Systematic Review.', *Sports Medicine* (Auckland, N.Z.), 48(5), pp. 1221–1246. Available at: <https://doi.org/10.1007/s40279-018-0878-4>.

95. Rizzo, N. (2021) 'Running Boom : 28 . 76 % of runners started during the pandemic', RunRepeat, (April), pp. 1–5. Available at: <https://runrepeat.com/new-pandemic-runners>.
96. Roy, J.P.R. and Stefanyshyn, D.J. (2006) 'Shoe midsole longitudinal bending stiffness and running economy, joint energy, and EMG', *Medicine and Science in Sports and Exercise*, 38(3), pp. 562–569. Available at: <https://doi.org/10.1249/01.mss.0000193562.22001.e8>.
97. Rueda, J. et al. (2017) 'Running pattern differences in gender and running level', 35th Conference of the International Society of Biomechanics in Sports [Preprint], (June).
98. Sadeghi, H. et al. (2000) 'Symmetry and limb dominance in able-bodied gait: a review', *Gait & Posture*, 12(1), pp. 34–45. Available at: [https://doi.org/10.1016/S0966-6362\(00\)00070-9](https://doi.org/10.1016/S0966-6362(00)00070-9).
99. Sarzynski, M.A. et al. (2013) 'Measured maximal heart rates compared to commonly used age-based prediction equations in the heritage family study', *American Journal of Human Biology*, 25(5), pp. 695–701. Available at: <https://doi.org/10.1002/ajhb.22431>.
100. Saucony Inc. (2017) Saucony shoe technology. Available at: <http://www.saucony-running.com/saucony-technology.html> (Accessed: 6 March 2023).
101. Saunders, P.U. et al. (2004) 'Factors Affecting Running Economy in Trained Distance Runners', *Sports medicine* (Auckland, N.Z.), 34(7), pp. 465–485. Available at: <https://doi.org/10.2165/00007256-200434070-00005>.

102. Scheerder J., Breedveld, K. and Borgers J. (2015) 'Who Is Doing a Run with the Running Boom?', in Scheerder J. and K.B.J. Breedveld (eds) *Running across Europe: The Rise and Size of One of the Largest Sport Markets*. London: Palgrave Macmillan UK, pp. 1–27. Available at: https://doi.org/10.1057/9781137446374_1.
103. Sejdíć, E. et al. (2016) 'Extraction of stride events from gait accelerometry during treadmill walking.', *IEEE Journal Of Translational Engineering In Health And Medicine*, 4. Available at: <http://search.ebscohost.com/login.aspx?direct=true&db=cmedm&AN=27088063&site=ehost-live>.
104. Seminati, E. et al. (2013) 'Anatomically Asymmetrical Runners Move More Asymmetrically at the Same Metabolic Cost', *PLoS ONE*, 8(9), pp. 1–8. Available at: <https://doi.org/10.1371/journal.pone.0074134>.
105. Senefeld, J.W. et al. (2021) 'Technological advances in elite marathon performance', *Journal of Applied Physiology*, 130(6), pp. 2002–2008. Available at: <https://doi.org/10.1152/japplphysiol.00002.2021>.
106. Shahabpoor, E. and Pavic, A. (2018) 'Estimation of vertical walking ground reaction force in real-life environments using single IMU sensor.', *Journal of Biomechanics*, 79, pp. 181–190. Available at: <https://doi.org/10.1016/j.jbiomech.2018.08.015>.
107. Snyder, K.L. and Farley, C.T. (2011) 'Energetically optimal stride frequency in running: the effects of incline and decline', *Journal of*

- Experimental Biology, 214(12), pp. 2089–2095. Available at: <https://doi.org/10.1242/jeb.053157>.
108. Snyder, K.L., Kram, R. and Gottschall, J.S. (2012) 'The role of elastic energy storage and recovery in downhill and uphill running', Journal of Experimental Biology, 215(13), pp. 2283–2287. Available at: <https://doi.org/10.1242/jeb.066332>.
 109. Soulard, J. et al. (2021) 'Spatio-temporal gait parameters obtained from foot-worn inertial sensors are reliable in healthy adults in single- and dual-task conditions', Scientific Reports, 11(1), pp. 1–15. Available at: <https://doi.org/10.1038/s41598-021-88794-4>.
 110. Stefanyshyn, D.J. and Nigg, B.M. (2000) Influence of midsole bending stiffness on joint energy and jump height performance, Med. Sci. Sports Exerc. Available at: <http://www.msse.org>.
 111. Steins, D. et al. (2014) 'A smart device inertial-sensing method for gait analysis.', Journal of Biomechanics, 47(15), pp. 3780–3785. Available at: <https://doi.org/10.1016/j.jbiomech.2014.06.014>.
 112. Tao, W. et al. (2012) 'Gait Analysis Using Wearable', Sensors, 12(2), pp. 2255–2283. Available at: <https://doi.org/10.3390/s120202255>.
 113. Tesio, L., Roi, G.S. and Möller, F. (1991) 'Pathological gaits: inefficiency is not a rule', Clinical Biomechanics, 6(1), pp. 47–50. Available at: [https://doi.org/10.1016/0268-0033\(91\)90041-N](https://doi.org/10.1016/0268-0033(91)90041-N).
 114. Verbitsky, O. et al. (1998) 'Shock transmission and fatigue in human running', Journal of Applied Biomechanics, 14(3), pp. 300–311. Available at: <https://doi.org/10.1123/jab.14.3.300>.

115. Wada, T. et al. (2018) '3D Visualisation of Wearable Inertial/Magnetic Sensors', *Proceedings*, 2(6), p. 292. Available at: <https://doi.org/10.3390/proceedings2060292>.
116. Whiting, C.S., Hoogkamer, W. and Kram, R. (2022) 'Metabolic cost of level, uphill, and downhill running in highly cushioned shoes with carbon-fiber plates: Graded running in modern marathon shoes', *Journal of Sport and Health Science*, 11(3), pp. 303–308. Available at: <https://doi.org/10.1016/j.jshs.2021.10.004>.
117. Wiltshire, G.R., Fullagar, S. and Stevinson, C. (2018) 'Exploring parkrun as a social context for collective health practices: running with and against the moral imperatives of health responsibilisation', *Sociology of Health & Illness*, 40(1), pp. 3–17. Available at: <https://doi.org/10.1111/1467-9566.12622>.
118. Winter, D. (2009) *Biomechanics and Motor Control of Human Movement*. Fourth. Ontario, Canada: John Wiley and Sons.
119. Worobets, J. et al. (2014) 'Softer and more resilient running shoe cushioning properties enhance running economy', *Footwear Science*, 6(3), pp. 147–153. Available at: <https://doi.org/10.1080/19424280.2014.918184>.
120. Yang, C.-C.C. and Hsu, Y.-L.L. (2010) 'A Review of Accelerometry-Based Wearable Motion Detectors for Physical Activity Monitoring', *Sensors (Basel)*, Aug(10), pp. 7772–7788. Available at: <https://doi.org/10.3390/s100807772>.
121. Youn, I.-H.H. et al. (2018) 'Biomechanical Gait Variable Estimation Using Wearable Sensors after Unilateral Total Knee

Arthroplasty.', *Sensors* (Basel, Switzerland), 18(5). Available at:
<https://doi.org/10.3390/s18051577>.